Distribution Agreement

In presenting this thesis or dissertation as a partial fulfillment of the requirements for an advanced degree from Emory University, I hereby grant to Emory University and its agents the non-exclusive license to archive, make accessible, and display my thesis or dissertation in whole or in part in all forms of media, now or hereafter known, including display on the world wide web. I understand that I may select some access restrictions as part of the online submission of this thesis or dissertation. I retain all ownership rights to the copyright of the thesis or dissertation. I also retain the right to use in future works (such as articles or books) all or part of this thesis or dissertation.

Signature:

_____ _____

Kevin Kimball Ogden Date

Molecular Basis of NMDA Receptor Allosteric Regulation by New Subunit-selective Modulators

By

Kevin Kimball Ogden
Doctor of Philosophy

Graduate Division of Biological and Biomedical Science
Molecular and Systems Pharmacology

_____
Stephen F. Traynelis, Ph.D.
Advisor

_____
Raymond Dingledine, Ph.D.
Committee Member

_____
Criss Hartzell, Ph.D.
Committee Member

_____
Yoland Smith, Ph.D.
Committee Member

Accepted:

_____
Lisa A. Tedesco, Ph.D.
Dean of the James T. Laney School of Graduate Studies

_____
Date

Molecular Basis of NMDA Receptor Allosteric Regulation by New Subunit-selective Modulators

By

Kevin Kimball Ogden
B.S., Michigan State University, 2007

Advisor: Stephen F. Traynelis, Ph.D.

An abstract of
a dissertation submitted to the Faculty of the
James T. Laney School of Graduate Studies of Emory University
in partial fulfillment of the requirements for the degree of
Doctor of Philosophy
in Graduate Division of Biological and Biomedical Science
Molecular and Systems Pharmacology
2013

Abstract

Molecular Basis of NMDA Receptor Allosteric Regulation by New Subunit-selective Modulators

By Kevin Kimball Ogden

NMDA receptors are glutamate-gated ion channels that mediate excitatory synaptic transmission in the central nervous system and are critical for learning, cognition, and neuronal development. Dysfunction of NMDA receptors has been implicated in neurological and psychiatric disorders ranging from stroke to schizophrenia. NMDA receptors are tetrameric ion channels comprising GluN1, GluN2, and GluN3 subunits. The four GluN2 subunits, GluN2A, GluN2B, GluN2C, and GluN2D, substantially contribute to functional diversity of NMDA receptors and have distinct expression patterns in the CNS. The promise that subunit-selective allosteric modulators differentially targeting the GluN2 subunit could provide an opportunity to modify the function of select groups of neurons for therapeutic gain has resulted in a handful of new compounds that appear to act at novel sites. In this dissertation, I present data that define the mechanism and site of action of two new classes of NMDA receptor allosteric modulators. I show that a class of tetrahydroisoquinolines, which selectively potentiates GluN2C- and GluN2D-containing NMDA receptors and is exemplified by the molecule CIQ, does not act at previously recognized modulatory sites. Rather, I identified critical determinants of CIQ modulation in the region near the first transmembrane helix of GluN2D, including in a putative pre-M1 cuff helix that may influence channel gating. Further, I investigated the mechanism and molecular determinants of selectivity for a new class of GluN2A-selective antagonists represented by the compound TCN-201. I found that TCN-201 inhibits GluN1/GluN2A receptors by decreasing the potency of the GluN1 agonist in an allosteric manner. Mutagenesis and chimeric data coupled with Schild analysis suggest that TCN-201 binds to a novel allosteric site located at the dimer interface between GluN1 and GluN2 agonist binding domains. Lastly, I show that the pre-M1 region of GluN2A affects desensitization and is critical for normal gating of NMDA receptors. Overall, the data presented here demonstrate new modulatory sites on the NMDA receptor and should facilitate development of novel tools and therapeutics with advantageous mechanisms of action and subunit-selectivity.

Molecular Basis of NMDA Receptor Allosteric Regulation by New Subunit-selective Modulators

By

Kevin Kimball Ogden
B.S., Michigan State University, 2007

Advisor: Stephen F. Traynelis, Ph.D.

A dissertation submitted to the Faculty of the
James T. Laney School of Graduate Studies of Emory University
in partial fulfillment of the requirements for the degree of
Doctor of Philosophy
in Graduate Division of Biological and Biomedical Science
Molecular and Systems Pharmacology
2013

Acknowledgements

Many people helped me succeed in the incredible, challenging, and rewarding experiment of earning my Ph.D. and I'd like to briefly thank those whose encouragement, guidance, and support were essential for me to achieve this goal. I'd like to thank my parents for teaching me to always do my best. I am grateful to my undergraduate mentor, Stephanie Watts, for giving me the opportunity to engage in science early in my development, which set me on the path that led me here. I would like to thank my Ph.D. advisor, Steve Traynelis, who gave me the right blend of independence, guidance, and motivation and provided particularly insightful advice on how to be a successful person and scientist. I am especially appreciative of Kasper Hansen for fruitful discussions and teaching me the practical aspects of making science your life. Lastly, I am forever indebted to my wife, Mindi, for providing endless emotional support, listening to all my unpolished ideas, for enduring my prolonged thesis writing, and for innumerable other acts of support.

Table of Contents

List of Figures

List of Tables

List of Abbreviations

ABD	agonist-binding domain
AMPA	α-amino-3-hydroxy-5-methyl-4-isoxazolepropionic acid
ATD	amino terminal domain
BAPTA	1,2-bis(2-aminophenoxy)ethane-N,N,N',N'-tetraacetic acid
CIQ	(3-chlorophenyl)(6,7-dimethoxy-1-((4-methoxyphenoxy)methyl)-3,4-dihydroisoquinolin-2(1H)-yl)methanone
CP-465,022	3-(2-chloro-phenyl)-2-[2-(6-diethylaminomethyl-pyridin-2-yl)-vinyl]-6-fluoro-3H-quinazolin-4-one
DQP-1105	4-(5-(4-bromophenyl)-3-(6-methyl-2-oxo-4-phenyl-1,2-dihydroquinolin-3-yl)-4,5-dihydro-1H-pyrazol-1-yl)-4-oxobutanoic acid
EC_{50}	Half-maximal effective concentration
GYKI-5365	1-(4-Aminophenyl)-3-methylcarbamyl-4-methyl-3,4-dihydro-7,8-methylenedioxy-5H-2,3-benzodiazepine
HEK	human embryonic kidney
IC_{50}	Half-maximal inhibitory concentration
MK-801	dizoclipine maleate
MTS	methanethiosulfonate
NMDA	N-methyl-D-aspartate
pA_2	Concentration of antagonist that produces a two-fold shift in agonist potency
P_{open}	open probability
QNZ46	(E)-4-(6-methoxy-2-(3-nitrostyryl)-4-oxoquinazolin-3(4H)-yl)-benzoic acid
TCN-201	3-chloro-4-fluoro-N-[(4-[(2-(phenylcarbonyl)hydrazino)carbonyl]phenyl)methyl]-benzenesulfonamide
TCN-213	N-(cyclohexylmethyl)-2-({5-[(phenylmethyl)amino]-1,3,4-thiadiazol-2-yl}thio)acetamide
TMD	transmembrane domain

Chapter 1: Introduction

The nervous system processes sensory information to globally regulate internal body functions and direct future actions, which includes generating thoughts and controlling movement. Trillions of nerve cells connected through complex networks throughout the brain, spinal cord, and periphery make up the nervous system. In addition to nerve cells, or neurons, the nervous system is composed of glial cells, including astrocytes, oligodendrocytes, and microglia. However, information processing in the brain is thought to arise from the activity of neurons with glial cells perhaps serving a modulatory role. Neuronal communication and the cellular responses it stimulates allow information to be stored for future use and produce the behavioral and regulatory outputs of the nervous system.

Communication between neurons occurs at specialized connections, called synapses. The vast majority of synapses in the nervous system use chemical neurotransmitters to transmit information between neurons. Around the same time the chemical nature of neurotransmission became widely accepted (Eccles et al., 1954), the amino acid glutamate was discovered to cause convulsions when injected into the cortex (Hayashi, 1954) and to increase action potential firing in neurons of the spinal cord (Curtis et al., 1959). Over the next 20 years, evidence accumulated for glutamate-mediated synaptic transmission and the existence of multiple glutamate receptor subtypes, and little doubt remained about the role of glutamate as a neurotransmitter following discovery of the antagonists D-α-aminoadipate, α,ε-diaminopimelic acid, and HA-966 (Biscoe et al., 1977; Evans et al., 1978a), which selectively blocked both synaptic excitation and the responses of glutamate versus other excitatory chemicals (for review see Watkins, 2000).

Glutamate synaptic transmission is mediated by two broad subtypes of receptors: ligand-gated ion channels (Traynelis et al., 2010) and G protein-coupled receptors (GPCRs) (Conn and Pin, 1997). The ligand-gated ion channels are grouped into three classes, namely AMPA receptors, NMDA receptors, and kainate receptors. These subdivisions were distinguished based on the agonists α-amino-3-hydroxy-5-methyl-4-isoxazole propionate (Krogsgaard-Larsen et al., 1980), N-methyl-D-aspartate (Watkins, 1962; Curtis and Watkins, 1963), and kainate (Shinozaki and Konishi, 1970; Johnston et al., 1974), respectively, which elicited currents from neurons that had varying relative potencies dependent on the brain region in which they were applied. Advances in antagonist pharmacology eventually confirmed the classification based on agonists (Biscoe et al., 1977; Evans et al., 1978a, 1979; McLennan and Lodge, 1979; Davies and Watkins, 1979). While the GPCRs mediating glutamatergic communication in the CNS play critical and diverse roles in synaptic physiology and disease (for review see Pin and Duvoisin, 1995; Conn and Pin, 1997; Niswender and Conn, 2010), this dissertation focuses on the ligand-gated ion channels, in particular the NMDA receptor.

Molecular Composition of NMDA Receptors

In the late 1980s and early 1990s, genes encoding AMPA, kainate, and NMDA receptors were cloned (reviewed by Hollmann and Heinemann, 1994). Initially, a single NMDA receptor subunit, originally called NMDAR1 and now called GluN1, was identified (Moriyoshi et al., 1991). This protein exhibited widespread expression in the brain and when expressed in *Xenopus* oocytes it yielded electrophysiological and pharmacological properties similar to neuronal NMDA receptors. NMDA receptors were therefore thought to be homomeric complexes, similar to AMPA and kainate receptors. However, subsequent cloning strategies discovered four additional subunits, originally called NR2A through NR2D (for rat proteins) or ε1 through ε4 (for mouse proteins) and now referred

to as GluN2A to GluN2D (Collingridge et al., 2009), which co-assemble with GluN1 to form functional NMDA receptors (Meguro et al., 1992; Monyer et al., 1992, 1994; Kutsuwada et al., 1992; Ikeda et al., 1992; Ishii et al., 1993). A few years later, two additional subunits, NR3A (also χ-1 or NMDAR-L) and NR3B (or χ-2), were cloned (Forcina et al., 1995; Ciabarra et al., 1995; Sucher et al., 1995). While these subunits did not yield glutamate-activated currents when expressed on their own, co-expression with GluN1 and GluN2 reduced glutamate-induced current responses. NR3A and NR3B, now called GluN3A and GluN3B, are the final members of the mammalian NMDA receptor gene family, as the complete genome demonstrated. In addition to the molecular and functional diversity arising from the seven subunits, GluN1, GluN2A, GluN2B, GluN2C, GluN2D, GluN3A, and GluN3B, that can comprise an individual NMDA receptor complex, the GluN1 subunit has eight splice variants that can contribute to the functional properties of the receptors (Sugihara et al., 1992; Durand et al., 1992; Hollmann et al., 1993).

NMDA receptors are tetrameric ion channels (Figure 1.1) (Laube et al., 1998; Schorge and Colquhoun, 2003; Ulbrich and Isacoff, 2008; Sobolevsky et al., 2009). GluN1 is an obligate subunit present in all NMDA receptors (Meguro et al., 1992; Monyer et al., 1992; Kutsuwada et al., 1992; Ciabarra et al., 1995; Sucher et al., 1995; Chatterton et al., 2002), and there are likely two GluN1 subunits in each tetramer (Behe et al., 1995; Laube et al., 1998; Ulbrich and Isacoff, 2008). In addition to two GluN1 subunits, NMDA receptor tetramers can contain two of the same type of GluN2 subunit (reviewed by Hollmann, 1999), two different GluN2 subunits (Hollmann, 1999; Brickley et al., 2003; Jones and Gibb, 2005; Brothwell et al., 2008), one GluN2 and one GluN3 subunit (Ciabarra et al., 1995; Sucher et al., 1995; Perez-Otano et al., 2001), or perhaps even two GluN3 subunits (Chatterton et al., 2002; Awobuluyi et al., 2007; Madry et al., 2007, 2010; Smothers and Woodward, 2007, 2009; Cavara et al., 2009). Thus, as

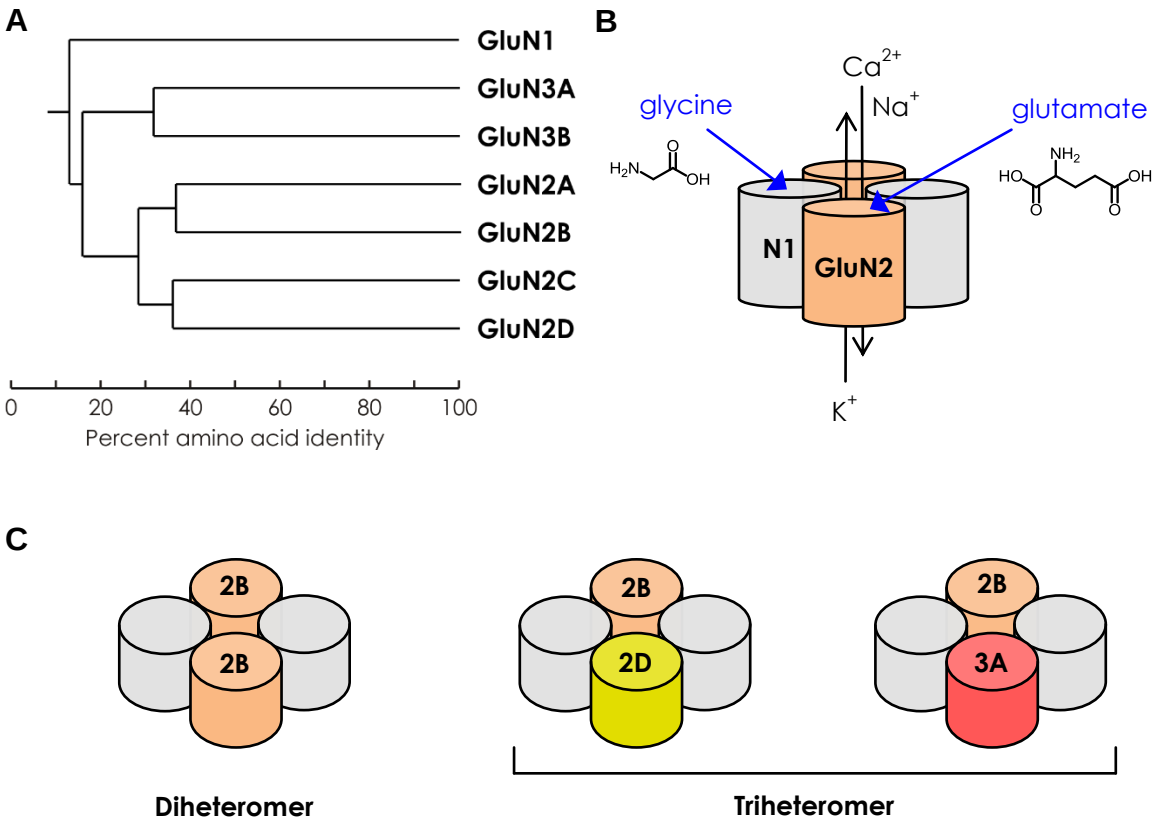

Figure 1.1. NMDA Receptor Subunit Composition

A. A dendrogram showing sequence identity of the subunits comprising NMDA receptors. **B.** A schematic illustrating the composition and key features of NMDA receptor ion channels. NMDA receptors are tetramers that are thought to form in a 1-2-1-2 arrangement with alternating GluN1 (gray) and GluN2 (orange) subunits. The GluN1 subunits bind the co-agonist glycine and the GluN2 subunits bind the co-agonist glutamate. Once all four subunits are bound by agonist, the ion channel pore opens, allowing Na^+, Ca^{2+}, and K^+ ions to permeate. **C.** NMDA receptors can form diheteromers, in which both GluN2 subunits are the same subtype, or triheteromers, in which the GluN2 subunits are different subtypes or in which there is a GluN2 subunit and a GluN3 subunit. GluN1 subunits are thought to be present in all NMDA receptors.

illustrated in Figure 1.1C, NMDA receptor tetramers can be diheteromeric (GluN1/GluN2 or GluN1/GluN3), or triheteromeric (e.g. GluN1/GluN2A/GluN2B, GluN1/GluN2/GluN3, or GluN1/GluN3A/GluN3B). Most studies of recombinant NMDA receptors have focused on diheteromeric receptors, although triheteromeric receptors have been widely observed in the brain (Sheng et al., 1994; Chazot and Stephenson, 1997; Luo et al., 1997; Brickley et al., 2003; Jones and Gibb, 2005; Brothwell et al., 2008; Delaney et al., 2012; Tovar et al., 2013) and may in fact be the majority of neuronal NMDA receptors (Rauner and Köhr, 2011; Gray et al., 2011; Tovar et al., 2013).

Architecture of NMDA Receptors

Each subunit in a tetramer folds into three semi-autonomous domains: an amino-terminal domain (ATD), an agonist-binding domain (ABD), and a transmembrane domain (Figure 1.2). Although high resolution crystallographic data for a tetrameric, membrane-spanning NMDA receptor are lacking, much information about the tertiary and quaternary arrangement of NMDA receptor has been inferred from X-ray crystal structures of isolated ATDs (Karakas et al., 2009, 2011; Farina et al., 2011) and ABDs (Furukawa and Gouaux, 2003; Furukawa et al., 2005; Vance et al., 2011) coupled with the structure of a tetrameric but C-terminal truncated GluA2 AMPA receptor that included the ion channel pore (Sobolevsky et al., 2009). Both the ATD and ABD form bi-lobed clamshell-shaped domains that have sequence and structural homology to bacterial periplasmic amino acid binding proteins. The transmembrane domain consists of three transmembrane helices, called M1, M3, and M4, and a re-entrant pore loop, called M2, that shares sequence and structural homology to the P-loop of potassium channels (Wo and Oswald, 1995; Wood et al., 1995; Kuner et al., 2003). In addition to an ATD, ABD, and transmembrane domain, NMDA receptor subunits have an intrinsically disordered intracellular carboxy-terminal region (Choi et al., 2011, 2013)

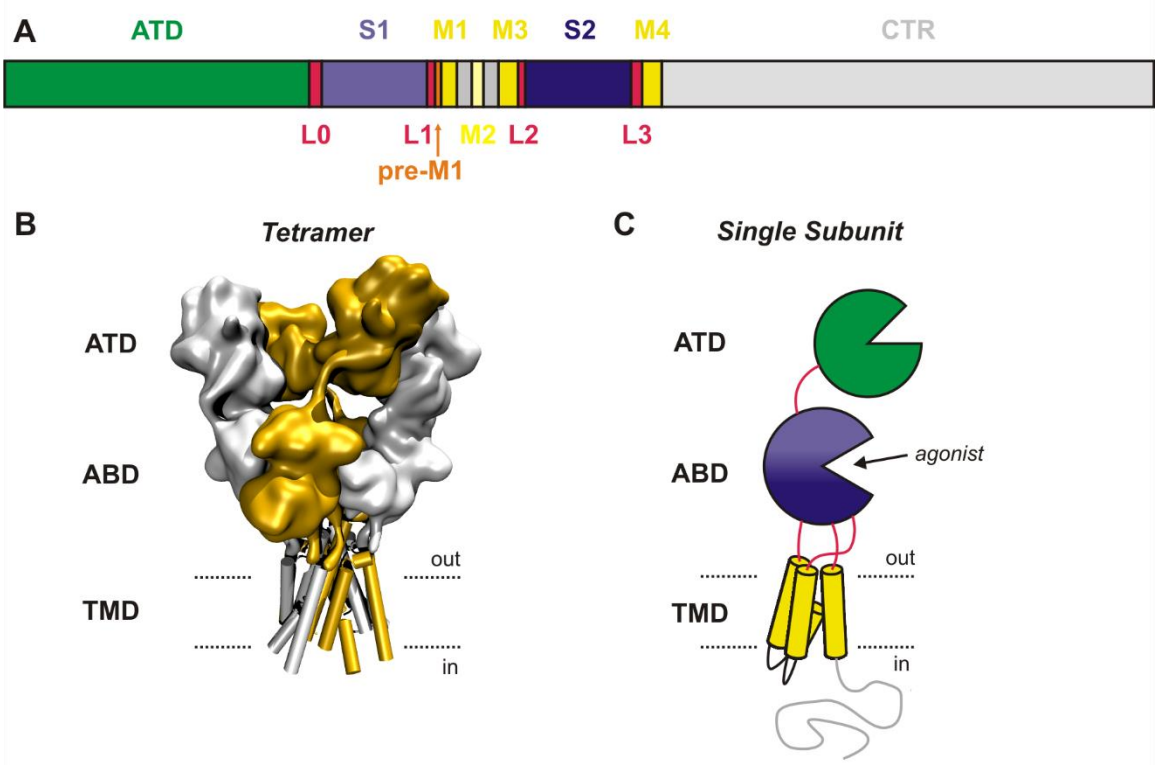

Figure 1.2 NMDA Receptor Architecture

A. NMDA receptor primary structure is depicted in a linear schematic. Regions comprising the main structural features of NMDA receptors are shown and include the amino-terminal domain (ATD), two non-adjacent sequences called S1 and S2 (Stern-Bach et al., 1994) that make up the agonist-binding domain (ABD), a putative pre-M1 helix (Sobolevsky et al., 2009), three transmembrane helices (M1, M3, and M4), a re-entrant pore loop (M2), a carboxy-terminal region (CTR), and the short peptide linkers that connect each region (L0, L1, L2, and L3). **B.** Overall quaternary arrangement of subunits in a glutamate receptor ion channel is shown as a volume representation of the GluA2 AMPA receptor tetrameric X-ray crystal structure (Sobolevsky et al., 2009). GluA2 subunits in a tetramer form two pairs of symmetrically distinct subunit pairs, called A/C (shown in silver) and B/D (shown in orange). Based on biochemical cross-linking, the GluN1 subunits are hypothesized to assemble in a manner similar to the A/C subunits, whereas GluN2 subunits are thought to arrange like the B/D subunits. **C.** A cartoon representation of one GluN2 subunit shows the three semi-autonomous domains, the ATD, ABD, and TMD, and intracellular carboxy-terminal region. The ATD and ABD form bi-lobed clamshell-shaped domains and agonists bind in the cleft between the upper and lower lobes.

following the M4 transmembrane helix that lacks fixed secondary and tertiary structure and is quite large in the case of GluN2 subunits, consisting of about 400-650 amino acids.

Carboxy-terminal region

The carboxy-terminal region is the most diverse region of NMDA receptor subunits, with only 2% sequence identity among the GluN2 subunits. The C-terminal region harbors sites for posttranslational modifications such as palmitoylation (Hayashi et al., 2009; Mattison et al., 2012) and phosphorylation by protein kinase C (Tingley et al., 1993), calcium/calmodulin-dependent protein kinase II (Omkumar et al., 1996), or casein kinase II (Chung et al., 2004), among other kinases (for review see Chen and Roche, 2007). All GluN2 subunits and four GluN1 splice variants (those utilizing exon 22', namely GluN1-3 and GluN1-4) also contain a binding motif for PSD-95 and other PDZ domain-containing proteins (Kornau et al., 1995; Niethammer et al., 1996; Bassand et al., 1999). Although the critical role of the carboxy terminus in normal trafficking of the receptors has been well-established (Standley et al., 2000; Scott et al., 2001; Xia et al., 2001; Chung et al., 2004; Foster et al., 2010; Chen et al., 2012; Chowdhury et al., 2013; Sanz-Clemente et al., 2013), the contribution of the C-terminus to the biophysical and pharmacological properties of the receptor is less clear (Köhr and Seeburg, 1996; Rossi et al., 2002; Puddifoot et al., 2009; Punnakkal et al., 2012; Maki et al., 2012).

Amino-terminal domain

The ATD is also a highly diverse region of NMDA receptors with only 19% sequence identity. The ATDs are locally organized as dimers of GluN1-GluN2 dimers (Lee and Gouaux, 2011; Karakas et al., 2011). Each ATD clamshell-shaped monomer is divided into an upper lobe, called R1, and a lower lobe, called R2. The lower lobe is twisted about 40-50º relative to the upper lobe (Karakas et al., 2009; Farina et al., 2011),

and consequently, the interface between GluN1 and GluN2 monomers in one ATD dimer is asymmetric and mediated by R1-R1 and R1-R2 interactions (Karakas et al., 2011). In all crystal structures of NMDA receptor ATDs, the cleft of the clamshell-shaped monomers is partially closed, despite speculation that closure of this cleft may lead to allosteric regulation of the receptor by modulators (Perin-Dureau et al., 2002; Gielen et al., 2009; Mony et al., 2009). Interestingly, the ATD of NMDA receptors has also been crystallized as a GluN1/GluN1 homodimer (Farina et al., 2011), highlighting the need for more complete structural information to elucidate the architecture of NMDA receptor ATDs, which likely differs from the arrangement in AMPA receptors and may explain how the ATD controls NMDA receptor function (Gielen et al., 2009; Yuan et al., 2009; Zhu et al., 2013).

In contrast to the ATD and C-terminal region, the ABD and the transmembrane domain are quite conserved, having about 63-75% identity. In the primary sequence of each subunit, the ABD is composed of two non-adjacent stretches of about 150 amino acids each (Kuryatov et al., 1994; Stern-Bach et al., 1994; Anson et al., 1998). These two segments, called S1 and S2 (Stern-Bach et al., 1994), are separated by two transmembrane helices, M1 and M3, and the re-entrant pore loop, called M2. Following the S2 region of the ABD is the third transmembrane helix, M4. By replacing M1, M2, and M3 with a glycine-threonine linker, soluble proteins of the S1-S2 region could be generated that allowed crystallographic studies of the ABD (Kuusinen et al., 1995, 1995; Chen and Gouaux, 1997).

Agonist binding in NMDA receptors

The ABD monomers of GluN1 (Furukawa and Gouaux, 2003), GluN2A (Furukawa et al., 2005; Hansen et al., 2013), and GluN2D (Vance et al., 2011) have been crystallized as have ABD dimers of GluN1/GluN2 (Furukawa et al., 2005). These

crystal structures revealed the molecular basis for agonist recognition and discrimination at NMDA receptors and have suggested a structural mechanism for coupling agonist binding to ion channel gating. Each ABD monomer forms a bi-lobed clamshell-shaped structure with an upper lobe termed D1 and a lower lobe termed D2. Glycine and glutamate bind the ABD of GluN1 and GluN2, respectively, in the cleft between D1 and D2. Not surprisingly, the residues directly interacting with agonist are highly conserved (Anson et al., 1998; Laube et al., 2004; Chen et al., 2005; Kinarsky et al., 2005; Hansen et al., 2005; Erreger et al., 2007). The α-carboxyl group of both glycine and glutamate interact with an Arg residue in the upper lobe of GluN1 and GluN2, respectively, which is conserved in all glutamate receptor ion channels. This interaction is the first step in a so-called Venus flytrap mechanism of activation, in which the agonist first makes low-affinity interactions with the upper D1 lobe. This interaction then allows subsequent higher affinity binding as the lower lobe moves upward to interact with the γ-carboxyl group of the agonist and the interaction with both the D1 and D2 lobes stabilizes the closed-cleft conformation (Mano et al., 1996; Laube et al., 1997; Abele et al., 1999, 2000).

The selectivity of GluN1 for glycine over glutamate can be explained by the hydrophobic environment created by Val689 (which is a Thr in GluN2A) and the steric barrier formed by Trp731 (a Tyr in GluN2A), both of which prevent binding of the γ-carboxyl group of L-glutamate to GluN1. The selectivity of N-methyl-D-aspartate for GluN2 subunits over other glutamate receptor ion channels arises from the presence of Asp731 in the binding pocket of GluN2A subunits instead of a glutamate residue, which occupies the homologous position in AMPA and kainate receptors. Asp731 in GluN2A is a methylene group shorter than the homologous glutamate residue in AMPA and kainate receptors, which thereby creates space in the GluN2A binding pocket for the N-methyl

group of NMDA and eliminates the steric clash that occurs between the N-methyl group and the glutamate residue in the binding pockets of AMPA and kainate receptors (Furukawa et al., 2005).

ABD cleft closure may contribute to NMDA receptor gating

The GluN1/GluN2 ABD dimer is arranged in a 'back-to-back' fashion, in contrast to the ATD dimers. Agonist-bound structures of NMDA receptor ABDs revealed a closed-cleft conformation, where the lower lobe of the agonist binding domain is in closer apposition to the upper lobe. Because the ABD dimer is formed by an interface between the upper D1 lobes, it is plausible that, in an intact receptor, binding of agonist leads to movement of the lower D2 lobe towards the upper D1 lobe and away from the membrane bilayer, while the upper D1 lobe remains relatively stationary, being stabilized by interactions at the ABD dimer interface. By virtue of the peptide linkers connecting the D2 lobe to the M1, M3 and M4 transmembrane helices, movement of the D2 lobe away from the lipid bilayer would thus separate the transmembrane helices away from each other thereby allowing the ion channel pore to open. However, data that could support this mechanism remains ambiguous. While the competitive antagonist DCKA stabilizes an open-cleft conformation of GluN1 (Furukawa and Gouaux, 2003), partial agonists at the GluN1 subunit induce a similar degree of domain closure as full agonists (Furukawa and Gouaux, 2003; Inanobe et al., 2005; Rambhadran et al., 2011). However, an intermediate conformational state with partial GluN1 agonists has been observed in molecular dynamics simulations (Ylilauri and Pentikäinen, 2012). At the GluN2 subunit, graded ABD cleft closure has been reported with partial agonists in full-length NMDA receptors using distances between residues in the ABD calculated from luminescence resonance energy transfer lifetimes (Rambhadran et al., 2011) and stabilizing the ABD in a closed-cleft conformation using engineered disulfide bonds

spanning the upper and lower lobes support a correlation between cleft stability and receptor activation (Blanke and VanDongen, 2008; Kussius and Popescu, 2010). However, crystal structures of the GluN2A and GluN2D ABDs in complex with partial agonists showed no discernible difference when compared to glutamate-bound structures (Hansen et al., 2013). The lack of correlation between the degree of ABD cleft closure and the extent of receptor activation for NMDA receptors is a departure from AMPA receptors, at which competitive antagonists stabilize the ABD in an open cleft conformation and partial agonists induce smaller degrees of ABD cleft closure than full agonists (Armstrong and Gouaux, 2000; Jin et al., 2003; Hogner et al., 2003; Lunn et al., 2003; Holm et al., 2005; Nielsen et al., 2005; Frandsen et al., 2005; Kasper et al., 2006).

Quaternary structure and subunit arrangement

The ATDs and ABDs of NMDA receptors are organized as dimers of GluN1/GluN2 dimers (Furukawa et al., 2005; Lee and Gouaux, 2011; Karakas et al., 2011), however the arrangement of these dimer pairs in an intact, functional receptor remains unclear. Based on sequence and structural homology, NMDA receptors are thought to share many features with AMPA receptors, so it is worth considering the quaternary arrangement of AMPA receptors, for which crystallographic data exists for a tetrameric receptor (Sobolevsky et al., 2009). In the tetrameric GluA2 crystal structure, individual subunits arrange in dimer-of-dimers, which leads to an overall two-fold symmetry at the level of the ABD and ATD and gives rise to two pairs of conformationally distinct subunits, denoted A/C and B/D, in a tetrameric complex (Sobolevsky et al., 2009). In GluA2 AMPA receptors, the A/B and C/D subunits form dimers at the level of the ATD whereas at the ABD, the A/D and B/C subunits form dimer pairs. Hence, the ATD and ABD of a single subunit do not stack on top of each other,

but rather each subunit crosses over between the ATD and the ABD. Additionally, these distinct subunit conformations cause a symmetry mismatch between the extracellular region of the receptor, which has overall two-fold rotational symmetry, and the ion channel pore, which in the membrane-spanning GluA2 structure has four-fold symmetry (Sobolevsky et al., 2009). The symmetry mismatch is resolved by a set of three peptides linking the ABD with the TMD within each subunit: the S1-M1, M3-S2, and S2-M4 linkers.

Assembly of NMDA receptors from two GluN1 subunits and two GluN2 subunits creates two possible tetrameric arrangements: the 1-1-2-2 arrangement in which the two GluN1 subunits are adjacent and the two GluN2 subunits are adjacent or the 1-2-1-2 arrangement made of alternating pairs of GluN1-GluN2 subunits. Initial studies using electrophysiological recordings of engineered tandem NMDA receptor subunits suggested a 1-1-2-2 arrangement (Schorge and Colquhoun, 2003). Then, studies using Forster resonance energy transfer measurements between GluN1 and GluN2 suggested that GluN1-GluN1 homodimers and GluN2-GluN2 homodimers could form, consistent with a 1-1-2-2 arrangement (Qiu et al., 2005). Elucidation of the GluA2 tetrameric structure provided hope that these studies would be confirmed, as homology models of NMDA receptors in either a 1-1-2-2 or 1-2-1-2 arrangement based on the GluA2 structure could direct engineering of cysteines for biochemically cross-linking that would differentiate between these two arrangements. However, in contrast to those initial experiments, biochemical crosslinking of engineered cysteine residues in NMDA receptors suggested that a 1-2-1-2 arrangement occurs in NMDA receptors (Sobolevsky et al., 2009; Salussolia et al., 2011b; Riou et al., 2012). Another study using luminescence resonance energy transfer lifetimes to estimate distances between residues in the ABD of GluN1 and GluN2A further suggested a 1-2-1-2 arrangement, although the receptors used in that study lacked ATDs (Rambhadran et al., 2010).

However, a recent report using atomic force microscopy of purified GluN1/GluN2A receptors tagged with antibodies showed that receptor complexes were tagged by either one or two antibodies (Balasuriya et al., 2013). When tagged by two antibodies, the distribution of angles between bound antibodies had a single peak at about 90º. This distribution differed from that of labelled AMPA receptors, which showed two peaks at ~90º and ~180º, and suggests a 1-1-2-2 arrangement of NMDA receptor subunits. Thus, the conclusions of seven studies explicitly probing NMDA receptor quaternary arrangement (Schorge and Colquhoun, 2003; Qiu et al., 2005; Sobolevsky et al., 2009; Rambhadran et al., 2010; Salussolia et al., 2011b; Riou et al., 2012; Balasuriya et al., 2013) favor an alternating 1-2-1-2 arrangement by a tally of 4 to 3. It will be interesting to see where the crystal structure of an NMDA receptor tetramer weighs in on this question and whether the stoichiometry and organization varies for the different GluN2 subunits; however even the crystal structure will provide only a snapshot of the complexity of NMDA receptor assembly.

Ion channel pore

The ion channel pore of NMDA receptors shares sequence and structural homology to the pore region of voltage-gated Na^+, K^+, and Ca^{2+} channels, all of which have two transmembrane helices separated by a membrane re-entrant loop (Wo and Oswald, 1995; Wood et al., 1995; Doyle et al., 1998; Catterall, 2000a, 2000b; Kuner et al., 2003; Zhorov and Tikhonov, 2004; Sobolevsky et al., 2009). NMDA receptors, however, have an additional third transmembrane helix, called M4, that is critical for normal assembly and trafficking of the receptor (Schorge and Colquhoun, 2003; Salussolia et al., 2011a; Kaniakova et al., 2012), and the membrane topology of NMDA receptors is inverted compared to the voltage-gated channels. Additionally, NMDA receptors do not discriminate among ions with a high degree of selectivity, being

permeable to Na^+, K^+, and Ca^{2+} as well as other divalent cations such as Mg^{2+} and organic ions. Thus, much has been learned about the NMDA receptor pore by analogy to K^+ channels, but a more complete understanding of NMDA receptor gating and permeation must account for their differing structure and function.

While a detailed atomic view of the NMDA receptor pore that explains its ion selectivity remains elusive, biophysical studies have shown that the narrow constriction of the pore, thought to be formed by crossing of adjacent M3 transmembrane helices (Sobolevsky et al., 2009), is located about midway through the lipid bilayer (Zarei and Dani, 1995; Villarroel et al., 1995; Wollmuth et al., 1996; Sobolevsky et al., 2002, 2003). Although a clear pathway for ions to access the pore was not present in the tetrameric GluA2 structure, there appears to be an extracellular vestibule in NMDA receptors (Jahr and Stevens, 1993; Paoletti et al., 1995; Premkumar and Auerbach, 1996; Sharma and Stevens, 1996) composed of a DRPEER sequence in the M3-S2 linker of GluN1 (Watanabe et al., 2002), that contributes to the high Ca^{2+} permeability (Burnashev et al., 1995; Wollmuth et al., 1996; Schneggenburger, 1996, 1998; Iino et al., 1997) of NMDA receptors. Moreover, mutagenesis and substituted cysteine accessibility studies have revealed that the M2 region lines the pore pathway and asparagine residues at the tip of the M2 loop controls Ca^{2+} permeability and block by extracellular Mg^{2+} (Kuner et al., 1996; Wollmuth et al., 1998). Interestingly, a single residue in the cytosolic half of the GluN2 M3 helix, Ser632 in GluN2A corresponding to Leu657 in GluN2D, controls relative Ca^{2+} permeability as well as other pore properties that differ between GluN2 subunits such as subconductance levels and Mg^{2+} block (Siegler Retchless et al., 2012). Mutation of Ser632 in GluN2A to leucine switched the Mg^{2+} inhibition, Ca^{2+} permeability and single-channel conductance of GluN2A to be more like the pore properties of GluN2D.

Despite the high degree of sequence and structural homology, NMDA receptors exhibit unique pore properties compared to K^+ channels and even AMPA and kainate receptors. For example, K^+ channels and GluA2 AMPA receptors are homomeric proteins and hence the transmembrane helices and pore loop from each subunit contribute equally to the pore. Already there is evidence that GluN1 and GluN2 subunits contribute unequally to pore properties (Sobolevsky et al 2007). Additionally, a homology model of the NMDA receptor pore based on the GluA2 membrane-spanning tetrameric structure did not reveal interaction of the GluN2 M3 helix with the p-loop of an adjacent GluN1 subunit that explained how GluN2A Ser632 primarily controlled GluN2 subunit-dependent pore properties (Siegler Retchless et al., 2012). Thus, a molecular understanding of ion permeation and block in NMDA receptors awaits elucidation of an atomic resolution structure.

NMDA Receptor Gating

Neuronal communication between pre- and postsynaptic neurons begins with release of neurotransmitter into an optimally designed 20 nm cleft (Savtchenko and Rusakov, 2007). Binding of the neurotransmitter to its receptor on the postsynaptic neuronal membrane converts that chemical signal into an electrical one. Unlike other ligand-gated ion channels such as the nicotinic acetylcholine receptor (Colquhoun and Sakmann, 1981, 1985), glycine receptors (Beato et al., 2002, 2004; Burzomato et al., 2004), 5-HT_3 receptors (Mott et al., 2001), and AMPA receptors (Rosenmund et al., 1998; Jin et al., 2003), NMDA receptors cannot open their ion channel pore until all four agonist binding sites, one on each subunit, are occupied. This conclusion was first reached on the basis of kinetic models of activation which accurately described whole-cell responses to synaptic-like concentration waveforms of glutamate (Benveniste and Mayer, 1991; Clements and Westbrook, 1991). Further support of the idea that NMDA

receptors must be fully occupied by agonist to open comes from observations in single channel recordings in which two agonist concentration-dependent phenomena that would be expected if partially liganded receptors could open were not observed (Schorge et al., 2005). First, mean open time distributions should exhibit an increased proportion of shorter open durations at low agonist concentrations, as partially liganded receptors, which would occur with greater frequency at low agonist concentrations, would stay open for a shorter time (or re-open less often) than fully bound receptors. Second, correlations between neighboring open and shut times should diminish at high agonist concentrations, as the proportion of partially bound receptors, which give rise to shorter duration openings that are followed by long shut times, decreases. Neither of these two phenomena were observed with low concentrations of either glutamate or glycine, suggesting NMDA receptors must be bound to four agonists before opening.

X-ray crystal structures of the ABDs of GluN1,GluN2, and GluN3 bound to competitive antagonists and full and partial agonists revealed that binding of agonist induces or at least stabilizes a closed-cleft conformation of the bi-lobed clamshell-shaped ABDs (Furukawa and Gouaux, 2003; Inanobe et al., 2005; Furukawa et al., 2005; Yao et al., 2008; Vance et al., 2011). How exactly closure of the ABD cleft relates to opening of the ion channel pore is still unclear. The M3 transmembrane helix has been implicated in conformational changes that couple agonist binding to channel gating because naturally-occurring and engineered mutations in this region cause spontaneously active receptors or receptors that are locked open after modification by cysteine-modifying methanethiosulfonate (MTS) reagents (Kohda et al., 2000; Jones et al., 2002; Yuan et al., 2005; Chang and Kuo, 2008). Additionally, the M3 helix seems to undergo large movements during gating (Sobolevsky et al., 2002; Dai and Zhou, 2013) An interesting inconsistency with the idea of the M3 helix being a critical regulatory element of gating, rather than simply a structural requirement, is that the M3 helix is

almost 100% conserved across the GluN2 subunits (a notable exception is the GluN2 S/L site Siegler Retchless et al., 2012). How, then, do gating properties such as mean open time, open probability, deactivation time course, and desensitization time course differ so widely between the GluN2 subunits?

Unfortunately, crystallographic data do not offer a full explanation for these differences because the overall conformations of GluN2A and GluN2D subunits bound to glutamate were quite similar (Vance et al., 2011; Hansen et al., 2013), only differing in the hinge loop region at the backside of the ABD that explains some of the differences in deactivation time course. A partial answer arises, however, from studies of chimeric NMDA receptors that swapped the ATD and the linker between the ATD and ABD across the GluN2 subunits (Gielen et al., 2009; Yuan et al., 2009). These investigations revealed that the ATD of GluN2A and GluN2B exert positive effects on NMDA receptor gating, enhancing channel open probability and accelerating deactivation, while the ATDs of GluN2C and GluN2D exert negative effects, greatly diminishing channel open probability. Moreover, the ATDs control glycine and glutamate potency. Thus, the ATD is a critical determinant of the pharmacological and kinetic properties of NMDA receptors.

How the ATD is allosterically coupled to the ion channel gate is still an open question. The overall architecture of full-length NMDA receptors will no doubt be critical in answering this question. A limitation of the available crystal structures of NMDA receptors is that the functional domains (i.e. ATD and ABD) were crystallized in isolation, so it is unclear how these domains are organized in an intact receptors. The local tertiary arrangement of these domains is probably correct, given that the domains in the crystal structure of GluA2 tetrameric but C-terminal truncated receptors were similar to the crystal structures of the isolated domains (Sobolevsky et al., 2009). However, arrangement of these domains in a functional NMDA receptors likely differs from the

quaternary arrangement in AMPA receptors (e.g. see the discussion on 1-1-2-2 vs. 1-2-1-2 arrangement, above). Nonetheless, a model explaining how the ATD regulates NMDA receptor gating has been proposed based on mutant receptors that alter the efficacy of allosteric antagonists acting at the ATD (Gielen et al., 2008). In this model, binding of antagonists to the ATD leads to a rearrangement of the ABD dimer interface. Rearrangement of the ABD dimer interface then leads to uncoupling of the ion channel gate from agonist binding because the tension caused by agonist binding is relieved by breakdown of the dimer interface rather than opening of the ion channel pore.

Recent work has focused on the linkers between the ABD and TMD (S1-M1, M3-S2 and S2-M4) as critical determinants of gating (Talukder and Wollmuth, 2011; Dai and Zhou, 2013; Kazi et al., 2013). These linkers seem to be an obvious candidate for coupling the large conformational change that occurs in the ABD upon agonist binding to channel gating because they are directly attached to the lower lobe of the ABD that pivots about 20º and expands about 5.5 Å upon agonist binding (Armstrong et al., 2006). Indeed, rearrangement of the peripheral M1 and M4 linkers upon channel gating has been suggested to occur based on kinetic modeling of receptors with engineered cross-links between the linkers (Kazi et al., 2013) or on molecular dynamics simulations (Dai and Zhou, 2013). The exact nature of the rearrangement of ABD-TMD linkers upon gating remains to be determined, but could involve rigid movements that pull the transmembrane helixes apart or perhaps more subtle changes such as rotation of helices. Interestingly, comparing the NMDA receptor pore to the open pore of MthK K^+ channels (Jiang et al., 2002a) suggests that a large kink or bend in the M3 helix of NMDA receptors would occur in the open state compared to the closed state. If the M3 helix kinks then it will require movement of both the pre-M1 helix and the top of the M4 helix.

A structure of the pore region of NMDA receptors will be invaluable for unraveling the details of NMDA receptor activation and will undoubtedly stimulate new ideas about NMDA receptor gating. New structural information together with molecular dynamics simulations may hold promise for achieving the lofty goal of linking conformational changes seen in static structures to the dynamic states proposed in kinetic mechanisms of NMDA receptor gating.

NMDA Receptor Function

A landmark discovery in neuroscience was that NMDA receptors are blocked at resting membrane potentials by the extracellular divalent cation Mg^{2+} (Evans et al., 1977; Ault et al., 1980; Nowak et al., 1984; Mayer et al., 1984). Voltage-dependent Mg^{2+} block allows NMDA receptors to serve as coincident detectors meaning they will only be permeable to ions when the membrane has been sufficiently depolarized (to a transmembrane potential of around -40 mV) and simultaneously glutamate is released. These conditions are thought to be met in highly active synapses, where previous excitatory postsynaptic potentials, mediated for example by AMPA receptors, or back-propagating action potentials have depolarized the postsynaptic membrane and hence subsequent synaptic release of glutamate can open the NMDA receptor pore.

The utility of coincidence detection is augmented by another critical property of NMDA receptors: Ca^{2+}-permeability (MacDermott et al., 1986; Mayer and Westbrook, 1987; Ascher and Nowak, 1988). Thus, activation of NMDA receptors allows entry of Ca^{2+} into the postsynaptic neurons. Ca^{2+} entry through NMDA receptors most notably activates Ca^{2+}/calmodulin-dependent protein kinase II (CaMKII) (Pettit et al., 1994; Lledo et al., 1995; Giese et al., 1998; Shen and Meyer, 1999; for review see Lisman et al., 2012), but may also activate protein kinase C (PKC) (Lovinger et al., 1987; Malinow et al., 1989; Wang and Feng, 1992; Hvalby et al., 1994; Sun and Liu, 2007; Luu and

Malenka, 2008), protein kinase A (PKA) (Chetkovich and Sweatt, 1993; Roberson and Sweatt, 1996), Src (Lu et al., 1998; Huang et al., 2001), nitric oxide synthase (NOS) (Sattler et al., 1999), phosphoinositide 3-kinase (PI3K) (Waxman and Lynch, 2005; Kim et al., 2011), superoxide (Lafon-Cazal et al., 1993) via NADPH oxidase (NOX-2) (Brennan et al., 2009) among myriad other possible effectors (see e.g. Sanes and Lichtman, 1999). Activation of these pathways initiates signaling events that are critical for longer-term activity-dependent changes in the strength of synaptic communication and for structural changes in synaptic connections that occur, for example, during development.

The voltage-dependent block of NMDA receptors by Mg^{2+} coupled with their Ca^{2+} permeability gives a molecular explanation for the phenomenon of long-term potentiation (Bliss and Gardner-Medwin, 1973; Bliss and Lømo, 1973), which was first observed as a long-lasting (hours to days) increase in the efficacy of synaptic transmission and excitability of dentate granule cells of the hippocampus following repetitive stimulation of the perforant path, but has since been observed under diverse stimulus patterns and in numerous brain regions (Malenka and Nicoll, 1999) and is thought to be a cellular correlate of learning and memory (Bliss and Collingridge, 1993). Block of NMDA receptors by Mg^{2+} would be relieved in active synapses, allowing Ca^{2+} entry into those neurons, which could trigger cellular events such as activation of CaMKII and phosphorylation of AMPA receptors that would lead to increases in synaptic strength. Moreover, the coincidence detection of NMDA receptors arms neurons with a mechanism for implementing the “Neurophysiological Postulate” proposed by Hebb (1949):

> *“When an axon of cell A is near enough to excite cell B and repeatedly or persistently takes part in firing it, some growth process or metabolic*

change takes place in one or both cells such that A's efficiency, as one of the cells firing B, is increased."

Further importance of voltage-dependent Mg^{2+} block to NMDA receptor function was highlighted recently by identification of a *de novo GRIN2A* mutation in a patient with early-onset epileptic encephalopathy (Endele et al., 2010). The mutation caused conversion of a critical asparagine in M2 to lysine ($GluN2A^{N615K}$) and NMDA receptors harboring this substitution were insensitive to block by Mg^{2+}, which could lead to over-activation of NMDA receptors and thereby underlie the severe seizures, myoclonic twitches, and abnormal EEG observed in the patient.

Another unique feature of NMDA receptors is that, although they mediate the actions of the neurotransmitter glutamate released into the synaptic cleft, they require glycine to bind as a co-agonist before they are activated (Johnson and Ascher, 1987; Kleckner and Dingledine, 1988). Cloning of the subunits comprising NMDA receptors allowed mutagenesis and crystallographic studies that demonstrated glycine binds the GluN1 subunit (Kuryatov et al., 1994; Hirai et al., 1996; Furukawa and Gouaux, 2003) and glutamate binds the GluN2 subunit (Laube et al., 1997; Anson et al., 1998; Furukawa et al., 2005). Moreover, NMDA receptors cannot open unless all four agonist binding sites are occupied (Schorge et al., 2005).

The requirement of glycine binding for activation provides another mechanism for controlling NMDA receptor function, namely by regulating the concentration of glycine at sites of receptor activation (e.g. synaptic versus extrasynaptic), perhaps both tonically and in an activity-dependent manner. Indeed, the glycine potency of NMDA receptors varies 10-fold depending on which GluN2 subunit comprises the receptor; the EC_{50} of glycine is 1.1 μM at GluN2A, 0.72 μM at GluN2B, 0.34 μM at GluN2C, and 0.13 μM at GluN2D (Chen et al., 2008b). Hence each NMDA receptor subtypes could be differentially sensitive to the concentration of glycine (Kalbaugh et al., 2009). Shortly

after the discovery that glycine potentiated NMDA receptor responses (Johnson and Ascher, 1987), glycine was reported to enhance NMDA receptor-mediated EPSPs (Thomson et al., 1989), but not NMDA-evoked depolarizations (Fletcher and Lodge, 1988), suggesting perhaps that glycine concentrations in the synapse were sub-saturating at NMDA receptors, but were saturating outside the synapse. Subsequent studies further supported the finding that glycine concentrations in the synapse are subsaturating (Vyklický et al., 1990; Abe et al., 1990; Collins, 1990; Thiels et al., 1992; Lukasiewicz and Roeder, 1995; Wilcox et al., 1996; Kalbaugh et al., 2009).

Although free glycine concentrations in the cerebrospinal fluid have been estimated at 8-20 μM (Ferraro and Hare, 1985; Matsui et al., 1995), an active uptake mechanism for glycine mediated by glycine transporters exists, with GlyT1 playing a role at glutamatergic synapses expressing NMDA receptors and GlyT2 taking up glycine at glycinergic inhibitory synapses (Zafra et al., 1995b, 1995a; Aragón and López-Corcuera, 2003; Cubelos et al., 2005; Harsing Jr. and Matyus, 2013). Furthermore, disruption of GlyT1 function by antagonists or genetic knockdown alters NMDA receptor-mediated synaptic transmission, for example by preventing glycine potentiation of NMDA receptors responses (Berger et al., 1998; Bergeron et al., 1998; Chen et al., 2003; Kinney et al., 2003; Tsai et al., 2004; Martina et al., 2005; Reed et al., 2009). Additionally, a release mechanism for glycine mediated by Asc-1 transporters has been recently reported (Rosenberg et al., 2013). Thus, glycine levels at the synapse seem to be tightly regulated and measurements of glycine concentrations in the CSF may not reflect the glycine concentration present at NMDA receptors.

In addition to glycine, D-serine is an endogenous coagonist at the GluN1 subunit of NMDA receptors (Mothet et al., 2000; Panatier et al., 2006; Martineau et al., 2006; Wolosker, 2006). While the identity of the coagonist most certainly varies in a synapse-specific manner, recent work advances a more provocative view that D-serine is the

coagonist at synapses whereas glycine is the coagonist at extrasynaptic locations (Papouin et al., 2012). In addition, coagonist concentration levels may be regulated by certain patterns synaptic activity (Li et al., 2009) and the identity of the coagonist acting at NMDA receptors may switch depending on synaptic activity (Li et al., 2013). A more active regulation of the NMDA receptor co-agonist is therefore emerging, which could allow more specific targeting of certain populations of NMDA receptors in disease states, for example synaptic versus extrasynaptic or NMDA receptors, or only those receptors involved in certain patterns of activity.

NMDA Receptors in Neurological and Psychiatric Disorders

Although the Ca^{2+} permeability of NMDA receptors allows synaptic transmission to couple to cellular signaling cascades under physiological conditions, under pathophysiological conditions such as stroke, ischemia, or traumatic brain injury, it can trigger a cell death cascade termed excitotoxicity (Olney, 1969; Choi, 1987, 1988; Choi et al., 1987; Rothman and Olney, 1987), which can lead to neuronal cell death that is thought to exacerbate the injury and symptoms observed in stroke, ischemia, traumatic brain injury, and neurodegenerative disorders (Dirnagl et al., 1999; Mattson, 2003; Arundine and Tymianski, 2004). The observation that glutamate concentrations in the brain dramatically increased after ischemia and edema in animals (Benveniste et al., 1984; Globus et al., 1988; Baethmann et al., 1989; Hillered et al., 1989; Nilsson et al., 1990; Adachi et al., 1995; Qureshi et al., 2003) and humans (Bondoli et al., 1981; Robertson et al., 1988; Persson and Hillered, 1992; Baker et al., 1993; Hamberger et al., 1995; Kanthan et al., 1995; Säveland et al., 1996; Persson et al., 1996; Yamamoto et al., 1999; Wagner et al., 2005; Srinivasan et al., 2005) spurred the hypothesis that elevated glutamate may mediate the neuronal death following stroke or traumatic brain injury. The concomitant finding that NMDA receptor antagonists significantly limited neuronal

loss following stroke and traumatic brain injury in animal models (Simon et al., 1984; Ozyurt et al., 1988; Novelli et al., 1988; Mcintosh et al., 1989; Faden et al., 1989; Swan and Meldrum, 1990; Lipton and Rosenberg, 1994; Mody and MacDonald, 1995; Block and Schwarz, 1996) prompted intense development of NMDA receptor antagonists for use in the neurological diseases.

Unfortunately all of the antagonists that were pursued in clinical trials for stroke and traumatic brain injury failed. Several reasons that led to failure of NMDA receptor antagonists in clinical trials have been identified by post-hoc analyses (Morris et al., 1999; Dawson et al., 2001; Danysz and Parsons, 2002; Gladstone et al., 2002; Ikonomidou and Turski, 2002; Muir, 2006; Kalia et al., 2008). These include (1) that on-target actions of NMDA receptors likely limit the dose of antagonists below the dose which would maximize the therapeutic benefits in neurological disorders, (2) a limited time window (a few hours) after injury in which antagonists will be effective, (3) a complex molecular pathogenesis including multiple pathways that lead to neuronal loss following injury, (4) the lack of quantifiable endpoints, and (5) poorly defined patient populations in the clinical trials. The latter two problems are likely to be solved by improved clinical trial design and management. The second limitation may also be overcome as advances in clinical trial design have shortened the time to deliver therapeutics after injury (Saver, 2013).

The first two problems highlight the idea that NMDA receptors are a double-edged target for stroke, traumatic brain injury, and possibly all disorders in which they are implicated because dysfunction of some NMDA receptors contributes to disease progression or detrimental endophenotypes, but attempts to correct dysfunctional receptors simultaneously disrupts normal NMDA receptor function in regions of the brain unaffected by the disease. This disruption of normal function leads to undesired consequences such as dissociated, psychotomimetic effects and limits the therapeutic

window for NMDA receptor antagonists. Thus, successfully targeting of NMDA receptors for therapeutic intervention will require innovative approaches, such as mechanistic-based inhibitors that preferentially inhibit overactive compared to normally functioning receptors. For example, new classes of NMDA receptor antagonists (e.g. QNZ46; Hansen and Traynelis, 2011; and DQP-1105; Acker et al., 2011, 2013) that require glutamate to bind the receptor before they can inhibit responses could inhibit NMDA receptors more at highly active synapses where glutamate is released more frequently.

At the same time that overactivation of NMDA receptors was recognized as mediating excitotoxicity and cell death following CNS injury, underactivation of NMDA receptors was being appreciated as a contributing factor to symptoms of schizophrenia. By the early 1960s, it was recognized that overdose of the anesthetic phencyclidine (PCP, Sernyl) led to clinical symptoms that were indistinguishable from those in schizophrenia including positive, negative, and cognitive symptoms (Luby et al., 1959; for reviews see Coyle, 2012; Domino and Luby, 2012). The discovery that PCP inhibits NMDA receptors in 1983 (Anis et al., 1983) fueled research into the link between NMDA receptors and schizophrenia. Subsequent work showed that other NMDA receptor channel blockers including MK-801 and ketamine could reproduce the full range of symptoms associated with schizophrenia when given to healthy individuals (Javitt and Zukin, 1991; Krystal et al., 1994) and to date, all compounds acting at the PCP site on NMDA receptors induce psychoses in humans (Moghaddam and Javitt, 2012).

Complex alterations in NMDA receptor expression at both the mRNA and protein level occur in human schizophrenic patients (Akbarian et al., 1996; Humphries et al., 1996; Woo et al., 2004; Makino et al., 2005; Kristiansen et al., 2007) and in PCP-treated rats (Lindahl and Keifer, 2004). Genetic linkage studies have shown a positive association between GluN1 (Begni et al., 2003) and GluN2B polymorphisms and

schizophrenia (Qin et al., 2005; Martucci et al., 2006; Allen et al., 2008). Additional components of the glutamatergic system including those handling production of the GluN1 co-agonist D-serine are altered in schizophrenia (Javitt, 2007; Labrie et al., 2009; Habl et al., 2009; Labrie and Roder, 2010). Further, schizophrenic patients exhibit deficits in mismatch negativity, an event-related potential indicating brain function at the level of auditory cortex that depends on NMDA receptor-mediated currents (Javitt et al., 1993, 1996; Näätänen and Kähkönen, 2009). Together these observations suggest that hypofunction of the NMDA receptor system might directly contribute to schizophrenic symptoms in patients.

Pharmacology of NMDA Receptors

Over three decades ago, the discovery of D-APV (Evans et al., 1982) and, a few years later, MK-801 (Wong et al., 1986) as antagonists with strong selectivity for NMDA receptors over AMPA and kainate receptors, provided neuroscientists studying physiology, behavior, development, and neurological disease powerful tools with which to dissect the role NMDA receptors play in a myriad of processes. Use of both competitive antagonists and NMDA receptor channel blockers provided key insights about the identity of receptors generating the excitatory postsynaptic current, and the role of various glutamate receptors in synaptic plasticity, neuronal death during CNS injury, and developmental biology. During the following dozen or so years, antagonists acting at the glycine binding site, the glutamate binding site, the channel pore, the amino terminal domain, and a region of the ligand binding domain encoded by the S2 region of the cDNA (e.g. neurosteroids) were described (Figure 1.3 and Table 1.1).

Discovery of the antihypertensive agent ifenprodil two decades ago as a subunit-selective antagonist for NMDA receptors containing the GluN2B subunit (Williams, 1993) was another watershed event in NMDA receptor pharmacology, offering the promise that

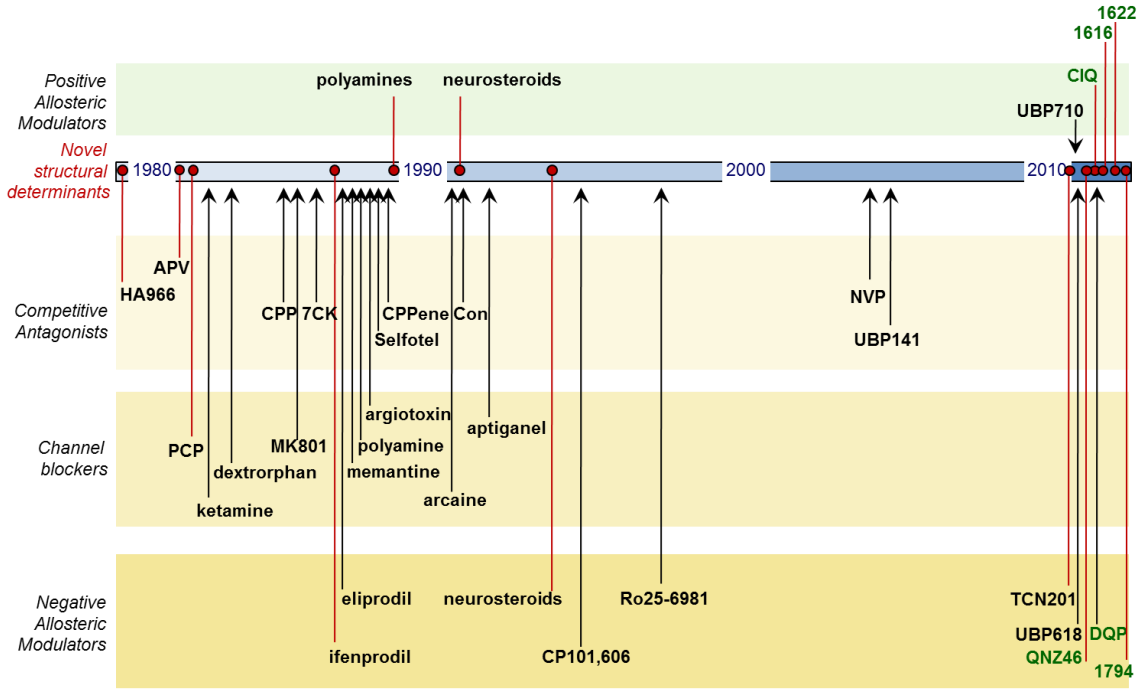

Figure 1.3 Discovery of NMDA Receptor Ligands

An active period for discovery of new ligands as well as new sites and mechanisms of action on the NMDA receptor occurred following the description of D-APV as a highly selective competitive NMDA receptor antagonist (Evans et al., 1982). The pace of discovery slowed over the next dozen years, with relatively few new prototypical compounds being described between 1995 and 2009. In 2010, however, discovery of new ligands accelerated as a number of new compounds acting on the receptor with unique structural determinants were reported. The figure provides a time line illustrating several different ligand classes acting by different mechanisms to inhibit or potentiate NMDA receptor function; a more comprehensive list of antagonists with K_i and IC_{50} values can be found elsewhere (see Tables 11, 13, and 15 in (Traynelis et al., 2010)). Identification of a new site of action is marked by the red circles within the time line. Representative examples for competitive antagonists (including both glycine site antagonists and glutamate site antagonists), channel blockers (acting at the ion channel pore), and negative allosteric modulators (acting at the amino terminal domain of

GluN2B-containg receptors) are shown, and include D-aminophosphonovaleric acid (APV (Evans et al., 1982)), the low efficacy agonist HA-966 (Evans et al., 1978b), phencyclidine (PCP (Anis et al., 1983)), ketamine (Anis et al., 1983), dextrorphan (Berry and Lodge, 1984), CPP (Davies et al., 1986), MK801 (Wong et al., 1986), 7-chlorokynurenic acid (7CK (Kemp et al., 1988)), ifenprodil (Carter et al., 1988; Reynolds and Miller, 1989), eliprodil (Carter et al., 1988), memantine (Bormann, 1989), argiotoxin (Raditsch et al., 1993), selfotel (Lehmann et al., 1988), CPPene (Aebischer et al., 1989), polyamines(Ransom and Stec, 1988; Williams et al., 1989), arcaine (Reynolds, 1990), conoantokins-G and -T (Con , (Haack et al., 1990; Mena et al., 1990)), aptiganel (CNS-1102, (Minematsu et al., 1993)), neurosteroids (Park-Chung et al., 1994), CP101,606 (Chenard et al., 1995), Ro25-6981 (Fischer et al., 1997), Conantokin-R (White et al., 2000), NVP-AAM077 (Liu et al., 2004), UBP141 (Morley et al., 2005). In addition, representative members of the few known classes of positive allosteric potentiators are shown, including polyamines (Williams et al., 1990; McGurk et al., 1990) and neurosteroids (Wu et al., 1991). Some of these ligands were exceptionally potent, highly-selective for NMDA receptors over kainate and AMPA receptors, and in some cases (ifenprodil and analogues acting at GluN2B) highly subunit-selective.

Table 1.1. Subunit-selectivity of compounds acting on recombinant NMDA receptors

Compound	GluN2A	GluN2B	GluN2C	GluN2D	Ref
Competitive Antagonists	*Ki (μM)*	*Ki (μM)*	*Ki (μM)*	*Ki (μM)*	
APV, (*R*)-AP5	0.28	0.46	1.6	3.7	(Feng et al., 2005)
(*R*)-AP7	0.49	4.1	6.4	17	(Feng et al., 2005)
Selfotel (CGS-19755)	0.15	0.58	0.58	1.1	(Feng et al., 2005)
(*R*)-CPP	0.041	0.27	0.63	1.99	(Feng et al., 2005)
NVP-AAM077	0.015	0.078	--	--	(Frizelle et al., 2006)
UBP-141	14	19	4.2	2.8	(Morley et al., 2005)
Conantokin-G	10	0.1	1	1	(Teichert et al., 2007)
Conantokin-R	1	1	7	10	(Teichert et al., 2007)
7-Cl-kynurenate[a]	0.6	0.2	--	--	(Priestley et al., 1995)
Channel blockers	*IC_{50} (μM)*	*IC_{50} (μM)*	*IC_{50} (μM)*	*IC_{50} (μM)*	
Argiotoxin636	0.009	0.005	0.46	--	(Raditsch et al., 1993)
(+)MK-801	0.015	0.009	0.024	0.038	(Dravid et al., 2007)
Memantine[b]	13	10	1.6	1.8	(Kotermanski and Johnson, 2009)
Ketamine[b]	5.4	5.1	1.2	2.9	(Kotermanski and Johnson, 2009)
Phencyclidine	0.82	0.16	0.16	0.22	(Dravid et al., 2007)
Dextrorphan	1.3	0.33	0.15	0.74	(Dravid et al., 2007)
CNS-1102 (aptiganel)	0.13	0.068	0.087	0.14	(Dravid et al., 2007)
Noncompetitive Antagonists	*IC_{50} (μM)*	*IC_{50} (μM)*	*IC_{50} (μM)*	*IC_{50} (μM)*	
Ifenprodil	39	0.15	29	76	(Hess et al., 1998)
Ro 25-6981	52	0.0090	--	--	(Fischer et al., 1997)
CP-101,606	>100	0.039	>100	>100	(Mott et al., 1998)
QNZ46	229	>300	6	3	(Mosley et al., 2010)
DQP-1105	206	121	9	3	(Acker et al., 2011)
DQP-69	13	26	0.22	0.17	(Acker et al., 2013)
TCN 201	0.109	>30	--	>30	(Bettini et al., 2010)
UBP-618	1.8	2.4	2.0	2.4	(Costa et al., 2010)
Dynorphin A (1-13)	19	29	228	57	(Brauneis et al., 1996)
Pregnanolone sulfate (3α5βS)	50	44	26	30	(Petrovic et al., 2005)
Allosteric Potentiators	*EC_{50} (μM)*	*EC_{50} (μM)*	*EC_{50} (μM)*	*EC_{50} (μM)*	
CIQ	NE	NE	2.8	3	(Mullasseril et al., 2010)
Spermine	NE[c]	163	NE	NE	(Williams et al., 1994; Williams, 1995; Traynelis et al., 1995)
Pregnenolone sulfate	21	33	NE[c]	NE[c]	(Malayev et al., 2002)
UBP-710	>30	>30	NE[c]	NE[c]	(Costa et al., 2010)

NE indicates no detectable effect, and -- indicates that data is not available.

[a] K_B values calculated from Cheng-Prusoff correction of IC_{50} values.

[b] IC_{50} values determined in extracellular Mg^{2+}, which alters subunit selectivity.

[c] Partially inhibits with IC_{50} value of 100 μM or greater.

subunit-selective agonists, antagonists, and modulators could be found, which would allow NMDA receptor function to be regulated in region-specific manner. Indeed, extensive pharmacology has been developed around the GluN2B subunit. However, shortly after this period of sustained progress, discovery of new ligands and pharmacological tools stalled. For over ten years there seemed to be little advance in development of subunit-selective antagonists and modulators for NMDA receptors comprised of subunits other than GluN2B. Nevertheless, academic interest in subunit-selective NMDA receptor antagonists persisted, as a need for tools to dissect subunit contribution to region-specific processes was acutely appreciated by those working on systems involving excitatory amino acids. This sustained need motivated multiple laboratories to search for subunit-selective compounds with which to answer important questions about the role of NMDA receptors in normal and neuropathological functions.

In the last few years, an acceleration in our understanding of the pharmacology of the NMDA receptor seems apparent (Figure 1.3), as the discovery of a handful of new binding sites on the receptor for positive and negative allosteric modulators has stimulated new thinking about NMDA receptor regulation and function (Mosley et al., 2010; Bettini et al., 2010; Costa et al., 2010; Mullasseril et al., 2010; Acker et al., 2011). This advance, fueled both by translational programs at the US National Institutes of Health (NIH) such as the Molecular Library Screening Centers Network (Lazo et al., 2007) and later the Molecular Libraries Program (http://mli.nih.gov/mli) as well as cross-cutting academic collaborations between neuropharmacologists and medicinal chemists, correlates with apparently renewed clinical interest in NMDA receptor pharmacology driven by a number of intriguing clinical trials (e.g. Preskorn et al., 2008; Mony et al., 2009). Thus, it appears that the glutamate receptor field may again be poised to witness a rapid set of advances as proof-of-concept compounds acting at new sites are refined

through medicinal chemistry into potent compounds with high degrees of subunit-selectivity that can serve as reliable new subunit-selective probes.

Recently identified positive modulators improve upon known endogenous potentiators

Throughout the early 1990s, several endogenous compounds including polyamines and other biogenic amines were recognized as NMDA receptor positive modulators, i.e. compounds that bind to the receptor and cause an increase in its maximal response or agonist affinity (or both), but do not act as agonists (Ransom and Stec, 1988; Williams et al., 1990; Reynolds, 1990; Rock and Macdonald, 1992; Benveniste and Mayer, 1993; Durand et al., 1993; Bekkers, 1993; Williams, 1994). Spermine can enhance the response of GluN2B-containing neurons through interactions with an extracellular site on the receptor (Ransom and Stec, 1988; Williams et al., 1990; Reynolds, 1990; Rock and Macdonald, 1992; Benveniste and Mayer, 1993; Durand et al., 1993) and has been suggested to bind at the GluN1-GluN2B amino terminal domain dimer interface, potentially shielding ionic interactions between residues that influence receptor function (Mony et al., 2011). Polyamine binding to NMDA receptors enhances the sensitivity of the receptors to glycine (Benveniste and Mayer, 1993) and relieves tonic proton inhibition of the receptors (Traynelis et al., 1995). However, the potency with which polyamines potentiate native NMDA receptor responses (EC_{50} of 10-125 μM) is higher than estimates of the basal extracellular spermine concentrations (4 uM; Fage et al., 1992).

There are extensive reports documenting interactions of dynorphin and the NMDA receptor system. Interestingly, dynorphin can both inhibit NMDA receptor-mediated currents, as well as potentiate responses in low glycine with an EC_{50} value for dynorphin A(1-13) of 2.8 μM (Zhang et al., 1997) (Table 1.1). Arachidonic acid can also enhance native NMDA receptor responses, presumably through direct interactions with a

fatty acid binding domain on the receptor (Miller et al., 1992). Furthermore, certain neurosteroids potentiate NMDA receptor function with some subunit selectivity (Wu et al., 1991). Pregnenolone sulfate (PS), for example, potentiates GluN1/GluN2A and GluN1/GluN2B, but inhibits GluN1/GluN2C and GluN1/GluN2D (Malayev et al., 2002; Horak et al., 2006) (Table 1.1). PS acts by increasing the peak open probability (Horak et al., 2004) in a manner controlled by phosphorylation (Petrovic et al., 2009). Moreover, portions of the S2 region between the M3 and M4 transmembrane helices are critical for PS activity (Jang et al., 2004; Horak et al., 2006). Although some neurosteroids are likely to have important roles in regulating receptor function in tissue, the neurosteroid scaffold has yet to be exploited for the development of potent and highly subunit-selective molecules that can discriminate between NMDA receptors containing different GluN2 subunits.

Recent evaluation of a series of tetrahydroisoquinoline analogues lead to the identification of (3-chlorophenyl)(6,7-dimethoxy-1-((4-methoxyphenoxy)methyl)-3,4-dihydroisoquinolin-2(1 H)-yl)methanone), or CIQ, which is a small drug-like molecule that is a highly selective allosteric potentiator of recombinant and native NMDA receptors that contain the GluN2C or GluN2D subunits (Mullasseril et al., 2010; Santangelo Freel et al., 2013). This compound has no detectable potentiating activity on AMPA or kainate receptors or on GluN2A- or GluN2B-containing NMDA receptors, but can enhance by over 2-fold the response amplitude of GluN2C- and GluN2D-containing NMDA receptors (Figure 1.4). Potentiation of GluN2D-containing receptors occurs with an EC_{50} value of 3 μM, whereas this compound is inactive at GluN2A- and GluN2B-containing receptors at 20 μM. CIQ has no agonist activity, does not alter agonist EC_{50} values, and is uninfluenced by agonist concentration (Mullasseril et al., 2010). Single channel analysis demonstrates that CIQ enhances channel opening frequency without impacting lifetime

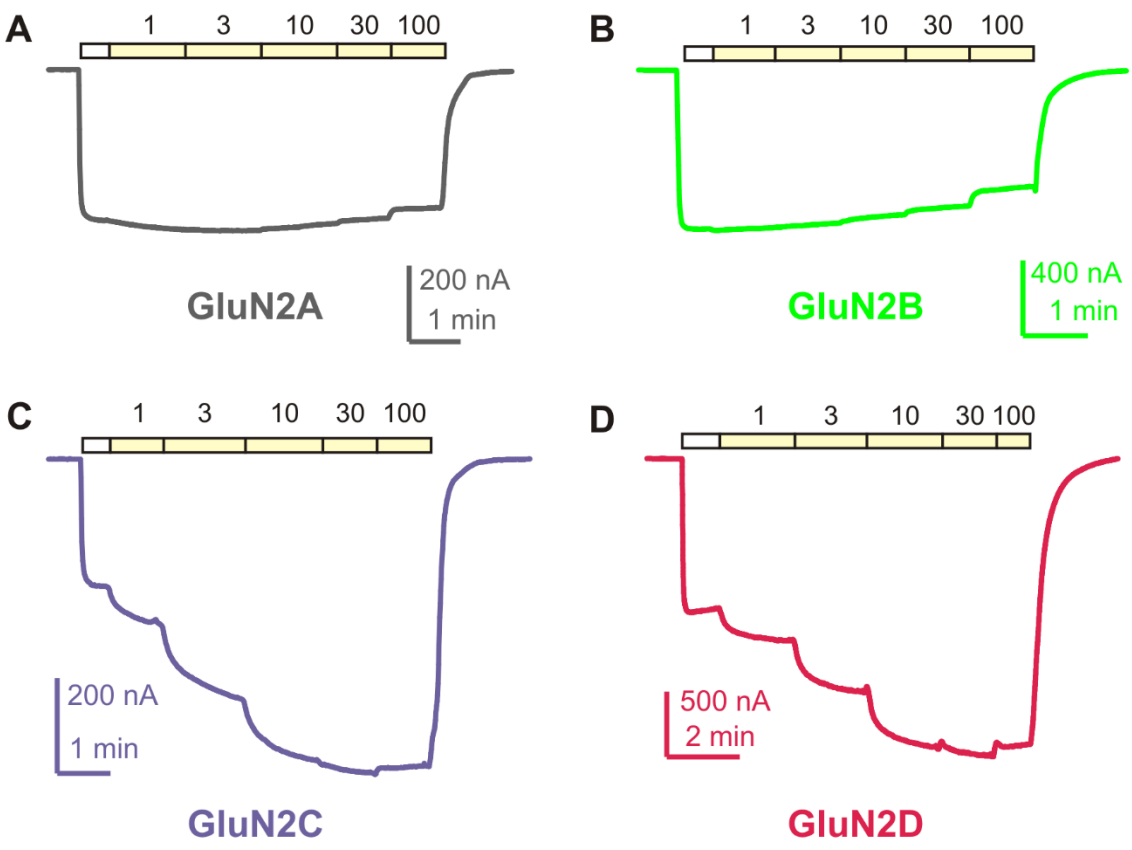

Figure 1.4 CIQ Selectively Potentiates GluN1/GluN2C and GluN1/GluN2D

Shown are two-electrode voltage-clamp recordings from *Xenopus* oocytes expressing GluN1-1a/GluN2A (**A**), GluN1-1a/GluN2B (**B**), GluN1-1a/GluN2C (**C**), or GluN1-1a/GluN2D (**D**). Currents were activated by 100 μM glutamate and 30 μM glycine (white bar above trace) and CIQ was co-applied (pale yellow bars) at the indicated concentrations (in μM) with agonists.

of the open state, suggesting that CIQ reduces the activation energy for channel opening.

A chimeric strategy using GluN2A and GluN2D revealed that the structural determinants of action involve membrane spanning elements as well as extracellular linker regions, and ensuing site-directed mutagenesis identified a single residue residing in the first transmembrane helix that can control CIQ function (Mullasseril et al., 2010). This residue (Thr592 in GluN2D) is conserved between GluN2C and GluN2D but divergent in GluN2A and GluN2B, suggesting it may interact directly with CIQ, although further experiments are needed to verify this (see Karakas et al., 2011 for an example where a crystal structure revealed a ligand binding site that was not predicted by chimera and mutagenesis data). Nevertheless, Thr592 and the nearby pre-M1 helix, a short helix running almost parallel to the membrane and acting as a 'cuff' at the extracellular region of the ion channel pore (Sobolevsky et al., 2009), are ideally positioned to influence the gating process (Talukder et al., 2010) and an interaction between CIQ and Thr592 would be consistent with the effects of CIQ at the single channel level. It is noteworthy that this region of the NMDA receptor has not previously been implicated in either gating or pharmacology, suggesting tetrahydroisoquinolines such as CIQ influence function in a manner that involves novel structural elements. Figure 1.5 illustrates the position of the residues that can control the actions of CIQ in homology model of GluN1/GluN2D. The discovery of a subunit-selective NMDA receptor potentiator and identification of its molecular determinants of action provides new opportunities to investigate mechanisms of NMDA receptor allosteric regulation as well as to explore the nature of channel gating at the single channel level.

CIQ can enhance the response of native NMDA receptors to exogenous application of NMDA in neurons in the subthalamic nuclei (Mullasseril et al., 2010), which has been suggested to express GluN2D (Standaert et al., 1994). By contrast, CIQ appears to

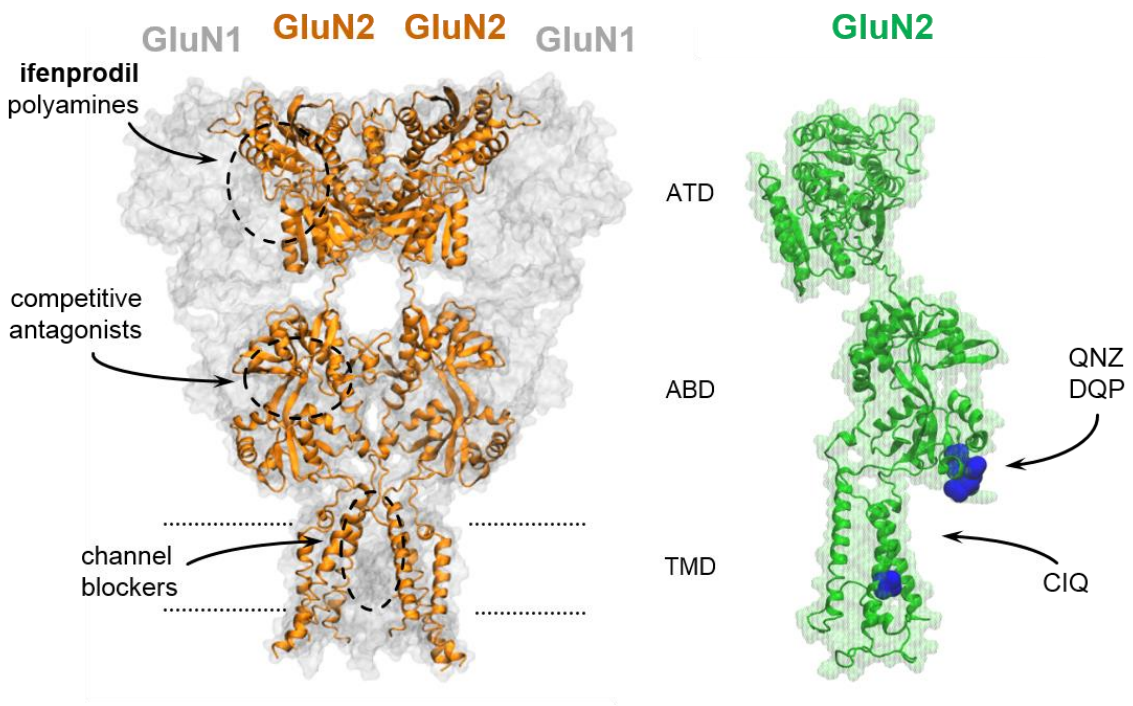

Figure 1.5 Ligand Binding Sites on NMDA Receptors

Major ligand binding sites on the NMDA receptor are depicted on a GluN1/GluN2D homology model based on X-ray structures of a GluA2 tetramer (PDB 3KG2), GluN1 amino terminal domain (PDB 3Q41), GluN1 ligand binding domain (PDB 2A5T), GluN2B ATD (PDB 3JPY), and GluN2D LBD (PDB 3OEN) (Modeller 9.9). Ifenprodil and related GluN2B-selective molecules bind to the amino terminal domain (ATD) as do polyamines. Competitive antagonists of glycine and glutamate bind to the agonist binding domain (ABD) of GluN1 and GluN2, respectively. Channel blockers bind in the transmembrane domain (TMD). Residues critical for the activity of QNZ46, DQP1105, or CIQ are shown in blue. *Right,* an individual GluN2 subunit from a tetrameric complex is shown with the sites for QNZ46, DQP-1105, and CIQ highlighted in blue.

have little effect on the response to NMDA of CA1 pyramidal cells, which have typically been thought to express GluN2A and GluN2B. Thus, CIQ can be used to probe the subunit composition of native NMDA receptors. Moreover, the existence of a small molecule allosteric potentiation provides an opportunity to test a number of hypotheses about the effects that enhancement of NMDA receptor function might have on circuits, behaviors, and in disease models.

In addition to CIQ, several structurally unrelated molecules (e.g. UBP710 and UBP646) have recently been reported to potentiate NMDA receptors (Costa et al., 2010) without agonist activity. At concentrations above 30 μM, UBP646 potentiated responses from GluN2A, 2B, 2C, and 2D. By contrast, UBP710 only potentiated GluN2A- and GluN2B-containing receptors. Recordings from chimeras of GluN2A and GluN2C suggest the entire S2 region between the M3 and M4 transmembrane helices is important for potentiation by UBP710. The existence of at least two structurally unrelated classes of subunit-selective NMDA receptor potentiators in addition to other potentiators with intriguing patterns of subunit-selectivity (Costa et al., 2010) suggests that either multiple potentiating sites exist or a single site can accommodate a variety of different scaffolds.

Non-competitive antagonists target unique modulatory sites with useful subunit-selectivity

The structure-activity relationship of GluN2B-selective antagonists that interact with the amino terminal domain has been extensively studied (for reviews see Borza and Domány, 2006; Beinat et al., 2010; Chenard and Menniti, 1999). An X-ray crystal structure of the GluN1/GluN2B amino terminal domain dimer has revealed the binding site for the GluN2B-selective antagonists ifenprodil and Ro 25-6891 (Karakas et al., 2011), which will no doubt aid in development of a clinically well-tolerated GluN2B-

selective antagonist as significant advances in medicinal chemistry continue to refine and embellish existing classes of GluN2B antagonists. In contrast to the abundant GluN2B-selective antagonists, no other highly subunit-selective non-competitive antagonists have been described. However, novel non-competitive antagonists of both GluN2A and GluN2C/D have been recently reported. Bettini *et al*. (2010) described a series of sulfonamides with high selectivity for GluN2A-containing receptors. For example, 3-chloro-4-fluoro-*N*-[(4-{[2-(phenylcarbonyl)hydrazino] carbonyl}phenyl)methyl]benzenesulfonamide (compound 1, referred to as TCN 201) is an apparent non-competitive antagonist whose actions cannot be surmounted by glutamate. It does partially displace glutamate site antagonists in radioligand binding assays in a manner similar to displacement of glutamate site ligands by glycine site antagonists. In contrast to glutamate, glycine can surmount the inhibition by TCN 201 in functional Ca^{2+} imaging assays, even though TCN 201 is minimally effective in displacing glycine site antagonists in radiolabelled binding studies. These data lead to the hypothesis that TCN 201 acts at a site allosterically modulated by glycine as well as the prediction that TCN 201 may act at the GluN1/GluN2A ligand binding domain interface (Bettini et al., 2010). A recent study by Costa *et al.* (Costa et al., 2010) has identified several phenanthrene and naphthyl analogues that act as non-competitive antagonists of GluN2C- and GluN2D-containing receptors. UBP618 shows robust inhibition with IC_{50} values of 1.8-2.4 μM (Table 1) that are minimally influenced by glutamate and glycine concentration (Costa et al., 2010). These compounds suggest a new negative modulatory site exists that could be exploited for the development of novel probes.

Another series of novel non-competitive antagonists were recently discovered through medicinal chemistry efforts to increase the potency of a quinazolin-4-one that was identified as an NMDA receptor inhibitor through a fluorescence-based multi-well

screen (Mosley et al., 2010). These antagonists had IC_{50} values ranging from 600 nM to 3 μM. A gain-of-function chimeric strategy utilizing one analogue (QNZ46) with greater than 50-fold selectivity for recombinant GluN2D over GluN2A identified unique structural determinants of action of these compounds (Hansen and Traynelis, 2011). The selectivity of QNZ46 for GluN2D can be transferred to GluN2A by residues within a loop region on the lower lobe of the ligand-binding bilobed clamshell (Figure 1.5). Subsequently, a handful of individual residues were identified that control the actions of these compounds. Interestingly, this class of antagonist shows a unique mechanism of action, with an unusual use-dependence that involves a 20-fold enhancement of IC_{50} when glutamate (but not glycine) binds to its recognition site. This enhancement suggests a simple mechanism of action that leads to an inhibition of opening frequency upon binding of inhibitors after glutamate binding. The dependence on glutamate (but not glycine) binding is consistent with the modular nature of glutamate receptor structure, as well as previous suggestions that different subunits may control independent conformational changes (Banke and Traynelis, 2003).

In addition to quinazoline-4-ones, structurally unrelated compounds that possess a pyrazoline scaffold appear to act at a similar site, as determined by the coordinated study of GluN2A-GluN2D chimeric receptors together with site-directed mutagenesis (Acker et al., 2011, 2013). These compounds, exemplified by DQP-1105, show an unusual property in that their potencies at the GluN2A subunit may be enhanced by desensitization that occurs following dialysis of the intracellular solution. Thus, in conventional patch mode, these antagonists do not appear as selective as they do in perforated patch recording mode. The mechanistic basis of this observation remains to be determined.

Competitive antagonists and channel blockers target highly conserved regions with little selectivity across NMDA receptor subtypes

The identification of D-APV as a competitive antagonist that is highly selective for NMDA receptors over AMPA and kainate receptors led to significant advances in our understanding of the role of NMDA receptors in numerous biological phenomena. D-APV has for years been the definitive antagonist to show NMDA receptor involvement in a neurological process or disease state (Herron et al., 1985; Morris et al., 1986; Hestrin et al., 1990). However, D-APV shows K_i values that vary less than ten-fold among NMDA receptors comprised of different GluN2 subunits, a level of selectivity generally considered too low to provide trustworthy dissection of subunit contribution, particularly in native tissue. Moreover, efforts to identify competitive antagonists with GluN2 subunit-selectivity have yet to improve much on D-APV (e.g. see table 11 in Traynelis et al., 2010). Considerable enthusiasm around NVP-AAM077, a proposed GluN2A-selective competitive antagonist (Liu et al., 2004), was short-lived as estimates of K_i values from IC_{50} values (Feng et al., 2004) and later determination of the K_i values by Schild analysis (Frizelle et al., 2006; Neyton and Paoletti, 2006) revealed that selectivity was less than 10-fold. Similarly, a handful of phenanthrene derivatives show 7- to 10-fold difference in estimated K_i values (Costa et al., 2009), favoring inhibition of GluN2D over GluN2A.

Crystal structures of the ligand binding domain among glutamate receptors offer an explanation for the difficulty in obtaining subunit-selective competitive antagonists. The key agonist contact residues are conserved almost universally across the glutamate receptor family and strongly conserved within the glutamate binding pocket across GluN2 subunits (Kinarsky et al., 2005; Mayer, 2006; Risgaard et al., 2010), although the hinge region in the GluN2 ligand binding domain shows agonist-dependent diversity (Vance et al., 2011). Whereas the glutamate binding pockets show some differences

(Erreger et al., 2007) that can be exploited to develop agonists with limited preference for different GluN2 subunits (Clausen et al., 2008), in general, the highly conserved nature of the agonist binding domain diminishes the prospect that strong subunit selectivity can be achieved through conventional modifications of competitive antagonist structure.

Uncompetitive antagonists, which are typically channel blockers, target perhaps the most highly conserved portion of the NMDA receptor, and thus there is little selectivity (<10 fold) for various channel blockers across NMDA receptor subunits (Dravid et al., 2007). The lone exception is a class of synthetic polyamines that contain a long chain with various aromatic headgroups (Igarashi et al., 1997). Some of these compounds can achieve up to 50-fold selectivity between GluN2A and GluN2D (with intermediate IC_{50} values at GluN2B and GluN2C), raising the possibility that these scaffolds could be modified in a manner that allows interaction with less conserved portions of the receptor. This may occur as the length of the blocker engages atomic interactions beyond the conserved ion permeation pore, potentially sensing more distinctive elements of the receptor. In addition, given the unusually large and diverse collection of molecules that can act as NMDA receptor blockers, it seems possible that some subunit selectivity might yet be encountered through extensive screening among GluN2 subunits; however, this awaits further study.

Conclusion

Our knowledge of NMDA receptor biology has been inextricably linked to the diverse array of small molecules acting on the receptors. For example, identification of NMDA receptors as a mediator of excitatory neurotransmission and some forms of synaptic plasticity relied heavily upon agonists and antagonists that were selective for NMDA over AMPA and kainate receptors. These pharmacological tools have been used

extensively to test important hypotheses about the contribution of the NMDA receptor family to neurological diseases including stroke, traumatic brain injury, dementia, epilepsy, and neuropathic pain. However, the numerous roles of NMDA receptors in normal brain function make it difficult to selectively target this receptor class in a disease state while preserving normal function in patients, which has limited the utility of NMDA receptor antagonists as therapeutics.

A promising approach to achieve the selective modulation of aberrant NMDA receptor function is to target the specific GluN2 subtypes, which are differentially expressed in the CNS. Additionally, there has been a growing appreciation that various NMDA receptor subtypes are likely to play unique roles in the neurophysiology of different brain regions. However, apart from the GluN2B subunit, it has been impossible to assess contribution of specific NMDA receptor subtypes to brain function or evaluate the potential therapeutic utility of targeting particular NMDA receptor subtypes because potent, subunit-selective antagonists that distinguish between NMDA receptors comprised of different GluN2 subunits simply have been unavailable. This mismatch finally is being resolved, as a handful of novel subunit-selective NMDA receptor modulators have been described recently (Figure 1.6). It is no accident that the newly discovered GluN2 subunit-selective molecules are largely allosteric modulators. Linker regions, the amino terminal domain, and portions of the ligand binding domain distal to the residues that contact the agonist are not well conserved among NMDA receptor subunits. Moreover, the highly modular arrangement of extracellular domains creates numerous potential regulatory sites at various protein-protein interfaces, and provides an opportunity to inhibit specific conformational changes that might take place within individual subunits en route to channel opening. New subunit-selective compounds acting at sites distinct from agonist binding pocket or the channel pore will likely continue to be found for the NMDA receptor. Almost certainly, medicinal chemistry efforts applied

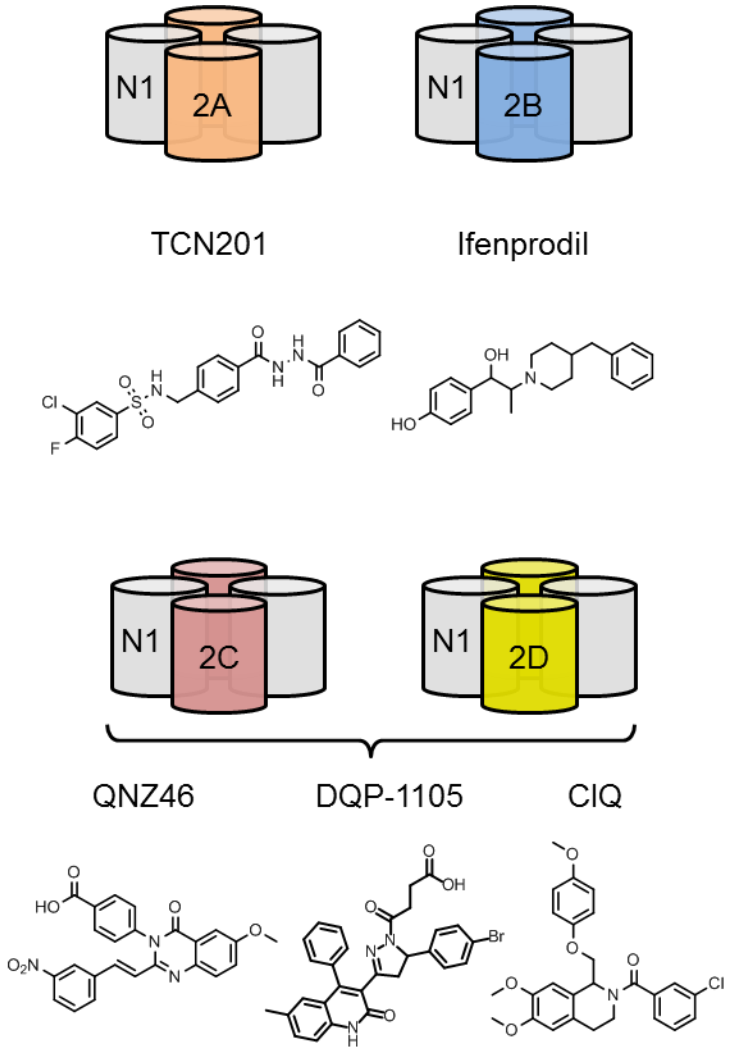

Figure 1.6. GluN2 Subunit-Selective Pharmacology

NMDA receptors are composed of two GluN1 (labeled N1) subunits and two GluN2 subunits (2A, 2B, 2C, or 2D) perhaps in a 1-2-1-2 arrangement. Receptors containing different GluN1 splice variants and/or a GluN3 subunit have distinct functional properties. Additionally, much of the diversity among receptor subtypes arises from the GluN2 subunits, which are critical in determining biophysical and pharmacological properties of the receptor. Representative compounds acting with greater than 50-fold selectivity at individual GluN2-containing receptors are shown below the receptor subtypes.

to the initial proof-of-concept molecules will improve the potency and selectivity of these new families of modulators. Availability of the resulting new pharmacological tools will stimulate experimental work that dissects the contribution of the different GluN2 subunits to various neurological processes and disease states, with potential for addressing unmet clinical need. Thus, our understanding of NMDA receptors seems poised again for explosive growth, triggered by the discovery of pharmacological tools.

The goal of this study was to identify the molecular determinants of selectivity for new NMDA receptor allosteric modulators and elucidate a detailed mechanistic understanding of how these modulators alter function of NMDA receptors. In this thesis I identified two unique, previously unrecognized modulatory regions of the NMDA receptor, one that is critical for positive allosteric modulation by a newly discovered class of GluN2C- and GluN2D-selective potentiators and one that is important for negative allosteric modulation by the GluN2A-selective inhibitor TCN-201. Further, I studied how modulators and mutations both impinge upon the function of a putative pre-M1 helix by evaluating the contribution of this region to NMDA receptor gating.

Chapter 2: Materials and Methods

DNA Constructs

cDNAs for recombinant rat NMDA receptor subunits were used. Table 2.1 gives the GenBank accession numbers for each subunit. For experiments using human embryonic kidney (HEK293) cells, cDNAs for GluN1-1a and GluN2D were subcloned into the pCI-neo mammalian expression vector (Promega catalog no. E1841; GenBank accession no. U47120), whereas cDNA for GluN2A was subcloned in the pcDNA1/Amp vector (Invitrogen). For experiments using *Xenopus laevis* oocytes, cDNA for GluN1-1a was subcloned in the pGEMHE vector (Liman et al., 1992), cDNAs for GluN2A, GluN2B, and GluN2D were in the pCI-neo vector, and cDNA for GluN2C was in the pRKW2 vector (GenBank accession no. DQ657243). cDNA for the green fluorescent protein variant maxGFP (formerly Amaxa, currently Lonza) was subcloned in the vector pmaxGFP. All plasmids contained a gene for ampicillin resistance, except for pmaxGFP, which contained a kanamycin resistance gene.

General Molecular Biology Procedures

cDNAs were propagated by transformation into chemically competent *E. coli*. Competent *E. coli* were prepared by inoculating a single colony of chemically competent TOP10 cells (Invitrogen product no. C4040-10) into 10 mL of SOB media and incubating at 37 °C overnight with shaking. The SOB media contained 2% (w/v) peptone, 0.5 % (w/v) yeast extract, 10 mM NaCl, 2.5 mM KCl, 10 mM $MgCl_2$, and 10 mM $MgSO_4$ at pH 7.0. The 10 mL of starter culture was then inoculated into 200 mL SOB media in a 2 L Erlenmeyer flask and incubated at 37 °C until the absorbance of 600 nm light by the SOB media was 0.4-0.6, approximately 1.5 hours. The SOB media was then collected in four 50 mL centrifuge tubes and chilled on ice for 15 minutes followed by centrifugation at 1000 g for 15 minutes at 4 °C. The cell pellet in each of the four 50 mL

Table 2.1 GenBank Accession Numbers for Rat (*Rattus norvegicus*) NMDA Receptor Subunits

Subunit	Accession Number
GluN1-1a	U11418 (pGEMHE) and U08261 (pCI-neo)
GluN1-1b	U08263
GluN2A	D13211
GluN2B	U11419
GluN2C	M91563
GluN2D	L31611

tubes was resuspended in 16.7 mL (one-third of the volume of SOB media collected) RF1 solution that contained 100 mM RbCl, 50 mM $MnCl_2$, 30 mM potassium acetate, 10 mM $CaCl_2$, 15% (w/v) glycerol at pH 5.8 (adjusted with 0.2 M acetic acid) sterilized by 0.22 μm membrane filtration. The cells were incubated on ice for 1 hour then centrifuged as above. The cell pellet in each tube was resuspended in 4 mL RF2 solution and then combined into a single 50 mL tube and incubated on ice for 15 minutes. RF2 solution contained 10 mM MOPS, 10 mM RbCl, 75 mM $CaCl_2$, 15% (w/v) glycerol adjusted to pH 6.8 with NaOH and sterilized by 0.22 μm membrane filtration. *E. coli* were then distributed in 50 μL aliquots into 1.5 mL microcentrifuge tubes, flash frozen in liquid nitrogen and stored at -80 °C.

For transformation of cDNA, competent *E. coli* were thawed on ice during which time SOC media (Invitrogen catalog no. 15544-034) was heated to 37 °C in a water bath. 1 μL cDNA (for retransformations) or 3.5 μL DNA (for Quikchange reactions or ligations) was added to the 50 μL of *E. coli*, mixed, and incubated on ice for 10-15 minutes. Microcentrifuge tubes containing the *E. coli*-DNA mix were placed in a 42 °C water bath for 45-60 s, placed on ice for 20 s, then set on the bench top. 250 μL of preheated SOC media was immediately added to *E. coli*-DNA mix. Cells were incubated at 37 °C for 45-60 minutes during which time an agar plate containing appropriate antibiotic was warmed in a 37 °C incubator with the lid partially open to allow condensation inside the plate to evaporate. For retransformations, 10 μL *E. coli* was spread on the agar plates, whereas for Quikchange reactions or ligations, all of the *E. coli* (about 300 μL) were plated. Plates were allowed to sit at room temperature for 5-15 minutes and then placed in a 37 °C incubator overnight.

For minipreparation of cDNA, individual colonies from transformations were inoculated into 2 mL 2x YT media with antibiotic in a 14 mL round-bottom tube and

incubated at 37 °C for 12-16 hours. Cells were collected in 2 mL microcentrifuge tubes and centrifuged at 13000 rpm for 3 minutes. DNA was then isolated and purified from *E. coli* using a QIAprep Spin Miniprep Kit (QIAGEN catalog no. 27104) according to the manufacturer's protocol, eluting the DNA with 50 μL Buffer EB. DNA was subsequently used for sequencing, test digests, *in vitro* cRNA synthesis, or Quikchange reactions.

For medium-scale (midi) preparation of cDNA, individual colonies from transformations were inoculated into 50 mL 2x YT media with antibiotic in a 500 mL Erlenmeyer flask and incubated at 37 °C overnight. Cells were collected in 50 mL centrifuge tubes and centrifuged at 6000 g for 15 minutes at 4 °C. DNA was then isolated and purified from *E. coli* using a HiSpeed Plasmid Midi Kit (QIAGEN catalog no. 12643) according to the manufacturer's protocol. The DNA was eluted with 0.5 mL TE buffer and the concentration of DNA isolated was then measured using UV spectrophotometry at 260 nm of a 1:100 dilution of DNA in TE buffer. A_{260} readings were between 0.1 and 1.0. A sample of DNA (1 μL) was also tested for quality by digestion with restriction enzymes and separation by 0.8% agarose gel electrophoresis. DNA of sufficient yield (>0.1 μg/μL) and quality was subsequently used for transfection of HEK cells, Quikchange reactions, or *in vitro* cRNA synthesis.

Quikchange Reactions

Site-directed mutagenesis was accomplished using Quikchange reactions. Each reaction was carried out in a total volume of 50 μL composed of 39 μL ultrapure water (Milli-Q), 5 μL 10x cloned Pfu reaction buffer (Agilent Technologies), 2 μL deoxyribonucleoside triphosphates (dNTPs, 10 mM each; Promega catalog no. U1511), 2 μL forward and reverse primers (10 μM each), 1 μL DNA template (about 0.2 μg/μL) and 1 μL PfuTurbo DNA polymerase (2.5 U/μL; Agilent Technologies catalog no. 600254). All reagents were thawed and mixed prior to use by flicking and/or inverting

the tube and were briefly spun down using a minicentrifuge then placed on ice during assembly of the reaction. Master mixes for several reactions containing all components except for the primers were made when convenient. Reactions were assembled at room temperature and the PfuTurbo DNA polymerase was added last. Reactions were thoroughly mixed by vigorously inverting the tubes 3-5 times and then placed in a thermal cycler (MJ Research PTC 200). Thermal cycling for the reactions consisted of 1 minute at 96 °C followed by 14 cycles of 30 s at 96 °C, 1 minute at 53 °C, and 15 minutes at 72 °C. When the reaction completed, it was kept at 4 °C for 4-8 hours. 1.5 μL DpnI was subsequently added to each reaction, the reactions were mixed and incubated at 37 °C for 3 hours. Reactions were then kept at 4 °C for 0-4 hours before transforming *E. coli* with 3.5 μL of the reaction mix.

If no colonies grew following transformation, reactions, which were kept at 4 °C following the first transformation, were re-transformed using chemically-competent TOP10 *E. coli* (Invitrogen). If colonies still did not grow, the primer sequences were cross-checked with the template DNA sequence to verify they would give the desired product and Quikchange reactions were re-run ensuring all the reagents were completely thawed and dissolved. If the reaction failed the second time, new primers were designed and ordered with higher purity and a new minipreparation of template DNA was generated. If reactions failed after ordering a new set of primers, the thermal cycling parameters were optimized according to recommendations from the PfuTurbo manual. About 5% of reactions required ordering of new primers and all Quikchange reactions were successful after ordering a new set of primers.

Oligodeoxynucleotide primers for Quikchange reactions were designed by replacing the wild type codon with a codon for the desired amino acid change in such a manner as to minimize the base pair mismatches. At least 9 bases were included

upstream of the targeted mismatch and at least 12 bases downstream were included. When feasible, primers were designed to start and end with GG, GC, CG, or CC. Primer lengths were generally kept under 40 bases. Primers used to generate alanine scan mutants of the GluN1 M1 and M4 were designed in an automated fashion using an algorithm written in ANSI C implementing these criteria (Ogden, unpublished) and Quikchange reactions run using these primers had a greater than 95% success rate.

ATD Deletion Constructs

The GluN2D ATD deletion construct (GluN2DΔATD) was generated by removing 384 base pairs from the 5' untranslated region (UTR) of a previously described GluN2D ATD deletion construct (Yuan et al., 2009). A restriction site for NheI was introduced into the previous ATD deletion construct 26 bp upstream of the initiating codon by Quikchange reaction and the product DNA was digested with NheI. The resulting 8241 bp band was isolated and self-ligated to generate the deletion construct. Removing the 384 base pairs from the 5' UTR dramatically improved expression of this construct in *Xenopus laevis* oocytes. The GluN2B ATD deletion construct was generated in a similar manner from a previously published GluN2B ATD deletion (Yuan et al., 2009). The GluN1 construct lacking the ATD (GluN1ΔATD) was generated by a modified Quikchange reaction (Makarova et al., 2000). Briefly, a forward primer was designed such that the 5' region was complementary to DNA encoding the first 18 amino acids of GluN1, which are predicted to comprise the signal peptide. The 3' region of the primer was complementary to DNA encoding the first residues in the agonist binding domain (i.e. M394, S395, etc.; see Furukawa and Gouaux, 2003). A successful reaction occurred when the template DNA folded in such a way as to allow the primer to anneal to both regions of the template simultaneously, which generated DNA products lacking the intervening 1125 bp because the primer was incorporated into the product.

DNA Ligations

DNA fragments for ligations were generated by digesting plasmid cDNAs with restriction enzymes. 3-5 μL of DNA from a miniprep was digested in a total reaction volume of 20 μL. Digested DNA was separated by 0.8% agarose gel electrophoresis. GeneMate LE Agarose (BioExpress catalog no. E-3120) was used for gels. Bands of interest in the gel were visualized under ultraviolet transillumination, minimizing the amount of time the DNA was exposed to UV light, and cut out of the gel with a scalpel blade and placed into a 1.5 mL microcentrifuge tube. DNA was isolated and purified from the gel using the illustra GFX PCR DNA and Gel Band Purification Kit (GE Healthcare) according to the manufacturer's protocol with the following modifications. 300 μL of Capture buffer type 3 was added regardless of the actual mass of the gel band; samples were washed twice with 500 μL wash buffer and spun twice to remove residual ethanol; DNA was eluted with 50 μL water. Following DNA recovery from the agarose gel, ligation reactions were assembled and run overnight at 16 °C. Ligation reactions consisted of 1 μL vector DNA, 3 μL insert DNA, 14 μL ultrapure water (Milli-Q), 2 μL 10x T4 ligation buffer (New England Biolabs), and 1.5 μL T4 DNA ligase (New England Biolabs). Ligation reaction product was then transformed into *E. coli*.

cRNA Synthesis

Plasmid cDNAs were linearized with restriction enzymes (Table 2.2) in a total reaction volume of 200 μL. Restriction enzymes were selected to cut the DNA at least 200 base pairs downstream from the stop codon of the cDNA insert. The digest reaction consisted of 20 μL 10x NEBuffer specific to the restriction enzyme, 20 μL 10x BSA if required by the enzyme, 5 μg DNA (or 20 μL of DNA from a miniprep), 5 μL restriction enzyme, and the volume of Milli-Q water needed to bring the final volume to 200 μL. Reactions were vortexed spun down, then incubated at 37 °C for 3 hours.

Table 2.2 Restriction Enzymes and RNA Promoters for cRNA Synthesis

Receptor	Vector	Enzyme	RNA Promoter Kit
GluN1-1a	pGEMHE	NheI	T7
GluN1-1a	pCI-neo	MfeI-HF	T7
GluN2A	pCI-neo	MfeI-HF	T7
GluN2B	pCI-neo	MfeI-HF	T7
GluN2C	pRKW2	NotI	SP6
GluN2D	pCI-neo	MfeI-HF	T7
GluN2D	SP6	NotI	SP6

The QIAquick PCR Purification kit (QIAGEN) was used to purify the linearized template DNA according to the manufacturer's protocol, eluting the DNA in 100 μL Buffer EB. Linearized cDNA was then purified using ethanol precipitation by adding 10 μL 3 M sodium acetate to the eluted DNA, mixing, adding 250 μL 100% ethanol, mixing, and then incubating on dry ice for 10 minutes or in the freezer at -80 °C for 30 minutes. Precipitated DNA was centrifuged at 14000 rpm for 30 minutes at 4 °C. The supernatant was removed and the pellet was washed with 200 μL 70% ethanol then re-centrifuged at 14000 rpm for 30 minutes at 4 °C. The supernatant was removed and the DNA pellet was allowed to dry for 3-5 minutes at 37 °C. The pellet was resuspended in 10.5 μL nuclease-free TE buffer by pipetting for 2-3 minutes until the pellet was no longer visible. The quality and quantity of the DNA and the completeness of the linearization was assessed by running 0.5 μL DNA on a 0.8% agarose gel at 100 V for 40-45 minutes and visualizing the DNA bands by ethidium bromide staining and UV transillumination.

cRNA was synthesized *in vitro* using the mMESSAGE mMACHINE Kit (Ambion) according to the manufacturer's protocol. All reagents were completely thawed at room temperature, vortexed and then placed on ice before assembly, except the RNA polymerase mix, which was simply placed on ice. The transcription reaction was assembled in a sterile 1.5 mL microcentrifuge tube at room temperature. The reaction was run in a total volume of 21 μL and reagents were added in the following order: 10 μL 2x NTP/CAP, the required amount of nuclease-free water to bring up to volume, 2 μL 10x reaction buffer, 3-6 μL linear DNA template (about 1 μg DNA), 1 μL GTP, and 2 μL RNA polymerase mix. GTP was included in the reaction to improve the yield of longer transcripts. The reaction was mixed by flicking the tube and then centrifuged briefly to collect the mixture at the bottom of the tube. The reaction ran at 37 °C for 1.5-2 hours. The template DNA was digested by addition of 1 μL TURBO DNase and incubating for

15 minutes at 37 °C. The cRNA reaction was then stopped and the cRNA precipitated by adding 30 μL LiCl Precipitation Solution and 30 μL nuclease-free water, mixing, and chilling at -20 °C for at least 1 hour, but up to 12 hours. The mixture was centrifuged at 14000 rpm at 4 °C for 15 minutes to pellet the RNA. The pellet was washed once with 0.5 mL 70% ethanol and re-centrifuged to maximize removal of unincorporated nucleotides. After removal of the supernatant, the pellet was dried at 37 °C for 5 minutes and resuspended in 20 μL nuclease-free water. The quality of the cRNA transcript was assessed by agarose gel electrophoresis. 1 μL cRNA product, 5 μL nuclease-free water, and 6 μL Gel Loading Buffer II (Ambion) were mixed and heated for 1-3 minutes at 95 °C. cRNA samples were then loaded in a 0.8% agarose gel and run at 85 V for 40 minutes. 1 μL 0.5-10 Kb RNA ladder (Invitrogen catalog no. 15623200) together with 5 μL nuclease-free water and 6 μL Gel Loading Buffer II was run along with the cRNA samples.

cRNA Injection of *Xenopus laevis* Oocytes

Healthy-looking, defolliculated stage V-VI *Xenopus laevis* oocytes (EcoCyte Bioscience) were selected for injection based on size (about 1 mm in diameter), uniform brown color of the animal pole, uniform light color of the vegetal pole with a lack of dark pigmentation, and the appearance of a clear demarcation between the animal and vegetal poles at the equator. cRNA for injection of oocytes was prepared by diluting the cRNA encoding each NMDA receptor subunit with nuclease-free water and then mixing the cRNA for GluN1 and GluN2 in a 1:2 ratio. cRNA was diluted so as to yield glutamate-activated currents of about 200-1000 nA when recorded 2-7 days post-injection. This was usually achieved with 1:3 to 1:10 dilutions of cRNA to water. 50 nL of GluN1:GluN2 cRNA mix was then injected into oocytes using a Nanoject II automated microinjection pipet (Drummond Scientific catalog no. 3-000-204) according to the

manufacturer's directions. Oocytes were lined up for injection on a Petri dish filled with Sylgard silicone elastomer that had a crevice cut in it. At least 2 seconds were allowed to elapse after injection of the cRNA before removing the pipet tip from the oocyte. Following injection, oocytes were maintained at 15-19 °C in Barth's culture medium containing (in mM) 88 NaCl, 2.4 $NaHCO_3$, 1 KCl, 0.33 $Ca(NO_3)_2$, 0.41 $CaCl_2$, 0.82 $MgSO_4$, 5 Tris-HCl (pH 7.4 with NaOH), 1 U/mL penicillin, 0.1 mg/mL gentamicin sulfate, and 1 µg/mL streptomycin.

Two-electrode Voltage-clamp Recordings

Recordings were performed on *Xenopus laevis* oocytes 2-7 days after injection. The extracellular recording solution contained (in mM) 90 NaCl, 1 KCl, 10 HEPES, 1 $BaCl_2$, 0.01 EDTA and was brought to pH 7.4 with 6 M NaOH. Stock solutions of glutamate (10 mM) and glycine (100 mM) were prepared using recording solution and brought to pH 7.4 using 6 M NaOH. Microelectrodes were fabricated from filamented borosilicate glass (1.5 mm outside diameter, 1.12 mm inside diameter, 10 cm length; World Precision Instruments catalog no. TW150F-4) in a two-step protocol using a vertical puller (Narishige PC-10). Both current and voltage electrodes were filled with saturated KCl (about 3 M) and had resistances of 0.3-1.0 MΩ when measured in recording solution. Silver wires for the current and voltage electrodes were coated with AgCl by placing the silver wire into household bleach (Clorox) for 1-5 minutes. Oocytes were placed in a custom chamber and continuously perfused at about 5 mL/min with recording solution. Voltage clamp and current monitoring were achieved with a two-electrode voltage clamp amplifier (Warner Instruments model no. OC-725C). Currents were anti-aliased lowpass filtered at 10 Hz (-3 dB; 4 pole Bessel filter, Dagan Corporation model no. FL4) and digitized at 20 Hz using a National Insturments PCI-6025E multifunction data acquisition device that was connected to a custom enclosure

with BNC interface panels (National Instruments model no. CA-1000) and controlled by EasyOocyte custom acquisition software. Solutions were perfused by gravity and solution exchange was regulated by an 8-port automated valve (Digital Modular Valve Positioner, Hamilton Company) controlled by EasyOocyte.

HEK Cell Culture

Human embryonic kidney (HEK) cells (ATCC CRL-1573) were grown in 60 mm tissue culture dishes in 5 mL Dulbecco's Modified Eagle Medium (DMEM) with GlutaMAX I (Gibco catalog no. 10569) supplemented with 10% dialyzed fetal bovine serum (Gibco catalog no. 26400), 10 U/mL penicillin, and 10 μg/mL streptomycin. Cells were split every 1-3 days when they reached 90-95% confluence by rinsing with Ca^{2+}-free Hank's Balanced Salt Solution (Gibco catalog n. 14175), incubating with 0.5 mL 0.05% trypsin-EDTA (Gibco catalog no. 25300) at 37 °C for 1-2 minutes then adding 4.5 mL media and gently pipetting up and down several times. Cells were seeded into new 60 mm dishes at ratios of 1:5, 1:10, or 1:20.

Transfection

For transfection and subsequent patch-clamp recordings, cells were plated on glass coverslips coated with poly-D-lysine (PDL) that had been placed into wells of a 24-well plate. Coverslips were coated with PDL by soaking them in 70% ethanol for 15 minutes, rinsing twice with sterile water, soaking in 0.1 mg/mL PDL (dissolved in sterile water) for 30 minutes, rinsing once with sterile water and allowing to dry for 24 hours at room temperature.

One day after cells were plated onto coverslips, cells were transiently transfected using the calcium phosphate precipitation method (Chen and Okayama, 1987) with plasmid cDNAs encoding GluN1, GluN2, and GFP (0.2 g/L total cDNA) at a ratio of 1:1:1. To transfect 4 wells of a 24 well plate, 65 μL water, 25 μL 1 M $CaCl_2$, and 10 μL

cDNA were mixed, 100 μL 2xBES was added, mixed and the solution incubated for 3-5 minutes at room temperature. 50 μL of this solution was then added dropwise to each well. 2xBES solution contained (in mM) 50 N,N-bis(2-hydroxyethyl)-2-aminoethanesulfonic acid (BES), 280 NaCl, 1.5 Na_2HPO_4 adjusted to pH 6.95 with NaOH and sterile filtered with 0.22 μm nylon filters. Cells incubated with cDNA mix for 4-6 hours at 37 °C then the media was changed and 200 μM D,L-2-amino-5-phosphonovalerate and 200 μM 7-chlorokynurenic acid were added to prevent activation of receptors by ambient glutamate and glycine present in the culture medium, which has been shown to lead to excessive Ca^{2+} influx and initiation of apoptosis (Hansen et al., 2008). The cells were used for experiments approximately 18-24 hours following transfection.

Whole-cell Patch-clamp Recordings

HEK cells transfected with NMDA receptors were transferred to a custom made recording chamber on an inverted Olympus IX-71 microscope and continuously perfused at 2 mL/min with recording solution containing (in mM) 150 NaCl, 3 KCl, 10 HEPES, 0.01 EDTA, 0.5 $CaCl_2$, and 11 D-mannitol. pH was adjusted to 7.4 with NaOH and recording solution was filtered (0.22 μm) to prevent clogging of the application tubing and improve pipette seal formation. Microelectrodes were fabricated using thin-walled filamented borosilicate glass (1.5 mm outside diameter, 1.12 inside diameter; WPI catalog no. TW150F-4) pulled using a Flaming/Brown horizontal puller (Sutter Instrument model no. P-1000) according to guidelines in the Sutter Instrument Pipette Cookbook (http://www.sutter.com/contact/faqs/pipette_cookbook.pdf). Pipettes were fire-polished by bringing the tip into proximity of a heated platinum-iridium wire (0.005" diameter; A-M systems catalog no. 767700). The internal pipette solution contained (in mM) 110 D-gluconic acid, 110 CsOH, 30 CsCl, 5 HEPES, 4 NaCl, 0.5 $CaCl_2$, 2 $MgCl_2$, 5 BAPTA, 2

Na_2ATP, 0.3 NaGTP adjusted to pH 7.35 with CsOH; the osmolality was adjusted to 300-310 mOsmol/kg using CsCl or water to increase or decrease, respectively, the osmolality. Pipette tips were filled with internal solution and had resistances of 3-4 MΩ when placed into recording solution. AgCl was deposited onto silver wire of the pipette electrode by placing the silver wire in bleach for 1-5 minutes. The membrane potential of HEK cells was clamped at -60 mV using an Axopatch 200B patch-clamp amplifier (Molecular Devices) and current responses to external application of glutamate (100 μM) and glycine (50 μM) were anti-alias filtered at 8 kHz (-3 dB, 8 pole Bessel filter, Frequency Devices model no. 900L8L) and digitized at 20 kHz using a Digidata 1440A data acquisition system (Molecular Devices) controlled by Clampex 10.3 (Molecular Devices).

Single-channel Recordings

Excised outside-out or cell-attached patches were formed from HEK293 cells transiently transfected with GluN1, GluN2, and GFP. The recording solution was the same as for whole-cell recordings, except the pH was adjusted to 8.0. For outside-out recordings, micropipettes were fabricated from filamented thick-walled borosilicate glass (1.5 mm OD, 0.86 ID, length 100 mm, Warner Instruments cat. no. GC150F-10), whereas for cell-attached patches, micropipettes were made using thin-walled glass as for whole-cell recordings above. For both cell-attached and outside-out recordings, pipettes were pulled using a Flaming/Brown horizontal puller (Sutter Instrument model no. P-1000), and coated with Sylgard silicone elastomer (DuPont), prepared according to the manufacturer's instructions, and cured using a heat gun. Pipette tips were fire-polished as for whole-cell recordings. For outside-out recordings, pipette tips were filled with the same internal solution as for whole-cell recordings; for cell-attached recordings, pipette tips were filled with recording solution supplemented with agonists. Tip

resistances for outside-out patches were 7-9 MΩ and for cell-attached patches were 4-6 MΩ. 1 mM glutamate and 50 μM glycine were used to activate receptors for both cell-attached and outside-out recordings. The holding potential was -80 mV for outside-out patches and +80 mV for cell-attached patches, which corresponded to a V_m of 100-120 mV as zero current was observed at -20 to -40 mV and the reversal potential for NMDA receptors is 0 mV. Currents were anti-aliased lowpass filtered at 8 kHz (-3 dB Bessel 8-pole; Frequency Devices) and digitized at 40 kHz.

Data Analysis

CIQ concentration-response data were analyzed using GraphPad Prism 5.2. The Hill equation

$$\text{Response} = \text{Max}+(100-\text{Max})/(1+(x/EC_{50})^{nH}) \quad (1)$$

where *Max* is the maximum current elicited by CIQ in the presence of glutamate and glycine as a percentage of the current elicited by just glutamate and glycine, *x* is the concentration of CIQ, EC_{50} is the concentration of CIQ that produces half-maximal response, and *nH* is the Hill slope, was fit to data from individual oocytes. For graphical presentation, data points from individual oocytes were normalized to the current response to saturating glutamate plus glycine in the same recording and averaged. The Hill equation was then fit to the average data points. For statistical testing, the logarithm of EC_{50} was used because EC_{50} values have a lognormal distribution (Gaddum, 1945; Christopoulos, 1998; Limpert et al., 2001).

Glutamate and glycine concentration-response data from each oocyte were individually fit to the equation

$$\text{Response} = \text{Max} + (\text{Min}-\text{Max})/(1+(x/EC_{50})^{nH}) \quad (2)$$

where *Min* and *Max* are the current responses elicited by no agonist and saturating agonist concentrations, respectively, *x* is the experimentally-controlled concentration of

agonist, EC_{50} is the concentration of agonist that elicits a half-maximal response, and *nH* is the Hill coefficient. For graphical presentations, current responses were normalized to *Min* and *Max*, averaged, and displayed with a fit of the Hill equation to the averaged data. Statistical tests were performed using the logarithm of the EC_{50}.

TCN-201 inhibition was evaluated using Schild plots (Arunlakshana and Schild, 1959). The agonist EC_{50} was determined in the absence of TCN-201 and EC_{50}' determined in the presence of increasing concentrations of TCN-201. The dose ratio ($DR = EC_{50}'/EC_{50}$) for each concentration of TCN-201 was then calculated and log (DR - 1) was plotted versus log (TCN-201 concentration). This plot was fitted with a straight line with variable slope. The slope of the Schild plot (i.e. Schild slope) is predicted to be 1 for a competitive antagonist at equilibrium according to the Schild equation:

$$\log (DR - 1) = pA_2 + \log [B], \quad (3)$$

where [B] is the TCN-201 concentration and pA_2 is the negative logarithm of the TCN-201 concentration that produces a 2-fold shift of the agonist EC_{50}.

The allosteric constant α and K_b for TCN-201 inhibition were determined using a global nonlinear least squares fitting method. All the agonist concentration-response data obtained at different TCN-201 concentrations were simultaneously fitted to the following equations (see Christopoulos and Kenakin, 2002):

$$\text{Response} = 1 / (1 + (EC_{50}' / [A])^{nH}) \quad (4)$$

$$EC_{50}' = EC_{50} (1 + [B] / K_b) / (1 + \alpha [B] / K_b) \quad (5)$$

where [A] is the agonist concentration, [B] is the TCN-201 concentration, EC_{50} is for the agonist alone in the absence of TCN-201, EC_{50}' values are for agonist in the presence of different concentrations of TCN-201, nH is the Hill slope, α is the allosteric constant, and K_b is the dissociation constant for TCN-201. This method will fit the data using EC_{50} in

the absence of TCN-201, the allosteric constantα, and K_b as global parameters, whereas the Hill slopes and EC_{50}' values are different for each concentration-response curve.

Current responses from whole-cell voltage-clamp recordings using HEK293 cells were analyzed using MATLAB (MathWorks, Inc.). The deactivation time courses of the current responses were fitted by two exponential components using:

$$I_{total} = I_{fast} \exp(-time / \tau_{fast}) + I_{slow} \exp(-time / \tau_{slow}), \quad (6)$$

where τ_{fast} and τ_{slow} are the deactivation time constants for the fast and slow components, respectively. The weighted deactivation time constant was calculated using:

$$\tau_{weighted} = (\tau_{fast} I_{fast} + \tau_{slow} I_{slow}) / (I_{fast} + I_{slow}) \quad (7)$$

Paired t-test (two-tailed), unpaired t-test (two-tailed) or analysis of variance (one-way ANOVA with Tukey-Kramer post test) were used for statistical comparisons as indicated (significance was set at the α=0.05 level). For Schild slopes, the 95% confidence intervals are calculated using the number of data points and the standard error for the best-fit value. All data are presented as mean $\pm$ SEM.

Single-channel analysis

GluN1-1a/GluN2A cell-attached patches with no observable double openings were pre-processed for kinetic analyses with the use of Clampfit 10.3 (Molecular Devices) by manually subtracting the baseline drift and eliminating occasional obvious brief noise artifacts, usually spikes of high amplitude, by matching them to the baseline level of adjacent events. Longer unusable stretches of noisy data (e.g. temporary patch breakdown) were not used for analysis and the recording was essentially divided into two recordings at that point. All patches analyzed had a probability <0.001 of containing 2 or more channels as estimated by the equation

$$E_r = (2/P_{o2})(1 - 0.5P_{o2} - 0.75P_{o2}^2) \quad (8)$$

where E_r is the mean number of consecutive single openings in a run of openings that originated from two individual channels but in which no double openings were observed, and P_{o2} is the fraction of time for which a channel was open during the run, i.e. the open probability during such a run (Colquhoun and Hawkes, 1990). For P_{o2} = 0.30, which is similar to the observed open probability of 0.34 for wild type GluN2A, E_r is 5.2, so patches with 36 openings or more in a run, i.e. 6.9*E_r, had p<0.001 for containing 2 or more active channels. In all GluN2A patches analyzed, E_r was greater than 94.

Kinetic analyses were performed using QuB software (available at http://www.qub.buffalo.edu) with a general 5 step procedure: 1) idealize entire record, 2) estimate transition rates to calculate a critical time, t_{crit}, between the longest duration shut state and the next longest shut state, 3) exclude prolonged shut durations longer than t_{crit} from analysis, 4) re-idealize clusters of openings, and 5) re-estimate rate constants using a model without desensitized states. Single-channel currents were first idealized into open and closed durations using the segmental k-means algorithm (SKM; Qin, 2004) with a linear C↔C↔C↔O model. The SKM algorithm relies on amplitudes of the open and shut states as well as the transition rates between states in the model, so care was taken to grab the amplitudes from clusters of openings that were representative of the average channel behavior in a patch and amplitudes were not re-estimated. Rate constants were then estimated using the maximum interval likelihood (MIL) algorithm (Qin et al., 1996, 1997) using a dead time of 50 μs (two sampling intervals). A t_{crit} was calculated between the longest and second-longest duration shut states so that there would be an equal number of misclassified events. Clusters of channel openings were then isolated using the Chop Idl function to exclude shut durations longer than t_{crit} and clusters were extracted to a new file. Clusters of openings were re-idealized using SKM with Scheme 1 and rate constants were re-estimated using MIL.

Scheme 1

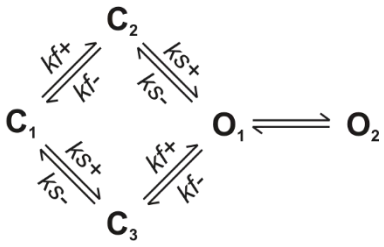

Simulations

Simulations of macroscopic current responses to concentration-jump waveforms were performed in MATLAB using the ode15s ordinary differential equation solver using the differential equations given by the Q matrix for each state in the activation mechanism (Colquhoun and Hawkes, 1977). Concentration-response data were simulated using the Q matrix to give the occupancy of each state in the activation mechanism at equilibrium (Colquhoun and Hawkes, 1995).

Chapter 3: Contribution of the M1 transmembrane helix and pre-M1 region to positive allosteric modulation and gating of N-methyl-D-aspartate receptors[1]

[1] This chapter has been published: Ogden KK, Traynelis SF (2013) Contribution of the M1 Transmembrane Helix and Pre-M1 Region to Positive Allosteric Modulation and Gating of N-Methyl-D-Aspartate Receptors. *Mol Pharmacol*

Abstract

N-methyl-D-aspartate (NMDA) receptors are glutamate-gated ion channels whose function is critical for normal excitatory synaptic transmission in the brain and whose dysfunction has been implicated in several neurological conditions. NMDA receptor function is subject to extensive allosteric regulation both by endogenous compounds and by exogenous small molecules. Elucidating the structural determinants and mechanism of action by which allosteric regulators control gating will enhance our understanding of NMDA receptor activation and facilitate the development of novel therapeutics. Here, we investigated the structural determinants for CIQ, a GluN2C/2D-selective positive allosteric modulator. We show that CIQ does not bind to the amino-terminal domain of the NMDA receptor and does not share structural determinants with modulators acting at the agonist-binding domain dimer interface or ion channel pore. Rather, we have identified critical determinants of CIQ modulation in the region near the first transmembrane helix of GluN2D, including in a putative pre-M1 cuff helix that may influence channel gating. We also show that mutations within the GluN2D pre-M1 region alter open probability of the NMDA receptor. These results suggest a novel site of action for potentiation of NMDA receptors by small molecules and implicate the pre-M1 region in NMDA receptor gating.

Introduction

N-methyl-D-aspartate (NMDA) receptors are ligand-gated ion channels that mediate excitatory synaptic transmission in the central nervous system (Traynelis et al., 2010). These non-selective cation channels are tetrameric complexes comprising GluN1, GluN2, and GluN3 subunits with typical NMDA receptors containing two GluN1 subunits and two GluN2 subunits (Ulbrich and Isacoff, 2008). The GluN1 subunit binds the co-agonist glycine or D-serine and the GluN2 subunit binds the co-agonist glutamate. There are four GluN2 subunits, GluN2A, 2B, 2C, and 2D, each of which is encoded by a separate gene (Hollmann and Heinemann, 1994). NMDA receptors composed of different GluN2 subunits exhibit markedly different biophysical and pharmacological properties (Vicini et al., 1998), which enables NMDA receptor subtypes to play distinct roles in brain physiology and development (Cull-Candy and Leszkiewicz, 2004).

NMDA receptor subunits are composed of three semi-autonomous domains: an amino-terminal domain (ATD), an agonist-binding domain (ABD), and a transmembrane domain (TMD). In addition, they contain a large intracellular region consisting of 100-600 amino acids. The TMD consists of three transmembrane helices—M1, M3, and M4—and a re-entrant pore loop, called M2. NMDA receptors have several allosteric sites including the side-to-side GluN1/GluN2 dimer interface of the ATD (Mony et al., 2011; Karakas et al., 2011), the back-to-back GluN1/GluN2 dimer interface of the ABD (Gielen et al., 2008; Hansen et al., 2012) and the ion channel pore (Antonov and Johnson, 1996; Kashiwagi et al., 2002; Blanpied et al., 2005).

NMDA receptors are potentiated by several endogenous molecules including arachidonic acid (Miller et al., 1992), dynorphin A (Zhang et al., 1997), sulfated neurosteroids (Wu et al., 1991), and polyamines (Ransom and Stec, 1988; Williams et al., 1990; McGurk et al., 1990; Reynolds, 1990). Also, aminoglycosides potentiate

NMDA receptors in a manner similar to potentiation by polyamines (Masuko et al., 1999). These compounds show varying subunit-selectivity and structural determinants of action. Additionally, the first class of positive allosteric modulators selective for GluN2C- and GluN2D-containing NMDA receptors was recently reported (Mullasseril et al., 2010). This class of potentiators doubles the current response to maximally effective concentrations of agonist for NMDA receptors containing GluN2C or GluN2D. These modulators are not agonists and do not affect the potency of either glutamate or glycine. Moreover, two regions of the GluN2 subunit were previously found to be critical for the selectivity of this class of potentiators: a 16 amino acid stretch linking the ATD with the ABD and a point mutation in the M1 transmembrane helix.

To gain a better understanding of allosteric potentiation of NMDA receptors, which could lead to therapeutics with novel selectivity and mechanisms of action, we sought to determine which regions of the receptor might contribute to the binding site and thereby control the actions of these allosteric potentiators.

Results

CIQ Does Not Act at Known Modulatory Sites

Previous work identified two distinct regions of GluN1/GluN2D that were critical for potentiation by CIQ and analogs: the ATD-ABD linker and the first transmembrane helix, M1 (Mullasseril et al., 2010). These regions are seemingly independent of each other based on homology to the GluA2 tetrameric crystal structure, with the ATD-ABD linker being about 65-70 Å extracellular to the M1 helix (Sobolevsky et al., 2009). Thus, it is unlikely that positive allosteric modulators could directly interact with both regions simultaneously. Moreover, it is unclear whether these regions might be allosterically coupled, as is the case for the ATD and the ABD in which ATD ligands such as Zn^{2+} and ifenprodil allosterically regulate glutamate binding (Kew et al., 1996; Paoletti et al., 1997;

Zheng et al., 2001; Erreger and Traynelis, 2005). Therefore, we sought to reconcile the contribution of these apparently discrete regions to potentiation by CIQ. To do so, we systematically explored the importance of both well-established and emerging regulatory sites on the NMDA receptor (Figure 3.1) for positive allosteric modulation of GluN1/GluN2D receptors. These sites, shown in Figure 1, are the interface between the GluN1 and GluN2 amino-terminal domains (Site I), the ion channel pore (Site II), the lower lobe of the agonist-binding domain (Site III), and the agonist-binding domain dimer interface (Site IV). These four modulatory sites are critical for the actions of GluN2B-selective antagonists (e.g. ifenprodil) and positive modulators (e.g. spermine), NMDA receptor channel blockers (e.g. ketamine), GluN2C/2D-selective antagonists (e.g. QNZ46), and GluN2A-selective antagonists (e.g. TCN-201), respectively.

To evaluate the importance of Site I in positive allosteric modulation of GluN1/GluN2D receptors, we recorded CIQ potentiation of receptors lacking the GluN2D ATD and the ATD-ABD linker (GluN2DΔATD) and found that CIQ potentiation was unaffected when then ATD was deleted from GluN2D (Figure 3.2B). These results suggest that CIQ does not bind solely to the ATD of GluN2D. However, the GluN2B-selective antagonist ifenprodil was recently shown to bind NMDA receptors at the interface of the GluN1/GluN2 ATD dimer (Karakas et al., 2011), raising the possibility that residues from the GluN1 ATD could contribute to the CIQ binding site. Contrary to this hypothesis, removal of the ATD and ATD-ABD linker from both GluN1 and GluN2D (GluN1ΔATD/GluN2DΔATD) did not reduce potentiation by CIQ (Figure 3.2C). These data eliminate the possibility that CIQ potentiates GluN2C- and GluN2D-containing NMDA receptors by binding to the amino-terminal domain (Site I).

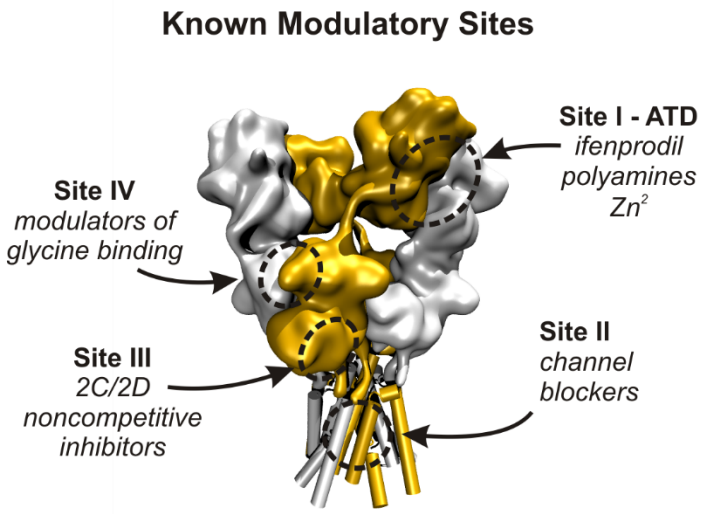

Figure 3.1. Known modulatory sites on the NMDA receptor are outlined on a volume representation of the GluA2 AMPA receptor with subunits corresponding to GluN1 shown in silver and those corresponding to GluN2 shown in orange. Site I, the amino-terminal domain (ATD), is involved in modulation by GluN2B-selective inhibitors such as ifenprodil, which bind to the GluN1-GluN2 ATD dimer interface. In addition, Zn^{2+} ions bind the ATD at the cleft of the GluN2 clamshell-like domain. Site II resides deep within the transmembrane pore of the receptor and is critical for binding of channel blockers such as Mg^{2+}, MK-801, ketamine, and memantine. Site III, located proximal to the membrane at the lower lobe of the GluN2 agonist-binding domain (ABD), is critical for block by noncompetitive, glutamate-dependent inhibitors such as QNZ46 and DQP-1105. Site IV is located at the GluN1-GluN2 ABD dimer interface and is critical for allosteric inhibition of glycine binding by TCN-201 and TCN-213.

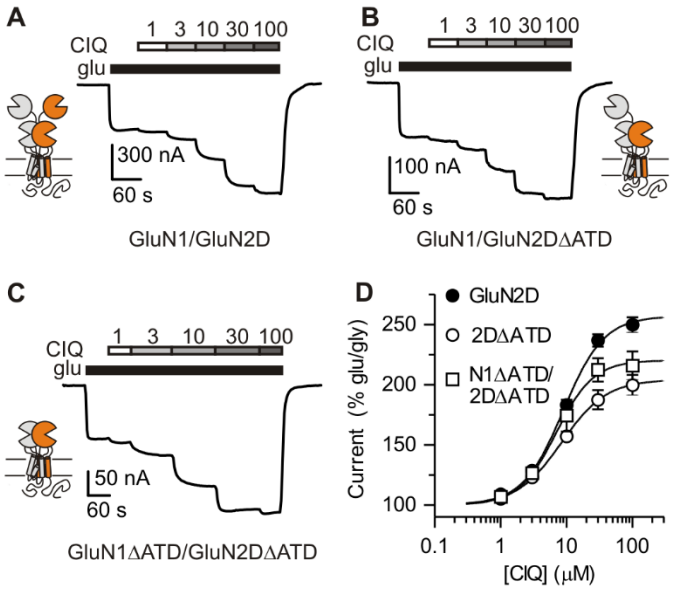

Figure 3.2. GluN1/GluN2D (**A**), GluN1/GluN2DΔATD (**B**) or GluN1ΔATD/GluN2DΔATD (**C**) receptors were expressed in *Xenopus laevis* oocytes and current responses recorded using two-electrode voltage-clamp. Currents were activated by 100 μM glutamate and 30 μM glycine and CIQ (1, 3, 10, 30, and 100 μM) was subsequently co-applied with agonists. (**D**) CIQ potentiated GluN1/GluN2D, GluN1/GluN2DΔATD (2DΔATD), and GluN1ΔATD/GluN2DΔATD (N1ΔATD/2DΔATD) with EC_{50} values of 8.9 μM, 8.4 μM, and 7.0 μM, respectively. Currents were normalized to the glutamate- and glycine-elicited currents. Data are shown as mean ± SEM and are from 3-32 oocytes.

We next assessed whether CIQ acts at the channel blocker site (Site II, Figure 3.3A) on GluN2C- and GluN2D-containing receptors by measuring concentration-response curves for two structurally distinct channel blockers, Mg^{2+} (Figure 3.3B) and ketamine (Figure 3.3C), at a holding potential of -80 mV in the absence or presence of 10 μM CIQ. We predicted that if CIQ binds to or in some way perturbs the channel blocker site, then the potency of channel blockers, the extent of inhibition, or both, would be altered in the presence of CIQ. Yet, CIQ affected neither the degree of inhibition nor the potency for both Mg^{2+} and ketamine at GluN1/GluN2D (Table 3.1). These data suggest CIQ does not compete for binding with channel blockers or dramatically alter the nature of the conduction pathway. These data are consistent with no effect of CIQ on the stability of the open channel, i.e. mean open time (Mullasseril et al., 2010), which is a key determinant of channel block.

The agonist-binding domain harbors several ligand binding sites, and thus we explored the potential interaction of CIQ with each of these sites. Agonists bind in the cleft of the clamshell-shaped ABD; however CIQ is unlikely to bind within the agonist-binding pockets for two reasons. First, CIQ neither activates nor inhibits the receptor, in contrast to other molecules binding at these sites, which are either agonists or competitive antagonists. Second, CIQ does not detectably alter glutamate or glycine potency (Mullasseril et al., 2010), suggesting the nature of the agonist-binding pockets is unchanged by CIQ. In addition to the agonist-binding sites, the ABD contains two regulatory sites that are critical for the actions of subunit-selective inhibitors. One site is located at the membrane-proximal lower lobe of the ABD (Site III in Figure 1) and is important for noncompetitive inhibition by quinazoline-4-ones (Hansen and Traynelis, 2011) and dihydroquinoline-pyrazolines (Acker et al., 2011). We tested whether this region may also be critical for positive allosteric modulation of GluN1/GluN2D by measuring CIQ potentiation of GluN2D receptors containing point mutations that

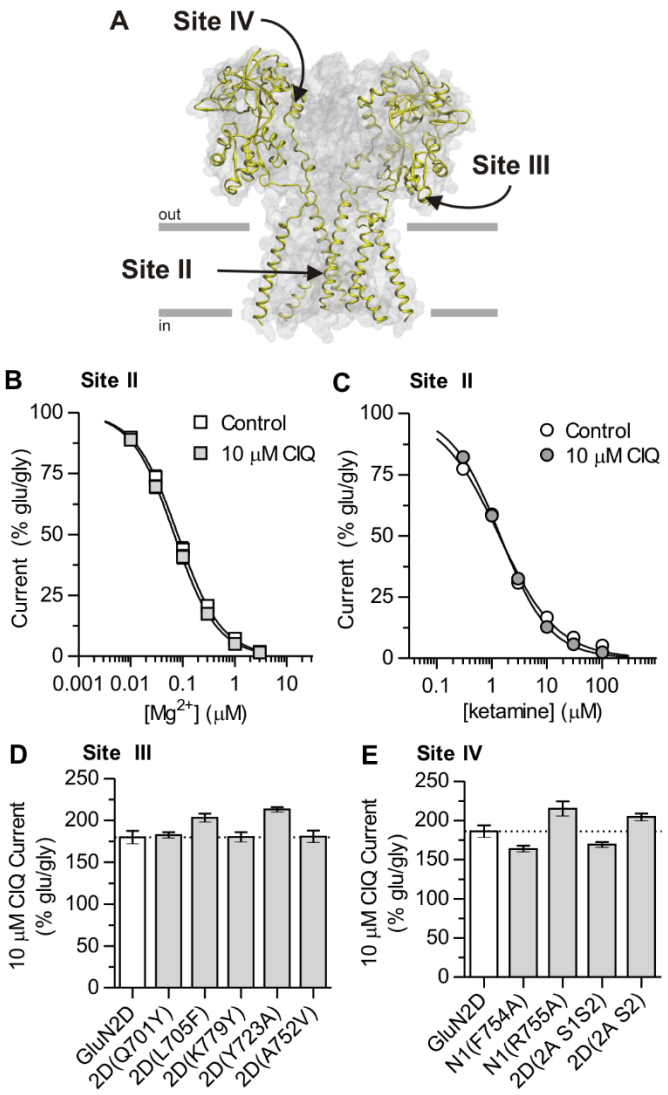

Figure 3.3. A, Modulatory sites II, III, and IV, are depicted on a homology model of GluN1/GluN2D (Acker et al., 2011). The GluN2 subunits are highlighted in yellow and the predicted location of the plasma membrane is represented by gray lines with the orientation indicated. For clarity, the ATD is not shown. **B** and **C**, Interaction of ClQ with Site II was assessed by measuring the potencies of two channel blockers, Mg^{2+} and ketamine, in the absence (control) or presence of 10 μM ClQ. Concentration-response curves were evaluated from current responses of GluN1/GluN2D receptors expressed in oocytes. Currents were normalized to a percentage of the initial glutamate- and glycine-activated currents in the absence

of inhibitor. Data are depicted as mean ± SEM and are from 6 oocytes for each condition. **D,** CIQ positive modulation was assessed at GluN1/GluN2D receptors containing point mutations at Site III that critically affected inhibition of GluN2D by QNZ46. **E,** CIQ potentiation was not affected by point mutations or chimeric NMDA receptors that significantly affected inhibition by TCN-201 at Site IV in GluN1/GluN2A receptors.

Table 3.1. CIQ Does Not Interact With Site II Modulators

Mg^{2+} and ketamine concentration response curves were measured at GluN1/GluN2D receptors expressed in oocytes and recorded using two-electrode voltage-clamp in the absence (control) or presence of CIQ (10 μM). Receptors were activated by 100 μM glutamate and 30 μM glycine at -80 mV. Mg^{2+} data are from 10 oocytes for control and 7 oocytes for CIQ while ketamine data are from 6 oocytes for both control and CIQ. The log IC_{50} values were not significantly different between control and CIQ for both Mg^{2+} and ketamine ($p>0.05$, unpaired t-test).

	IC_{50} (μM)		Minimum Response (% glutamate)	
	Control	CIQ	Control	CIQ
Mg^{2+}	80 ± 10	66 ± 6	1.8 ± 0.8	1.6 ± 0.6
Ketamine	1.58 ± 0.08	1.41 ± 0.12	5.4 ± 0.8	2.4 ± 0.6

markedly impacted inhibition by quinazoline-4-ones (Hansen and Traynelis, 2011) and dihydroquinoline-pyrazolines (Acker et al., 2011). CIQ potentiation, however, was unaffected by mutations in this region that alter inhibition by both quinazoline-4-ones and dihydroquinoline-pyrazolines (Figure 3.3C), suggesting the lower portion of the ABD clamshell proximal to the membrane helices of the receptor does not contribute to the molecular determinants for positive allosteric modulation of GluN1/GluN2D receptors.

A second modulatory site for subunit-selective inhibitors resides at the dimer interface between GluN1 and GluN2 ABDs (Site IV in Figure 3.1) and is critical for glycine-dependent inhibition by TCN-201 and TCN-213 (Hansen et al., 2012; McKay et al., 2012). Given the role of the ABD dimer interface in mediating allosteric coupling between the ATD and the ion channel gate (Gielen et al., 2008, 2009), and the importance of the ABD dimer interface of AMPA receptors for the activity of positive modulators such as cyclothiazide (Sun et al., 2002), we asked if the ABD dimer interface of NMDA receptors might contribute to potentiation by CIQ. Two residues in GluN1 contributing to the dimer interface, Phe754 and Arg755, were critical for inhibition of GluN1/GluN2A receptors by TCN-201 (Hansen et al., 2012), and mutation of these residues to alanine altered the binding of TCN-201. By contrast, CIQ potentiation was not altered at GluN1(F754A)/GluN2D and GluN1(R755A)/GluN2D receptors (Figure 3.3D). The S2 segment of the GluN2 ABD also contributes residues to the ABD dimer interface and introducing this region of GluN2A into GluN2D conferred inhibition by TCN-201 to GluN2D (Hansen et al., 2012). Yet, CIQ potentiation was not diminished in GluN2D chimeric receptors containing the entire ABD from GluN2A, i.e. 2D(2A S1S2), or just the S2 segment, as in the chimera 2D(2A S2) (Figure 3.3D). These data suggest positive allosteric modulation of GluN2C- or GluN2D-containing receptors is not mediated through the ABD dimer interface. These results are consistent with the

molecular determinants for CIQ residing outside the ATD and being more membrane-proximal than the ABD dimer interface.

Residues in the M1 helix affect CIQ potentiation

Previous studies identified a single amino acid residue in the M1 transmembrane helix of GluN2D, Thr592, that when mutated to the corresponding GluN2A residue (isoleucine) eliminated potentiation by CIQ (Mullasseril et al., 2010). To further explore the importance of the M1 helix in mediating potentiation by CIQ, we utilized alanine scanning mutagenesis of this region. A sequence alignment of the GluN1 and GluN2 NMDA receptor subunits together with the GluA2 AMPA receptor (Figure 3.4A) was used as a guide to individually mutate twenty-three residues in GluN2D to alanine (or cysteine if the wild type residue was alanine). These residues correspond to the residues comprising the M1 transmembrane helix in the GluA2 membrane-spanning crystal structure (Sobolevsky et al., 2009) and are shown in a homology model of GluN1/GluN2D in Figure 4B. We assessed the effects of 10 μM CIQ on these mutants and found six residues in GluN2D that when mutated to alanine reduced potentiation by CIQ: Val582, Trp583, Phe587, Val588, Leu591, and Thr592 (Figure 3.4C). Additionally, we found two residues that increased the potentiation by CIQ: Val584 and Met586 (Figure 3.4C). CIQ concentration-response curves (Figure 3.5, A and B) revealed varying effects of these mutations on CIQ potency and efficacy. CIQ potency, but not efficacy, was reduced at 2D(L591A) and 2D(T592A). By contrast, the efficacy of CIQ at 2D(V582A) and 2D(V588A) was significantly attenuated. CIQ caused no detectable potentiation at 2D(F587A). CIQ efficacy increased at 2D(V584A) and 2D(M586A) with little to no decrease in CIQ potency (Table 3.2). Currents elicited from 2D(W583A), however, were small (< 50 nA) and showed linear run down with agonist application, preventing reliable estimation of CIQ potency, consistent with previous studies

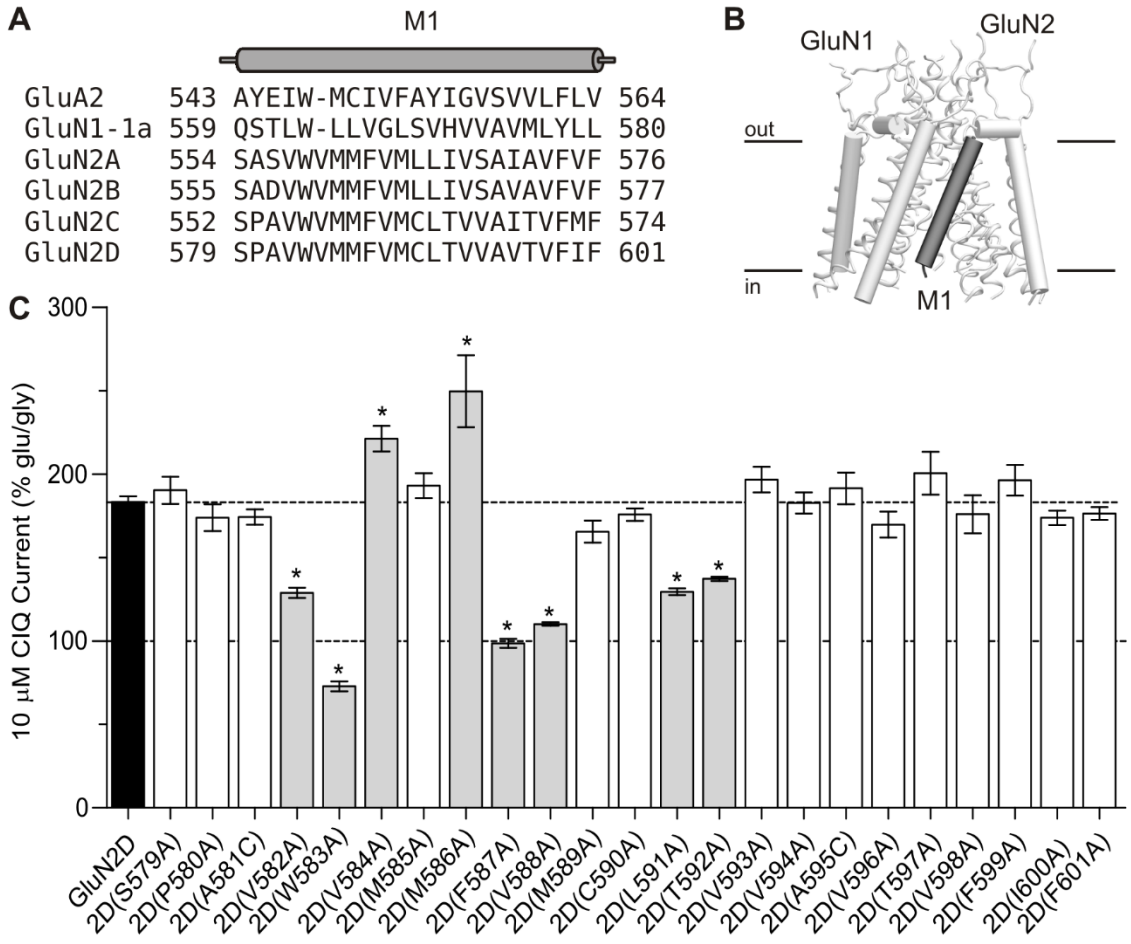

Figure 3.4. A, A sequence alignment of NMDA receptor subunits with GluA2 is shown. The M1 helix of GluA2 (Sobolevsky et al., 2009) is indicated as a cylinder above the alignment. **B,** The position of the GluN2D M1 helix is highlighted in a side-on view of the transmembrane region of a homology model of GluN1/GluN2D (Acker et al., 2011). **C,** GluN2D subunits with point mutations in the M1 transmembrane helix were co-expressed with GluN1 in *Xenopus laevis* oocytes and current responses recorded using two-electrode voltage clamp. Currents were first activated by 100 μM glutamate and 30 μM glycine and then 10 μM ClQ was co-applied with glutamate and glycine. * indicates a statistically significant change from wild type GluN1/GluN2D ($p<0.05$ One-way ANOVA with Dunnett's post-test) and those mutants are highlighted in gray. Responses were normalized to the glutamate- and glycine-induced current. Data are from 4-52 oocytes.

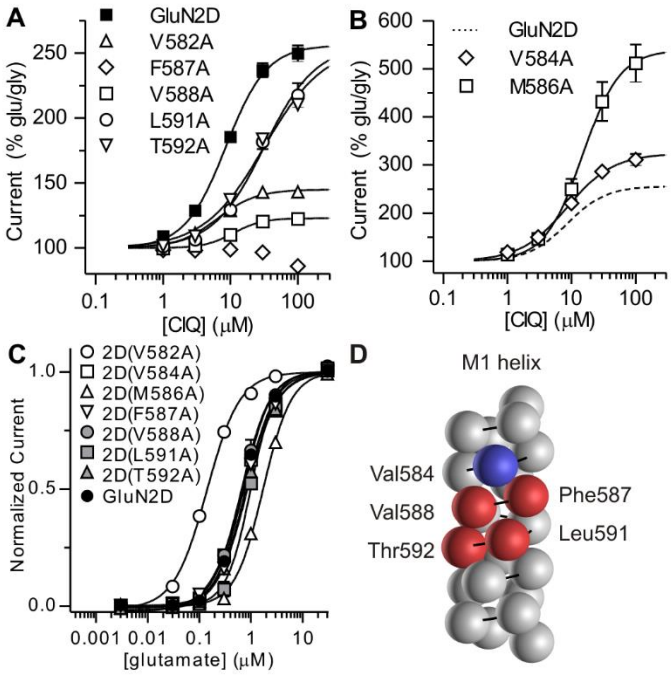

Figure 3.5. Currents were recorded under two-electrode voltage clamp in response to increasing concentrations of CIQ co-applied with glutamate (100 μM) and glycine (30 μM) to oocytes expressing GluN2D point mutants that attenuated CIQ potentiation (**A**) or enhanced CIQ potentiation (**B**). See Table II for CIQ EC_{50} values. Responses were normalized to the currents elicited by glutamate and glycine in the absence of CIQ. Data are from 4-32 oocytes. **C,** Glutamate concentration-response curves were measured using two-electrode voltage-clamp recordings of oocytes expressing the GluN2D point mutants from **A** and **B**. 30 μM glycine was co-applied with all glutamate concentrations. Glutamate EC_{50} values (Table II) measured for 2D(V582A) and 2D(M586A) were significantly different from GluN2D. Data are shown as mean ± SEM from 6-9 oocytes. **D,** Residues comprising the M1 helix are depicted as spheres on a generic protein α helix. Residues with diminished CIQ potentiation are colored red and those with increased CIQ potentiation are colored blue. The residues impacting modulation by CIQ but not glutamate potency cluster on one side of the α helix.

Table 3.2. CIQ, Glutamate, and Glycine EC_{50} Values for GluN2D Point Mutants

EC_{50} values were determined from two-electrode voltage-clamp recordings of *Xenopus laevis* oocytes expressing the indicated GluN1/GluN2D receptor. For CIQ EC_{50} determination, receptors were activated by 100 μM glutamate and 30 μM glycine at -40 mV; 5 mM 2-(hydroxypropyl)-β-cyclodextrin was present in all solutions. For glutamate EC_{50} measurements, glycine was 30 μM. For glycine EC_{50} measurements, glutamate was 100 μM. Data are from 4-36 oocytes. NE indicates no effect and ND indicates not determined

Mutant	Region	CIQ EC_{50} (μM)	100 μM CIQ Response (% glu/gly)	Glutamate EC_{50} (μM)	Glycine EC_{50} (μM)
GluN2D	--	9.3 ± 0.3	253 ± 5	0.82 ± 0.07	0.14 ± 0.02
2D(F574A)	pre-M1	13.0 ± 1.5*	150 ± 1	0.057 ± 0.003*	0.060 ± 0.001*
2D(L575A)	pre-M1	38 ± 18	53 ± 4	0.24 ± 0.03*	0.15 ± 0.02
2D(E576A)	pre-M1	10.7 ± 0.4	321 ± 12	0.178 ± 0.009*	0.106 ± 0.002
2D(P577A)	pre-M1	7.2 ± 0.6*	127 ± 2	0.398 ± 0.014	0.147 ± 0.002
2D(Y578A)	pre-M1	4.5 ± 0.4*	320 ± 30	0.0027 ± 0.0002*[a]	0.0011 ± 0.0001*[a]
2D(V582A)	M1	6.6 ± 0.6*	143 ± 3	0.17 ± 0.01*	0.04 ± 0.01*
2D(V584A)	M1	8.7 ± 0.7	311 ± 12	0.78 ± 0.04	0.14 ± 0.02
2D(M586A)	M1	15.3 ± 1.1*	510 ± 40	1.90 ± 0.12*	0.26 ± 0.01*
2D(F587A)	M1	NE	86 ± 3	0.80 ± 0.05	0.25 ± 0.02*
2D(V588A)	M1	11.3 ± 1.2	123 ± 3	0.93 ± 0.09	0.12 ± 0.02
2D(L591A)	M1	34.6 ± 5.9*	218 ± 9	0.99 ± 0.06	0.18 ± 0.01
2D(T592A)	M1	32.5 ± 2.9*	210. ± 4	1.06 ± 0.08	0.12 ± 0.02
N1(M813A)	M4	11.0 ± 0.7	337 ± 19	0.168 ± 0.008*	0.082 ± 0.003
N1(F817A)	M4	12.1 ± 0.6	430 ± 30	ND	ND

* $p<0.05$ vs. GluN2D, one-way ANOVA with Dunnett's post-hoc test

[a] The lowest concentration of glutamate tested, 3 nM, elicited currents greater than 100 nA from GluN1/GluN2D(Y578A) receptors. Therefore, the EC_{50} of glutamate was calculated by fixing the minimum current to be 0 pA.

(Kashiwagi et al., 2002; Thomas et al., 2006). In addition, mutation of this tryptophan to phenylalanine, 2D(W583F), did not affect CIQ modulation (10 μM CIQ response (% glu/gly) was 179 ± 6 for 2D(W583F) vs. 201 ± 7 for GluN2D, $p>0.05$ unpaired t-test, n=4). Hence, it is likely that this tryptophan residue is a critical structural element for the M1 helix and not necessarily involved with modulation by CIQ.

To assess the effects of these GluN2 M1 mutations on channel function, we recorded glutamate and glycine concentration-response curves (Figure 3.5C and Figure 3.6). We found glutamate and glycine potencies were significantly increased at 2D(V582A) (Table 3.2). By contrast, glutamate potency was reduced at 2D(M586A) (Table 3.2). No other M1 mutations affected glutamate or glycine potency. Although agonist potency is determined by both the affinity and efficacy of the agonist at the receptor, these residues do not comprise the agonist binding pocket (Furukawa et al., 2005; Vance et al., 2011) and therefore we expect that the affinity of glutamate and glycine remain unchanged at these mutants. Thus, we interpret the change in glutamate potency at 2D(V582A) and 2D(M586A) to reflect a change in the efficacy of glutamate, i.e. the ability of glutamate binding to cause the ion channel pore to open, and suggest these mutations alter gating of the receptor.

Next we asked whether the residues in the M1 helix that when mutated affect CIQ potentiation, but not glutamate potency, clustered in three-dimensional space. We plotted the residues comprising the M1 helix as spheres on a generic protein alpha helix, having 3.6 amino acids per turn and a 5.4 Å translation per turn, and highlighted the residues affecting CIQ potentiation (Figure 3.5D). Strikingly, the residues seemed to reside on only one side of the helix, suggesting these residues could all potentially interact directly with CIQ. It is also noteworthy that the equivalent residues in the GluA2 tetrameric crystal structure line “gaps” between the transmembrane domains that were

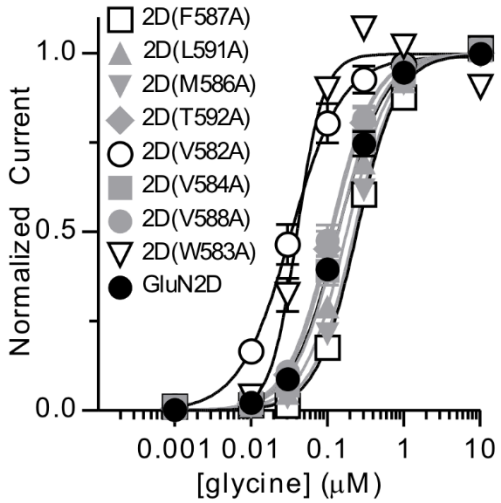

Figure 3.6 Glycine concentration-response curves were measured at the indicated GluN2D point mutant, co-expressed with GluN1, using two-electrode voltage-clamp recordings of oocytes. Receptors were co-activated by 100 μM glutamate at -40 mV. Individual curves were fit to the Hill equation, normalized to the fitted minimum and maximum and averaged. Data are mean ± SEM from 5-8 oocytes.

hypothesized to be occupied by amino acid residues from TARPs (Sobolevsky et al., 2009).

If CIQ interacts with residues in the M1 transmembrane helix, there may be other residues in this region of the receptor on either GluN1 or GluN2 that mediate potentiation by CIQ. To explore this idea, we used a homology model of GluN1/GluN2D (Acker et al., 2011) to identify residues located within 5 Å of the GluN2 M1 helix. The residues we identified resided in the M4 transmembrane helix of GluN1 and a short stretch of amino acids immediately extracellular to the GluN2 M1 helix. We mutated these residues and assessed potentiation by 10 μM CIQ. Only two residues in the M4 helix of GluN1 affected CIQ potentiation: GluN1(M813A) and GluN1(F817A) (Figure 3.7). While these residues do not cluster in three-dimensional space with the amino acids from the GluN2 M1 helix that affected CIQ modulation, they do occupy a provocative location in a homology model of GluN1/GluN2D. They are positioned on the GluN1 M4 helix such that their side chains protrude into a region between the M1 helix and the GluN2 M3 gate helix. For example, Met813 of GluN1 is about 4.5 Å from the serine in the SYTANLAAF motif of GluN2D. Thus, Met813 and Phe817 of the GluN1 M4 helix may be positioned to mediate interactions between the GluN2D M1 helix and the GluN2D M3 gate helix.

Additionally, we identified four residues in the GluN2D S1-M1 linker that influence positive modulation by CIQ: Phe574, Leu575, Pro577, and Tyr578 (Figure 3.8). These residues, which are immediately extracellular to the GluN2 M1 helix, are of interest because they form a purportedly crucial gating element for glutamate receptor ion channels. The corresponding amino acids in the tetrameric crystal structure of a GluA2 AMPA receptor form a cuff helix that is parallel to the membrane and makes Van der Waals contacts with the M3 helix that forms the gate (Sobolevsky et al., 2009). Moreover, the pre-M1 cuff helices in AMPA receptors have been proposed to be a key

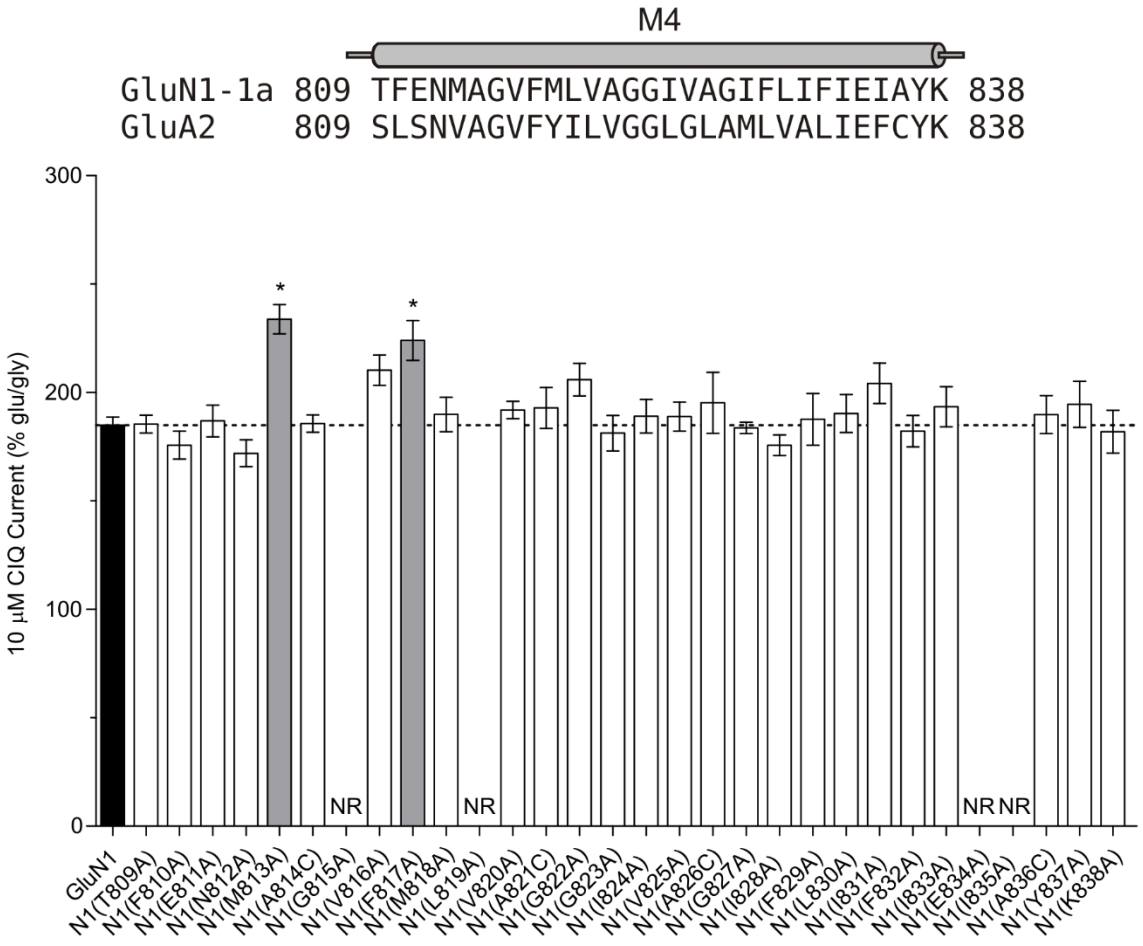

Figure 3.7. Residues comprising the M4 helix of GluN1 were individually mutated to alanine and co-expressed with GluN2D in oocytes. CIQ potentiation of glutamate- and glycine-stimulated currents was then measured using two-electrode voltage-clamp recordings. * indicates residues displaying significantly altered CIQ potentiation, which are also highlighted in gray ($p<0.05$, one-way ANOVA with Dunnett's post-hoc test). NR signifies that oocytes expressing the corresponding GluN1 point mutant failed to generate agonist-evoked currents larger than 5 nA in at least three separate injections of cRNA. Shown above the graph is an amino acid sequence alignment of the M4 region of GluN1 and GluA2; the M4 helix from the GluA2 crystal structure (Sobolevsky et al., 2009) is depicted as a cylinder on top of the alignment. Amino acids are numbered with the initiating methionine as 1.

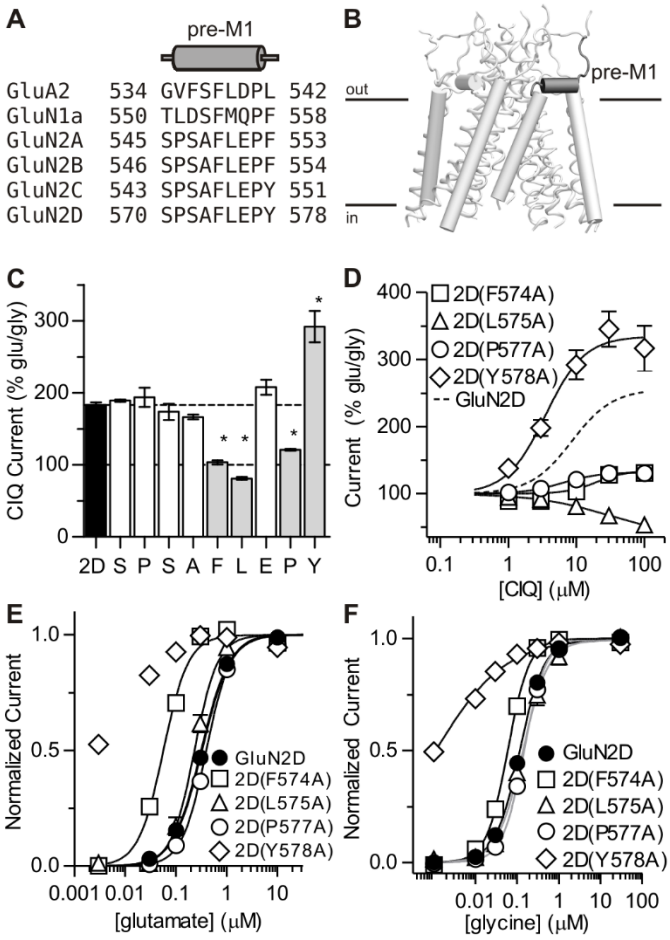

Figure 3.8. A, An amino acid sequence alignment of the preM1 region of NMDA receptor subunits and the GluA2 subunit is shown with the preM1 helix of the GluA2 crystal structure depicted above as a cylinder. **B,** The position of the GluN2D preM1 helix is illustrated in a homology model of GluN1/GluN2D viewed parallel to the membrane. The ATD and ABD are omitted for clarity. **C,** Residues comprising the GluN2D preM1 region were mutated to alanine and potentiation by 10 μM CIQ was measured using two-electrode voltage-clamp recordings of oocytes. Residues highlighted in gray and marked with an asterisk exhibited CIQ potentiation that was significantly different from GluN2D ($p<0.05$, one-way ANOVA with Dunnett's post-hoc test). **D,** CIQ concentration-response curves were evaluated on point mutants from **C** with altered CIQ modulation. CIQ EC_{50} values are given in Table II. The data from GluN2D is replicated from Figure **5A** for comparison. Data are depicted as mean ±

SEM and are from 3-4 oocytes. **E** and **F**, Glutamate and glycine concentration-response curves for the GluN2D mutants in **D** were measured using two-electrode voltage-clamp recordings (see Table II for EC_{50} values). Individual curves were normalized to fitted minimum and maximum currents for that curve except for 2D(Y578A). The lowest concentration of glutamate (3 nM) or glycine (1 nM) tested at 2D(Y578A) produced currents that were larger than 100 nA and were at least half of the maximal agonist-evoked response. Hence, curves for 2D(Y578A) were fixed to a minimum of zero. Data are presented as mean ± SEM and are from 3-6 oocytes.

determinant of receptor gating by restricting movement of the M3 helices in the closed state of the ion channel, but mediating channel opening upon agonist binding (Sobolevsky et al., 2009). The proposed role of the pre-M1 region in receptor gating is quite interesting given that CIQ increases the channel opening frequency in a gating step that precedes channel opening (Mullasseril et al., 2010). Consistent with the proposed role of these pre-M1 residues in receptor gating, we observed profound changes in both glutamate (Figure 3.8 and Table 3.2) and glycine (Figure 3.8 and Table 3.2) potencies for 2D(F574A) and 2D(Y578A).

Pre-M1 residues control channel open probability

We further explored the potential of these GluN2D pre-M1 residues to contribute to channel gating by estimating the open probability of the 2D pre-M1 alanine mutants using the onset of MK-801 inhibition (Blanke and VanDongen, 2008; Gielen et al., 2009; Vance et al., 2011). We expected that mutations at residues influencing gating would accelerate or decelerate MK-801 binding depending on whether the mutations increased or decreased gating efficiency, respectively. The time-course of MK-801 inhibition was dramatically slowed for 2D(F574A), 2D(L575A), 2D(E576A), and 2D(Y578A) (Figure 3.9), suggesting these residues are involved in mediating ion channel opening following agonist binding. Surprisingly, mutation of Pro577, which corresponds to an 'elbow' in the pre-M1 helix of GluA2 and is highly conserved across glutamate receptor ion channels but absent from K^+ channels (Sobolevsky et al., 2009), caused only a modest increase in the rate of onset of MK-801 inhibition. These results suggest that molecular determinants of CIQ potentiation converge on key determinants of receptor gating and imply an interesting mechanism of action whereby CIQ binding to the M1 helix of GluN2D increases the efficiency by which the pre-M1 region can promote channel opening.

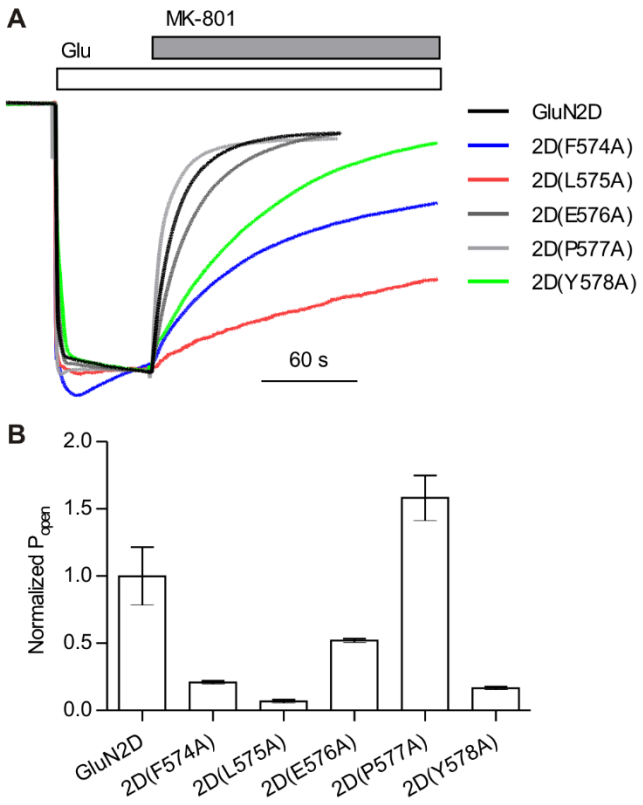

Figure 3.9. A, Shown are two-electrode voltage-clamp recordings illustrating the rate of block by MK-801 of GluN1/GluN2D receptors containing point mutations in the GluN2D preM1 helix. Currents were activated by 100 μM glutamate and 30 μM glycine at a holding potential of -60 mV followed by co-application of 200 nM (+)-MK-801. Traces were normalized to the glutamate/glycine current. **B,** Open probability (P_{open}) of GluN2D point mutations, calculated as the reciprocal of the time constant of onset of MK-801 block ($\tau_{MK\text{-}801\ block}$) and normalized to the values for GluN2D, are shown. Bars represent mean ± SEM for 3-10 oocytes.

CIQ cannot reach its modulatory site by diffusion through the membrane

The location of multiple residues that impact the action of CIQ clustered in the transmembrane region raised the possibility that CIQ was required to partition into the plasma membrane to exert its effects. To determine if this was the case, we recorded GluN1/GluN2D currents in the whole-cell configuration and included 10 μM CIQ in the recording pipette. We waited for 10 minutes after achieving the whole cell configuration to allow for dialysis of the cell and then co-applied 10 μM CIQ with glutamate and glycine to the exterior of the cell. We reasoned that if CIQ must partition into the membrane, then it could do so equally well from the intracellular or extracellular face. If CIQ included in the patch pipette entered the plasma membrane to access its site, then the receptors should pre-bind CIQ and no further potentiation would be observed when CIQ is applied extracellularly. However, when CIQ was included in the pipette solution, GluN1/GluN2D receptors were still potentiated by extracellular CIQ to the same extent as control cells with normal internal solution (Figure 3.10; $p>0.05$ vs. control pipette solution).

One possible caveat to this experiment is that CIQ could be a substrate for transporters in the cell, degradative enzymes, or otherwise be moved into organelles with a consequent decrease in its effective intracellular concentration. We therefore repeated this experiment in excised outside-out patches that lack all organelles and contain only about 1 μm^2 of membrane and associated cytoskeletal components. We selected patches containing multiple GluN1/GluN2D channels so as to avoid potential complications of variable activity of a single channel throughout the duration of the experiment and to maximize our ability to measure an increase in the average current response of the patch. The potentiation of GluN1/GluN2D receptors by CIQ applied to the exterior of the patch was comparable when the internal pipette solution contained no CIQ (control) or contained 10 μM CIQ (Figure 3.10; $p>0.05$ CIQ pipette solution vs.

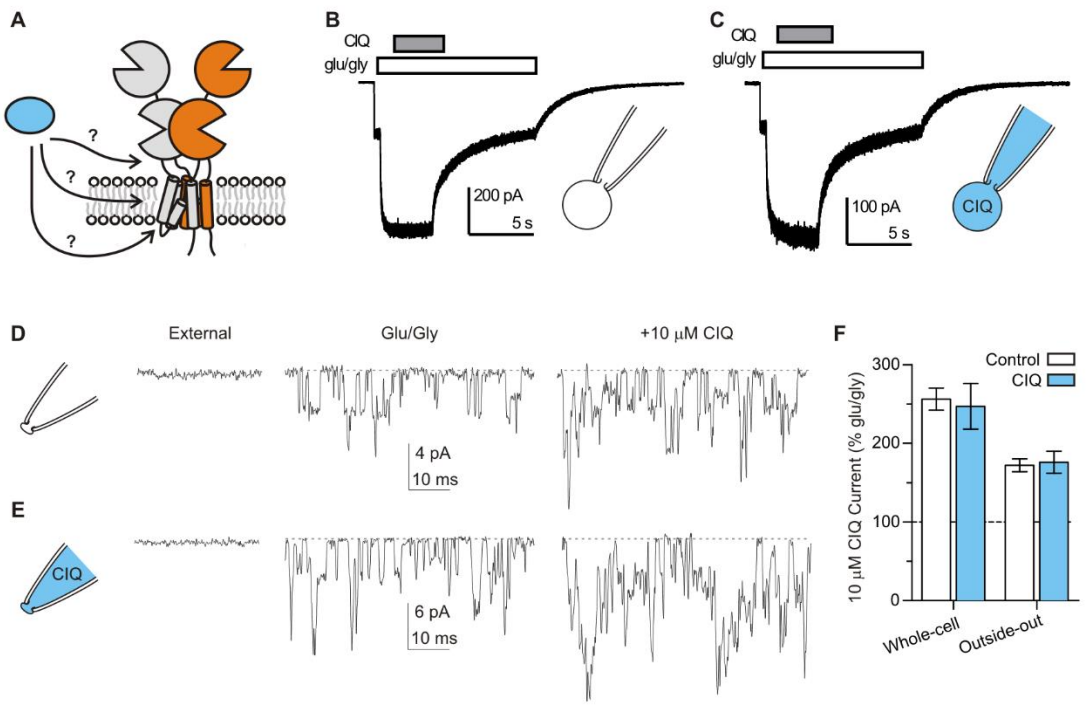

Figure 3.10. A, Potential routes by which CIQ can access residues in the M1 helix are illustrated in a schematic representation of GluN1/GluN2D receptors. For simplicity, only one pair of GluN1/GluN2 subunits is shown. CIQ could access its site directly from the extracellular solution, by first partitioning into the plasma membrane and then laterally diffusing to its site, or by first crossing the plasma membrane and then accessing the M1 helix from the cytosolic face of the receptor. **B,** A whole-cell voltage-clamp recording of an HEK cell expressing GluN1/GluN2D receptors is shown. Currents were activated by 100 μM glutamate and 50 μM glycine and then 10 μM CIQ was rapidly co-applied with glutamate and glycine. The pipette tip contained control internal solution and currents were recorded at least 10 minutes after breaking through the cell membrane. **C,** A whole-cell recording similar to **B** is shown, except the pipette tip contained internal solution that included 10 μM CIQ. **D,** An outside-out patch-clamp recording of GluN1/GluN2D receptors is shown at different times with the applied extracellular solution indicated above. Channels were activated by 100 μM glutamate and 50 μM glycine. Co-application of 10 μM CIQ with glutamate and

glycine increased the current response to 170% that of glutamate/glycine. **E,** An outside-out patch-clamp recording similar to **D** is shown except the pipette tip contained internal solution plus 10 μM CIQ. CIQ applied in the extracellular solution increased the current response to 220% that of glutamate/glycine. In both **D** and **E**, channel openings were recorded at least 5 minutes after pulling the patch. **F,** The results from experiments in **B-E** are summarized. Potentiation of GluN2D receptors by externally applied CIQ was not affected by pre-incubating the cytosolic face of the receptor with CIQ. Bars represent mean ± SEM from 5 cells or 3 patches.

control). These results are similar to those obtained in the whole cell configuration, and together suggest that CIQ cannot access its modulatory site from the intracellular side of the receptor nor by diffusion into the plasma membrane. Rather, direct extracellular aqueous access to the receptor appears necessary for positive modulation by CIQ.

Discussion

The most important conclusion of this study is that CIQ, a positive allosteric modulator of GluN2C- and GluN2D-containing NMDA receptors, does not bind the ATD. Rather, our data suggest that CIQ interacts with residues in the M1 transmembrane helix, and that CIQ potentiation is mediated by residues in the GluN2 pre-M1 region and the GluN1 M4 transmembrane helix. Moreover, we show for the first time that the GluN2 pre-M1 region may be a critical determinant of NMDA receptor gating. Mutations in this region not only influence allosteric regulation by CIQ, but also alter receptor open probability, assessed by the rate of onset of MK-801 channel block.

Structural determinants of CIQ potentiation reside in the transmembrane region

Although the linker between the ATD and ABD had been previously identified as a molecular determinant of CIQ action (Mullasseril et al., 2010), CIQ does not bind this region of the receptor because removal of the ATD and the ATD-ABD linker from both GluN1 and GluN2D did not affect CIQ potentiation. The actions of CIQ are in contrast to positive modulation of GluN1/GluN2B receptors by polyamines such as spermine, which seems to involve positive charges located on the lower lobe of the GluN2B ATD (Mony et al., 2011) and alternatively-spliced GluN1 ATD (Traynelis et al., 1995). Hence, the structural determinants of positive allosteric modulation by CIQ are distinct from those of polyamines. It remains to be determined whether the ATDs of GluN2C and GluN2D harbor binding sites for allosteric modulators and whether the downstream mechanisms of GluN2B potentiation by polyamines are conserved at GluN2C and GluN2D receptors.

The majority of residues in the GluN2D M1 helix critical for potentiation by CIQ cluster on one side of the helix (Figure 3.5D). However two of those residues (Val582 and Met586) are located on the opposite side of the helix. Mutation of both of these residues to alanine also changes glutamate potency, which likely reflects changes in gating of these mutants because these residues are situated far outside the agonist binding pocket. Perhaps mutation of these residues alters the conformation of the M1 helix thereby preventing CIQ from binding. Alternatively, these mutations change the manner in which the M1 helix moves upon agonist binding and by extension disrupt the changes that occur in gating when CIQ is present. In this context, it is interesting to note that in a homology model of GluN1/GluN2D, Val582 and Met586 of GluN2D are positioned within ~3 Å of Met813 and Phe817 in the GluN1 M4 helix, raising the possibility that these residues interact during channel gating. Moreover, these residues are also located adjacent to the M3 gate helix, in particular the serine in the conserved SYTANLAAF gating motif and two phenylalanines that are one and two helical turns below SYTANLAAF (Figure 3.11). Although further experiments would be needed to confirm interaction of these residues, it is tempting to speculate that Val582 and Met586 of GluN2D together with Met813 and Phe817 of GluN1 couple movement of the M1 helix upon agonist binding to movement of the M3 gate helix.

Of the five residues we identified in the GluN2 M1 helix that appear critical specifically to potentiation by CIQ (Val584, Phe587, Val588, Leu591, and Thr592; Figure 3.5D), only one of those residues, Thr592, differs between GluN2A/2B and GluN2C/2D. Indeed, CIQ did not potentiate GluN2D(T592I) receptors, in which this residue had been mutated to the homologous residue in GluN2A/2B (Mullasseril et al., 2010). We have further observed that mutation of this residue to valine also eliminates CIQ potentiation, whereas mutation to serine has no effect on CIQ potentiation (data not shown). Hence, hydrogen bond capabilities at this residue might be critical for the actions of CIQ and

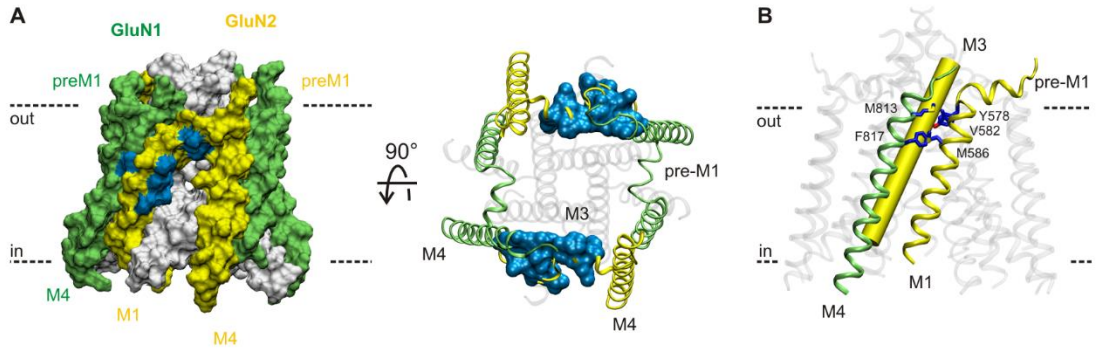

Figure 3.11. A, Amino acid residues at which mutations altered CIQ potentiation are depicted in a homology model of GluN1/GluN2D. For clarity, only the transmembrane region is shown. *Left*, The outside of the receptor viewed parallel with the membrane is shown as a surface representation. GluN1 is colored in green and GluN2D is colored in yellow. Residues affecting positive modulation by CIQ are highlighted in blue. *Right*, A view from the extracellular side of the receptor down the pore axis is shown. The preM1, M1, and M4 helices from all four subunits are colored (GluN1 in green and GluN2D in yellow). Residues impacting CIQ activity are highlighted in blue. **B,** The proximity of the GluN2D pre-M1 region and M1 helix, GluN1 M4 helix, and M3 gate helix is shown in a side-on view of the receptor. Residues Tyr578, Val582, and Met586 in GluN2D and Met813 and Phe817 in GluN1 are highlighted. These residues impacted both CIQ potentiation and glutamate potency when mutated to alanine. GluN1 is colored in green and GluN2D is colored in yellow.

may help explain the selectivity of CIQ for GluN2C/2D over 2A/2B. For example, CIQ may directly interact with the side chain of Thr592 and loss of the hydroxyl group, which occurs with the isoleucine residue at this position in GluN2A/2B, may prevent CIQ from binding. Alternatively, the side chain of Thr592 may be critical for conformational changes that occur downstream of CIQ binding and lead to increased channel openings.

Selectivity of CIQ for GluN2C/2D over GluN2A/2B could also arise from differences in the arrangement of the transmembrane helices in GluN2A/2B vs. GluN2C/2D. Perhaps the M1 helix of 2A/2B is rotated compared to the M1 helix in 2C/2D and thus the residues on the outside of the transmembrane region that could potentially interact with modulators are different. It is also likely that movements of the transmembrane helices upon agonist binding differs between 2A/2B and 2C/2D given the markedly different open and closed times of these receptors (Traynelis et al., 2010). Hence, functional rearrangements of the transmembrane helices may be differentially sensitive to modulation by CIQ.

Role of pre-M1 region in gating

Several lines of evidence implicate the pre-M1 region in gating of glutamate receptors. In AMPA receptors, changes in receptor leak currents occur when amino acids on the M3 helix facing the pre-M1 helix are mutated to cysteine and reacted with MTS reagents, suggesting these residues are important for gating of AMPA receptors (Sobolevsky et al., 2003). Additionally, residues at the interface of the pre-M1 and M4 helices were critical for noncompetitive inhibition of AMPA receptors by GYKI- 53655 and CP-465,022 (Balannik et al., 2005). In NMDA receptors, mutations in the pre-M1 region of GluN1 (Gln556 and Pro557; (Kashiwagi et al., 2002)) and GluN2C (Glu530 and Ser533; (Sobolevsky et al., 2007)) result in either spontaneously active channels or channels that become spontaneously active upon modification by MTS reagents.

Moreover, introduction of cysteines at several residues in the preM1 region of GluN2A resulted in channels with small or abnormal glutamate-activated currents (Thomas et al., 2006). Mutations in the preM1 region giving rise to spontaneously active channels (either alone or after reaction with MTS reagents) may reflect a shift in the gating equilibrium towards the open state, that is, an increase in the gating efficiency, which has been shown for several residues in the S1-M1 linker (Talukder et al., 2010). In a complementary way, mutations yielding receptors with small glutamate-activated currents may be due to uncoupling of the ion channel pore from agonist binding.

In this study, mutations in the pre-M1 region of GluN2D at Phe574, Leu575, and Pro577, disrupted positive modulation by CIQ. CIQ potentiates the receptor by accelerating a pre-gating step, thereby increasing the opening frequency of the receptor (Mullasseril et al., 2010). Hence, mutations at these pre-M1 residues likely disrupt the gating steps accelerated by CIQ. By contrast, mutation at Tyr578 enhanced both the potency and maximum effect of CIQ potentiation. This effect may be explained by increased space for CIQ to interact with the receptor as the larger side chain of tyrosine was replaced with the smaller methyl group of alanine. However, the alanine also lacks the hydrogen bond capabilities of the tyrosine, which may interact with the thioether of Met813 on GluN1 (Figure 3.11). It is worth noting that both 2D(Y578A) and N1(M813A) receptors displayed large leak currents in the absence of glutamate. These leak currents were blocked by 1 mM Mg^{2+} and 1 μM (+)-MK-801 and could be potentiated by 10 μM CIQ (data not shown) suggesting these currents were mediated by NMDA receptors.

While residues in pre-M1 region seem critical for potentiation of NMDA receptors by CIQ, residues in a similar region of AMPA receptors mediate noncompetitive inhibition (Balannik et al., 2005) and it remains an open question whether noncompetitive inhibition of NMDA receptors may be achieved through the pre-M1

region. We hypothesize that compounds exist that can act at this site to bring about negative allosteric modulation, rendering it functionally analogous to the benzodiazepine site on GABA receptors at which ligands can have positive, neutral, or negative actions.

Chapter 4: Subunit-Selective Allosteric Inhibition of Glycine Binding to NMDA Receptors[1]

[1] This chapter has been published: Hansen KB, Ogden KK, and Traynelis SF (2012) Subunit-Selective Allosteric Inhibition of Glycine Binding to NMDA Receptors. *J. Neurosci.* 32:6197–6208

Abstract

NMDA receptors are ligand-gated ion channels that mediate excitatory neurotransmission in the brain, and are involved in numerous neuropathological conditions. NMDA receptors are activated upon simultaneous binding of co-agonists glycine and glutamate to the GluN1 and GluN2 subunits, respectively. Subunit-selective modulation of NMDA receptor function by ligand binding to modulatory sites distinct from the agonist binding sites could allow pharmacological intervention with therapeutically beneficial mechanisms. Here, we show the mechanism of action for TCN-201, a new GluN1/GluN2A-selective NMDA receptor antagonist whose inhibition can be surmounted by glycine. Electrophysiological recordings from chimeric and mutant NMDA receptors suggest that TCN-201 binds to a novel allosteric site located at the dimer interface between the GluN1 and GluN2 agonist binding domains. Furthermore, we demonstrate that occupancy of this site by TCN-201 inhibits NMDA receptor function by reducing glycine potency. TCN-201 is therefore a negative allosteric modulator of glycine binding.

Introduction

Ionotropic glutamate receptors, which include N-methyl-D-aspartate (NMDA), α-amino-3-hydroxy-5-methyl-4-isoxazolepropionate (AMPA), and kainate receptors, are ligand-gated ion channels that mediate fast excitatory neurotransmission in the central nervous system (Traynelis et al., 2010). NMDA receptors are involved in a myriad of neurological processes, including neuronal development and experience-dependent plasticity, but are also implicated in numerous neuropathological conditions, such as stroke, traumatic brain injury, Alzheimer's, and Parkinson's diseases (Kalia et al., 2008; Traynelis et al., 2010). NMDA receptors are tetramers comprising two GluN1 and two GluN2 subunits (Ulbrich and Isacoff, 2007). The GluN1 subunit is an obligate part of all NMDA receptors and is widely expressed in the central nervous system. By contrast, the different GluN2 subunits (GluN2A-D) have distinct temporal and spatial expression in the brain (Watanabe et al., 1992; Ishii et al., 1993; Monyer et al., 1994). Furthermore, the different GluN2 subunits endow NMDA receptors with markedly different biophysical and pharmacological properties (Monyer et al., 1992; Vicini et al., 1998; Gielen et al., 2009; Yuan et al., 2009).

Since the discovery of ifenprodil as a non-competitive NMDA receptor antagonist with over 500-fold selectivity for GluN2B-containing NMDA receptors (Williams, 1993), there has been considerable focus on the development of subunit-selective antagonists for therapeutic gain (Kalia et al., 2008; Ogden and Traynelis, 2011). Ifenprodil and related GluN2B-selective antagonists have proven to be invaluable tools to dissect the contribution of specific NMDA receptor subtypes to neurophysiological processes (Mony et al., 2009; Hansen et al., 2010). Despite the utility of GluN2B-selective antagonists, there has been a lag in discovery of antagonists selective for other GluN2 subunits. However, several recent reports describe novel subunit-selective ligands for GluN2C- and GluN2D-containing receptors (Mosley et al., 2010; Costa et al., 2010; Mullasseril et

al., 2010; Hansen and Traynelis, 2011; Acker et al., 2011). In addition, a new class of antagonists selective for GluN2A- over GluN2B-containing NMDA receptors was recently described (Bettini et al., 2010; McKay et al., 2012). Inhibition of GluN1/GluN2A receptors by a compound in this class, 3-chloro-4-fluoro-N-[(4-[(2-(phenylcarbonyl)hydrazino)carbonyl]phenyl)methyl]-benzenesulfonamide (hereafter referred to as TCN-201; see Figure 4.1A), was surmounted by glycine, but not glutamate, suggestive of competitive inhibition at the glycine binding site. However, it remains unclear how TCN-201 inhibition can discriminate between GluN2 subunits and yet, at the same time, be surmounted by agonist binding to the GluN1 subunit.

To facilitate development of therapeutic agents, it is important to identify modulatory binding sites on the NMDA receptor. To this end, we investigated the mechanism of action for TCN-201 inhibition. We show that TCN-201 binding reduces potency of agonists at the GluN1 subunit and vice versa. We identify residues located at the dimer interface between the GluN1 and GluN2 agonist binding domains that control the subunit-selectivity of TCN-201 inhibition. The results demonstrate that TCN-201 is a negative allosteric modulator of glycine binding, and implicate the agonist binding domain interface between GluN1 and GluN2 as a putative binding site for allosteric modulators of NMDA receptors.

Results

Binding of TCN-201 reduces potency of glycine at the GluN1 subunit

To assess the selectivity profile of TCN-201 across the different NMDA receptor subtypes, we determined the concentration-effect relationship for TCN-201 at recombinant GluN1/GluN2A, GluN1/GluN2B, GluN1/GluN2C, or GluN1/GluN2D receptors expressed in Xenopus oocytes using two-electrode voltage-clamp recordings.

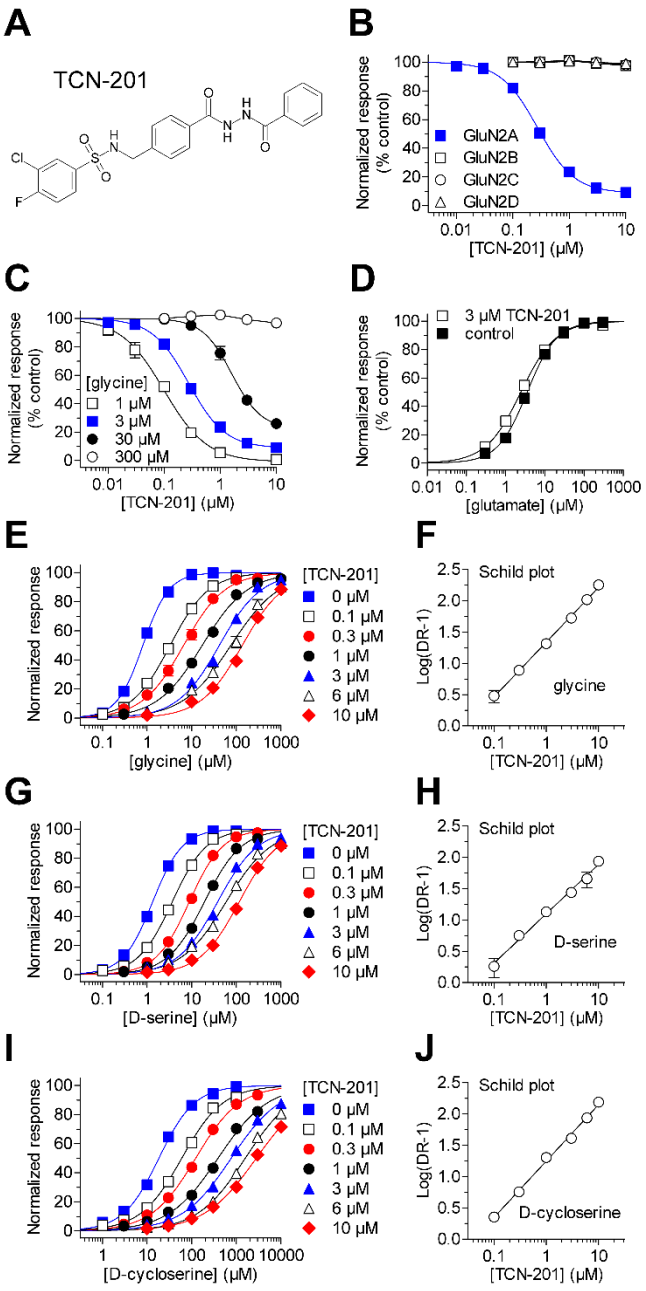

Figure 4.1 TCN-201 Selectively Inhibits GluN1/GluN2A Receptors

(**A**) Chemical structure of 3-chloro-4-fluoro-N-[(4-[(2-(phenylcarbonyl)hydrazino)carbonyl]phenyl)methyl]-benzenesulfonamide (TCN-201; Bettini et al., 2010). (**B**) The effects of increasing concentrations of TCN-201 on responses to 100 μM glutamate plus 3 μM glycine from recombinant NMDA receptors expressed in *Xenopus* oocytes were measured using two-electrode voltage-clamp

recordings. Data are from 4-25 oocytes. (**C**) Concentration-response data for TCN-201 inhibition of GluN1/GluN2A activated by 100 µM glutamate plus different concentrations of glycine (1 - 300 µM). The data obtained in the presence of 300 µM glycine could not be fitted to the Hill equation. Data are from 5-25 oocytes. (**D**) Glutamate concentration-response data for GluN1/GluN2A co-activated by 30 µM glycine in the absence (control) and presence of 3 µM TCN-201. Glutamate EC_{50} was 3.6 $\pm$ 0.2 µM (N = 8) in the absence of TCN-201 and 2.5 $\pm$ 0.1 µM (N=7) in the presence of TCN-201. (**E**) Glycine concentration-response data for GluN1/GluN2A co-activated by 100 µM glutamate in the absence (0 µM) and presence of increasing concentrations of TCN-201. Data are from 5-7 oocytes. (**F**) A Schild plot of the glycine concentration-response data produced a pA_2 value of 7.53 corresponding to 30 nM and a Schild slope of 0.87 (95% confidence interval 0.83-0.92). (**G**) D-serine concentration-response data for GluN1/GluN2A in 100 µM glutamate. Data are from 6-8 oocytes. (**H**) A Schild plot of the D-serine concentration-response data produced a pA_2 value of 7.39 corresponding to 41 nM and a Schild slope of 0.79 (95% confidence interval 0.69-0.89). (**I**) D-cycloserine concentration-response data for GluN1/GluN2A in 100 µM glutamate. Data are from 5-7 oocytes for each condition. (**J**) A Schild plot of the D-cycloserine concentration-response data produced a pA_2 value of 7.39 corresponding to 41 nM and a Schild slope of 0.90 (95% confidence interval 0.82-0.98).

TCN-201 completely inhibited responses from GluN1/GluN2A receptors activated by 100 μM glutamate plus 3 μM glycine with an IC_{50} value of 320 nM (Fig. 4.1B and Table 4.1). In contrast to its effects on GluN2A-containing receptors, TCN-201 did not inhibit responses from GluN2B-, GluN2C-, or GluN2D- containing NMDA receptors (Fig. 4.1B and Table 4.1). Moreover, TCN-201 inhibition was not affected by the presence of exon 5 in GluN1, which encodes 21 amino acids in the amino terminal domain. GluN1-1a/GluN2A receptors, which lack exon 5, were inhibited to 45 ± 3% of control (N = 7), and GluN1-1b/GluN2A receptors, which contain exon 5, were inhibited to 49 ± 2% of control (N = 6) by 3 μM TCN-201 in the presence of 30 μM glycine. In addition, 10 μM TCN-201 did not affect responses activated by 100 μM glutamate from GluA1 AMPA receptors (N = 8) or GluK2 kainate receptors (N = 10) (data not shown). Thus, TCN-201 displays strong selectivity, estimated to be >1000-fold, for GluN2A-containing NMDA receptors at a glycine concentration of 3 μM.

Because TCN-201 inhibition was surmounted by high glycine concentrations (Bettini et al., 2010), we evaluated the extent to which glycine shifts TCN-201 potency at GluN1/GluN2A by generating TCN-201 concentration-inhibition data at different concentrations of glycine (Fig. 4.1C and Table 4.1). In agreement with previously published observations (Bettini et al., 2010), TCN-201 potency was reduced by increasing concentrations of glycine. For example, the IC_{50} of TCN-201 was increased 16-fold from 100 nM in the presence of 1 μM glycine to 1.6 μM in the presence of 30 μM glycine. There was no detectable inhibition of GluN1/GluN2A by 10 μM TCN-201 in the presence of 300 μM glycine. In a reciprocal manner, the potency of glycine at GluN1/GluN2A was reduced in the presence of increasing TCN-201 concentrations with no effects on the maximal response (Fig. 4.1E and Table 4.1). The EC_{50} of glycine increased 100-fold from 1.5 μM in the absence of TCN-201 to 150 μM in the presence of 10 μM TCN-201 (Table 4.1). By contrast, the EC_{50} of glutamate at GluN1/GluN2A was

Table 4.1. TCN-201 and glycine potencies for wild type and mutant NMDA receptors.

	TCN-201 activity					Glycine activity			
NMDA receptor (GluN1/GluN2X)	**[glycine]** (μM)	**IC_{50}** (μM)	**n_H**	**Max. % inhibition**	**N**	**[TCN-201]** (μM)	**EC_{50}** (μM)	**n_H**	**N**
GluN2A	1	0.10 ± 0.01	1.2	100 ± 1	5	0	1.1 ± 0.1	1.4	7
GluN2A	3	0.32 ± 0.04	1.5	81 ± 1	25	10	150 ± 10	0.9	6
GluN2A	30	1.6 ± 0.2	2.2	73 ± 2	12				
GluN2A	300	N.E.			6				
2A-(2D S1)	3	0.23 ± 0.02	1.5	97 ± 1	8		N.D.		
2A-(2D S2)	3	N.E.					N.D.		
GluN2B	3	N.E.			5	0	0.3 ± 0.1	1.2	6
GluN2B						10	0.6 ± 0.2	1.1	4
GluN2B F784V	3	6.8 ± 0.4	1.2	N.D.	6	0	0.8 ± 0.4	1.2	4
GluN2B F784V						10	5.5 ± 0.5	1.5	4
GluN2B L783F+F784V	3	4.4 ± 0.2	1.3	N.D.	5	0	0.6 ± 0.1	1.2	5
GluN2B L783F+F784V						10	9.5 ± 0.5	1.5	6
GluN2C	3	N.E.			4		N.D.		
GluN2D	3	N.E.			4		N.D.		
GluN2D L808V	3	72% control at 10 μM TCN-201			5		N.D.		
2D-(2A S1)	3	N.E.					N.D.		
2D-(2A S2)	3	1.6 ± 0.1	2.1	91 ± 4	6		N.D.		
GluN2A V783L	3	70% control at 10 μM TCN-201			5	0	0.6 ± 0.1	1.4	3
GluN2A V783L						10	3.7 ± 0.3	1.3	4
GluN2A G786D	3	1.4 ± 0.1	1.7	82 ± 3	5	0	0.4 ± 0.01	1.5	3
GluN2A G786D						10	22 ± 2	1.1	4
GluN2A E790M	3	0.60 ± 0.04	1.4	90 ± 3	6	0	1.0 ± 0.01	1.4	6
GluN2A M788I	3	1.0 ± 0.1	1.3	79 ± 3	5	0	0.8 ± 0.1	1.5	4
GluN2A T793R	3	0.32 ± 0.03	2.2	94 ± 2	6	0	2.4 ± 0.4	1.5	6
GluN2A V783A	3	0.23 ± 0.02	1.1	91 ± 2	5	0	2.4 ± 0.1	1.0	4
GluN2A V783F	3	1.9 ± 0.1	1.8	80 ± 2	4	0	0.5 ± 0.1	1.3	5
GluN2A V783W	3	0.036 ± 0.003	1.0	95 ± 2	4	0	4.6 ± 0.2	1.4	4
GluN2A V783S	3	0.66 ± 0.06	1.4	89 ± 3	4	0	1.4 ± 0.1	1.3	4
GluN2A V783T	3	0.81 ± 0.06	1.5	91 ± 1	4	0	1.5 ± 0.1	1.2	4
GluN2A V783H	3	0.060 ± 0.010	0.9	93 ± 4	4	0	3.8 ± 0.2	1.4	4
GluN2A V783D	3	0.27 ± 0.01	1.2	92 ± 2	4	0	6.3 ± 0.7	1.3	4
GluN2A P527A	3	0.48 ± 0.06	1.4	91 ± 3	4	0	1.5 ± 0.1	1.2	6
GluN2A L777A	3	0.072 ± 0.017	1.2	98 ± 1	4	0	2.0 ± 0.1	1.3	6
GluN2A L779A	3	0.52 ± 0.07	1.3	88 ± 5	4	0	1.1 ± 0.1	1.3	6
GluN2A L780A	3	67% control at 10 μM TCN-201			6	0	1.3 ± 0.1	1.1	6
GluN2A Q781A	3	0.78 ± 0.03	1.9	94 ± 2	4	0	0.6 ± 0.07	1.1	6
GluN2A G786A	3	1.1 ± 0.1	1.8	87 ± 3	5	0	0.4 ± 0.03	1.0	6
GluN2A M788A	3	0.62 ± 0.02	1.4	90 ± 3	4	0	1.1 ± 0.1	1.3	6
GluN2A E789A	3	0.15 ± 0.01	1.4	96 ± 1	4	0	4.6 ± 0.4	1.3	6
GluN1 I519A	3	1.1 ± 0.1	1.9	80 ± 2	8	0	1.5 ± 0.1	1.3	4
GluN1 F754A	3	0.048 ± 0.002	1.4	98 ± 1	4	0	2.3 ± 0.1	1.6	4
GluN1 R755A	3	79% control at 10 μM TCN-201			4	0	4.4 ± 0.2	1.1	4

TCN-201 IC_{50} ± SEM and glycine EC_{50} ± SEM was determined using two-electrode voltage-clamp recordings at wild type and mutant GluN2 subunits co-expressed with GluN1 in *Xenopus* oocytes (GluN1/GluN2X). The receptors were activated by 100 µM glutamate plus the indicated concentration of glycine in the presence of the indicated concentration of TCN-201. Maximal inhibition (± SEM) was calculated as control response in the absence of TCN-201 minus residual current at saturating concentrations of TCN-201 relative to control response. GluN1 mutants were co-expressed with GluN2A. N.E. indicates no effect at 10 µM TCN-201. N.D. indicates not determined. N is the number of oocytes used to generate the data, and n_H is the Hill slope.

only slightly reduced from 3.6 ± 0.2 μM (N = 8) in the absence of TCN-201 to 2.5 ± 0.1 μM (N=7) in the presence of 3 μM TCN-201 (Fig. 4.1D). One potential interpretation of these results could be that TCN-201 is a competitive antagonist at the glycine binding site of the GluN1 subunit. However, a competitive mechanism at the GluN1 subunit would be unexpected, since TCN-201 displays a remarkable selectivity for GluN1/GluN2A over other NMDA receptor subtypes that contain different GluN2 subunits.

TCN-201 is not a competitive antagonist at the GluN1 subunit

Schild analysis is a valuable approach to determine pA_2, an empirical measure of potency defined as the negative logarithm of the antagonist concentration that produces a 2-fold shift of the agonist concentration-response curves (i.e. agonist EC_{50}) (Arunlakshana and Schild, 1959; see also Wyllie and Chen, 2007). For competitive antagonists, pA_2 can be considered a measure of the equilibrium constant for binding (i.e. $pA_2 = -\log K_b$), and a linear fit of the Schild plot should have unitary slope (see Materials and Methods) (Arunlakshana and Schild, 1959). However, a slope that is significantly different from 1 suggests a noncompetitive mechanism of action, such as negative allosteric modulation of agonist binding (Kenakin, 2009).

We generated a Schild plot to evaluate the actions of TCN-201. Using the glycine EC_{50} at increasing concentrations of TCN-201, we calculated a dose-ratio (DR) for each antagonist concentration. The linear fit to the data in the resulting Schild plot produced a pA_2 value of 7.53 corresponding to 30 nM and a Schild slope of 0.87, which is significantly different from 1 (95% confidence interval 0.83-0.92) (Fig. 4.1F). Since the Schild slope is less than unity, the pA_2 value is only an estimate of $-\log K_b$ for TCN-201. We also evaluated the effects of TCN-201 on the potency of two other GluN1 agonists, D-serine and D-cycloserine (Figs. 4.1G-J). For both D-serine and D-cycloserine, Schild

plots of the TCN-201 antagonism gave pA_2 values of 7.39 corresponding to 41 nM, similar to the pA_2 value for TCN-201 shift of glycine potency. For D-serine the Schild slope was 0.79 (95% confidence interval 0.69-0.89) and for D-cycloserine the slope was 0.90 (95% confidence interval 0.82-0.98); in both cases the slope was significantly different from 1. Thus, Schild plots produced slopes significantly lower than 1 for all three GluN1 agonists, suggesting that the mechanism of TCN-201 inhibition is not direct competitive antagonism between TCN-201 and GluN1 agonist at the orthosteric agonist binding site. One possible mechanism of action that can explain the observed results could be that TCN-201 is a negative allosteric modulator of agonist binding to the GluN1 subunit.

Inhibition by TCN-201 is controlled by the agonist binding domain interface

To evaluate the structural determinants of TCN-201 inhibition, we used a chimeric strategy exploiting the selectivity between GluN2A and GluN2D subunits. We first replaced the GluN2A amino-terminal domain, agonist binding domain, and transmembrane domain with homologous regions of the GluN2D subunit and evaluated inhibition by 3 μM TCN-201 of the chimeric receptors activated by 100 μM glutamate plus 30 μM glycine (Figs. 4.2A and B). Replacing the GluN2A amino-terminal domain or transmembrane region with those of GluN2D did not reduce inhibition by TCN-201. Similarly, deleting the entire amino-terminal domain of GluN2A also did not reduce inhibition by TCN-201. By contrast, TCN-201 inhibition was abolished when the entire agonist binding domain of GluN2A was replaced with that of GluN2D. We further divided the agonist binding domain into segments S1 and S2 (Hansen and Traynelis, 2011). Replacing S1 of GluN2A with that of GluN2D did not affect TCN-201 sensitivity, whereas no inhibition was observed upon replacement of S2 (Fig. 4.2C and Table 4.1). Consistent with this results, replacing S2 in GluN2D with that of GluN2A resulted in

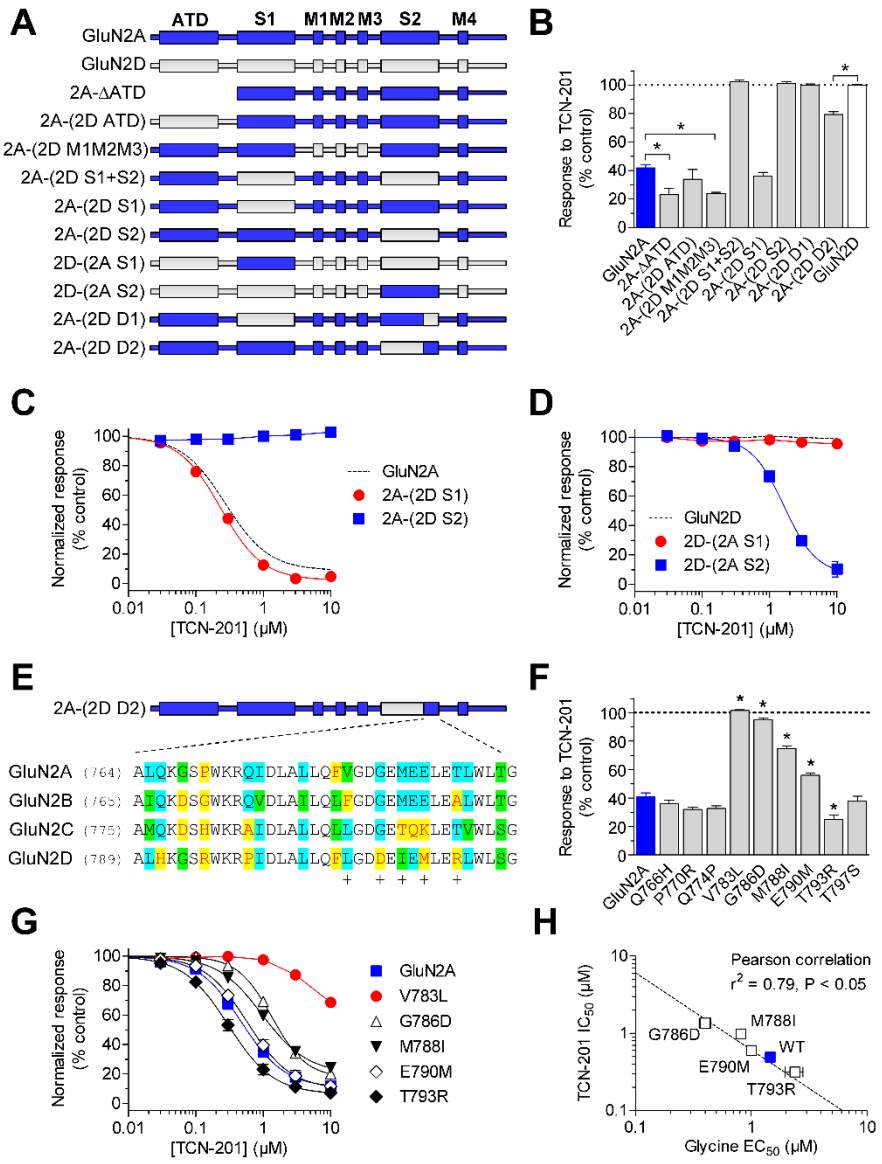

Figure 4.2. Structural determinants for TCN-201 activity are located in the S2 segment of the agonist binding domain. (**A**) Linear representations of the polypeptide chains of GluN2A (blue) and GluN2D (grey), as well as chimeric GluN2A-GluN2D subunits (see Materials and Methods for chimeric junctions) show the amino terminal domain (ATD), S1 and S2 segments of the agonist binding domain, transmembrane helices (M1, M3, and M4), and the re-entrant pore loop (M2). (**B**) Bar graph summarizing inhibition by 3μM TCN-201 of responses to 100 μM glutamate plus 30 μM glycine for wild type and chimeric GluN2 subunits co-expressed with GluN1. Data

are from 4-9 oocytes. * indicates significantly different from GluN1/GluN2A (blue bar) or GluN1/GluN2D (white bar) ($P < 0.05$; one-way ANOVA with Tukey-Kramer post test). TCN-201 concentration-response data for inhibition of responses to 100 µM glutamate plus 3 µM glycine were generated for (**C**) 2A-(2D S1) and 2A-(2D S2) chimeras, as well as for (**D**) 2D-(2D S1) and 2D-(2A S2) chimeras co-expressed with GluN1 in *Xenopus* oocytes. Dashed lines are data for wild type NMDA receptors as shown in Figure 4.1B. Data are from 4-25 oocytes. (**E**) Amino acid sequence alignment of the last residues of the S2 segment from GluN2A-D, which contains the structural determinants for TCN-201 inhibition. + below the sequences indicates that TCN-201 sensitivity was significantly changed when the residue in GluN2A was mutated. (**F**) Inhibition by 3 µM TCN-201 of responses to 100 µM glutamate plus 30 µM glycine from wild type and mutant GluN2A subunits co-expressed with GluN1. Data are from 4-7 oocytes. * indicates significantly different from GluN1/GluN2A (blue bar) ($P < 0.05$; one-way ANOVA with Tukey-Kramer post test). (**G**) Concentration-response data for TCN-201 inhibition of NMDA receptors activated by 100 µM glutamate plus 3 µM glycine. Data are from 5-10 oocytes. (**H**) TCN-201 IC_{50} values plotted versus glycine EC_{50} values for mutant GluN2A subunits. Data for GluN2A V783L is excluded from this analysis, since the TCN-201 IC_{50} could not be determined for this mutant. There is a significant correlation between glycine EC_{50} values and TCN-201 IC_{50} values for the depicted GluN2A mutants (Pearson test for correlation, $r^2 = 0.79$, $P < 0.05$). See Table 4.1 for IC_{50} values and EC50 values.

TCN-201 inhibition with an IC_{50} of 1.6 ± 0.1 µM (N = 6), whereas replacing S1 of GluN2D with that of GluN2A did not introduce TCN-201 sensitivity (Fig. 4.2D and Table 4.1).

We subsequently divided the agonist binding domain into the upper D1 lobe of the clamshell-like structure and the lower D2 lobe (Furukawa et al., 2005). Replacing the D1 lobe of GluN2A with that of GluN2D eliminated TCN-201 inhibition, but some TCN-201 activity was retained upon replacement of the D2 lobe (Fig. 4.2B). In these chimeric GluN2 subunits, replacement of the D1 lobe is equivalent to the combined replacement of the entire segment S1, which has no effect on TCN-201 inhibition, as well as a smaller portion of segment S2 (Fig. 4.2A). The molecular determinants of TCN-201 action could therefore be located in this smaller portion of S2, since these residues are sufficient to eliminate TCN-201 activity.

The portion of S2 that comprises the determinants of TCN-201 action differs by only nine amino acids between GluN2A and GluN2D (Fig. 4.2E). We individually mutated these nine residues in GluN2A to the corresponding residues in GluN2D and found that five of these mutations (GluN2A V783L, G786D, M788I, E790M, and T793R) significantly affected the inhibition by 3 µM TCN-201 (Fig. 4.2F). TCN-201 concentration-inhibition data of responses activated by 100 µM glutamate plus 3 µM glycine confirmed effects of these five mutations on TCN-201 potency (Fig. 4.2G and Table 4.1). The most prominent reduction in TCN-201 potency was observed for GluN2A V783L, which was only inhibited to 70% of control by 10 µM TCN-201. To evaluate potential interactions between glycine binding and TCN-201 activity on NMDA receptors containing mutant GluN2A subunits, we determined glycine EC_{50} values in the absence of TCN-201. Interestingly, all of the GluN2A mutations identified by the chimeric approach affected glycine potency (Table 4.1). There was significant correlation between glycine EC_{50} values and TCN-201 IC_{50} values for four of the GluN2A mutants (Fig. 4.2H). Since it was not possible to reliably determine TCN-201 IC_{50} for GluN2A V783L given the limits of

TCN-201 solubility (see Materials and Methods), data for this mutant was not included in the test for correlation. Glycine EC_{50} for NMDA receptors containing GluN2A V783L was 0.6 µM, which is 1.8-fold lower than the EC_{50} of 1.1 µM for wild type GluN1/GluN2A (Table 4.1). Because inhibition of GluN2A V783L could not be accounted for by a shift in glycine potency, we speculate that GluN2A Val783 could be directly involved in TCN-201 binding. By contrast, the effects of the other GluN2A mutations on TCN-201 activity are primarily mediated through changes in glycine potency.

Residue Val783 in GluN2A influences binding of TCN-201

To evaluate the idea that the GluN2A V783L mutation directly affects binding of TCN-201, we used Schild plots to estimate a pA_2 value for TCN-201 potency. According to the correlation shown in Figure 4.2H, only a minor change in TCN-201 binding affinity would be expected for GluN2A G786D, since the reduction of TCN-201 potency is primarily caused by an increase in glycine potency for this mutation. The Schild plot of TCN-201 antagonism on GluN2A G786D produced a pA_2 value of 7.40 corresponding to 40 nM (Figs. 4.3A and B), which is close to the 30 nM derived from the pA_2 value for wild type GluN1/GluN2A. By contrast, the Schild plot for GluN2A V783L produced a pA_2 value of 5.67 corresponding to 2.1 µM, which is 70-fold higher compared to wild type GluN1/GluN2A (Figs. 4.3C and D). These results are consistent with the idea that residue Val783 of GluN2A participates in TCN-201 binding.

If the residue in GluN2 subunits at the same position as GluN2A Val783 is an important determinant of TCN-201 binding, we predict that TCN-201 will gain some activity on GluN2B with the mutation F784V, as Phe784 in GluN2B corresponds to GluN2A Val783 (Fig. 4.2E). Indeed, TCN-201 had a pronounced effect on glycine potency of mutant GluN1/GluN2B F784V receptors and the Schild plot gave a pA_2 value of 5.86 corresponding to 1.4 µM (Figs. 4.3E and F). By contrast, glycine potency at wild

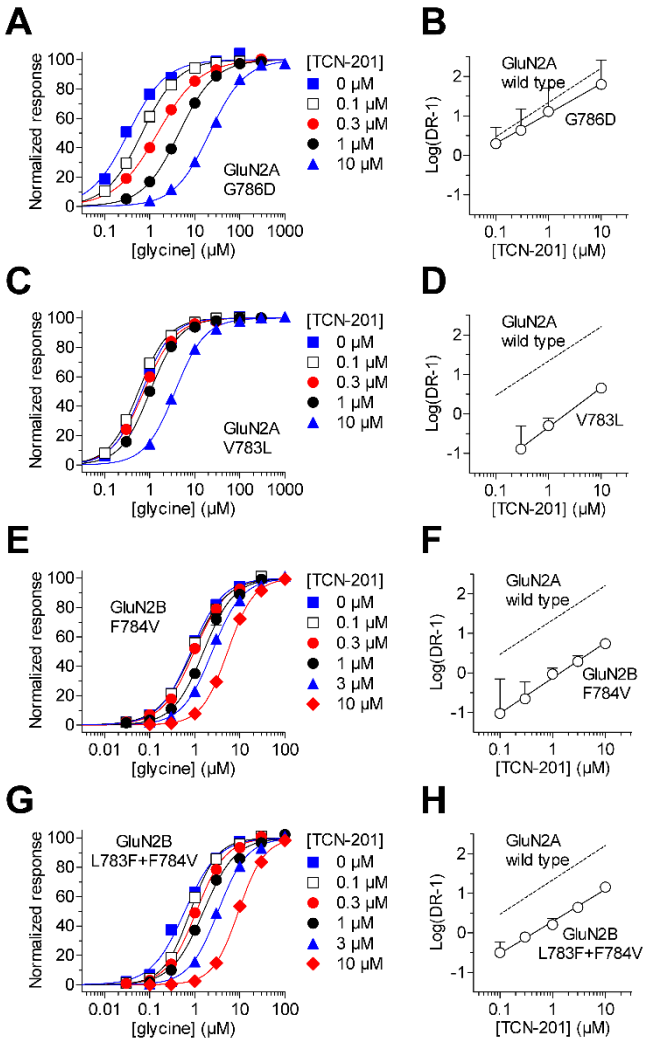

Figure 4.3. Residue Val783 of GluN2A controls TCN-201 binding. Glycine concentration-response data for (**A**) GluN1/GluN2A G786D, (**C**) GluN1/GluN2A V783L, (**E**) GluN1/GluN2B F784V, and (**G**) GluN1/GluN2B L783F+F784V in the absence (0 μM) and presence of increasing concentrations of TCN-201. Data are from 4-6 oocytes. Schild plots for (**B**) GluN1/GluN2A G786D, (**D**) GluN1/GluN2A V783L, (**F**) GluN1/GluN2B F784V, and (**H**) GluN1/GluN2B L783F+F784V yield pA_2 values of 7.40, 5.67, 5.86, and 6.36 corresponding to 40 nM, 2.1 μM, 1.4 μM, and 440 nM, respectively. For all experiments, responses were activated by increasing concentrations of glycine plus 100 μM glutamate.

type GluN1/GluN2B was only marginally reduced in the presence of 10 μM TCN-201, preventing determination of pA_2 from the Schild plot (Table 4.1). Glycine EC_{50} values for wild type GluN1/GluN2B in the absence of TCN-201 and in the presence 10μM TCN-201 were 0.3 ± 0.1 μM (N = 6) and 0.6 ± 0.2 μM (N = 4), respectively ($P < 0.05$; unpaired two-tailed t-test). Glycine EC_{50} values for mutant GluN1/GluN2B F784V in the absence of TCN-201 and in the presence 10μM TCN-201 were 0.8 ± 0.4 μM (N = 4) and 5.5 ± 0.5 μM (N = 4), respectively ($P < 0.05$; unpaired two-tailed t-test). The residue immediately before GluN2A Val783 is also not conserved between GluN2A and GluN2B (Fig. 4.2E). The double mutant GluN2B L783F+F784V, in which both of these residues are converted to the corresponding residues in GluN2A, exhibited even greater antagonism by TCN-201. The Schild plot produced a pA_2 value of 6.36 corresponding to 440 nM (Figs. 4.3G and H). Glycine EC_{50} values for mutant GluN1/GluN2B L783F+F784V in the absence of TCN-201 and in the presence 10μM TCN-201 were 0.6 ± 0.1 μM (N = 5) and 9.5 ± 0.5 μM (N = 6), respectively ($P < 0.05$; unpaired two-tailed t-test). TCN-201 concentration-response data for GluN1/GluN2B F784V and GluN1/GluN2B L783F+F784V in the presence of 3 μM glycine produced IC_{50} values of 6.8 ± 0.4 μM (N = 6) and 4.4 ± 0.2 μM (N = 5), respectively (Table 4.1). In addition, TCN-201 sensitivity could also be introduced to GluN2D by a single point mutation (GluN2D L808V) at the residue corresponding to Val783 in GluN2A (72% of control at 10 μM TCN-201; Table 4.1).

To further evaluate the role of residue Val783 in TCN-201 binding to GluN2A, we mutated this position to residues with charged, polar, and non-polar side-chains and determined TCN-201 IC_{50} and glycine EC_{50} values (Table 4.1). GluN2A V783A resulted in a 2.2-fold increase in glycine EC_{50} and a 1.4-fold reduction in TCN-201 IC_{50} compared to wild type GluN2A. By contrast, GluN2A V783F resulted in a 2.2-fold reduction in glycine EC_{50} and a 5.9-fold increase in TCN-201 IC_{50}. Comparison of TCN-201 activities

at GluN2A V783A and GluN2A V783F with the marked decrease in TCN-201 IC_{50} for GluN2A V783L (See Table 4.1) suggests that the effect of mutating residue V783 to leucine is not solely due to steric occlusion of TCN-201 binding. Additional substitutions yielded no significant correlation between glycine EC_{50} values and TCN-201 IC_{50} values for the GluN2A V783 mutants (Pearson test for correlation, $r^2 = 0.40$, $P > 0.05$; GluN2A V783L not included in the test) and did not show a clear relationship between the size or hydrophobicity of the side chain and TCN-201 potency (see Table 4.1). This result suggests the Val783 substitutions likely have multiple effects on receptor structure in addition to potentially changing the nature of the hypothetical binding pocket. Nonetheless, Schild analysis of GluN1/GluN2A V783L inhibition by TCN-201 demonstrated that the V783L mutation directly impacts TCN-201 binding (Fig. 4.3).

TCN-201 inhibition is mediated by residues from both GluN1 and GluN2A

To identify additional residues that mediate TCN-201 inhibition, we mutated residues in both GluN1 and GluN2A that are located within 8 angstrom of residue Val783 in GluN2A and have side chains protruding into the dimer interface according to the crystal structure of the isolated agonist binding domains from GluN1/GluN2A (Furukawa et al., 2005) (Fig. 4.4A). In GluN1, 7 residues were mutated and 3 of these mutations affected inhibition by 3 µM TCN-201 of responses to 100 µM glutamate plus 30 µM glycine TCN-201 inhibition (Fig. 4.4B). In GluN2A, 15 residues were mutated to alanine and 8 of these mutations affected TCN-201 inhibition (Fig. 4.4C).To assess whether changes in TCN-201 sensitivity could be influenced by changes in glycine potency, we also determined TCN-201 IC_{50} and glycine EC_{50} values for the mutants (Table 4.1). There was no significant correlation between glycine EC_{50} values and TCN-201 IC_{50} values for the GluN2A or the GluN1 mutants (Pearson test for correlation, $P > 0.05$; GluN2A L780A and GluN1 R755A not included in the test). Interestingly, the GluN2A L777A and

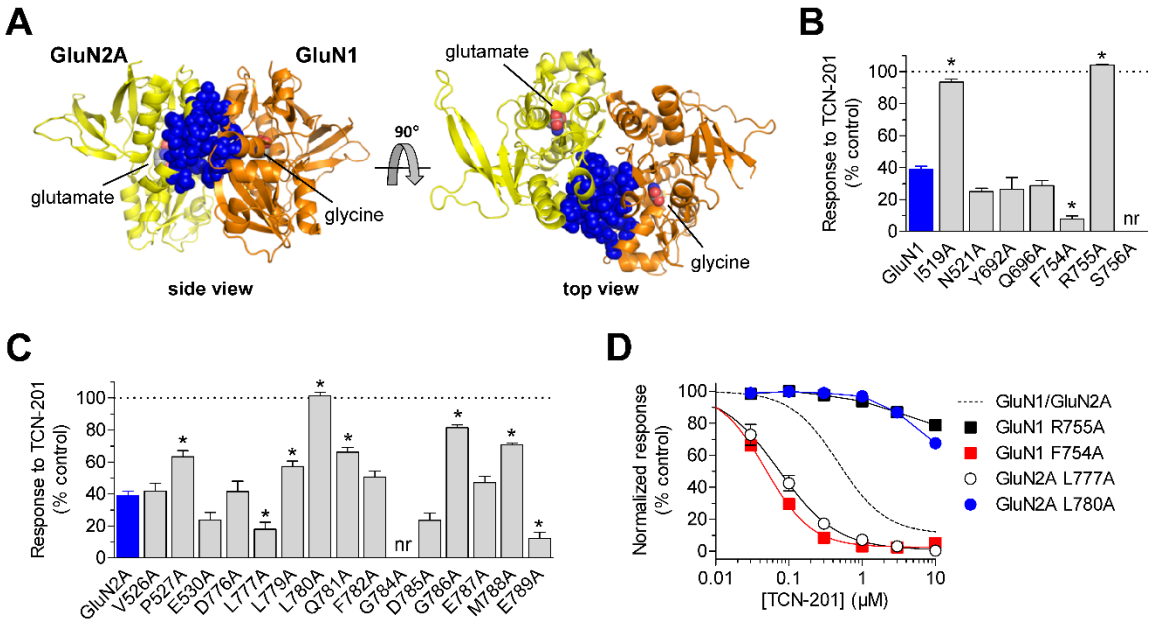

Figure 4.4. TCN-201 inhibition is mediated by residues from both GluN1 and GluN2A. (**A**) Residues that are located within 8 angstrom of residue V783 in GluN2A and have side chains protruding into the dimer interface are highlighted as blue spheres in the structure of the isolated agonist binding domains from GluN1/GluN2A with bound glutamate and glycine (PDB ID 2A5T; Furukawa et al., 2005). GluN2A is shown in yellow and GluN1 is shown in orange. The highlighted residues were mutated to alanine in order to identify additional residues implicated in TCN-201 inhibition. Inhibition by 3 μM TCN-201 of responses to 100 μM glutamate plus 30 μM glycine from (**B**) mutant GluN1 subunits co-expressed with GluN2A or (**C**) mutant GluN2A subunits co-expressed with GluN1. Data are from 4-12 oocytes. * indicates significantly different from wild type GluN1/GluN2A (blue bar) ($P < 0.05$; one-way ANOVA with Tukey-Kramer post test). nr indicates that responses to 100 μM glutamate plus 30 μM glycine were not detected (N = 10-12), suggesting that these mutations have pronounced effects on subunit biosynthesis or receptor function. (**D**) TCN-201 concentration-response data are shown for GluN1 and GluN2A mutants with marked changes in TCN-201 inhibition. Responses to 100 μM glutamate plus 3 μM glycine were measured from receptors expressed in

Xenopus oocytes using two-electrode voltage-clamp recordings. Dashed line is data for wild type GluN1/GluN2A as shown in Figure 4.1B. Data are from 4-25 oocytes. See Table 4.1 for IC_{50} values.

GluN2A L780A mutations markedly affected TCN-201 potency without any noticeably change in glycine potency (Fig. 4.4D and Table 4.1), suggesting that these residues are involved in TCN-201 binding. Residues Leu777 and Leu780 in GluN2A are located two and one helical turns away from residue Val783 (Fig. 4.5), and a previous study has implicated Leu780 in the arrangement of the agonist binding domain dimer interface, as well as in inhibition by proton and zinc (Gielen et al., 2008). In GluN1, the F754A mutation resulted in a 6.7-fold reduction in TCN-201 IC_{50} and a 2.1-fold increase in glycine EC_{50} compared to wild type GluN1/GluN2A, whereas the R755A mutation almost completely abolished TCN-201 inhibition (79% of control at 10 μM TCN-201; Fig. 4.4D and Table 4.1). The GluN1 R755A mutation increased both glycine EC_{50} (4.0-fold) and TCN-201 IC_{50}, (> 30-fold), suggesting a role for this residue in TCN-201 binding. Residues Phe754 and Arg755 in GluN1 are located directly opposite from Val783 in GluN2A in the dimer interface (Fig. 4.5). In summary, the expanded mutagenesis identified several residues in both GluN1 and GluN2A that affect inhibition by TCN-201.

Based on evaluation of changes in TCN-201 and glycine potencies caused by the mutations, we suggest that residues Phe754 and Arg755 in GluN1, as well as Leu777, Leu780, and Val783 in GluN2A are important structural determinants of inhibition by TCN-201. These residues are located at the subunit dimer interface in the structure of the isolated agonist binding domains of heteromeric agonist-bound GluN1/GluN2A (Furukawa et al., 2005) (Fig. 4.5). The side chain of GluN2A Val783 is directly facing the hinge region of the bilobed GluN1 agonist binding domain. Upon agonist binding, the hinge region of the agonist binding domain undergoes a conformational change that allows closure of the clamshell-like agonist binding domain around the agonist. In the GluN1/GluN2A agonist binding domain structure, GluN2A Val783 and the glycine agonist in GluN1 are separated by 16 Å (Cα-Cα distance). However, three residues in the GluN1 hinge region (GluN1 Phe754 and Arg755, and

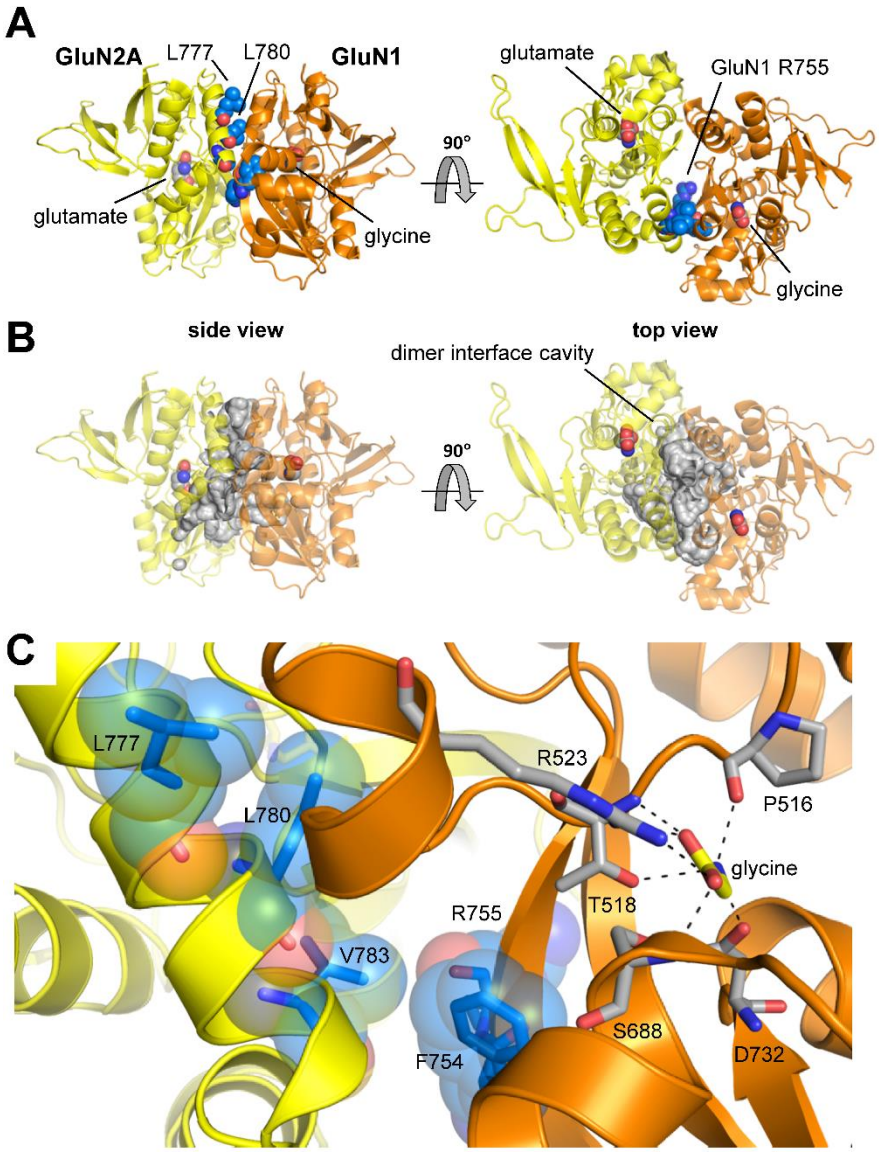

Figure 4.5. TCN-201 sensitivity is controlled by the agonist binding domain dimer interface between GluN1 and GluN2. (**A**) Residues Leu777, Leu780 and Val783 of GluN2A, as well as F754 and R755 of GluN1, which substantially influence TCN-201 sensitivity, are located at the dimer interface in the crystal structure of the isolated agonist binding domains from GluN1/GluN2A with bound glutamate and glycine (PDB ID 2A5T; Furukawa et al., 2005). These residues are highlighted as blue spheres. GluN2A is shown in yellow and GluN1 is shown in orange. (**B**) The residues that influence TCN-201 sensitivity are lining part of a large water-filled cavity (~5200 Å3) in the dimer

interface that can accommodate a modulatory binding site. The cavity was identified using the CASTp server (Dundas et al., 2006 p.200) and the surface of the cavity is highlighted in grey. (**C**) The side chain of GluN2A Val783 (shown as blue sticks with transparent blue spheres) is directly facing the hinge region of the bilobed GluN1 agonist binding domain. The path between GluN2A Val783 and the glycine agonist is blocked by Phe754 and Arg755 in the GluN1 hinge region. GluN2A Leu777 and Leu780 are located two and one helical turns away from Val783 in the dimer interface. The distance (Cα-Cα) between GluN2A Val783 and the glycine agonist in GluN1 is 16 Å. Selected residues important for glycine binding are shown as grey sticks and interactions with glycine are indicated by black dashed lines.

Ser756; Fig. 4.5) lie directly between GluN2A Val783 and the agonist glycine. Interestingly, residues Phe754 and Arg755 in GluN1, as well as Leu777, Leu780 and Val783 are lining part of a large water-filled cavity (~5200 Å3) in the dimer interface that can accommodate a modulatory binding site (Fig. 4.5B). A binding site for TCN-201 at the subunit dimer interface would be ideally positioned to allosterically couple to binding of GluN1 agonists by influencing the conformation of the agonist binding pocket and, at the same time, discriminate between GluN2 subunits by contacting GluN2 residues.

TCN-201 inhibition is mediated by a multi-step mechanism

To further investigate the mechanism of action for TCN-201, we recorded whole-cell current responses under voltage-clamp from recombinant GluN1/GluN2A receptors expressed in HEK293 cells. We evaluated the time course and concentration-dependence of TCN-201 inhibition of steady-state responses to saturating concentration of glutamate (50 μM) and glycine (10 μM) (Fig. 4.6). The onset and offset of TCN-201 inhibition were adequately described by single exponential functions. Interestingly, both the time constants for inhibition ($\tau_{inhibition}$) and recovery from inhibition ($\tau_{recovery}$) were dependent on the TCN-201 concentration (Figs. 4.6B and C). Furthermore, $\tau_{inhibition}$ and $\tau_{recovery}$ were inversely correlated in that higher concentrations of TCN-201 that produced faster onset of inhibition also yielded a slower recovery from inhibition. The dependence of $\tau_{recovery}$ on the TCN-201 concentration used to inhibit the receptor as well as the inverse correlation between $\tau_{inhibition}$ and $\tau_{recovery}$ are distinct from previously described properties of competitive NMDA receptor antagonists (Benveniste et al., 1990), as well as other subunit-selective non-competitive antagonists (e.g. Ro 8-4304, QNZ46, and DQP-1105; Kew et al., 1998; Hansen and Traynelis, 2011; Acker et al., 2011). Moreover, the changes in $\tau_{inhibition}$ and $\tau_{recovery}$ with TCN-201 concentration differ from those predicted by a bimolecular interaction for which $1/\tau_{inhibition}$ is linearly related to the

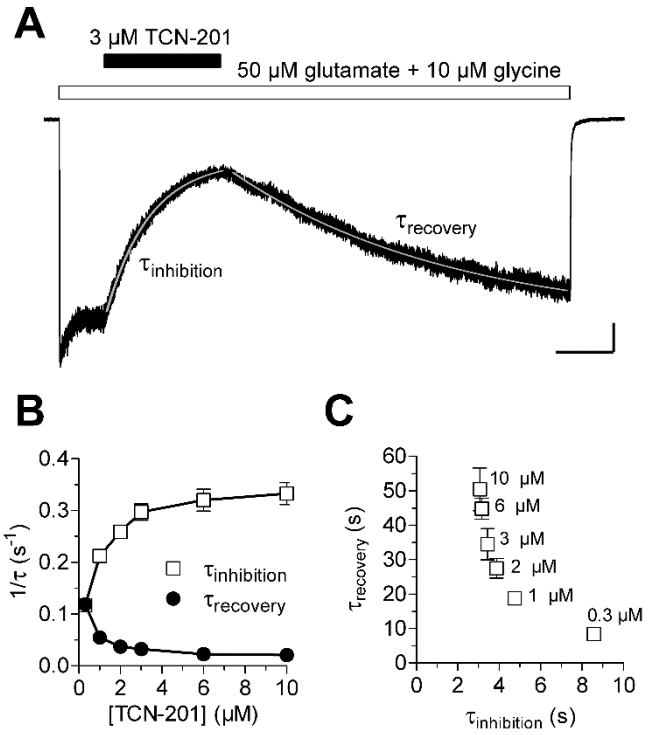

Figure 4.6. Time course of the onset and recovery of TCN-201 inhibition. (**A**) Representative whole-cell current responses recorded under voltage-clamp from recombinant GluN1/GluN2A receptors expressed in an HEK293 cell using rapid solution exchange. Fitted single exponential functions are superimposed as white lines. Vertical and horizontal scale bars are 100 pA and 5 seconds, respectively. (**B**) The rates for the onset of inhibition ($1/\tau_{inhibition}$) and recovery from inhibition ($1/\tau_{recovery}$) are plotted versus TCN-201 concentration. Both the time constants for inhibition ($\tau_{inhibition}$) and recovery from inhibition ($\tau_{recovery}$) are dependent on the TCN-201 concentration. Data are averaged from 3-7 cells for each condition. (**C**) $\tau_{recovery}$ is plotted versus $\tau i_{nhibition}$ for the indicated concentrations of TCN-201.

concentration of antagonist, whereas $1/\tau_{recovery}$ is independent of antagonist concentration. Thus, the time course of action for TCN-201 modulation is incompatible with competitive inhibition, and suggests a more complex mechanism of action.

TCN-201 binding is differentially modulated by glutamate and glycine binding

To determine if binding of TCN-201 is influenced by glutamate binding or receptor activation, we performed experiments in which the receptors were pre-incubated with 3 μM TCN-201 in the presence of either no agonist, glutamate alone (50 μM), or glycine alone (10 μM) immediately prior to activation by 50 μM glutamate plus 10 μM glycine. We compared responses following increasing periods of TCN-201 pre-incubation to control responses in the same recording prior to TCN-201 pre-incubation (Fig. 4.7A). This protocol allowed us to monitor the time course of TCN-201 binding in the presence or absence of agonist. Minimal binding of TCN-201 was observed in the presence of glycine alone and $\tau_{inhibition}$ could not be reliably determined (Fig. 4.7B). In the absence of any agonists, the time constant for TCN-201 binding ($\tau_{inhibition}$) was 3.5 ± 0.3 seconds (N = 4) (Figs. 4.7B and C), and was not significantly different than the $\tau_{inhibition}$ value of 3.4 ± 0.2 seconds (N = 7) observed in the presence of both glutamate and glycine ($P > 0.05$; one-way ANOVA with Tukey-Kramer post-test; Fig. 4.6). Interestingly, binding of TCN-201 was markedly accelerated ($\tau_{inhibition} = 1.1 \pm 0.1$ seconds; N = 4) when TCN-201 was pre-incubated in the presence of glutamate alone (Figs. 4.7B and C). These results show that TCN-201 binding is differentially modulated by glutamate and glycine binding. Glutamate binding alone appears to shift the receptor into a conformation with increased rate of TCN-201 binding, whereas binding of glycine alone promotes a conformation with low rate of TCN-201 binding (Fig. 4.7D). Receptors in the apo-state (i.e. absence of agonist binding) and activated receptors (i.e. with both glutamate and glycine bound) have similar time courses of TCN-201 inhibition with

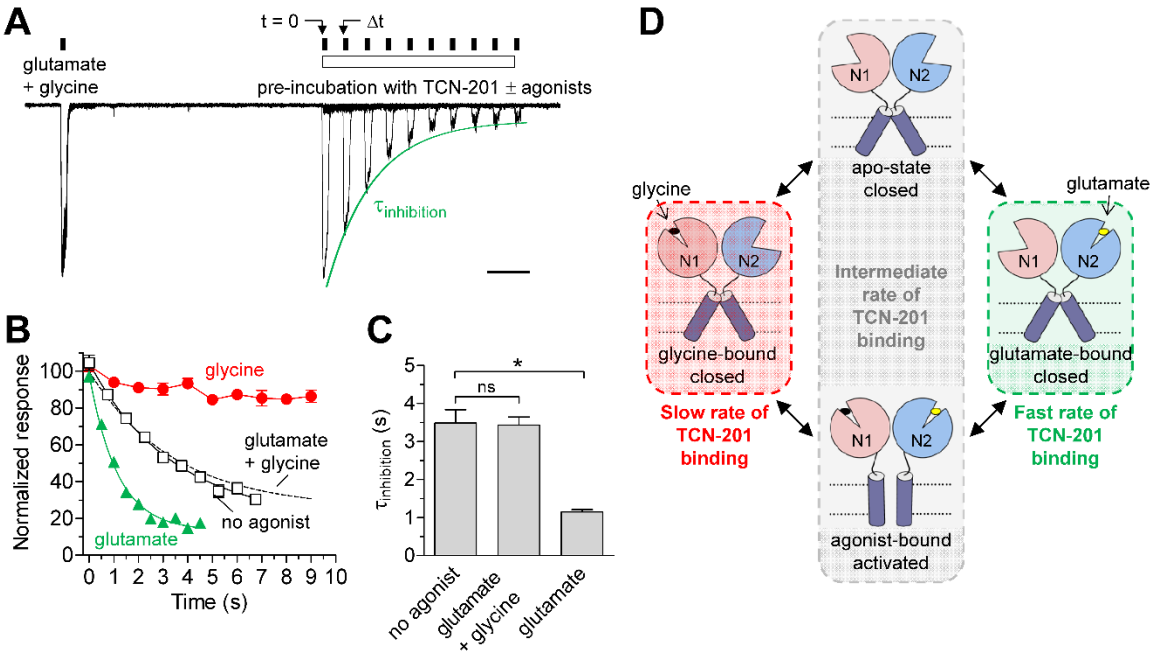

Figure 4.7. TCN-201 binding is differentially modulated by glutamate and glycine binding. (**A**) Representative overlay of 10 paired-pulse whole-cell current recordings from one HEK293 cell expressing recombinant GluN1/GluN2A receptors. The cell was initially stepped into glutamate (50 µM) plus glycine (10 µM) to obtain the control response amplitude before pre-incubation with TCN-201. Subsequent to this control response, the cell was stepped into TCN-201 without agonists (indicated as time zero, t = 0). The cell was then stepped back into glutamate plus glycine at different time intervals (Δt) on subsequent sweeps. TCN-201 was pre-incubated either with no agonist, with glutamate alone (50 µM), or with glycine alone (10 µM). TCN-201 binding occurred from t = 0 to Δt, and the time constant for TCN-201 inhibition ($\tau_{inhibition}$) was obtained by a mono-exponential fit to the response amplitudes at Δt as percent of control amplitude. The recording shown here is with TCN-201 plus glutamate in the pre-incubation and the mono-exponential fit is shown as a green line. Scale bar is 1 second. (**B**) Time course of TCN-201 inhibition in the presence of either no agonist (white), with glutamate alone (50 µM; green), or with glycine alone (10 µM; red). The dashed line is the time course of

TCN-201 inhibition observed in the continuous presence of both glutamate (50 μM) plus glycine (10 μM) as depicted in Figure 4.6. In the presence of glycine alone, the time course of inhibition could not be reliably determined. Data are averaged from 3-7 cells for each condition. (**C**) Mean $\tau_{inhibition}$ values obtained from individual cells for different conditions. * indicates significantly different ($P < 0.05$) and ns indicates not significantly different ($P > 0.05$) (one-way ANOVA with Tukey-Kramer post-test). (**D**) Cartoon scheme depicting differences in TCN-201 binding to the different conformations of the NMDA receptor.

$\tau_{inhibition}$ values intermediate of those in the presence of either glutamate or glycine alone. The similarity of binding rates in these two conditions suggests that TCN-201 binding does not require receptor activation per se. Furthermore, the indistinguishable $\tau_{inhibition}$ values obtained for activated receptors and receptors in the apo-state indicate that the TCN-201 binding site or the accessibility of this site is similar for these two receptor conformations (Fig. 4.7D).

TCN-201 binding accelerates glycine deactivation

These results suggest a working hypothesis in which a negative allosteric interaction exists between TCN-201 and glycine binding. To test this hypothesis, we evaluated the effects of TCN-201 on the time course of deactivation following rapid removal of glycine for recombinant GluN1/GluN2A receptors expressed in HEK293 cells. We compared deactivation with or without TCN-201 for responses to brief (10 ms) and long (5 seconds) applications of a high concentration of glycine (1 mM) in the continuous presence of glutamate (50 μM) (Fig. 4.8). In the case of negative allosteric interaction, a brief glycine application in the presence of TCN-201 could show accelerated glycine deactivation time course compared to control, since bound TCN-201 reduces glycine potency presumably in part by increasing the microscopic dissociation rate constant. Furthermore, prolonged glycine application should result in dissociation of bound TCN-201 as glycine binding reduces TCN-201 affinity. In this scenario, the deactivation time course following prolonged agonist application will become indistinguishable from control as TCN-201 unbinds from the receptor. As predicted from this hypothesis, the weighted time constant for glycine deactivation ($\tau_{weighted}$) of responses to a brief glycine application was significantly reduced (i.e. glycine deactivation is accelerated by TCN-201) from 123 $\pm$ 11 ms (N = 6) in the absence of TCN-201 to 27 $\pm$ 2 ms (N = 6) in the presence of 1 μM TCN-201 ($P < 0.05$; one-way ANOVA with Tukey-Kramer post-test) (Figs. 4.8D and J;

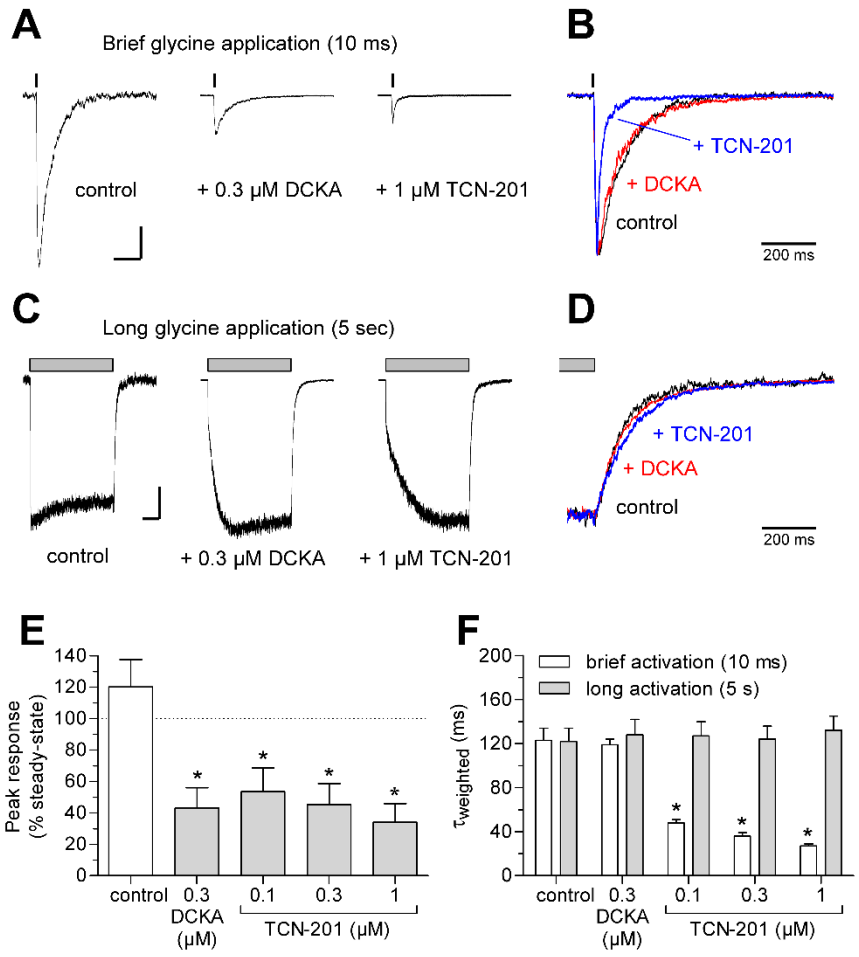

Figure 4.8. TCN-201 binding accelerates glycine deactivation. (**A**) Representative whole-cell current responses recorded under voltage-clamp from recombinant GluN1/GluN2A receptors expressed in HEK293 cells using rapid solution exchange. The receptors were activated by brief application of 1 mM glycine in the continuous presence of 50 μM glutamate and either no antagonist, 0.3 μM 5-7-dichlorokynurenic acid (DCKA), or 1 μM TCN-201. Vertical and horizontal scale bars are 200 pA and 200 ms, respectively. (**B**) Overlay of normalized responses from panel A. (**C**) Representative whole-cell current responses from recombinant GluN1/GluN2A receptors activated by long application of 1 mM glycine in the continuous presence of 50 μM glutamate and either no antagonist, 0.3 μM 5-7-dichlorokynurenic acid (DCKA), or 1 μM TCN-201. Vertical and horizontal scale bars are 200 pA and 1 second, respectively. (**D**)

Overlay of normalized responses from panel C. (**E**) Mean peak responses from brief applications of glycine as percent of steady-state responses from long applications of glycine. Data are from 6 cells. * indicates significantly different from control (white bar; $P < 0.05$; one-way ANOVA with Tukey-Kramer post-test). (**F**) Summary of $\tau_{weigthed}$ for glycine deactivation of responses to brief and long glycine applications. Data are from 6 cells. See Table 4.2 for τ_{fast} and τ_{slow} values. * indicates significantly different from control ($P < 0.05$; one-way ANOVA with Tukey-Kramer post-test).

Table 4.2. Time constants for deactivation of GluN1/GluN2A NMDA receptors.

Antagonist	**Concentration** (μM)	**N**	τ_{fast} (ms)	τ_{slow} (ms)	**% fast**
			Brief application (10 ms)		
control	-	6	74 ± 20	171 ± 18	41 ± 17
7CKA	0.3	6	46 ± 7	158 ± 10	34 ± 6
TCN-201	0.1	6	20 ± 1	131 ± 7	74 ± 2
TCN-201	0.3	6	18 ± 1	123 ± 11	82 ± 1
TCN-201	1	6	16 ± 2	116 ± 19	89 ± 2
			Long application (5 seconds)		
control	-	6		122 ± 12	
7CKA	0.3	6		128 ± 14	
TCN-201	0.1	6		127 ± 13	
TCN-201	0.3	6		124 ± 12	
TCN-201	1	6		132 ± 13	

The deactivation time courses of current responses following removal of 1000 μM glycine in the continuous presence of 50 μM glutamate plus either TCN-201 or 7-chlorokynurenic acid (7CKA) (as shown in Figure 4.8). The deactivation time courses for brief (10 ms) glycine applications were best described using dual-exponential fits and two time constants are listed (τ_{fast} and τ_{slow}), whereas the deactivation time courses for long (5 second) glycine applications were best described using mono-exponential fits and only one time constant is listed (τ_{slow}). All values are mean ± SEM.

see Table 4.2 for τ_{fast} and τ_{slow} values). Acceleration of glycine deactivation by TCN-201 demonstrates that activated NMDA receptors can simultaneously bind glycine and TCN-201, and again is incompatible with a competitive mechanism of action for TCN-201. For prolonged application of glycine in the presence of TCN-201, we observed a rapidly rising current response followed by a slower increase to steady-state that reflects additional glycine binding and resulting TCN-201 dissociation subsequent to a reduction of TCN-201 affinity (Fig. 4.8G). Since prolonged application of glycine results in complete unbinding of TCN-201 under these experimental conditions, there was no significant difference between $\tau_{weighted}$ for glycine deactivation of responses to a long glycine application in the presence or absence of TCN-201 (Figs. 4.8H and J).

In contrast to negative allosteric modulation of glycine binding, the time course of glycine deactivation should be unaffected by a glycine-site competitive antagonists, since it is not possible for glycine and the competitive antagonist to simultaneously bind to activated NMDA receptors. As expected, the competitive glycine-site antagonist 7,5-dichlorokynurenic acid (DCKA; 0.3 µM) did not alter the deactivation time course for either brief (10 ms) or long (5 seconds) applications of 1 mM glycine in the continuous presence of 50 µM glutamate compared to control in the absence of DCKA (Figs. 4.8D, H, J). DCKA inhibited the peak response to a brief glycine application to 43 $\pm$ 13% of control (N = 6) (Figs. 4.8B and I).

TCN-201 is a negative allosteric modulator of glycine binding

A straight-forward model for allosteric modulation of agonist binding without any change in agonist efficacy is shown in Figure 4.9A. In this model, the dissociation constant for agonist binding (K_a) is changed by a factor of $1/\alpha$ upon binding of the allosteric modulator, where α is the allosteric constant (Ehlert, 1988; Christopoulos and Kenakin, 2002). Similarly, the dissociation constant for modulator binding (K_b) is

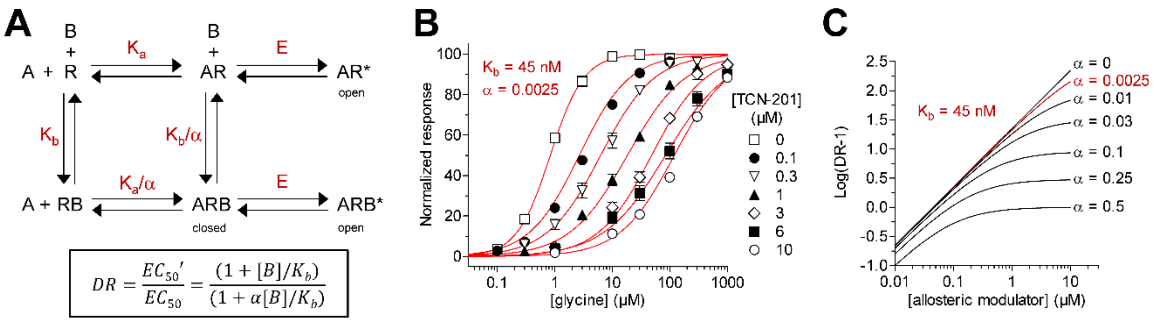

Figure 4.9. TCN-201 is a negative allosteric modulator of glycine binding.

(**A**) Proposed model for TCN-201 inhibition, where TCN-201 allosterically modulates agonist binding without changing agonist efficacy. A is the agonist glycine, B is the inhibitor TCN-201, and R is the receptor. The dissociation constant for agonist binding (K_a) is changed by an allosteric constant α upon binding of the allosteric modulator. Similarly, the dissociation constant for modulator binding (K_b) is changed by α upon agonist binding. In this model, the agonist efficacy E is not changed upon modulator binding. Positive allosteric modulation is achieved if $\alpha > 1$ and negative modulation is achieved if $\alpha < 1$. The relationship describing the dose ratio DR (EC_{50}'/EC_{50}, the ratio of agonist EC_{50} values in presence and absence of modulator) is shown below. DR is a function of the modulator concentration [B], modulator binding affinity K_b, and the allosteric constant α. (**B**) Analysis of the glycine concentration-response data shown in Figure 4.1E by directly fitting to the relationship for the dose ratio DR shown in panel A using a global nonlinear regression method (see Materials and Methods). The regression gave a K_b value of 45 nM and an allosteric constant α of 0.0025 for TCN-201 inhibition of GluN1/GluN2A activated by glutamate and glycine. (**C**) The Schild plots illustrating of the effects of changing the allosteric constant α with constant K_b (45 nM). Low allosteric constants produce Schild plot with only small deviations from the line dictated by the Schild equation ($\alpha = 0$).

changed by a factor 1/α upon agonist binding. We assume that agonist efficacy E is not changed by modulator binding, which renders the inhibition fully surmountable by increased concentrations of agonist. Positive allosteric modulation is achieved if $\alpha > 1$ and negative modulation is achieved if $\alpha < 1$. Figure 4.9A also shows the relationship describing the dose ratio DR (i.e. the ratio of agonist EC_{50} values in presence and absence of modulator EC_{50}'/EC_{50}) as a function of the modulator concentration [B], modulator binding affinity K_b, and the allosteric constant α (Ehlert, 1988; Christopoulos and Kenakin, 2002). From this it can be seen that this type of allosteric modulation is saturable, meaning that an infinite concentration of modulator B will maximally shift the agonist EC_{50}' value to EC_{50}/α. In addition, it can be seen that if $\alpha = 0$, the model in Figure 4.9A reduces to a competitive mechanism and the relationship becomes the Schild equation. In the case of negative allosteric modulation by TCN-201, we predict that the allosteric constant α will be close to 0 and that binding affinity will be close to the pA_2 value obtained in the Schild plot shown in Figure 4.1F.

In order to determine α and K_b for TCN-201 inhibition of GluN1/GluN2A, we re-analyzed the glycine concentration-response data shown in Figure 4.1E by simultaneously fitting the relationship shown in Figure 4.9A to all of the data using a global nonlinear regression method (see Christopoulos and Kenakin, 2002). This analysis gave a K_b value of 45 nM and an allosteric constant α of 0.0025 (Fig. 4.9B). The allosteric constant $\alpha = 0.0025$ implies that TCN-201 can maximally cause a 400-fold (i.e. 1/α) increase in glycine EC_{50}. Since glycine EC_{50} is 1.5 µM in the absence of TCN-201, an infinite concentration of TCN-201 will increase glycine EC_{50} to 600 µM. However, TCN-201 concentrations well above the limit of solubility, estimated to be 18 µM, would be required to maximally shift the glycine EC_{50}. In fact, the K_b of 45 nM for TCN-201 in the absence of glycine is predicted to increase 400-fold to 18 µM in the presence of an

infinite concentration of glycine. Figure 4.9C illustrates the effect of different values for the allosteric constant α on the Schild plot for negative allosteric modulators with K_b = 45 nM.

Discussion

The results from this study suggest that a binding site for allosteric modulators of NMDA receptor exists at the dimer interface between the GluN1 and GluN2 agonist binding domains. The dimer interface between agonist binding domains of AMPA receptor subunits is a well-described binding site for allosteric modulation (Sun et al., 2002; Jin et al., 2005; Hald et al., 2009; Ptak et al., 2009; Ahmed et al., 2010), and positive allosteric modulators of AMPA receptor function are currently being evaluated for the treatment of depression and attention-deficit hyperactivity disorder (ADHD), as well as for the improvement of cognitive deficits in Alzheimer's disease (Ward et al., 2010). Allosteric AMPA receptor modulators enhance receptor function by reducing desensitization and/or by slowing deactivation of the receptor response. Similarly, it has been shown that Na^+ and Cl^- ions bind and stabilize the dimer interface in kainate receptors to attenuate desensitization (Wong et al., 2006, 2007; Plested and Mayer, 2007; Plested et al., 2008), and that Ca^{2+} ions stabilize the dimer interface of the structurally related glutamate-like receptor GluD2 (Naur et al., 2007; Hansen et al., 2009). By contrast, modulators that bind the dimer interface between the agonist binding domains of GluN1 and GluN2 in NMDA receptors have not been described prior to this study. This GluN1-GluN2 dimer interface buries ~2600 Å of solvent-accessible surface area and harbors a large water-filled pocket that can accommodate a modulatory binding site (Furukawa et al., 2005) (Fig. 4.5).

The data presented here provide multiple lines of evidence to suggest that TCN-201 is a negative allosteric modulator of glycine binding to the GluN1 subunit of NMDA

receptors. First, TCN-201 binding reduces glycine potency and vice versa (Figs. 4.1C and E). Second, the Schild slope was significantly lower than unity, indicating TCN-201 is not a competitive antagonist (Fig. 4.1F). Third, the rates of inhibition and recovery depended on the TCN-201 concentration in a manner that is incompatible with a competitive mechanism of action (Fig. 4.6). Finally, TCN-201 and glycine can simultaneously bind activated NMDA receptors, resulting in acceleration of glycine deactivation (Fig. 4.8). This mechanism of TCN-201 action is strikingly different from those of compounds or ions that bind to and stabilize the agonist binding domain interface of AMPA and kainate receptors.

The allosteric constant α has been used to describe the effectiveness of allosteric modulators of G protein-coupled receptors (Lazareno and Birdsall, 1995; Schetz and Sibley, 1997; Hedlund et al., 1999). We estimated the allosteric constant α for TCN-201 to be 0.0025, which results in inhibition that is difficult to distinguish from a competitive mechanism of action. The small allosteric constant α prevented us from observing saturation of the increase in glycine EC50 at the TCN-201 concentrations evaluated here. It was therefore not possible to determine whether TCN-201 modulates agonist efficacy (i.e. NMDA receptor gating) in addition to its effects on glycine binding. This distinction would require functional data at saturating concentrations of both glycine and TCN-201 to eliminate allosteric effects on binding, however, the solubility of TCN-201 precludes this determination. For comparison, the allosteric GluN2B subunit-selective modulator ifenprodil increases potency of GluN2 agonists, such as NMDA and glutamate, but at the same time reduces agonist efficacy (Kew et al., 1996; Zhang et al., 2000). Since allosteric interactions are reciprocal, the GluN2 agonists also increase potency of ifenprodil as NMDA receptor antagonist.

Studies that seek to understand the structure-activity relationship of allosteric modulators at the TCN-201 binding site could potentially identify ligands with different subunit-selectivity and mechanism of action (e.g. allosteric modulation of glutamate binding). Moreover, compounds acting at the TCN-201 binding site seem capable of achieving considerable subunit-selectivity, as demonstrated by the >1000-fold selectivity of TCN-201 for GluN1/GluN2A over other NMDA receptor subtypes. The characterization of TCN-201 inhibition described here reveals previously unrecognized features of NMDA receptor structure and function, and provides compelling data suggesting that novel allosteric regulators of NMDA receptor function exist with high subunit-selectivity. Such compounds could provide an opportunity for the development of new pharmacological tools and therapeutic agents with novel mechanisms underlying their subunit-selectivity.

Chapter 5: The pre-M1 region is a critical gating element in NMDA receptors

Abstract

Glutamate receptor ion channels, which include AMPA receptors, kainate receptors, and NMDA receptors, mediate the majority of excitatory synaptic transmission in the central nervous system. A fundamental question is how these ligand-gated ion channels transduce binding of the amino acid glutamate into opening of the ion channel pore. X-ray crystallographic data from a tetrameric AMPA receptor revealed a short 7 residue "cuff" helix in the pre-M1 region of the receptor that is situated parallel to the lipid bilayer and may act a critical structural determinant of channel gating by restricting movement of pore-forming transmembrane helices until agonist binds. Whether a similar element exists in NMDA receptors and what its role in gating is remains unknown. Using cell-attached patch clamp, we recorded single-channel currents from NMDA receptors containing mutations in the pre-M1 region of GluN2A. Mutations at several residues in the pre-M1 region to alanine or to the homologous residue in the GluN2D subunit reduced channel open probability. The most dramatic changes occurred with 2A(L550A), which reduced open probability from 0.12 ± 0.05 (control, n=7) to 0.0012 ± 0.0003 (n=7). Open durations were described by a mixture of two exponential distributions with τ_1=1.54 ms (area = 74%) and τ_2= 0.12 ms for control. The fitted time constants were markedly shorter in 2A(L550A), with τ_1=0.55 ms (area=66%) and τ_2=0.10 ms. These data suggest the pre-M1 region of GluN2A is critical for normal gating of NMDA receptors. The pre-M1 region of GluN2D was recently implicated in the actions of the GluN2C/2D-selective positive allosteric modulator CIQ. Thus, understanding how the pre-M1 region impacts gating of NMDA receptors may reveal new mechanisms for regulation of the receptor by endogenous and exogenous modulators and interacting proteins.

Introduction

The majority of synaptic transmission occurs by activation of post-synaptic membrane proteins upon binding of neurotransmitter. In the case of ligand-gated ion channels, conformational changes induced by neurotransmitter binding rapidly transduce the free energy of binding into opening of the ion channel pore in a process called gating. Glutamate receptor ion channels, which include AMPA, kainate, and NMDA receptors, are tetrameric complexes that mediate fast excitatory neurotransmission in the central nervous system (Traynelis et al., 2010). Each subunit in the tetramer is made of three semiautonomous domains, an amino-terminal domain (ATD), an agonist-binding domain (ABD), and a transmembrane domain (TMD), together with a cytosolic carboxy-terminal region. The ABDs of all glutamate receptor ion channels fold into a bi-lobed clamshell-shaped structure (Figure 6.1), with an upper lobe called D1 and a lower lobe called D2. Crystal structures of isolated ABDs of glutamate receptor ion channels revealed that upon agonist binding, atomic contacts between the agonist and both the D1 and D2 lobes promote a closed-cleft conformation of the ABD (Armstrong et al., 1998; Sun et al., 2002; Jin et al., 2003; Inanobe et al., 2005; Furukawa et al., 2005; Mayer, 2011a). For AMPA receptors there is strong evidence that the degree of cleft closure correlates with activation of the receptor (for review see Hansen et al., 2007; Mayer, 2011a; Kumar and Mayer, 2013) and it has been speculated that this closure leads to translation of the M3 transmembrane helices away from the central axis of the pore, creating a path for ions to traverse the lipid bilayer. However, direct functional evidence for the conformational changes that occur after ABD cleft closure and that couple this closure to opening of the ion channel pore are lacking and the structural elements involved are not well understood.

An X-ray crystal structure of a tetrameric, membrane-spanning AMPA receptor revealed novel structural features perfectly positioned to transduce agonist binding into

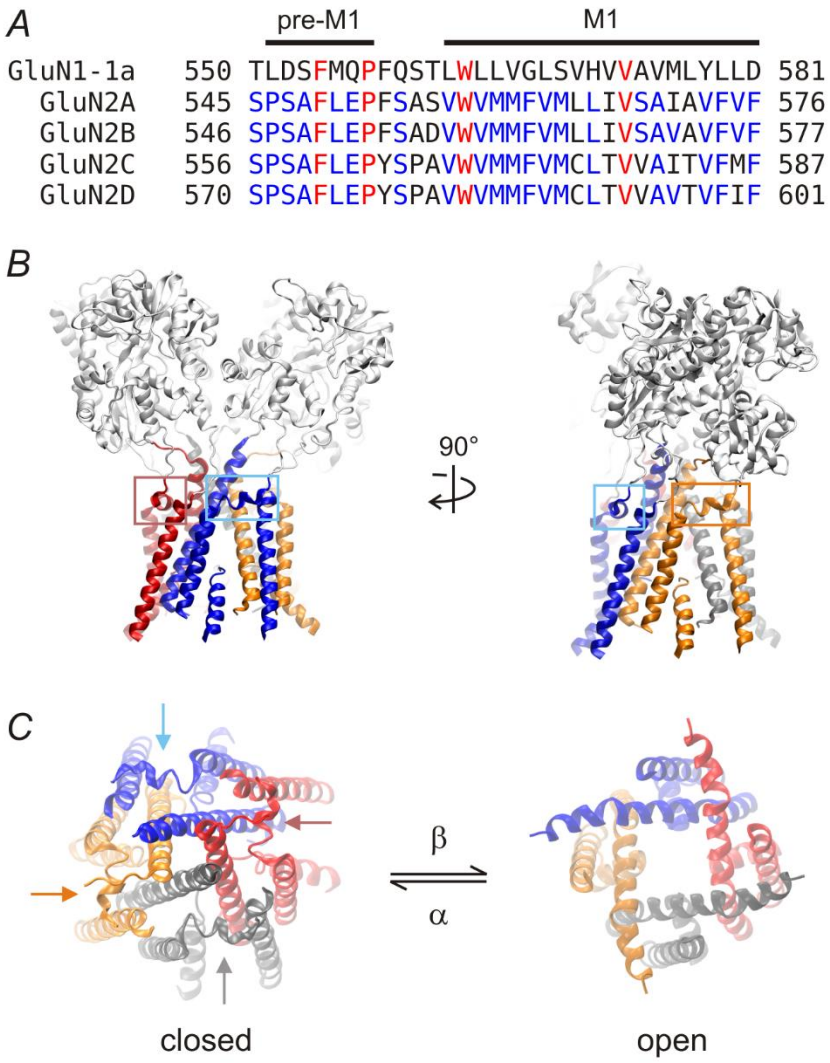

Figure 5.1 The pre-M1 helix

A, An amino acid sequence alignment of the pre-M1 and M1 region of NMDA receptor subunits is shown. Conserved residues are highlighted in blue and identical residues are in red. *B*, The position of the pre-M1 helix is shown in two side-on views of the X-ray structure of a GluA2 AMPA receptor tetramer (PDB code 3KG2, Sobolevsky et al., 2009). The ATD is omitted for clarity. The pre-M1 helix is boxed in two of the four subunits, which are colored blue, red, orange, and gray. *C*, A top-down view of the pore region from the GluA2 membrane-spanning crystal structure. The structure was solved in the presence of a competitive

antagonist and therefore represents the closed state of the pore. Upon agonist binding, conformational changes lead to opening of the ion channel pore, represented on the right by the open NaK structure (PDB code 3E83, Alam and Jiang 2009). The pre-M1 helices are indicated by arrows. Note that NaK channels lack a region homologous to the pre-M1 helix. Also note the large displacement of the M3 helix compared with the closed state. Individual subunits are colored blue, red, orange, and gray.

channel opening (Sobolevsky et al., 2009). The pre-M1 region of the receptor between the ABD and first transmembrane helix forms a short “cuff” helix that is parallel to the lipid bilayer and may act to constrain movement of the M3 gate helices (Figure 6.1). In NMDA receptors, several lines of evidence suggest the pre-M1 region may be involved in gating. First, mutation of individual residues in this region to cysteine caused receptors to have small currents with abnormal kinetics (Beck et al., 1999; Kashiwagi et al., 2002; Thomas et al., 2006). Second, MTS modification of cysteine substituted residues in this region caused significant changes in leak current (Sobolevsky et al., 2007). Third, mutation of residues in this region to alanine generated spontaneously active receptors (Chang and Kuo, 2008).

It is important to understand the role of the pre-M1 region in glutamate receptor gating because several allosteric modulators have structural determinants of action in this region. In AMPA receptors, inhibition by the noncompetitive antagonists CP-465,022 and GYKI-53655 was greatly diminished by chimeric receptors in which the S1-M1 and S2-M4 linkers were exchanged with homologous regions of the non-sensitive kainate receptor, GluK1 (Balannik et al., 2005). Further, inhibition was also reduced by point mutations in these linkers and sensitivity to these inhibitors could be transferred to GluK1 by substituting GluK1 pre-M1 residues with GluA3 pre-M1 residues (Balannik et al., 2005). In NMDA receptors, the positive allosteric modulator CIQ interacts with the pre-M1 and M1 region to increase the opening frequency of the ion channel (Ogden and Traynelis, 2013). Thus the pre-M1 region might be an important modulatory site that could be exploited for design of new therapeutics. Interestingly, recent genomics studies have identified mutations in the pre-M1 region of GluN2A and GluN2B in patients with neurological disorders, however direct effects of those mutations on channel function were not reported (de Ligt et al., 2012; O’Roak et al., 2012a, 2012b; Epi4K Consortium

et al., 2013). Hence, mutations in this region may lead to disease states so it is important to determine what role the pre-M1 region plays in NMDA receptor function.

Here, we explored the contribution of the pre-M1 region of NMDA receptors to channel gating. We used single channel recordings of receptor currents to directly monitor the gating isomerization and to infer the proportion of other states of the receptor, such as agonist-bound closed states and desensitized states. We chose to study the pre-M1 region of GluN1/GluN2A receptors because the gating mechanism of this channel has been well studied (Wyllie et al., 1998; Popescu and Auerbach, 2003; Erreger et al., 2005; Auerbach and Zhou, 2005; Schorge et al., 2005; Kussius and Popescu, 2009; Yuan et al., 2009; Talukder and Wollmuth, 2011) and because the open probability of this receptor is about 0.5, which should easily allow us to identify both increases or decreases in gating efficiency. To explore the importance of the pre-M1 region to gating, we introduced mutations into specific residues within the pre-M1 region. We chose a mutagenesis strategy because the residues in the pre-M1 region are highly conserved across the GluN2 subunits (Figure 5.1A) suggesting that the side chain of each residue is critical for either direct interaction with other regions of the receptor or for indirectly positioning the main chain backbone atoms. Thus, we introduced alanine residues to remove most side chain interactions without introducing excessive flexibility, as would occur with glycine for example. We found that the pre-M1 region generally contributes to the slow conformational change that has been associated with GluN2 subunits. In addition, the pre-M1 region may also determine the mean open time (stability of the open state) as mutation at two residues in this region caused a profound reduction of mean open time.

Results

Single-channel activity of GluN1/GluN2A NMDA Receptors

To determine how the pre-M1 region of NMDA receptors contributes to gating, we recorded single-channel NMDA receptor currents from cell-attached patches ($V_{pipette}$ = +80 mV) of HEK cells expressing GluN1-1a with wild type GluN2A or with GluN2A pre-M1 point mutants (Figure 5.1). We mutated residues individually to alanine to probe the importance of side chain interactions made by this region of the protein during gating, which are likely to be important given the high percentage identity of pre-M1 residues across GluN2 subunits (Figure 5.1). Additionally, we sought to take advantage of the approximately 50-fold difference in open probability between GluN2A-containing receptors and GluN2D-containing receptors by mutating divergent residues in GluN2A to the homologous residue in GluN2D. Currents were recorded at pH 8.0 to minimize the effects of by protons, which inhibit GluN1-1a/GluN2A receptors with an IC_{50} that corresponds to pH 6.9-7.2 (Traynelis et al., 1995; Low et al., 2003). Additionally, saturating concentrations of glutamate (1 mM) and glycine (50 μM) were used to ensure receptors were bound by agonists and thereby focus analysis mainly to effects of the pre-M1 region on gating rather than binding of agonists. EDTA (10 μM) was included in the pipette solution to chelate contaminating Zn^{2+}.

Single channel activity occurred in bursts separated by long periods of inactivity, which reflect desensitization of the receptor, as previously described (Popescu and Auerbach, 2003; Erreger et al., 2005; Auerbach and Zhou, 2005; Schorge et al., 2005). Figure 5.2 illustrates the protocol that was used to isolate bursts of activity for analysis. Single-channel activity was idealized into a sequence of openings and closings and the components of the shut time histogram were determined by maximum likelihood estimates of the rate constants in the gating model $D \leftrightarrow C_1 \leftrightarrow C_2 \leftrightarrow O_1 \leftrightarrow O_2$.

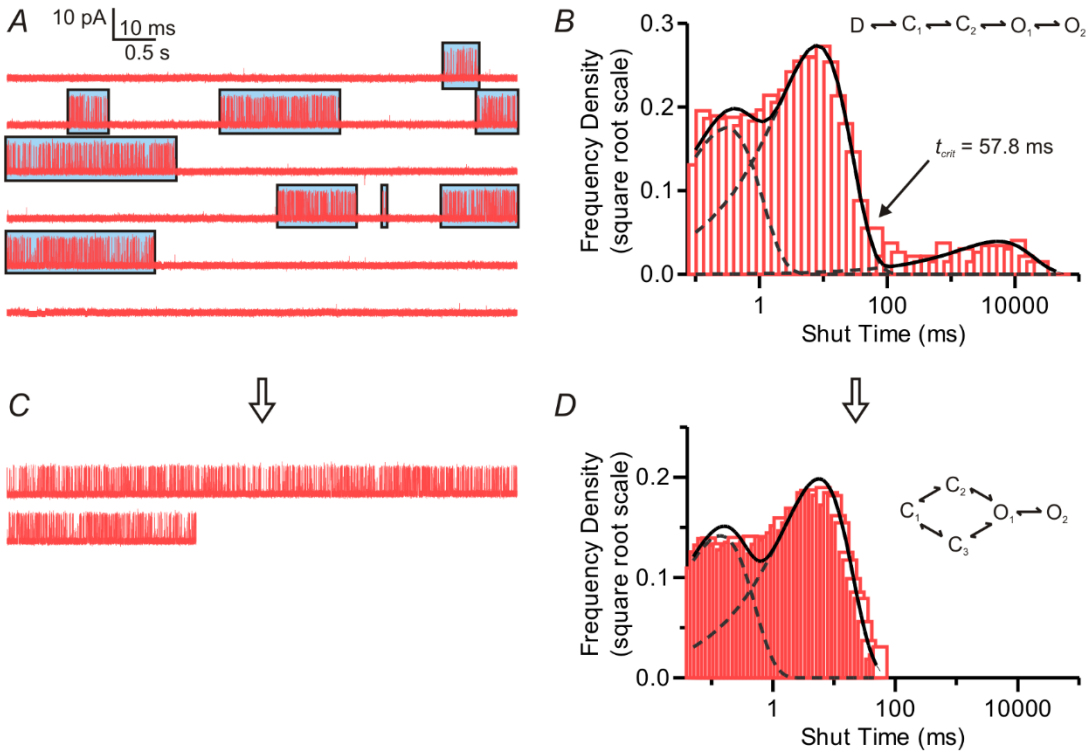

Figure 5.2 Protocol for analyzing bursts of openings

A, An example single-channel recording from a cell-attached patch illustrates clusters of channel openings separated by prolonged closed periods. Clusters, or bursts, of openings separated by a critical shut time, t_{crit}, are boxed and shaded in blue. *B*, Channel activity was idealized into a sequence of open and shut periods using the SKM algorithm in QuB software with the model shown in the inset. The model includes three closed states, C_1, C_2, and D (the desensitized state) and two open states, O_1 and O_2. A histogram of shut time durations is shown and the probability density functions of each closed state, is overlaid (dashed lines). *C*, The boxed clusters of openings shown in panel *A* were concatenated into one trace for analysis of gating rate constants. *D*, The shut time histogram after excluding the desensitized states is shown. The gating rate constants of the model (inset) were estimated by maximum likelihood fitting.

Conceptually, this model incorporates a desensitized state, *D*, a pregating step, $C_1 \rightarrow C_2$, a gating step, $C_2 \rightarrow O_1$, and a coupled open state, $O_1 \leftrightarrow O_2$, and is the minimum activation scheme needed to fit the prolonged closed (i.e. desensitized) states and explain the two components observed in the open time distribution. Overall channel properties were measured from this idealization and subsequently the longest closed events (i.e. desensitized states) were excluded using a critical shut time (t_{crit}) that was chosen to give an equal number of misclassified events between the desensitized state and the next slowest shut state (Jackson et al., 1983; Magleby and Pallotta, 1983; Colquhoun and Sigworth, 1995). Bursts of activity were then used for kinetic modeling by re-idealizing the openings using the model in Scheme 1 and estimating the rate constants using a maximum likelihood approach.

Scheme 1

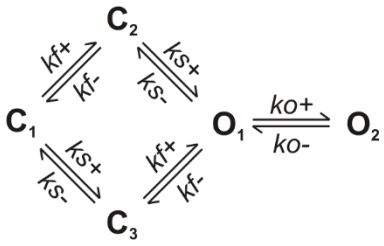

Effects of pre-M1 Mutations

Single-channel activity of pre-M1 mutants occurred in patterns similar to wild type GluN1/GluN2A (Figures 5.3 to 5.8) with bursts of openings separated by long durations in non-conducting, desensitized states. Both wild type GluN2A and pre-M1 mutants displayed only a single prominent peak in histograms of the current amplitude, with no obvious subconductance levels (data not shown). Moreover, unitary current amplitudes were comparable between mutants and wild type, suggesting pre-M1 mutations did not cause a change in the single-channel conductance. By contrast, mutations at every position in the pre-M1 region of GluN2A, except Ala555, considerably altered overall

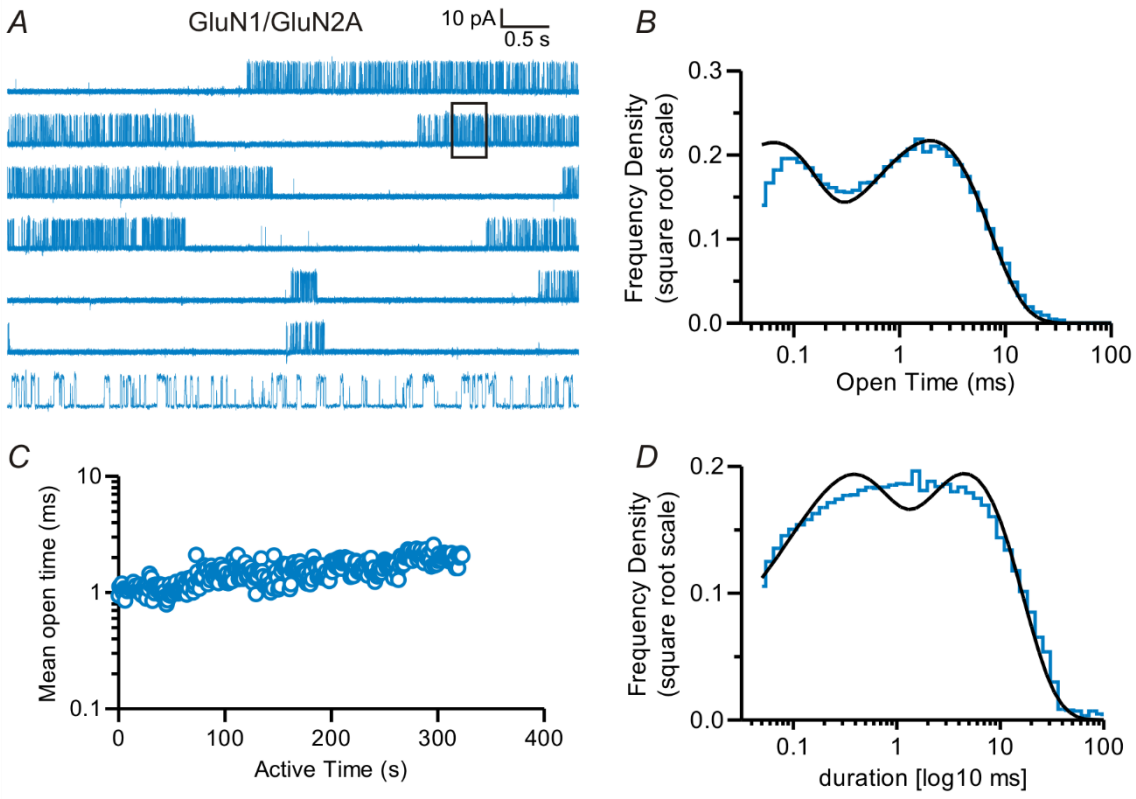

Figure 5.3 Steady-state activation of GluN1/GluN2A in cell-attached patches

A, Single channel currents from a representative cell-attached patch activated by saturating concentrations of glutamate (1 mM) and glycine (50 μM). Openings are upward in this and subsequent traces (V_m = +80 mV). A 360 ms segment of the recording (the boxed region) is shown below on an expanded time scale. *B*, The open time distribution of clusters of openings is shown together with the probability density functions of the two open states in Scheme 1 (solid line). *C*, A stability plot of mean open times for the recording in *A* is shown. Clusters of openings were concatenated and then analyzed in one second increments, called active time. *D*, The shut duration histogram for clusters of single-channel activity is shown. The probability density function predicted from maximum likelihood fits to Scheme 1 is overlaid (solid line).

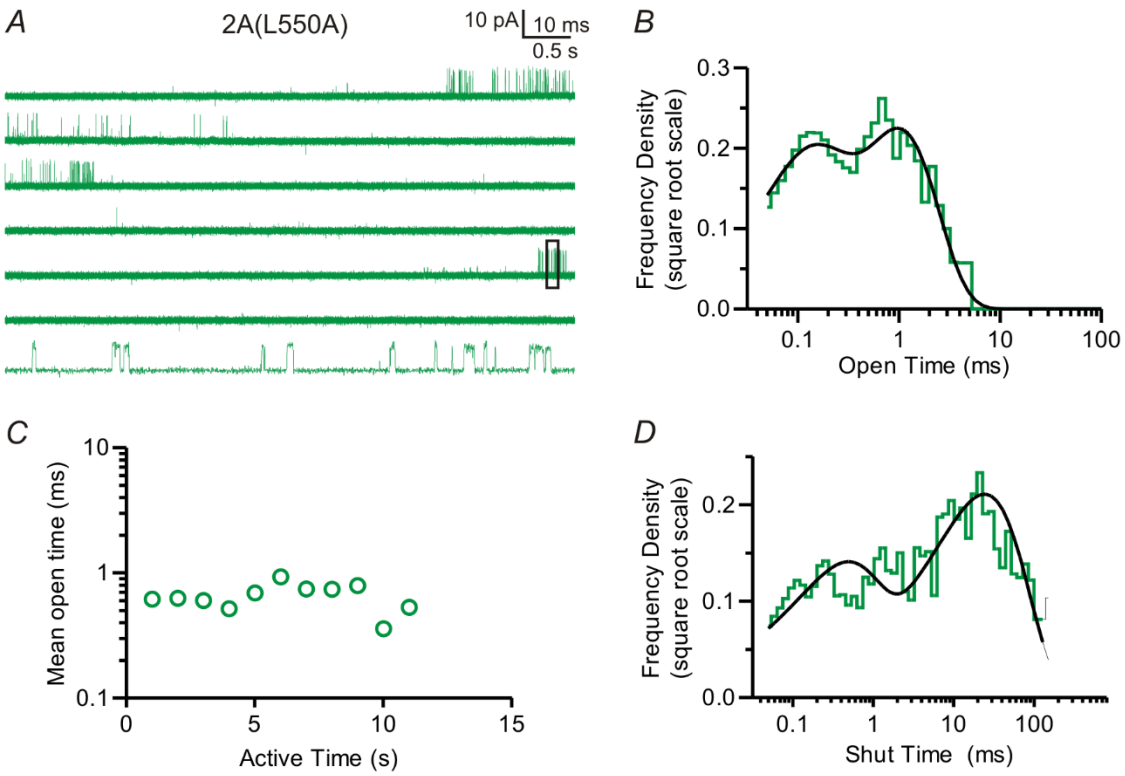

Figure 5.4 Single-channel currents from GluN2A(L550A)

A, Single channel openings from a representative cell-attached patch containing a single active GluN1/GluN2A(L550A) receptor are shown. 1 mM glutamate and 50 μM glycine were included in the patch pipette and the $V_{pipette}$ was +80 mV. The boxed region is shown below on an expanded time scale. *B*, The open duration histogram for the clusters of openings from the patch shown in *A* is depicted along with the predicted open time distribution from maximum likelihood estimation of the rates in the mechanism from Scheme 1. *C*, The mean open time was stable throughout the recording as illustrated by the stability plot of 1 s active time periods. *D*, The closed duration histogram for bursts of activity from the patch in *A* is shown. The black line is the predicted shut time distribution from maximum likelihood estimation of the rates in Scheme 1 for this patch.

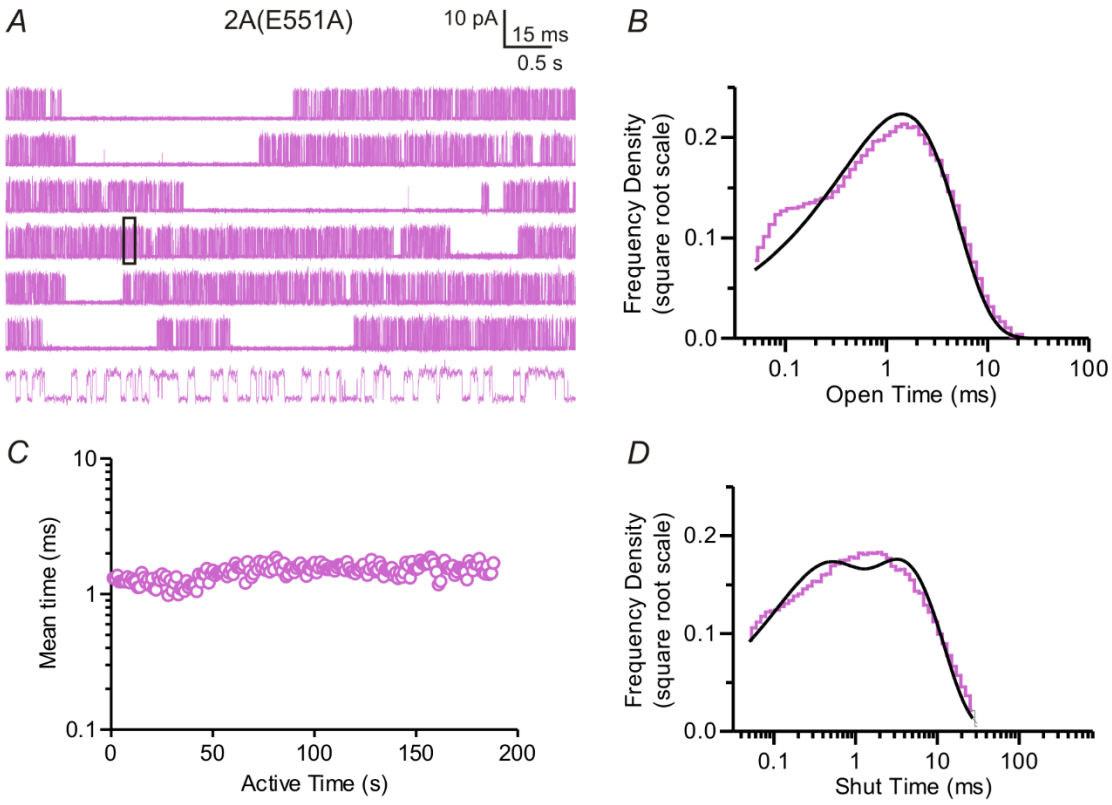

Figure 5.5 Activation of GluN2A(E551A)

A representative cell-attached patch recording containing a single active GluN1/GluN2A(E551A) receptor is shown in *A*. The boxed region is displayed on an expanded time scale in the last line. Saturating glutamate (1 mM) and glycine (50 μM) were included in the pipette tip and the holding potential was +80 mV. *B*, The open time histogram for clusters of openings from the patch shown in *A* is plotted together with the predicted distribution from maximum likelihood fitting of the rates in Scheme 1 to the idealized list of open and shut times. *C*, Stability plot of the mean open time in the patch from *A*. *D*, Shut time histogram and probability density function predicted by maximum likelihood fitting of rates in Scheme 1 for the patch in *A*.

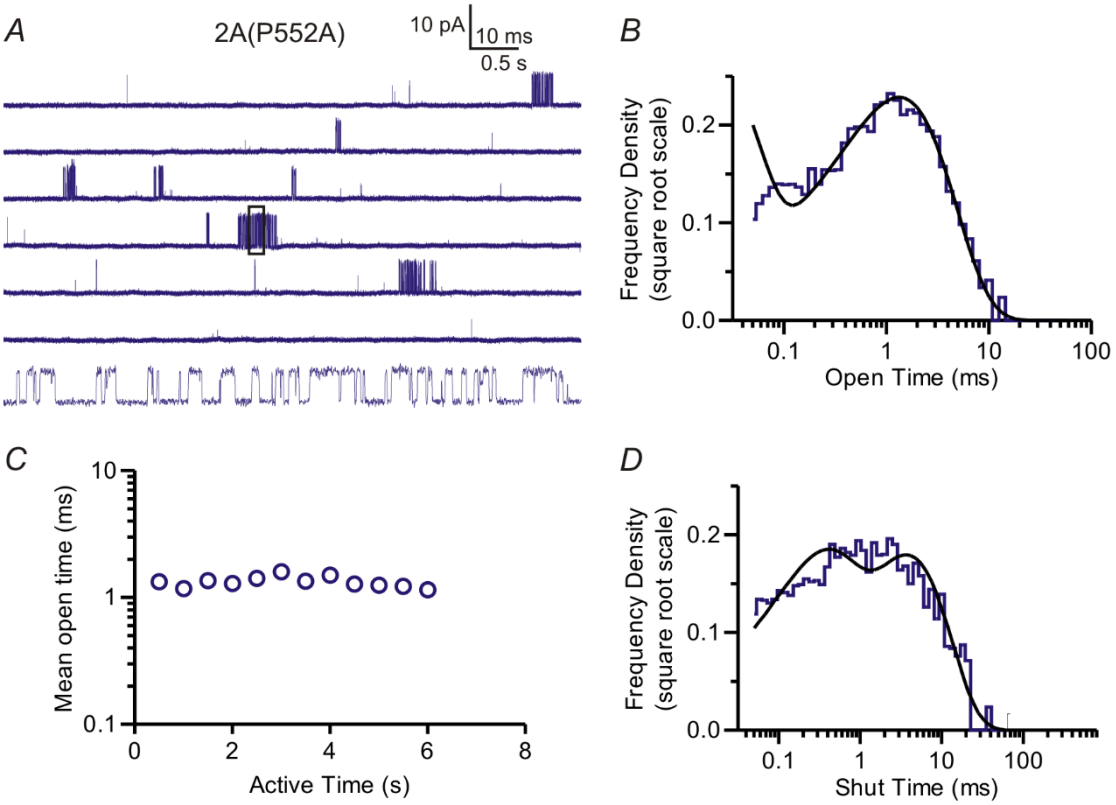

Figure 5.6 Single-channel recording of GluN2A(P552A)

A, GluN1/GluN2A(P552A) single channel currents from a representative cell-attached patch are shown. *B, D*, Dwell time histograms and probability density functions predicted by fitting Scheme 1 for the patch shown in *A*. *C*, Stability plot of the mean open time for each second of active time in the recording shown in panel *A*.

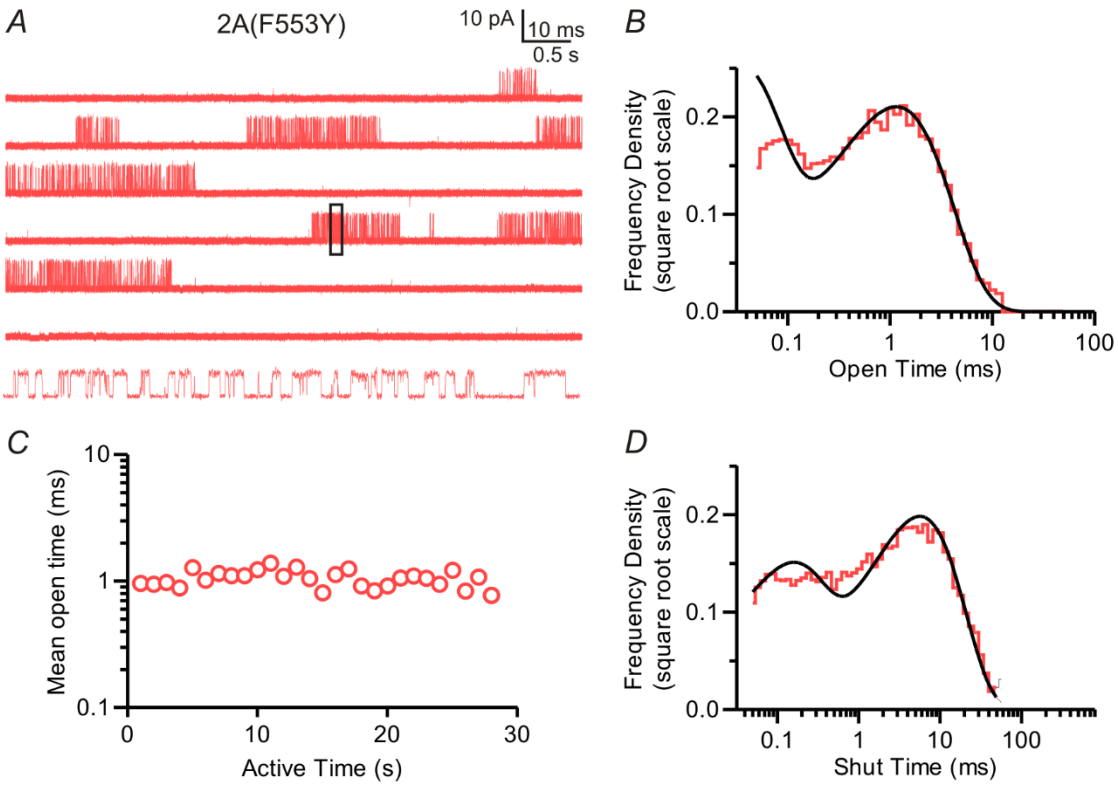

Figure 5.7 Steady-state GluN2A(F553Y) currents in cell-attached patches

A, steady-state recording of a patch with a single GluN1/GluN2A(F553Y) channel displayed on two different time scales ($V_{pipette}$ = +80 mV, digitized at 40 kHz, filtered at 8 kHz). The box highlights the region shown in detail in the bottom trace. The open time histogram (*B*) and shut duration histogram (*D*) for this patch are shown. The solid lines are probability density functions calculated from the rate constants of Scheme 1 obtained by maximum likelihood estimation. The open times were stable throughout this recording (*C*).

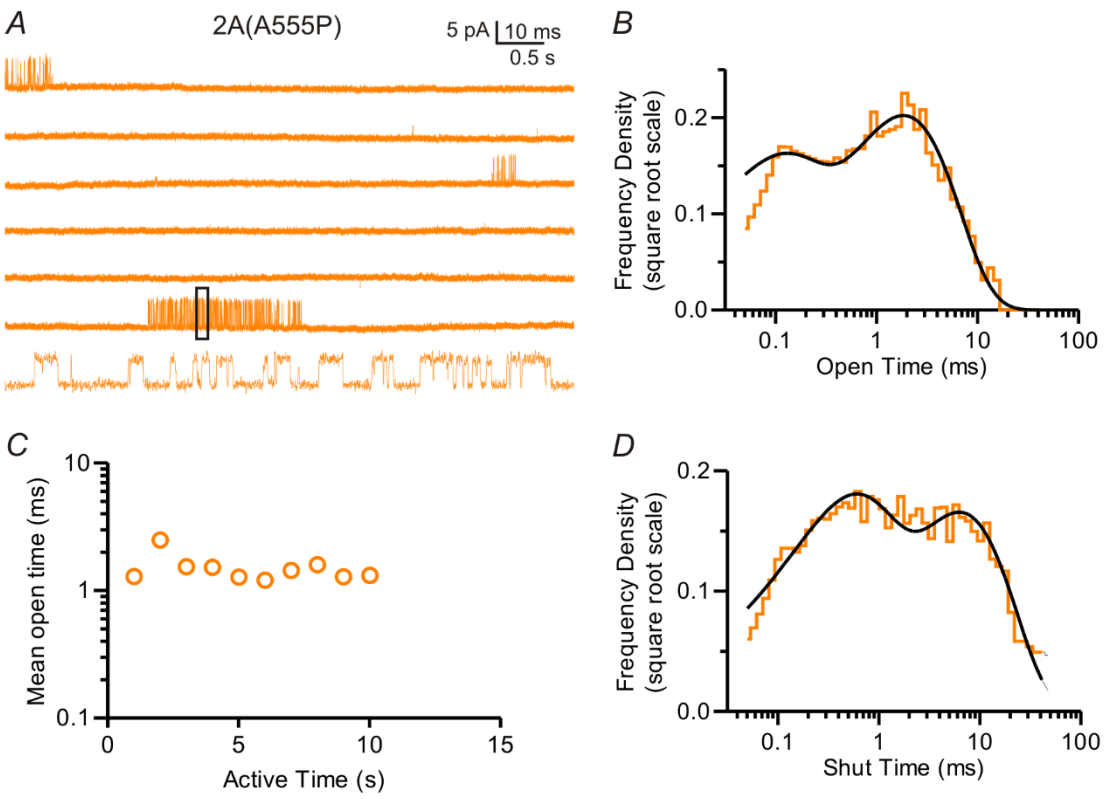

Figure 5.8 GluN2A(A555P) single-channel activity

A, representative single-channel traces (36 s, shown filtered at 8 kHz with openings upward; $V_{pipette}$ = +80 mV) recorded with saturating concentrations of glutamate and glycine. The boxed region (120 ms) is shown in the bottom trace. *B, D* Histograms of open and closed durations for the record shown in *A* superimposed with the probability density functions (solid lines) estimated from fits of Scheme 1 to the idealized data. *C*, Mean open durations are shown for each second of active time.

open probability (Table 5.1). The most dramatic changes in single channel properties occurred with GluN2A(F549A). Single-channel openings of this receptor were very brief, roughly one-third as long as openings of wild type GluN2A, and were separated by exceptionally prolonged durations in non-conducting states (Table 5.1). In addition, it is noteworthy that mutation of Phe553 to homologous residue in GluN2D, tyrosine, did not change the overall open probability while mutation of this residue to alanine dramatically reduced open probability, suggesting that hydrophobic and/or aromatic properties of the side chain at residue 553 are important for gating.

We hypothesized that some of the differences in gating between GluN2A and GluN2D might result from divergent residues between these two subunits in the pre-M1 region. GluN2A Ala555 was a particularly intriguing residue in this context because the homologous residue in GluN2D is a proline, which has exceptional conformational rigidity and could uniquely contribute to the secondary structure of the pre-M1 region of GluN2D. However, the overall open probability, mean open time, and mean shut time of GluN2A(A555P) did not differ from GluN2A (Table 5.1), suggesting that the amino acid in this position is not an essential structural determinant of channel gating.

Gating Impairments in the GluN2 pre-M1 Region Disrupt the Slow Gating Isomerization of NMDA Receptors

To examine in more detail the effects of pre-M1 mutations and define the specific kinetically distinct conformational transitions in the NMDA receptor gating mechanism affected by the pre-M1 region we fit a previously described model of NMDA receptor activation (Scheme 1) (Banke and Traynelis, 2003; Erreger et al., 2005; Schorge et al., 2005) to the idealized sequence of openings and closings in bursts of activity in single-channel records using maximum likelihood estimation of the rate constants. Conceptually, Scheme 1 postulates that two independent conformational changes must

Table 5.1 Overall single-channel properties of GluN2 pre-M1 mutants

	n	Events	Overall P_o	Overall MOT (ms)	Overall MST (ms)
GluN2A	6	311314	0.09 ± 0.03	1.49 ± 0.11	29 ± 12
2A(F549A)	3	546	0.00030 ± 0.00006*	0.53 ± 0.07*	1650 ± 180*
2A(L550A)	7	7126	0.0012 ± 0.0004*	0.66 ± 0.05*	900 ± 300*
2A(E551A)	3	307463	0.26 ± 0.07*	1.30 ± 0.11	4.2 ± 1.1
2A(P552A)	7	18899	0.011 ± 0.003*	1.25 ± 0.06	160 ± 40
2A(F553Y)	3	67738	0.03 ± 0.02	1.38 ± 0.09	70 ± 30
2A(F553A)	3	4448	0.0012 ± 0.0003*	0.199 ± 0.003*	180 ± 40
2A(A555P)	3	82659	0.05 ± 0.04	1.67 ± 0.05	100 ± 50

* indicates $p<0.05$ vs. GluN2A (one-way ANOVA with Dunnett's post-test)

occur before the channel can open. The two transitions are distinguished kinetically based on the microscopic rate constants, with one relatively fast transition, *f*, and one slow transition, *s*. Moreover, the conformational changes can occur in either order. At least two lines of evidence support the notion that the faster rate reflects GluN1-specific conformational changes and the slower rate reflects GluN2-specific transitions. First, partial agonists at the glycine binding site only affected a fast component of the shut time distribution, while glutamate site partial agonists only affected the slow component of the shut time distribution (Banke and Traynelis, 2003). Second, only the rate constant for the slow transition differed between GluN2A and GluN2B receptors (Erreger et al., 2005). Scheme 1 additionally contains two coupled open states that account for the two components in the open time distribution of wild type GluN1/GluN2A channels (Popescu and Auerbach, 2003; Auerbach and Zhou, 2005; Schorge et al., 2005; Erreger and Traynelis, 2008).

Open times for all mutants except 2A(F553A) and 2A(E551A) appeared to be mixtures of two exponential components (Figure 5.9). By contrast, only a single exponential component was observed for open times of 2A(E551A) and 2A(F553A), leading to significant differences in the relative areas (Figure 5.9B). Table 5.3 gives the values (in ms) and relative areas of each open time component as estimated from maximum likelihood fitting of Scheme 1 to idealized dwell times from clusters of single channel activity. The mean open times of 2A(L550A) and 2A(F553A) were significantly shorter than for GluN2A (Table 5.2), whereas mean open times for other pre-M1 mutants were similar to GluN2A.

The distribution of shut times from clusters of single-channel openings were fit reasonably well by Scheme 1. Compared to wild type GluN2A, there were no changes in any shut time component or the relative proportions from single-channel currents of 2A(P552A), 2A(F553Y), or 2A(A555P). Conversely, shut times for 2A(L550A) and

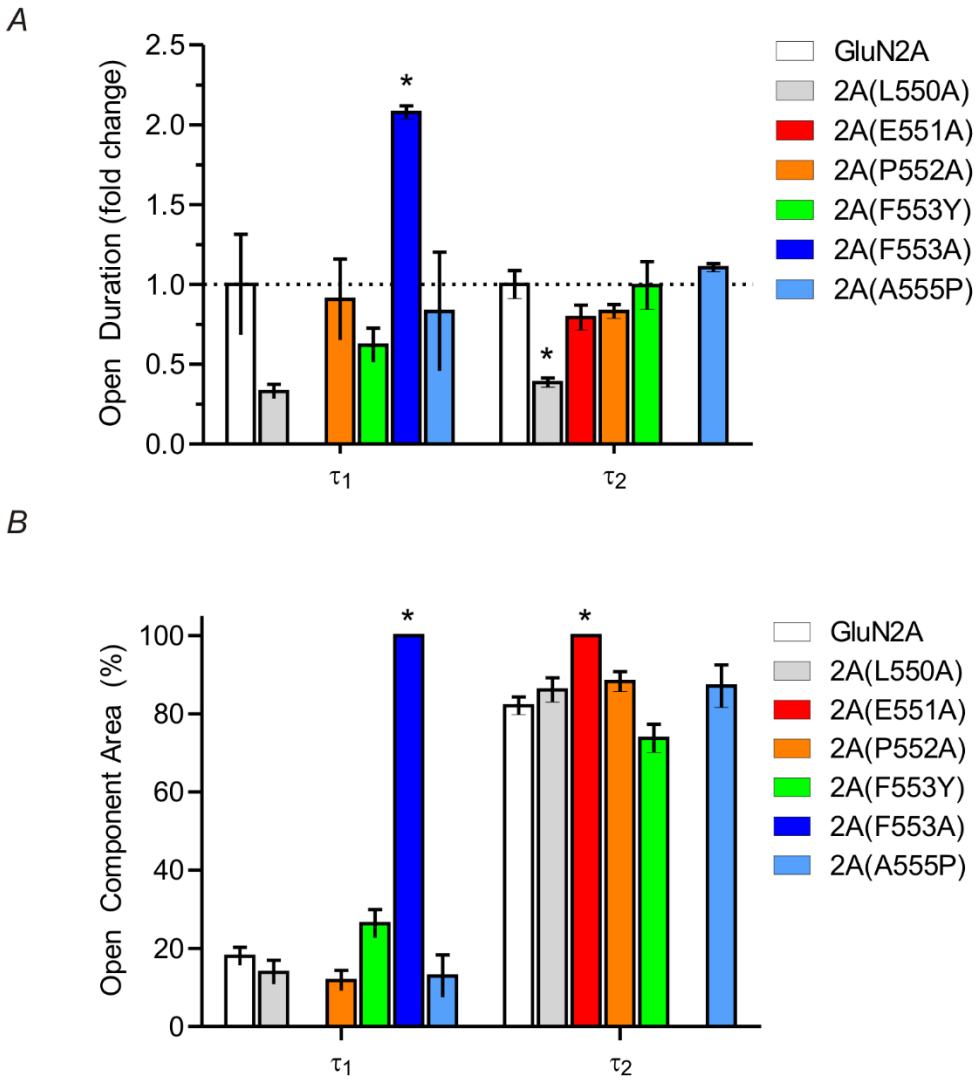

Figure 5.9 Leu550 and Phe553 of GluN2A contribute to stability of the open state

A, Mean (± SEM) fold change in the two open time components as calculated from maximum likelihood estimation of the rate constants in Scheme 1 using idealized dwell times from clusters of single channel activity. For GluN2A, the short duration component, τ_1, was 0.058 ± 0.018 ms and the long duration component, τ_2, was 1.51 ± 0.13 ms. *B*, The effect of pre-M1 mutation on mean (± SEM) relative areas of each open time component is summarized. For 2A(E551A) and 2A(F553A), only a single component was detected. For 2A(E551A), the open durations were similar to τ_2 for GluN2A whereas for 2A(F553A), open durations were similar to τ_1 of GluN2A.

Table 5.2 Single-channel properties of **bursts** of activity from GluN2 pre-M1 mutants

	n	Events	Burst P_o	Burst MOT (ms)	Burst MST (ms)
GluN2A	6	315130	0.342 ± 0.008	1.52 ± 0.11	2.9 ± 0.2
2A(L550A)	7	6519	0.033 ± 0.006*	0.66 ± 0.05*	22 ± 3*
2A(E551A)	3	307463	0.38 ± 0.04	1.33 ± 0.13	2.3 ±0.3
2A(P552A)	7	17623	0.34 ± 0.02	1.29 ± 0.06	2.51 ± 0.16
2A(F553Y)	3	67723	0.23 ± 0.02*	1.35 ± 0.15	4.58 ± 0.07
2A(F553A)	3	3484	0.020 ± 0.005*	0.211 ± 0.007*	12 ± 3*
2A(A555P)	3	74905	0.39 ± 0.06	1.73 ± 0.10	2.8 ± 0.5

Clusters of activity were not analyzed for 2A(F549A) receptors because there was not a clear desensitized state that could be excluded based on a critical shut time, t_{crit}.

* indicates $p<0.05$ vs. GluN2A (one-way ANOVA with Dunnett's post-test)

2A(F553A) were significantly prolonged. The briefest shut time component, which often reflects the opening rate of terminal steps in the gating mechanism as receptors close briefly then reopen, was not detectable in 2A(L550A) receptors; in contrast, the longest shut time was increased 6.5 fold (Figure 5.10A and Table 5.3). For 2A(F553A) receptors, the two longest shut times were each prolonged about 3 fold and the longest shut times comprised a larger proportion of openings (Figure 5.10).

2A(E551A) receptors had interesting patterns of activation. Compared to wild type GluN2A, they displayed a substantial decrease in the number of desensitized periods as demonstrated by the elevated overall P_{open} (Table 5.1) and the smaller increase in P_{open} when excluding desensitized periods (Table 5.2). However, the briefest shut time component was prolonged while its proportion was increased (Figure 5.10). Hence, the burst P_{open} was not decreased even though one of the shut times was increased because there was a decrease in the proportion of longer duration closings.

Table 5.3 compares the rate constants of the NMDA receptor gating mechanism in Scheme 1 for the GluN2 pre-M1 mutants. Rate constants for both the fast and slow transitions were affected by pre-M1 mutants. By contrast, rate constants governing the transition between open states were unaffected by pre-M1 mutants. Figure 5.11 shows free energy plots of the two activation routes from the initial closed state, C_1, to the open state, O_1, and the transition between open states, O_1—O_2. In Figure 5.11A, the fast conformational change occurs first whereas for Figure 5.11B the slow conformational change occurring first. Except for 2A(E551A), all pre-M1 mutations increased the energy barrier for both the slow and fast gating transitions without much effect on the transition between open states. By contrast, 2A(E551A) lowered the energy barrier for the slow gating transition (C_2—O_1 and C_1—C_3) and caused the overall energy change from C_1 to O_1 to be downhill, consistent with the increased burst open probability of 2A(E551A).

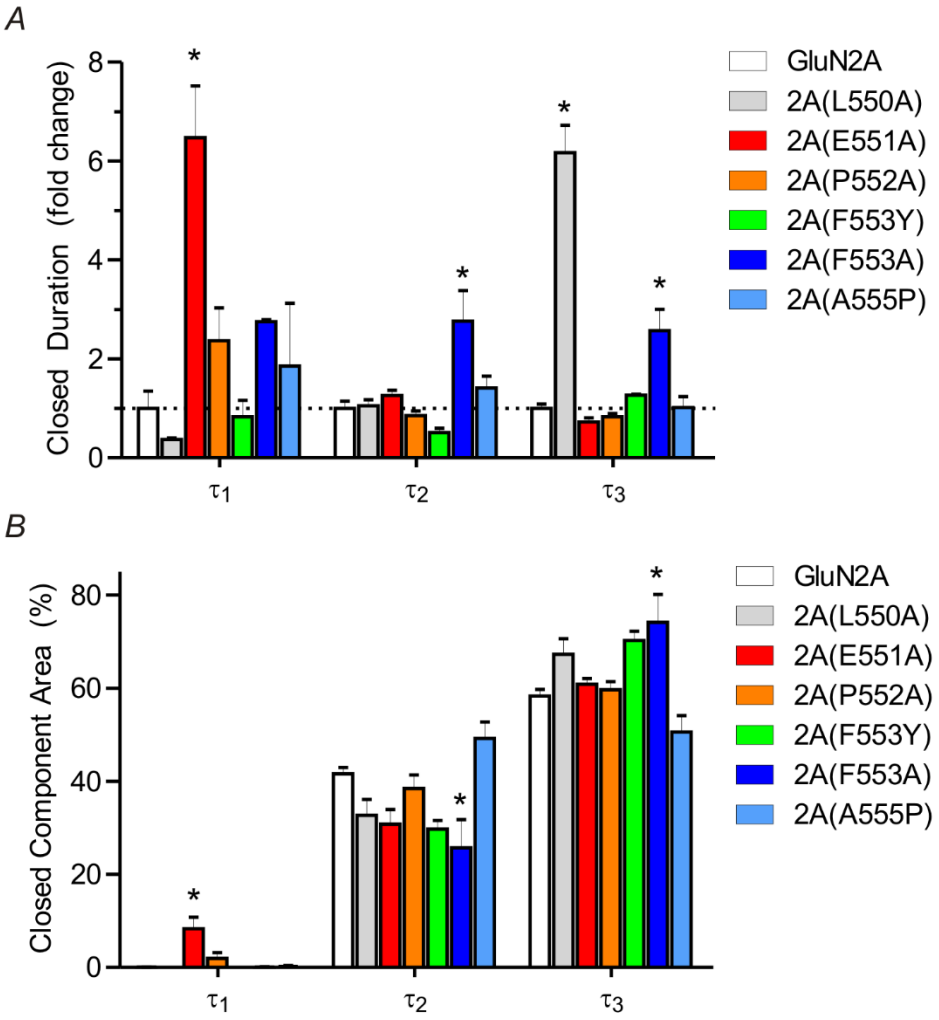

Figure 5.10 Mutations in the pre-M1 region alter the distribution of channel shut times.

A, Fold changes relative to wild type GluN1/GluN2A in the three components of the closed time distributions as determined by MIL fitting of idealized single-channel data. See Table 5.2 for the values of each component. *B*, Relative areas of the closed time components. Data are mean ± SEM.

Table 5.3 Rates predicted by maximum likelihood fitting of Scheme 1 to idealized data

	kf+ (s^{-1})	kf- (s^{-1})	ks+ (s^{-1})	ks- (s^{-1})	ko+ (s^{-1})	ko- (s^{-1})
GluN2A	15000 ± 9000	38000 ± 14000	420 ± 30	1200 ± 200	8200 ± 1700	1090 ± 40
2A(L550A)	7300 ± 1000	60000 ± 5000	103 ± 9*	1700 ± 200	11000 ± 2000	2250 ± 140
2A(E551A)	2300 ± 200	510 ± 80*	1000 ± 700	410 ± 20*	—	—
2A(P552A)	5100 ± 900	17000 ± 8000	440 ± 40	1240 ± 130	12000 ± 3000	2200 ± 500
2A(F553Y)	9000 ±3000	28000 ± 8000	390 ± 30	2800 ± 400*	9000 ± 700	1040 ± 150
2A(F553A)	600 ± 100*	7940 ± 70	260 ± 30	600 ± 200	—	—
2A(A555P)	5000 ± 2000	27000 ± 13000	400 ± 110	650 ± 140	10000 ± 2000	1100 ± 200

* indicates $p<0.05$ vs. GluN2A (one-way ANOVA)

Table 5.4 Open dwell times predicted by fitting of Scheme 1 to idealized data

	τ_{O1} (ms)	τ_{O2} (ms)	$Area_{O1}$ (%)	$Area_{O2}$ (%)
GluN2A	0.058 ± 0.018	1.51 ± 0.13	18 ± 2	82 ± 2
2A(L550A)	0.019 ± 0.003	0.58 ± 0.04*	14 ± 3	86 ± 3
2A(E551A)	—	1.19 ± 0.12	—	100*
2A(P552A)	0.052 ± 0.015	1.25 ± 0.07	12 ± 3	88 ± 3
2A(F553Y)	0.035 ± 0.006	1.5 ±0.2	26 ± 4	74 ± 4
2A(F553A)	0.120 ± 0.002*	—	100*	—
2A(A555P)	0.05 ±0.02	1.66 ± 0.04	13 ± 5	87 ± 5

* indicates $p<0.05$ vs. GluN2A (one-way ANOVA)

Table 5.5 Shut dwell times predicted by fitting of Scheme 1 to idealized data

	τ_{C1} (ms)	τ_{C2} (ms)	τ_{C3} (ms)	$Area_{C1}$(%)	$Area_{C2}$ (%)	$Area_{C3}$ (%)
GluN2A	0.041 ±0.014	0.32 ± 0.05	4.3 ± 0.4	0.07 ± 0.04	41.6 ± 1.4	58.3 ±1.4
2A(L550A)	—	0.34 ± 0.04	26 ± 2*	—	33 ± 4	67 ± 3
2A(E551A)	0.27 ± 0.04*	0.41 ± 0.03	3.1 ± 0.3	8 ± 2*	31 ± 3	60.9 ± 1.2
2A(P552A)	0.10 ± 0.03	0.28 ± 0.03	3.5 ± 0.3	1.9 ± 1.3	38 ± 3	59.6 ± 1.8
2A(F553Y)	0.034 ± 0.014	0.16 ± 0.03	5.38 ± 0.07	0.03 ± 0.03	29.7 ± 1.9	70.3 ± 1.9
2A(F553A)	0.113 ± 0.002	0.9 ± 0.2*	11.0 ± 1.8*	0.10 ± 0.04	26 ± 6*	74 ± 6*
2A(A555P)	0.07 ± 0.05	0.46 ± 0.08	4.3 ±0.9	0.2 ± 0.2	49 ± 4	51 ± 3

* indicates $p<0.05$ vs. GluN2A (one-way ANOVA)

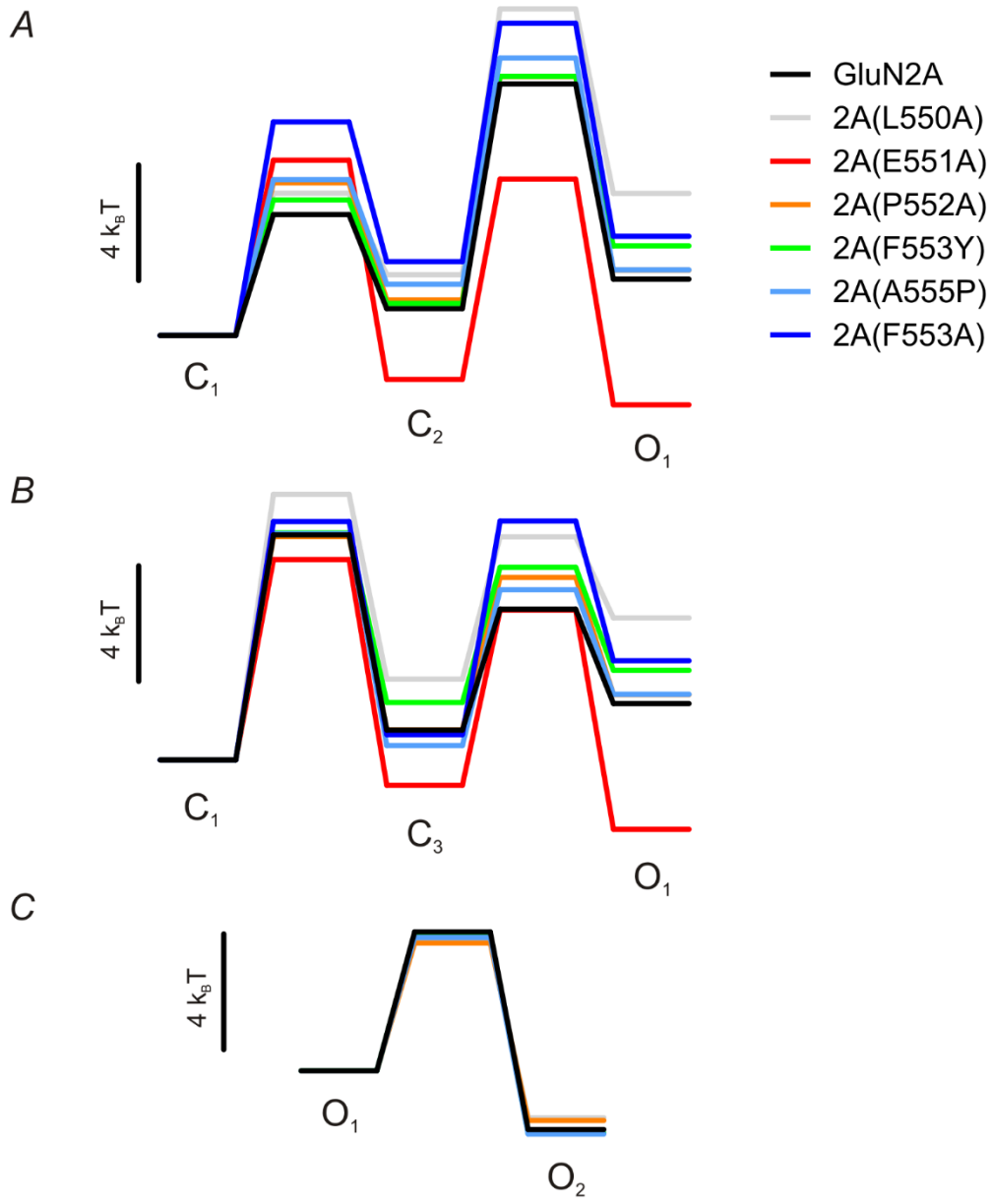

Figure 5.11 Effects of pre-M1 mutations on NMDA rececptor gating mechanism

Free energy landscapes of the GluN1/GluN2A gating mechanism with respect to C_1. Two pathways can lead from state C_1 to state O_1. In the first pathway, the fast gating step associated with GluN1 occurs first (*A*). The slow gating step occurs first in the second pathway (*B*). The relative free energy landscape of the transition between open states is shown, aligned to the first open state, O_1.

Discussion

The conformational transitions that underlie coupling of agonist binding to pore opening in ligand-gated ion channels are fundamental to their physiological roles in synaptic signaling. Structural studies of isolated agonist-binding domains (ABDs) of NMDA receptors have revealed much information about some of the conformational changes that occur upon agonist binding (Inanobe et al., 2005; Furukawa et al., 2005; Vance et al., 2011; Hansen et al., 2013), but how these changes are transduced into opening of the ion channel pore remains an open question. We have sought to address this question by exploring the importance of the pre-M1 region to NMDA receptor gating. This region, together with the M3-S2 and S2-M4 linkers, connects the ABD to the channel pore. Using single-channel recordings of GluN1/GluN2A receptors we have shown that point mutations at several residues in the GluN2 pre-M1 region lead to reduced channel activation due to increased energetic barriers for both the slow and fast gating transition as well as increased durations of desensitized states. Additionally, one mutation, 2A(E551A), increased receptor activation by lowering the energy barrier of the slow, GluN2-specific transition rate as well as the energy of the open state.

The pre-M1 region of GluN2A has previously been implicated in desensitization of NMDA receptors (Thomas et al., 2006). Our work supports these findings because the equilibrium open probability of several pre-M1 mutants was significantly lower than the P_{eq} for wild type GluN2A, but excluding the longest-lived shut state, which is commonly referred to as the desensitized state, eliminated differences in open probability (compare overall P_{open} from Table 5.1 to the burst P_{open} in Table 5.2). In addition, we extend the role of the pre-M1 region to contributing to pre-open gating transitions. Although the phenomenon of desensitization in NMDA receptors is complex and not as well understood as for AMPA receptors, it is generally thought that NMDA receptor desensitization is similar to AMPA receptor desensitization, in which the ABD

dimer interface breaks down leading to a relaxation of the lower lobe of the ABD to a more apo-like position. It is therefore plausible that residues in the pre-M1 region of NMDA receptors, which is located between the lower lobe of the ABD and the ion channel pore, make interactions (or structurally position the M1 helix to make interactions) that are important for transitions to the desensitized state.

Interestingly, the role of pre-M1 region in channel gating seems to differ from that of the M3-S2 and S2-M4 linkers. Whereas pre-M1 mutations mainly affected the early gating transitions but not the O_1—O_2 transition, a previous study found that constraining the M3-S2 and S2-M4 linkers with engineered intrasubunit disulfide bonds dramatically impaired entry into the long-lived open state, but largely did not affect early gating transitions, e.g. C_1—C_2 (Talukder and Wollmuth, 2011). Moreover, constraints in the linkers of both GluN1 and GluN2 seemed to impair receptor gating to the same extent (Talukder and Wollmuth, 2011). Whether the pre-M1 regions of GluN1 and GluN2 also contribute equally to receptor gating is an open question that will require future studies to address.

In the crystal structure of a membrane-spanning tetrameric GluA2 AMPA receptor, the pre-M1 region formed a short “cuff” helix perpendicular to the membrane and immediately adjacent to the it on the extracellular side (Sobolevsky et al., 2009). The four pre-M1 helices, one from each subunit, were directly flanking the central M3 helices and associated M3-S2 linkers, which are thought to be central gating elements in NMDA receptors (Kohda et al., 2000; Jones et al., 2002; Yuan et al., 2005; Chang and Kuo, 2008). Although the secondary structure of the pre-M1 region of NMDA receptors remains unknown, it is worth noting that the two residues at which mutations most dramatically impacted open probability, Leu550 and Phe553, are roughly one helical turn apart, consistent with the predicted alpha-helical secondary structure.

Although structural data of the pore-forming region of NMDA receptors are lacking, much information about NMDA receptor structure and function has been inferred from the sequence and structural homology between glutamate receptor ion channels and K^+ channels (Wo and Oswald, 1995; Wood et al., 1995; Kuner et al., 2003; Sobolevsky et al., 2003, 2009). In the context of gating, two observations between K^+ channels and NMDA receptors are worth noting. First, NMDA receptors lack a glycine in the critical M3 gate helix, which was a critical structural element for K+ channel gating (Doyle et al., 1998; Jiang et al., 2002a, 2002b). Second, the space occupied by the pre-M1 helix in the GluA2 membrane-spanning structure overlaps with the critical S4 voltage-sensing helix in KvAP voltage-dependent K^+ channels (Jiang et al., 2003) when the pore regions are aligned. Similarly, the pre-M1 region also overlaps with two gate-forming inner helices, which may underlie mechanosensitivity, in a human TRAAK channel (Brohawn et al., 2012). Although there are clearly differences between K^+ channels and glutamate receptor ion channels, the observation that critical gating elements in other ion channels occupy a space similar to that of the pre-M1 helix in GluA2 AMPA receptors suggests this region of the receptor could play an important regulatory role in glutamate receptor gating.

Some studies have described distinct “modes” of GluN1/GluN2A receptor gating, characterized by shifts in the mean open times and open probability occurring on the order of seconds (Popescu and Auerbach, 2003; Popescu et al., 2004; Zhang et al., 2008; Kussius and Popescu, 2009; Talukder and Wollmuth, 2011), however several other studies have not observed such shifts in GluN1/GluN2A mean open times (Erreger et al., 2005; Auerbach and Zhou, 2005; Schorge et al., 2005; Yuan et al., 2009). To test for modal gating in our recordings, we concatenated all isolated bursts into a continuous “active time” record, and divided this active time record into 1 second segments to calculate the mean open time, mean shut time, and open probability for each segment.

In our experiments, we never observed shifts in the mean open time characteristic of "modal gating" of NMDA receptors (see Figure 5.3C) even in recordings lasting longer than 1 hour. Similarly, we did not observe modal gating in any of the pre-M1 mutants.

Modal gating has previously been attributed to intracellular binding of proteins and second messengers (Popescu and Auerbach, 2003), Zn^{2+} (Schorge et al., 2005), and transfection system (Auerbach and Zhou, 2005). One possibility that may explain why modal gating was not observed in these studies is that there are differences in the sequences of the recombinant GluN2A subunits used in these experiments and those in which modal gating was reported. In particular GluN2A Thr758 used here is a serine in the subunits used by others. This threonine residue is situated at the ABD dimer interface (Site III from Furukawa et al., 2005), which has been shown to impact NMDA receptor properties (Furukawa et al., 2005; Gielen et al., 2008; Borschel et al., 2011; Hansen et al., 2012). Additionally, GluN2A Phe246 used here is a leucine in other studies. This residue is located in the ATD and seems to be located on a solvent-exposed loop (Karakas et al., 2009), although the functional importance of this residue has not been explored. Moreover, depending on the quaternary arrangement of NMDA receptor ATDs, this residue could be located at an interface between ATD dimers. Future studies are necessary to determine the effect of these two sequence differences on NMDA receptor gating.

Chapter 6: Discussion

The findings presented in this dissertation broadly advance our understanding of allosteric regulation of ion channel function by small molecules. The studies here focused on regulation of the NMDA receptor because it is a critical signaling protein in the brain, important for numerous CNS functions including learning, memory, synapse formation and development, and has been implicated in myriad neurological and psychiatric disorders. The results will likely have implications for the other members of the glutamate receptor ion channel family, and the new mechanisms of allosteric regulation I defined could transfer to other ligand-gated ion channels. My work sheds significant light on allosteric modulators for which no mechanisms of action were understood: a new non-competitive NMDA receptor antagonist and an emerging class of NMDA receptor potentiators. The structural and functional detail of NMDA receptor allosteric regulation that emerged from these studies will most likely carry over to future drugs acting with the same mechanism and together with emerging NMDA receptor crystal structures could allow for rational design of modulators targeting these sites.

Together, these findings embellish the sophisticated mechanisms by which NMDA receptors can be modulated. Although all of the modulators described in this work are exogenous, the possibility exists that endogenous molecules or yet unidentified interacting partners of NMDA receptors also utilize the mechanisms described here. Further, understanding the modulatory sites on the receptor and how molecules interact with the receptor should allow development of therapeutic agents with improved clinical properties and could allow design of subunit-selective modulators

TCN-201: a new non-competitive GluN2A-selective antagonist

I report that TCN-201 is the first antagonist discovered with over 100-fold selectivity for GluN2A-containing NMDA receptors versus GluN2B-, GluN2C-, or

GluN2D-containing receptors. My work demonstrates that TCN-201 inhibits NMDA receptors in an allosteric mechanism by decreasing the affinity of the receptor for the glycine-site agonist. Further, I show that TCN-201 likely binds to a new modulatory site on NMDA receptors located at the GluN1/GluN2 ABD dimer interface.

GluN2A-Selective Antagonism

The discovery of multiple subunits comprising NMDA receptor subtypes in the early 1990s shed light upon the vast molecular and functional diversity that NMDA receptors possess (Moriyoshi et al., 1991; Monyer et al., 1992; Ishii et al., 1993). These findings set the stage for each brain region, neuron type, and synapse in the CNS to express their own repertoire of NMDA receptor subtypes, with varying biophysical properties that could allow each subtype to fulfill diverse roles in CNS physiology (Cull-Candy and Leszkiewicz, 2004; Wyllie et al., 2013; Paoletti et al., 2013). In a similar manner, this diversity could also give rise to particular subtypes being dysfunctional in specific diseases, which would allow therapeutic agents targeting individual NMDA receptor subtypes to restore normal function while avoiding side effects caused by modulating all NMDA receptor subtypes. Elucidation of the mechanism and site of action of TCN-201 should aid in achieving this goal.

There is considerable interest in deciphering which NMDA receptor subunits are involved in excitatory synaptic transmission, neuronal development, and other central nervous system processes (see, for example, Liu et al., 2004; Weitlauf et al., 2005; Bartlett et al., 2007; Gray et al., 2011; Delaney et al., 2012; Volianskis et al., 2012) as individual NMDA receptors subtypes vary considerably in biophysical and pharmacological properties (Monyer et al., 1992; Vicini et al., 1998; Erreger et al., 2007; Yuan et al., 2009) as well as spatiotemporal CNS expression (Monyer et al., 1994; Sheng et al., 1994; Akazawa et al., 1994). Moreover, the subunit combinations are

plastic (Philpot et al., 2001; Bellone and Nicoll, 2007; Matta et al., 2011; Hunt and Castillo, 2012), changing with development and experience. Indeed, NMDA receptor plasticity at mature synapses may shape NMDA receptor function in physiology and disease (Kwon and Castillo, 2008; Rebola et al., 2008, 2011; Hunt et al., 2013).

Perhaps the two most important tools available to neuroscientists to demonstrate unique roles of each NMDA receptor subtype are 1) genetic manipulations to knockdown, knockout, or overexpression specific subunits with cellular and temporal precision in whole animals and isolated tissue, and 2) specific pharmacological tools with sufficient selectivity to rapidly and reversibly modulate individual NMDA receptor subtypes. Since the introduction of Cre-Lox technology to neuroscience by Tonegawa's group in 1996 (Tsien et al., 1996a, 1996b), genetic manipulation of NMDA receptors has continued to improve in the cellular and temporal precision, with recent studies reporting ablation of GluN1 subunits only in interneurons of adolescent mice (Belforte et al., 2010; Korotkova et al., 2010). Unfortunately pharmacological tools with greater than 100-fold selectivity for any NMDA receptor subunit have only been available for the GluN2B subunit. Consequently, many studies have been able to draw strong conclusions about the role of this subunit in CNS physiology and disease. Meanwhile, understanding of the roles of GluN2A, 2C, 2D, and GluN3 in CNS function has lagged behind GluN2B, in part because of the lack of selective pharmacological tools.

Due to the prominent and widespread expression of GluN2A, along with GluN2B, the adult forebrain, GluN2A-selective antagonists have long been sought after to dissect the role of this subunit in normal brain physiology and neurological and psychiatric disorders. While highly-selective GluN2B antagonists have been known since 1993, no antagonists that block GluN2A versus GluN2B with more than 5-fold selectivity were reported until NVP-AAM077 (Auberson et al., 2002; Liu et al., 2004). This competitive antagonist was initially reported to be >100 fold selective for GluN2A over GluN2B

receptors. However, those estimates did not account for the agonist concentration used to activate the receptor. Subsequently, detailed analysis of NVP-AAM077 antagonism at GluN2A and GluN2B receptors using Schild analysis revealed that the K_i at GluN2A and GluN2B varied less than 5-fold (Frizelle et al., 2006). The competitive nature of NVP antagonism together with the 5-fold difference in affinity between GluN2A and GluN2B means that there is no concentration of NVP-AAM077 that can be used to inhibit synaptic GluN2A receptors without also substantially inhibiting synaptic GluN2B receptors (Frizelle et al., 2006). It is interesting to note that D-AP7, an analog of the widely used NMDA receptor antagonist D-AP5, is actually more selective for GluN2A over GluN2B than NVP, having K_i values varying about 8 fold between the two receptors (Table 1.1).

In contrast to NVP-AAM077, my work in chapter 3 shows that TCN-201 displays no measurable inhibition on GluN2B receptors up to its solubility limit, rendering TCN-201 completely selective for GluN2A over not only GluN2B but also GluN2C and GluN2D receptors. Furthermore, my work shows that TCN-201 inhibits NMDA receptors in an allosteric mechanism by decreasing the affinity of the receptors for the GluN1 co-agonist (e.g. glycine or D-serine). Concomitantly, binding of the GluN1 co-agonist decreases the affinity of the receptor for glycine. This mechanism of TCN-201 inhibition creates an important caveat: the degree of inhibition is dependent on the concentration of GluN1 co-agonist. Hence, while TCN-201 will not inhibit GluN2B, even at low glycine concentrations, its inhibition of GluN2A receptors may be less than maximal at higher glycine concentrations. Despite this important caveat to TCN-201 inhibition, TCN-201 will most likely prove useful for inhibiting synaptic GluN2A receptors because glycine concentrations in the synapse appear to be subsaturating at NMDA receptors (Berger et al., 1998; Kalbaugh et al., 2009; Rosenberg et al., 2013 and see “NMDA Receptor Function” section in Introduction).

TCN-201 Site of Action – ABD Dimer Interface

TCN-201 clearly does not act at the GluN2 ATD because it inhibited receptors lacking the GluN2 ATD. As the only highly subunit-selective antagonists known to date (ifenprodil and related GluN2B-selective antagonists) act at the ATD (Perin-Dureau et al., 2002; Karakas et al., 2011; Burger et al., 2012), this finding suggests that TCN-201 represents a class of modulators acting at a new site that could have rich pharmacology and allow development of potent and selective inhibitors of GluN2A. However, it is possible that TCN-201 binds to the ATD of GluN1. I could not rule this out as a possibility because receptors lacking the ATD of both GluN1 and GluN2 are difficult to express in heterologous expression systems due to the fact that the ATD serves as a key interacting domain for assembly of intact, functional receptors (Mayer, 2011b; Herguedas et al., 2013) and formation of ATD dimers is a critical checkpoint for assembly (Meddows et al., 2001; Papadakis et al., 2004; Qiu et al., 2005; Farina et al., 2011).

Nonetheless, the chimeric and mutant data from Chapter 3 suggest that TCN binds to a previously unrecognized modulatory site on the NMDA receptor: the ABD dimer interface. In particular, TCN-201 sensitivity could be transferred to both GluN2B and GluN2D by introducing a single point mutation, GluN2B(F784V) and GluN2D(L808V), that converted divergent residues to the homologous residue in GluN2A, Val783. Additionally, residues that controlled TCN-201 inhibition on both GluN1 and GluN2A resided in the ABD dimer interface.

The ABD dimer interface was first recognized as a critical subunit interface in GluA2 AMPA receptors from crystallographic studies of isolated ABD dimers (Sun et al., 2002). In those studies, mutations that prevented desensitization of the receptor were found to stabilize formation of ABD dimers and were located in the dimer interface in crystal structures. Additionally, positive AMPA receptor modulators, such as

cyclothiazide, that block desensitization were also found to stabilize dimer formation. Moreover, crystal structures revealed a binding site for these modulators in the dimer interface. A mechanism of activation was therefore proposed in which the ABD closes and traps the agonist in the cleft between the upper and lower lobes. Upon activation, the stability of the dimer interface allows the conformational strain caused by domain closure to then transfer to the ion channel gate, opening the pore. On desensitization, however, the dimer interface rearranges, which decouples domain closure from the channel gate. Because the energy barrier for activation is lower than that for desensitization, the ion channel opens faster than it desensitizes.

Subsequently, other positive AMPA receptor modulators were shown to act at the ABD dimer interface (Jin et al., 2005; Ahmed and Oswald, 2010) and desensitization of GluK1, GluK2, and GluK3 kainate receptors also involves rearrangement of the dimer interface (Weston et al., 2006; Nayeem et al., 2009). Furthermore, the ABD dimer interface of kainate receptors and GluD2 receptors, as in AMPA receptors, is a site for allosteric modulation. In GluK1 and GluK2, binding of sodium and chloride ions at discrete sites in the dimer interface are required to maintain kainate receptors in an active conformation by stabilizing the ABD dimer (Plested et al., 2008). Similarly, in GluD2 receptors, Ca^{2+} binding stabilized the ABD dimer interface (Hansen et al., 2009).

My finding that TCN-201 acts at the GluN1-GluN2 ABD dimer interface is the first to demonstrate a site for allosteric modulators at the ABD dimer interface of NMDA receptors. This is in agreement with studies suggesting the NMDA receptor ABD dimer interface couples allosteric modulation by ATD ligands to the channel gate (Gielen et al., 2008). In those studies, several mutations that purportedly disrupt atomic contacts between ABD dimers were shown to increase sensitivity of the receptor to allosteric antagonists that bind the ATD, such as Zn^{2+}. Because of the importance of the ABD dimer interface for allosteric modulation, my experiments showing affinity, and not simply

efficacy, of TCN-201 decreased at GluN2A(V783L) were particularly important to show that TCN-201 directly interacts with the ABD dimer interface.

Effects of TCN-201 on Triheteromeric NMDA Receptors

Many, if not all, neuronal NMDA receptors are thought to be triheteromeric complexes composed of GluN1 and two different GluN2 subunits, or possibly a GluN2 and a GluN3 subunit (Henson et al., 2010; Rauner and Köhr, 2011; Gray et al., 2011; Delaney et al., 2012; Tovar et al., 2013) . Therefore, it is important to know how modulators acting on NMDA receptors will affect the function of triheteromeric receptors.

Will TCN-201 inhibit triheteromeric receptors? Antagonists such as Zn^{2+} and ifenprodil inhibit triheteromeric receptors with similar potency as diheteromeric receptors, albeit with reduced efficacy (Hatton and Paoletti, 2005), so it is possible that TCN-201 could inhibit triheteromeric receptors. However, the mechanisms by which Zn^{2+} and ifenprodil inhibit the receptor are quite different from the mechanism of TCN-201. Zn^{2+} and ifenprodil also act at the ATD, a site distinct from that of TCN-201. Yet, if the binding site for TCN-201 is at the ABD dimer interface as suggested by experiments from Chapter 4, then its binding site will be present in a triheteromeric NMDA receptor because the ABDs are locally arranged as a pair of GluN1/GluN2 dimers (Sobolevsky et al., 2009; Salussolia et al., 2011b; Riou et al., 2012). Therefore it is likely that TCN-201 will inhibit triheteromeric receptors with similar potency. Whether binding of TCN-201 to one ABD dimer could influence the conformation (and therefore the glycine affinity) of the other ABD dimer is unclear and could affect TCN-201 potency or the extent to which glycine potency is shifted by TCN-201.

With what efficacy might TCN-201 inhibit triheteromeric receptors? If NMDA receptors require fully occupied binding sites at all four subunits (two glycines on the two GluN1 subunits, and two glutamates on the two GluN2 subunits) as proposed

(Benveniste and Mayer, 1991; Clements and Westbrook, 1991; Schorge et al., 2005), then reducing the affinity of glycine for only one subunit should be just as efficacious as reducing it at both GluN1 subunits, because there is little cooperativity between glycine binding sites, as suggested by the Hill slope of glycine concentration response curve of 1.2 (Chen et al., 2008b) and as explicitly modeled in NMDA receptor activation mechanisms (Schorge et al., 2005).

Does TCN-201 Change the Gating Equilibrium?

Although Chapter 4 demonstrates that TCN-201 can shift the potency of glycine at GluN1/GluN2A receptors, TCN-201 could additionally change the efficiency of gating. However, the observation that 300 μM glycine completely eliminated any TCN-201 inhibition (see Figure 4.1C) strongly suggests that TCN-201 did not change the gating efficiency; if it did, then some degree of TCN-201 inhibition would still be observed, even at very high glycine concentrations. Nonetheless, one way to test this directly is by recording single-channel currents in the presence of TCN-201. It would be difficult to determine in a strictly quantitative manner the effect of TCN-201 on the gating equilibrium, however, because the solubility limit of TCN-201 (~18 μM) prevents saturation of the shift in glycine potency, a key feature of allosteric antagonists that would occur at >200 μM TCN-201. Thus, it could not be assumed that TCN-201 is always bound to a receptor during such experiments. Still, the simple allosteric mechanism from Figure 4.9 would suggest that with 10 μM TCN-201 and 3 μM glycine about 85% of the openings would be with TCN-201 bound, so it might be possible to get a qualitative answer to whether TCN-201 changes the gating equilibrium.

Clinical Utility of a GluN2A-Selective Antagonist

In general, overactivation of NMDA receptors has been implicated in neuronal loss that occurs in diseases with either acutely elevated glutamate, such as stroke and

traumatic brain injury, or chronically elevated glutamate, such as degenerative disorders (Muir, 2006). The mechanism proposed for all these cases is that overactivation of NMDA receptors allows excessive entry of Ca^{2+} into the neuron, triggering excitotoxicity. Many general NMDA receptor antagonists, which are not selective for a particular subtype, have been neuroprotective in preclinical animal models and pursued in clinical trials (Gladstone et al., 2002; Muir, 2006; Kalia et al., 2008). Investigations of the NMDA receptor subtype or subtypes that might underlie neuronal loss in these diseases have largely focused on GluN2B-containing NMDA receptors, in large part because of the availability of highly-selective GluN2B antagonists. These studies have revealed significant neuroprotective effects of GluN2B-specific antagonists (for review see Mony et al., 2009). By contrast, activation of GluN2A-containing receptors has been shown to promote survival of neurons (Liu et al., 2007; Chen et al., 2008a), although the pro-survival role of GluN2A remains contested (Martel et al., 2012). Some of the ambiguity of these studies undoubtedly stems from the use of NVP-AAM077 in attempts to selectively-block GluN2A receptors. Because NVP-AAM077 is, in fact, rather non-selective, a questions arises whether some of the effects observed with NVP treatment are due to off-target effects. In contrast to NVP-AAM077, TCN-201 is completely selective for GluN2A receptors across the glutamate receptor ion channel family. Hence, TCN-201 or future related GluN2A-selective antagonists will surely help to clarify how GluN2A-containing receptors contribute to these disease states.

In animal models of Parkinson's disease, overactivation of glutamate projections to the striatum and basal ganglia occurs upon loss of nigral dopaminergic neurons (Sgambato-Faure and Cenci, 2012) and upregulation of synaptic GluN2A receptors in the striatum occurs (Hallett et al., 2005). Further, disrupting GluN2A synaptic localization concomitant with L-DOPA treatment decreased the percentage of parkinsonian rats that developed dyskinesias (Gardoni et al., 2012). Given that non-

selective NMDA receptor antagonists showed anti-parkinsonian effects (Hallett and Standaert, 2004) further studies with GluN2A-selective antagonists such as TCN-201 seem warranted.

Alteration of NMDA receptor signaling has also been implicated in mood disorders such as anxiety and depression (Paul and Skolnick, 2003; Sanacora et al., 2012; Riaza Bermudo-Soriano et al., 2012). GluN2A knock-out mice showed decreased anxiety-related phenotypes and antidepressant-like profiles in multiple behavioral paradigms (Boyce-Rustay and Holmes, 2006). The effects of GluN2A knock-out appeared to be somewhat specific to emotional behaviors because no deficits in locomotion, sensory reflexes, or prepulse inhibition were observed. However, intra-amygdala infusions of NVP-AAM077 suggested that GluN2A was more broadly involved in amygdalar synaptic transmission and not necessarily in fear-specific synaptic plasticity (Walker and Davis, 2008). Yet, GluN2A could participate in synaptic plasticity in the lateral amygdala depending on the pattern of synaptic activation (Müller et al., 2009). Hence, GluN2A-selective antagonists may prove useful for treating some anxiety-related disorders, depending on what circuits are dysregulated in the specific disorder.

A strong theoretical framework exists for NMDA receptors in neuronal circuits important in chronic pain. Chronic pain, either inflammatory or neuropathic, involves neuronal plasticity at one or several sites within the pain transmission pathway that leads to hypersensitivity in nociceptive systems (Woolf and Salter, 2000). As NMDA receptors are critical for induction and expression of synaptic plasticity throughout the brain, it is not surprising that they play similar roles in the spinal cord. NMDA receptors are expressed in the spinal cord (in fact some of the earliest studies demonstrating the existence of NMDA receptors utilized spinal cords neurons (Evans et al., 1978b, 1982; Mayer et al., 1984)), and, importantly, are localized to synapses (Nagy et al., 2004). Interest in NMDA receptor antagonists for the relief of chronic pain was first generated

when ketamine and AP5 were shown to inhibit the hyperexcitability of spinal cord nociceptive neurons caused by excessive stimulation of C fibres in the late 1980s (Dickenson and Sullivan, 1987; Davies and Lodge, 1987). Subsequently, GluN2B-selective antagonists received considerable attention as efficacious antinociceptive agents (Chizh et al., 2001; Petrenko et al., 2003; Wu and Zhuo, 2009).

In addition to GluN2B, inhibition of other NMDA receptor subtypes may also have analgesic properties. Deletion of GluN1 in the spinal cord reduced formalin-induced pain without altering heat or cold paw-withdrawal latencies, suggesting NMDA receptors are important specifically for injury-induced pain (South et al., 2003). PSD-93 knockout mice had reduced surface expression of GluN2A and GluN2B and exhibited decreased NMDA receptor-dependent pain responses in inflammatory and neuropathic pain models (Tao et al., 2003). Preventing enhancement of NMDA receptor currents by disrupting their interaction with the tyrosine kinase Src suppressed pain hypersensitivity by peripheral nerve injury without affecting normal sensory thresholds or acute nociception (Liu et al., 2008). Furthermore, GluN2A knock-in mice that were insensitive to inhibition by Zn^{2+} showed enhanced allodynia in models of inflammatory and neuropathic pain (Nozaki et al., 2011). Thus GluN2A-containing receptors represent an intriguing, but underexplored therapeutic target for inflammatory and chronic pain.

CIQ: a novel GluN2C- and GluN2D-selective positive allosteric modulator

CIQ is the first small molecule NMDA receptor positive allosteric modulator. Interestingly, it is selective for GluN2C- and GluN2D-containing NMDA receptors, having no activity at GluN2A-, or GluN2B-containing receptors. Previous work by myself and others has shown that CIQ potentiates NMDA receptors by increasing the channel opening frequency without changing glutamate deactivation time course (Mullasseril et al., 2010). In studies presented here, I have extended these findings to demonstrate

that CIQ acts a previously unrecognized modulatory site in the region of the M1 transmembrane helix.

Effects of CIQ on Triheteromeric NMDA Receptors

To determine how CIQ affects triheteromeric receptors, Mullasseril et al (2010) co-applied CIQ with agonists on oocytes injected with cRNA for GluN1, GluN2A, and GluN2C (or GluN2D). In these oocytes, three populations of receptors should form, two of which are diheteromeric—GluN1/GluN2A and GluN1/GluN2C—and one of which is triheteromeric—GluN1/GluN2A/GluN2C (Hatton and Paoletti, 2005; Ulbrich and Isacoff, 2008). The GluN2A subunit in these experiments had two point mutations; one mutation reduced the block by Mg^{2+} and one mutation reduced glutamate potency by over 1000-fold. These mutations thus allowed isolation of responses from triheteromeric receptors by recording currents in 1 mM Mg^{2+}, which would block GluN2C, but not GluN2A or GluN2A/GluN2C, and eliciting responses with 10 mM glutamate, which would activate GluN2C and GluN2A/GluN2C, but not GluN2A. When CIQ was co-applied with agonists under these conditions, an increase in current amplitude was observed that could not be explained by potentiation of GluN1/GluN2C alone. Since CIQ has no activity on GluN1/GluN2A receptors, the increased current above what was accounted for by potentiation of GluN1/GluN2C must have arisen from potentiation of triheteromeric GluN1/GluN2A/GluN2C receptors. Therefore, CIQ likely potentiates triheteromeric receptors to a similar extent as diheteromeric receptors.

The ability of CIQ is significant because, in wild type mice, GluN2C and GluN2D have only been identified in neurons that also express GluN2A and/or GluN2B (Momiyama et al., 1996; Misra et al., 2000; Brickley et al., 2003; Jones and Gibb, 2005; Brothwell et al., 2008). Moreover, GluN2C and GluN2D subunits often coassemble with GluN2A and GluN2B, respectively, as evidenced by single-channel recordings of

somatic NMDA receptors in which currents from a single ion channel containing openings that exhibited amplitudes and durations characteristic of two different GluN2 subunits (Cathala et al., 2000; Brickley et al., 2003; Jones and Gibb, 2005). The ability of CIQ to potentiate triheteromerics likely explains its ability to potentiate NMDA-evoked responses from neurons of the subthalamic neurons, which express both GluN2B and GluN2D (Standaert et al., 1994; Mullasseril et al., 2010).

Given the site of action of CIQ in the pre-M1/M1 region, its ability to potentiate triheteromeric receptors containing two different GluN2 subunits suggests that the M1 region of GluN2D has a negative regulatory role on channel gating, similar to the GluN2D ATD (Gielen et al., 2009; Yuan et al., 2009), because CIQ binding to this subunit alone was sufficient to increase channel function. It is tempting to speculate, then, that triheteromeric receptors containing e.g. GluN2B and GluN2D will have reduced function compared to diheteromeric GluN2B receptors, however further investigations are needed to establish this.

Effect of CIQ on Glutamate Potency

CIQ causes an approximate doubling of currents from GluN2C- and GluN2D-containing receptors (see Figure 1.1), but has minimal effects on the potency of either glutamate or glycine (Mullasseril et al., 2010). The increased current response caused by CIQ could be due to 1) an increase in the single-channel conductance, 2) an increase in the gating equilibrium (i.e. an increase in open probability), 3) an increase in the number of functional receptors expressed at the cell surface, or 4) a decrease in receptor desensitization. Case 4 is unlikely because GluN1/GluN2C and GluN1/GluN2D receptors exhibit very little observable desensitization (Dravid et al., 2008; Vance et al., 2011, 2012). Although case 3 cannot be ruled out without an independent measure of total number of receptors on the cell surface (see for example Chang and Weiss, 1999),

it most certainly would not be due to an increase in trafficking of the receptor, because the time course of potentiation occurs on the order of seconds (Mullasseril et al., 2010), much too quickly for CIQ to cross the cell membrane and initiate biochemical events leading to increased insertion of receptors in the cell membrane. An increase in "functional" receptors could arise, then, from a change in some "nonfunctional" receptors that are already expressed at the cell surface, but then we are simply referring to an increase in the efficacy of gating, which is 0 in the case of nonfunctional receptors. Fortunately, analysis of single-channel recordings allowed observation of the effects of CIQ on channel conductance, which, if anything, decreased with CIQ (Mullasseril et al., 2010) and therefore cannot explain the potentiation.

Hence, a reasonable assertion is that CIQ increases the gating equilibrium. It has been well established that an increase in gating efficiency will cause an increase in the EC_{50} for agonists (Colquhoun, 1998). It is therefore surprising, at least at first, that CIQ does not increase the potency of glutamate given that it increases the gating equilibrium. The reason for this discrepancy is likely that GluN1/GluN2C and GluN1/GluN2D receptors have such a low open probability: 0.01 for 2C (Dravid et al., 2008) and 0.02 for 2D (Vance et al., 2012), which correspond to gating equilibrium constants (*E* in Scheme 1) of 0.0101 for 2C and 0.0204 for 2D. Previous discussions of effects of gating changes on current responses (e.g. Colquhoun, 1998), did not consider such low values of *E*. Extending those discussions to *E* values around 0.01 reveal that doubling the value of *E* (e.g. from 0.01 to 0.02), which would result in an approximate doubling of the maximum response (i.e. P_{open} would increase from 0.0099 to 0.0196), has absolutely no change in the agonist potency or the Hill slope. In a more general case, marked changes in the agonist potency would not be observed until the value of *E* increased to about 1, which for GluN1/GluN2D would correspond to an approximate 50-fold increase in the maximum current response to a P_{open} of 0.5.

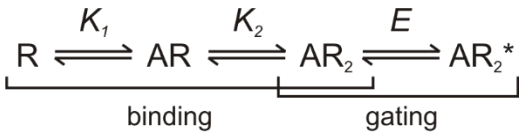

Scheme 1

The potentiation of current responses by CIQ is entirely consistent with an increase in the gating equilibrium. Moreover, a change in only the binding equilibrium (i.e. K_1 or K_2) and not the gating equilibrium cannot account for the increase in maximum current response caused by CIQ because the maximum response is only a function of the efficiency of gating, specifically, E / ($E+1$). Therefore, CIQ must affect the gating equilibrium. Can an effect of CIQ on the binding equilibrium, and thus the agonist potency, be ruled out, though? Two potential lines of evidence to address this are whether CIQ affects the agonist activation and deactivation rates and whether the increase in current response caused by CIQ is dependent on the concentration of agonist used. While CIQ did not affect the glutamate activation rate (10-90% rise time at GluN2D was 13 ± 1 ms for control and 15 ± 2 ms for CIQ) and had minimal effects on the glutamate deactivation time course (for GluN2D τ_{fast} = 2.1 ± 0.15 s and τ_{slow} = 5.7 ± 0.5 s (53%) for control and τ_{fast} = 2.0 ± 0.3 s and τ_{slow} = 5.8 ± 0.6 s (60%) for CIQ), this information alone is insufficient to settle the question for two reasons. First, for NMDA receptors, the relationship between potency and deactivation time course is non-linear such that approximately 10-fold changes in EC_{50} have been observed with only about 2-fold changes in the deactivation time course (Vance et al., 2011). Hence, minor changes in the EC_{50} (e.g. 2-fold) may not produce detectable changes in the deactivation time course. Second, the recent description of a gating mechanism for GluN1/GluN2D had 14 states (Vance et al., 2012), and therefore the $\tau_{deactivation}$ should be a mixture of 13 exponentials (Colquhoun and Hawkes, 1977). However $\tau_{deactivation}$ for GluN2D can be well-described by a mixture of two exponentials (Vance et al., 2012).

Thus, the ability to infer changes in the gating mechanism based on macroscopic properties such as $\tau_{deactivation}$ is inadequate. Actually, $\tau_{deactivation}$ remains poorly understood. The best gating mechanism described for GluN1/GluN2D (among more than 50 mechanisms tested) explains many of the properties of GluN2D activation, including the low open probability, rapid response time, and mean open time, but did not produce a dual exponential deactivation time course (Vance et al., 2012).

In contrast to effects of CIQ on agonist activation and deactivation rates, the dependence of maximal CIQ potentiation on agonist concentration is potentially more revealing. Figure 6.1 shows glutamate-concentration response curves from GluN1/GluN2D receptors expressed in oocytes in the absence and presence of 10 μM CIQ. The glutamate current response was increased in the presence of CIQ (Figure 6.1A) with a small, but significant increase in the glutamate potency (Figure 6.1B). Although the current response at every concentration of glutamate was increased in the presence of CIQ, the degree of CIQ potentiation was greater at low glutamate concentrations (Figure 6.1C). A simple sequential mechanism of activation (Scheme in Figure 6.1) in which both glutamate binding sites are equivalent (i.e. $K_2 = 4K_1$) and have to be occupied for the channel to open provides a nice conceptual framework for understanding how changes in both binding and gating equilibria give rise to the increased CIQ potentiation at low glutamate concentrations. Figure 6.1D shows a simulated control glutamate concentration-response curve with a binding equilibrium constant of 0.1128 μM and a gating equilibrium constant of 0.01 (blue curve). If CIQ caused a doubling of the gating efficiency and a small decrease in the binding equilibrium constant, the glutamate curve would look like that shown in red. When normalized to the maximum current response for each condition, these two curves would be almost indistinguishable (Figure 6.1E), although a slight increase in glutamate

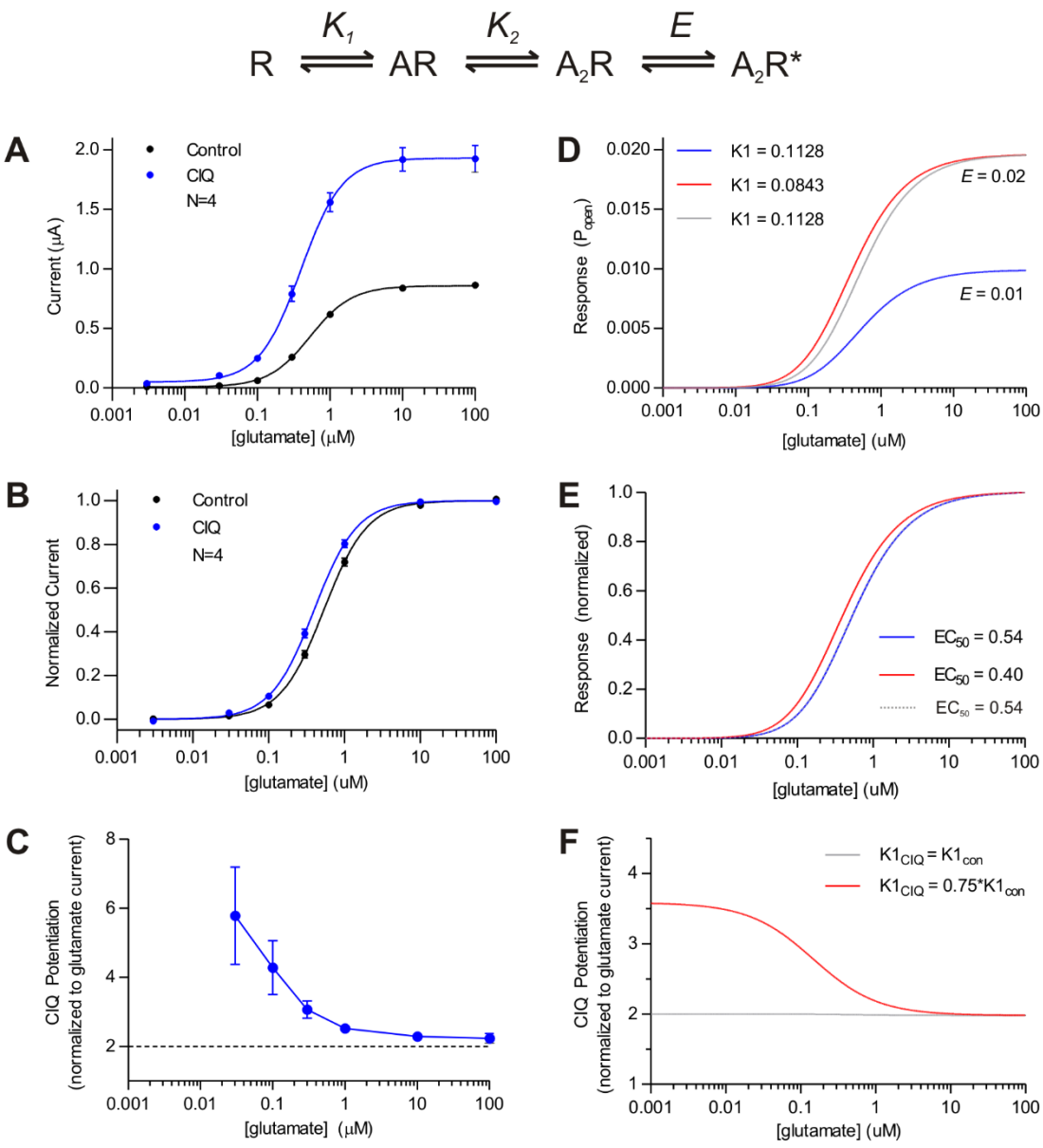

Figure 6.1 ClQ Affects Glutamate Binding Equilibrium

The effect of ClQ on glutamate concentration-response curves was measured using two-electrode voltage-clamp recordings of GluN1/GluN2D receptors expressed in oocytes. Currents were activated by 30 μM glycine and increasing concentrations of glutamate at -40 mV. **A**, Glutamate concentration-response curves were measured on each oocyte in the absence (control) and subsequently

in the presence of 10 μM CIQ. **B**, The same glutamate curves from panel A are shown normalized to the maximum current for each condition. Individual curves from each oocytes were fit to the Hill equation. The glutamate EC_{50} (mean ± sem) in the absence of CIQ was 0.54 ± 0.03 μM while in the presence of CIQ it was 0.40 ± 0.02 μM. The logarithm of the EC_{50}values was significantly different in the presence of CIQ compared to control ($t_{0.05(2)}$=4.012, df=3, p=0.03; paired t-test). **C**, The glutamate curves from panel A in the presence of CIQ are shown normalized to the glutamate curves in the absence of CIQ. CIQ increased the current response at every concentration of glutamate, but the extent of potentiation was greater at lower concentrations of glutamate. To understand why CIQ caused larger potentiation at low glutamate concentrations, GluN2D current responses were simulated using the gating mechanism shown at the top. For these simulations, *K2* was fixed to be 4**K1* because the two glutamate binding sites on NMDA receptors have been modeled as equivalent (Lester and Jahr, 1992; Schorge and Colquhoun 2005; Erreger et al., 2005; Dravid et al., 2008; Vance et al., 2012). The value of *E* was also fixed to match the open probability from single channel recordings: $E = P_{open} / (1-P_{open})$. For GluN2D, P_{open} is about 0.01, corresponding to an *E* value of 0.01. With *E* = 0.01, an observed glutamate EC_{50} for control of 0.54 μM implies that *K1* = 0.1128 μM (blue curves). To simulate the effects of CIQ (red curve), the value of *E* was doubled, which would lead to an approximate doubling of the maximum current. The glutamate EC_{50} observed in the presence of CIQ (10 μM) was 0.40 μM, implying *K1* decreased to 0.0843 μM (red curves). For comparison, a simulation was done in which only the value of *E* changed (gray curves). **D**, Simulated glutamate curves are shown as the fraction of open receptors (P_{open}), which corresponds to the maximum current response. **E**,

The simulated curves from panel D are shown normalized to the maximum P_{open} for each curve. Note that the gray and blue curves are indistinguishable. **F**, The red and gray curves from panel A are shown normalized to the blue curve also in panel A. This is the degree of potentiation that occurs when the binding and gating equilibriums are affected (red) or only the gating equilibrium changes (gray). Only when both the binding and gating equilibriums are changed is the extent of potentiation at low glutamate concentrations greater than at high glutamate concentrations.

potency would occur. In fact, this is what was observed with CIQ (Mullasseril et al., 2010) although the change in glutamate potency was not statistically significant, perhaps due to insufficient power of the experiment, which is estimated to be 0.43 to detect a 1.3-fold change in glutamate EC_{50} with n=6 using an independent two-sample t-test. Nevertheless, this small shift in glutamate potency would lead to quite dramatic changes in the maximum degree of potentiation by CIQ when control current responses are activated by low concentrations of agonist, e.g. EC_{10}. This is illustrated in Figure 6.1F, which shows the CIQ potentiation normalized to the current elicited by glutamate alone (i.e. the red, and gray curves divided by the blue curve in Figure 6.1D). For the case when only the gating equilibrium changes (gray), CIQ potentiation would be (almost) the same at every concentration of glutamate, only varying from 2 at concentrations less than 0.03 μM to 1.98 at concentrations greater than 3 μM. However, if the binding equilibrium also changes (red curve), CIQ potentiation should be much greater at lower concentrations of glutamate. This increased potentiation could be quite remarkable; even if CIQ only caused a 2-fold increase in glutamate potency, it would still quadruple the response to an EC_{10} concentration of glutamate. Indeed, CIQ potentiation is greater at lower glutamate concentrations (Figure 6.1C), suggesting that CIQ enhances both binding of glutamate and the subsequent gating conformational change.

An intriguing possibility raised by the effects of CIQ on both binding of agonist and gating is that these effects arise from two different CIQ binding sites on the receptor, perhaps even one site in GluN1 and one site in GluN2. While it is certainly not necessary that this must be the case to explain the actions of CIQ (e.g. mutations at a single site, tyrosine 190, in the α subunit of mouse nicotinic receptors affected both binding and gating (Chen et al., 1995)), there are several reasons to investigate this possibility. First, conferring CIQ potentiation onto GluN2A using chimeras required

transferring two disparate regions of GluN2D into GluN2A. Second, modifying the chemical structure of CIQ yielded some analogues that seemed to primarily affect potency and some that primarily affected the maximum potentiation (Santangelo Freel et al., 2013). Third, the M1 helix is highly conserved across the GluN2 subunits, yet CIQ only potentiates GluN2C and GluN2D, with no detectable potentiation at GluN2A or GluN2B. Fourth, analogs of CIQ with modest changes to the chemical scaffold potentiate GluN2B (Santangelo-Freel, Strong, Ogden, and Traynelis, unpublished observations), which already has an isoleucine at the homologous M1 residue that when mutated in GluN2D to isoleucine abolished CIQ potentiation. Moreover, one of these analogs, 1180-55, potentiates, albeit modestly, GluN2D(T592V) receptors that are insensitive to CIQ (Ogden and Traynelis, unpublished observations). Fifth, chimeric receptors of GluN2D that had the ATD and its linker to the ABD swapped for those regions of GluN2A—GluN2D(2A ATD+L)—showed a pronounced decrease in CIQ potentiation whereas chimeras only having the linker swapped—GluN2D(2A L)—showed no change in CIQ potentiation (Mullasseril et al., 2010). Knowing whether there are two binding sites for CIQ and whether the effects of CIQ on binding and gating are separable could allow design of modulators that affect only binding or only gating and could allow selectivity to be directed toward any of the four subunits.

Effects of CIQ on fear/emotional conditioned learning

Fear is a normal emotional response that results in a heightened state of arousal in response to an immediate threat or aversive situation. The acquisition of fear is thought to share some of the same molecular underpinnings as cognitive processes such as learning and memory (for review, see Johansen et al., 2011). Given the central role of NMDA receptors in mediating plasticity, such as LTP, their involvement has been

explored in the context of fear learning and in particular the GluN2C subtype may be critical for modulating emotional learning.

Amygdala infusions of the competitive NMDA receptor antagonist AP5 blocked NMDA receptors and prevented acquisition of learned fear (Miserendino et al., 1990). Subsequently, studies using the GluN2B-selective antagonists ifenprodil or CP-101,606 suggested that GluN2B-containing NMDA receptors may mediate fear memory formation and the underlying synaptic plasticity (Rodrigues et al., 2001; Walker and Davis, 2008). In addition to fear acquisition, NMDA receptors are also critical for the extinction of fear. NMDA receptor antagonists blocked extinction (Falls et al., 1992; Baker and Azorlosa, 1996; Lee and Kim, 1998; Santini et al., 2001; Lin et al., 2003; Suzuki et al., 2004) and D-cycloserine (DCS), an agonist at the GluN1 subunit, enhanced fear extinction (Walker et al., 2002). Interestingly, DCS is a partial agonist at GluN2A, 2B, and 2D receptors but elicits greater currents than saturating concentrations of glycine from GluN2C receptors (Sheinin et al., 2001; Dravid et al., 2010). This finding creates the possibility that DCS increases retention of fear extinction by at least two mechanisms. First, when endogenous glycine concentrations are submaximal DCS can augment the activity of all NMDA receptors by increasing occupancy of the glycine site. Second, DCS can selectively enhance the response of GluN2C receptors when it replaces glycine as the co-agonist bound to GluN1/GluN2C receptors. The idea that the effects of DCS on fear extinction are mediated by GluN1/GluN2C receptors is consistent with a recent finding that acquisition of fear learning is impaired in GluN2C knockout mice (Hillman et al., 2011). The deficit in fear learning was observed for both cued and contextual conditioned fear and was observed with either a tone or a light as the conditioned stimulus. Further, these mice did not exhibit plasticity at thalamo-amygdala synapses normally induced by fear conditioning.

Given the effects of GluN2C knockout and DCS on the acquisition and extinction of learned fear, we hypothesized that GluN2C-containing NMDA receptors play an important role in the acquisition, retention, and extinction of fear. To further evaluate the role of GluN2C receptors in fear acquisition and extinction, we therefore initiated a collaboration with Drs. Scott Heldt and Kerry Ressler to infuse CIQ bilaterally into the basolateral amygdala (3, 10 or 30 μg/side) immediately following either fear conditioning or fear extinction training (Ogden et al., submitted).

In the first experiment to test whether CIQ would affect fear response, mice were given one session of conditioned fear training followed immediately by injection of CIQ *via* a cannula implanted into the basolateral amygdala. When mice were tested one day later without drug, mice that received CIQ injections exhibit a dose-dependent increase the conditioned freezing response, suggesting CIQ enhanced the retention of fear when assessed 24 hr after training. In a second set of experiments to assess the effects of CIQ on fear extinction, a new cohort of mice were given fear training. Two days later, mice were given an extinction session and immediately following the session mice received injections of CIQ. When mice were tested for fear responses one day after the extinction session, mice that received CIQ injections showed significant differences in levels of conditioned freezing, indicating that post-extinction training intra-amygdala infusions of CIQ dose-dependently enhanced the retention of fear extinction when assessed 24 hr after training.

These results support a critical role for GluN2C receptors in the amygdala in the consolidation of learned fear responses and suggest that increased activity of GluN2C receptors may underlie the therapeutic actions of D-cycloserine. Moreover, these findings hold several important implications for learning. First, they show that positive allosteric modulation of NMDA receptors by small molecules can enhance learning in vivo. Second, they suggest the GluN2C subunit, a subunit about which little is known,

plays a central role in plasticity of certain brain circuits. More broadly, our findings raise the possibility that enhancement of learning involving specific brain regions can be selectively achieved through targeted allosteric potentiation of the receptors expressed in those regions. Hence, CIQ and other selective NMDA receptor allosteric modulators (Monaghan et al., 2012) may be useful pharmacological tools for dissecting which receptors may underlie learning and memory. Moreover, as human anxiety disorders likely result from disruptions in some of the same neuronal circuitry that underlies fear learning in animal models (Cryan and Sweeney, 2011; Graham et al., 2011), potentiation of GluN2C-containing receptors may be an attractive strategy to treat a wide range of neurological diseases with altered fear learning, including post-traumatic stress disorder and anxiety disorders.

Conclusion

The unique biophysical properties of NMDA receptors place them at the center of many physiological phenomenon in the central nervous system and also implicate them in many neurological and psychiatric disorders. The discovery of multiple subunits comprising several NMDA receptor subtypes each with unique biophysical and pharmacological properties as well as region-specific expression profiles expanded the repertoire of potential roles NMDA receptors might play in normal brain function. However, dissection of the unique contribution of each NMDA receptor subtype to physiology and disease has been hindered by the lack of subunit-selective pharmacological tools. The work in this dissertation helps to fill this gap by describing the mechanism of action of two new subunit-selective NMDA receptor modulators, TCN-201 and CIQ. Coupled with future elucidation of NMDA receptor structure may allow further embellishment of the structure-activity relationship of NMDA receptor modulators and a more complete understanding of how this intricate molecular machine works.

Chapter 7: References

Abe K, Xie F, Watanabe Y, Saito H (1990) Glycine facilitates induction of long-term potentiation of evoked potential in rat hippocampus. *Neurosci. Lett.* 117:87–92

Abele R, Keinänen K, Madden DR (2000) Agonist-induced Isomerization in a Glutamate Receptor Ligand-binding Domain A KINETIC AND MUTAGENETIC ANALYSIS. *J. Biol. Chem.* 275:21355–21363

Abele R, Svergun D, Keinänen K, Koch MHJ, Madden DR (1999) A Molecular Envelope of the Ligand-Binding Domain of a Glutamate Receptor in the Presence and Absence of Agonist. *Biochemistry (Mosc.)* 38:10949–10957

Acker TM, Khatri A, Vance KM, Slabber C, Bacsa J, Snyder JP, Traynelis SF, Liotta DC (2013) Structure–Activity Relationships and Pharmacophore Model of a Noncompetitive Pyrazoline Containing Class of GluN2C/GluN2D Selective Antagonists. *J. Med. Chem.* 56:6434–6456

Acker TM, Yuan H, Hansen KB, Vance KM, Ogden KK, Jensen HS, Burger PB, Mullasseril P, Snyder JP, Liotta DC, Traynelis SF (2011) Mechanism for noncompetitive inhibition by novel GluN2C/D N-methyl-D-aspartate receptor subunit-selective modulators. *Mol. Pharmacol.* 80:782–795

Adachi H, Fujisawa H, Maekawa T, Yamashita T, Ito H (1995) Changes in the extracellular glutamate concentrations in the rat cortex following localized by hyperthermia. *Int. J. Hyperth. Off. J. Eur. Soc. Hyperthermic Oncol. North Am. Hyperth. Group* 11:587–599

Aebischer B, Frey P, Haerter H, Herrling PL, Mueller W, Olverman HJ, Watkins JC (1989) Synthesis and NMDA Antagonistic Properties of the Enantiomers of 4-(3-phosphonopropyl)piperazine-2-carboxylic acid (CPP) and of the unsaturated analogue (E)-4-(3-phosphonoprop-2-enyl)piperazine-2-carboxylic acid (CPP-ene). *Helv. Chim. Acta* 72:1043–1051

Ahmed AH, Oswald RE (2010) Piracetam defines a new binding site for allosteric modulators of alpha-amino-3-hydroxy-5-methyl-4-isoxazole-propionic acid (AMPA) receptors. *J. Med. Chem.* 53:2197–2203

Ahmed AH, Ptak CP, Oswald RE (2010) Molecular Mechanism of Flop Selectivity and Subsite Recognition for an AMPA Receptor Allosteric Modulator: Structures of GluA2 and GluA3 in Complexes with PEPA. *Biochemistry (Mosc.)* 49:2843–2850

Akazawa C, Shigemoto R, Bessho Y, Nakanishi S, Mizuno N (1994) Differential expression of five N-methyl-D-aspartate receptor subunit mRNAs in the cerebellum of developing and adult rats. *J. Comp. Neurol.* 347:150–160

Akbarian S, Sucher NJ, Bradley D, Tafazzoli A, Trinh D, Hetrick WP, Potkin SG, Sandman CA, Bunney WE Jr, Jones EG (1996) Selective alterations in gene expression for NMDA receptor subunits in prefrontal cortex of schizophrenics. *J. Neurosci. Off. J. Soc. Neurosci.* 16:19–30

Allen NC, Bagade S, McQueen MB, Ioannidis JPA, Kavvoura FK, Khoury MJ, Tanzi RE, Bertram L (2008) Systematic meta-analyses and field synopsis of genetic association studies in schizophrenia: the SzGene database. *Nat. Genet.* 40:827–834

Anis NA, Berry SC, Burton NR, Lodge D (1983) The dissociative anaesthetics, ketamine and phencyclidine, selectively reduce excitation of central mammalian neurones by N-methyl-aspartate. *Br. J. Pharmacol.* 79:565–575

Anson LC, Chen PE, Wyllie DJA, Colquhoun D, Schoepfer R (1998) Identification of Amino Acid Residues of the NR2A Subunit That Control Glutamate Potency in Recombinant NR1/NR2A NMDA Receptors. *J. Neurosci.* 18:581–589

Antonov SM, Johnson JW (1996) Voltage-dependent interaction of open-channel blocking molecules with gating of NMDA receptors in rat cortical neurons. *J. Physiol.* 493:425–445

Aragón C, López-Corcuera B (2003) Structure, function and regulation of glycine neurotransporters. *Eur. J. Pharmacol.* 479:249–262

Armstrong N, Gouaux E (2000) Mechanisms for Activation and Antagonism of an AMPA-Sensitive Glutamate Receptor Crystal Structures of the GluR2 Ligand Binding Core. *Neuron* 28:165–181

Armstrong N, Jasti J, Beich-Frandsen M, Gouaux E (2006) Measurement of Conformational Changes accompanying Desensitization in an Ionotropic Glutamate Receptor. *Cell* 127:85–97

Armstrong N, Sun Y, Chen GQ, Gouaux E (1998) Structure of a glutamate-receptor ligand-binding core in complex with kainate. *Nature* 395:913–916

Arundine M, Tymianski M (2004) Molecular mechanisms of glutamate-dependent neurodegeneration in ischemia and traumatic brain injury. *Cell. Mol. Life Sci. CMLS* 61:657–668

Arunlakshana O, Schild HO (1959) Some quantitative uses of drug antagonists. *Br. J. Pharmacol. Chemother.* 14:48–58

Ascher P, Nowak L (1988) The role of divalent cations in the N-methyl-D-aspartate responses of mouse central neurones in culture. *J. Physiol.* 399:247–266

Auberson YP, Allgeier H, Bischoff S, Lingenhoehl K, Moretti R, Schmutz M (2002) 5-Phosphonomethylquinoxalinediones as competitive NMDA receptor antagonists with a preference for the human 1A/2A, rather than 1A/2B receptor composition. *Bioorg. Med. Chem. Lett.* 12:1099–1102

Auerbach A, Zhou Y (2005) Gating Reaction Mechanisms for NMDA Receptor Channels. *J. Neurosci.* 25:7914–7923

Ault B, Evans RH, Francis AA, Oakes DJ, Watkins JC (1980) Selective depression of excitatory amino acid induced depolarizations by magnesium ions in isolated spinal cord preparations. *J. Physiol.* 307:413–428

Awobuluyi M, Yang J, Ye Y, Chatterton JE, Godzik A, Lipton SA, Zhang D (2007) Subunit-Specific Roles of Glycine-Binding Domains in Activation of NR1/NR3 N-Methyl-D-aspartate Receptors. *Mol. Pharmacol.* 71:112–122

Baethmann A, Maier-Hauff K, Schürer L, Lange M, Guggenbichler C, Vogt W, Jacob K, Kempski O (1989) Release of glutamate and of free fatty acids in vasogenic brain edema. *J. Neurosurg.* 70:578–591

Baker AJ, Moulton RJ, MacMillan VH, Shedden PM (1993) Excitatory amino acids in cerebrospinal fluid following traumatic brain injury in humans. *J. Neurosurg.* 79:369–372

Baker JD, Azorlosa JL (1996) The NMDA antagonist MK-801 blocks the extinction of Pavlovian fear conditioning. *Behav. Neurosci.* 110:618–620

Balannik V, Menniti FS, Paternain AV, Lerma J, Stern-Bach Y (2005) Molecular Mechanism of AMPA Receptor Noncompetitive Antagonism. *Neuron* 48:279–288

Balasuriya D, Goetze TA, Barrera NP, Stewart AP, Suzuki Y, Edwardson JM (2013) AMPA and NMDA receptors adopt different subunit arrangements. *J. Biol. Chem.*

Banke TG, Traynelis SF (2003) Activation of NR1/NR2B NMDA receptors. *Nat Neurosci* 6:144–152

Bartlett TE, Bannister NJ, Collett VJ, Dargan SL, Massey PV, Bortolotto ZA, Fitzjohn SM, Bashir ZI, Collingridge GL, Lodge D (2007) Differential roles of NR2A and NR2B-containing NMDA receptors in LTP and LTD in the CA1 region of two-week old rat hippocampus. *Neuropharmacology* 52:60–70

Bassand P, Bernard A, Rafiki A, Gayet D, Khrestchatisky M (1999) Differential interaction of the tSXV motifs of the NR1 and NR2A NMDA receptor subunits with PSD-95 and SAP97. *Eur. J. Neurosci.* 11:2031–2043

Beato M, Groot-Kormelink PJ, Colquhoun D, Sivilotti LG (2002) Openings of the Rat Recombinant α1 Homomeric Glycine Receptor as a Function of the Number of Agonist Molecules Bound. *J. Gen. Physiol.* 119:443–466

Beato M, Groot-Kormelink PJ, Colquhoun D, Sivilotti LG (2004) The Activation Mechanism of α1 Homomeric Glycine Receptors. *J. Neurosci.* 24:895–906

Beck C, Wollmuth L., Seeburg P., Sakmann B, Kuner T (1999) NMDAR Channel Segments Forming the Extracellular Vestibule Inferred from the Accessibility of Substituted Cysteines. *Neuron* 22:559–570

Begni S, Moraschi S, Bignotti S, Fumagalli F, Rillosi L, Perez J, Gennarelli M (2003) Association between the G1001C polymorphism in the GRIN1 gene promoter region and schizophrenia. *Biol. Psychiatry* 53:617–619

Behe P, Stern P, Wyllie DJA, Nassar M, Schoepfer R, Colquhoun D (1995) Determination of NMDA NR1 Subunit Copy Number in Recombinant NMDA Receptors. *Proc. R. Soc. Lond. B Biol. Sci.* 262:205–213

Beinat C, Banister S, Moussa I, Reynolds AJ, McErlean CSP, Kassiou M (2010) Insights into structure-activity relationships and CNS therapeutic applications of NR2B selective antagonists. *Curr. Med. Chem.* 17:4166–4190

Bekkers JM (1993) Enhancement by histamine of NMDA-mediated synaptic transmission in the hippocampus. *Science* 261:104–106

Belforte JE, Zsiros V, Sklar ER, Jiang Z, Yu G, Li Y, Quinlan EM, Nakazawa K (2010) Postnatal NMDA receptor ablation in corticolimbic interneurons confers schizophrenia-like phenotypes. *Nat. Neurosci.* 13:76–83

Bellone C, Nicoll RA (2007) Rapid Bidirectional Switching of Synaptic NMDA Receptors. *Neuron* 55:779–785

Benveniste H, Drejer J, Schousboe A, Diemer NH (1984) Elevation of the Extracellular Concentrations of Glutamate and Aspartate in Rat Hippocampus During Transient Cerebral Ischemia Monitored by Intracerebral Microdialysis. *J. Neurochem.* 43:1369–1374

Benveniste M, Mayer ML (1991) Kinetic analysis of antagonist action at N-methyl-D-aspartic acid receptors. Two binding sites each for glutamate and glycine. *Biophys. J.* 59:560–573

Benveniste M, Mayer ML (1993) Multiple effects of spermine on N-methyl-D-aspartic acid receptor responses of rat cultured hippocampal neurones. *J. Physiol.* 464:131–163

Benveniste M, Mienville JM, Sernagor E, Mayer ML (1990) Concentration-jump experiments with NMDA antagonists in mouse cultured hippocampal neurons. *J. Neurophysiol.* 63:1373–1384

Berger AJ, Dieudonné S, Ascher P (1998) Glycine Uptake Governs Glycine Site Occupancy at NMDA Receptors of Excitatory Synapses. *J. Neurophysiol.* 80:3336–3340

Bergeron R, Meyer TM, Coyle JT, Greene RW (1998) Modulation of N-methyl-d-aspartate receptor function by glycine transport. *Proc. Natl. Acad. Sci.* 95:15730–15734

Berry SC, Lodge D (1984) Benz(f)isoquinolines as excitatory amino acid antagonists: an indication of their mechanism of action? *Biochem. Pharmacol.* 33:3829–3832

Bettini E, Sava A, Griffante C, Carignani C, Buson A, Capelli AM, Negri M, Andreetta F, Senar-Sancho SA, Guiral L, Cardullo F (2010) Identification and Characterization of Novel NMDA Receptor Antagonists Selective for NR2A- over NR2B-Containing Receptors. *J. Pharmacol. Exp. Ther.* 335:636–644

Biscoe TJ, Evans RH, Francis AA, Martin MR, Watkins JC, Davies J, Dray A (1977) D-α-Aminoadipate as a selective antagonist of amino acid-induced and synaptic excitation of mammalian spinal neurones. *Nature* 270:743–745

Blanke ML, VanDongen AMJ (2008) Constitutive Activation of the N-Methyl-d-aspartate Receptor via Cleft-spanning Disulfide Bonds. *J. Biol. Chem.* 283:21519–21529

Blanpied TA, Clarke RJ, Johnson JW (2005) Amantadine Inhibits NMDA Receptors by Accelerating Channel Closure during Channel Block. *J. Neurosci.* 25:3312–3322

Bliss TV, Gardner-Medwin AR (1973) Long-lasting potentiation of synaptic transmission in the dentate area of the unanaesthetized rabbit following stimulation of the perforant path. *J. Physiol.* 232:357

Bliss TV, Lømo T (1973) Long-lasting potentiation of synaptic transmission in the dentate area of the anaesthetized rabbit following stimulation of the perforant path. *J. Physiol.* 232:331–356

Bliss TVP, Collingridge GL (1993) A synaptic model of memory: long-term potentiation in the hippocampus. *Nature* 361:31–39

Block F, Schwarz M (1996) Memantine reduces functional and morphological consequences induced by global ischemia in rats. *Neurosci. Lett.* 208:41–44

Bondoli A, Barbi S, Camaioni D, Della Morte F, Magalini SI (1981) Plasma and cerebrospinal fluid free amino acid concentration in post-traumatic cerebral oedema in patients with shock. *Resuscitation* 9:119–124

Bormann J (1989) Memantine is a potent blocker of N-methyl-D-aspartate (NMDA) receptor channels. *Eur. J. Pharmacol.* 166:591–592

Borschel WF, Murthy SE, Kasperek EM, Popescu GK (2011) NMDA receptor activation requires remodelling of intersubunit contacts within ligand-binding heterodimers. *Nat. Commun.* 2:498

Borza I, Domány G (2006) NR2B selective NMDA antagonists: the evolution of the ifenprodil-type pharmacophore. *Curr. Top. Med. Chem.* 6:687–695

Boyce-Rustay JM, Holmes A (2006) Genetic Inactivation of the NMDA Receptor NR2A Subunit has Anxiolytic- and Antidepressant-Like Effects in Mice. *Neuropsychopharmacology* 31:2405–2414

Brauneis U, Oz M, Peoples RW, Weight FF, Zhang L (1996) Differential sensitivity of recombinant N-methyl-D-aspartate receptor subunits to inhibition by dynorphin. *J. Pharmacol. Exp. Ther.* 279:1063–1068

Brennan AM, Won Suh S, Joon Won S, Narasimhan P, Kauppinen TM, Lee H, Edling Y, Chan PH, Swanson RA (2009) NADPH oxidase is the primary source of superoxide induced by NMDA receptor activation. *Nat. Neurosci.* 12:857–863

Brickley SG, Misra C, Mok MHS, Mishina M, Cull-Candy SG (2003) NR2B and NR2D Subunits Coassemble in Cerebellar Golgi Cells to Form a Distinct NMDA Receptor Subtype Restricted to Extrasynaptic Sites. *J. Neurosci.* 23:4958 –4966

Brohawn SG, Mármol J del, MacKinnon R (2012) Crystal Structure of the Human K2P TRAAK, a Lipid- and Mechano-Sensitive K+ Ion Channel. *Science* 335:436–441

Brothwell SLC, Barber JL, Monaghan DT, Jane DE, Gibb AJ, Jones S (2008) NR2B- and NR2D-containing synaptic NMDA receptors in developing rat substantia nigra pars compacta dopaminergic neurones. *J. Physiol.* 586:739–750

Burger PB, Yuan H, Karakas E, Geballe M, Furukawa H, Liotta DC, Snyder JP, Traynelis SF (2012) Mapping the binding of GluN2B-selective N-methyl-D-aspartate receptor negative allosteric modulators. *Mol. Pharmacol.* 82:344–359

Burnashev N, Zhou Z, Neher E, Sakmann B (1995) Fractional calcium currents through recombinant GluR channels of the NMDA, AMPA and kainate receptor subtypes. *J. Physiol.* 485:403–418

Burzomato V, Beato M, Groot-Kormelink PJ, Colquhoun D, Sivilotti LG (2004) Single-Channel Behavior of Heteromeric α1β Glycine Receptors: An Attempt to Detect a Conformational Change before the Channel Opens. *J. Neurosci.* 24:10924–10940

Carter C, Benavides J, Legendre P, Vincent JD, Noel F, Thuret F, Lloyd KG, Arbilla S, Zivkovic B, MacKenzie ET (1988) Ifenprodil and SL 82.0715 as cerebral anti-ischemic agents. II. Evidence for N-methyl-D-aspartate receptor antagonist properties. *J. Pharmacol. Exp. Ther.* 247:1222–1232

Cathala L, Misra C, Cull-Candy S (2000) Developmental Profile of the Changing Properties of NMDA Receptors at Cerebellar Mossy Fiber–Granule Cell Synapses. *J. Neurosci.* 20:5899–5905

Catterall WA (2000)(a) Structure and regulation of voltage-gated Ca2+ channels. *Annu. Rev. Cell Dev. Biol.* 16:521–555

Catterall WA (2000)(b) From Ionic Currents to Molecular Mechanisms: The Structure and Function of Voltage-Gated Sodium Channels. *Neuron* 26:13–25

Cavara NA, Orth A, Hollmann M (2009) Effects of NR1 splicing on NR1/NR3B-type excitatory glycine receptors. *BMC Neurosci.* 10:32

Chang H-R, Kuo C-C (2008) The activation gate and gating mechanism of the NMDA receptor. *J. Neurosci. Off. J. Soc. Neurosci.* 28:1546–1556

Chang Y, Weiss DS (1999) Channel opening locks agonist onto the GABAC receptor. *Nat. Neurosci.* 2:219–225

Chatterton JE, Awobuluyi M, Premkumar LS, Takahashi H, Talantova M, Shin Y, Cui J, Tu S, Sevarino KA, Nakanishi N, Tong G, Lipton SA, Zhang D (2002) Excitatory glycine receptors containing the NR3 family of NMDA receptor subunits. *Nature* 415:793–798

Chazot PL, Stephenson FA (1997) Molecular Dissection of Native Mammalian Forebrain NMDA Receptors Containing the NR1 C2 Exon: Direct Demonstration of NMDA Receptors Comprising NR1, NR2A, and NR2B Subunits Within the Same Complex. *J. Neurochem.* 69:2138–2144

Chen B-S, Gray JA, Sanz-Clemente A, Wei Z, Thomas EV, Nicoll RA, Roche KW (2012) SAP102 Mediates Synaptic Clearance of NMDA Receptors. *Cell Reports* 2:1120–1128

Chen B-S, Roche KW (2007) Regulation of NMDA Receptors by Phosphorylation. *Neuropharmacology* 53:362–368

Chen C, Okayama H (1987) High-efficiency transformation of mammalian cells by plasmid DNA. *Mol. Cell. Biol.* 7:2745–2752

Chen G-Q, Gouaux E (1997) Overexpression of a glutamate receptor (GluR2) ligand binding domain in Escherichia coli: Application of a novel protein folding screen. *Proc. Natl. Acad. Sci.* 94:13431–13436

Chen J, Zhang Y, Akk G, Sine S, Auerbach A (1995) Activation kinetics of recombinant mouse nicotinic acetylcholine receptors: mutations of alpha-subunit tyrosine 190 affect both binding and gating. *Biophys. J.* 69:849–859

Chen L, Muhlhauser M, Yang CR (2003) Glycine Tranporter-1 Blockade Potentiates NMDA-Mediated Responses in Rat Prefrontal Cortical Neurons In Vitro and In Vivo. *J. Neurophysiol.* 89:691–703

Chen M, Lu T-J, Chen X-J, Zhou Y, Chen Q, Feng X-Y, Xu L, Duan W-H, Xiong Z-Q (2008)(a) Differential Roles of NMDA Receptor Subtypes in Ischemic Neuronal Cell Death and Ischemic Tolerance. *Stroke* 39:3042–3048

Chen PE, Geballe MT, Katz E, Erreger K, Livesey MR, O'Toole KK, Le P, Lee CJ, Snyder JP, Traynelis SF, Wyllie DJA (2008)(b) Modulation of glycine potency in rat recombinant NMDA receptors containing chimeric NR2A/2D subunits expressed in Xenopus laevis oocytes. *J. Physiol.* 586:227–245

Chen PE, Geballe MT, Stansfeld PJ, Johnston AR, Yuan H, Jacob AL, Snyder JP, Traynelis SF, Wyllie DJA (2005) Structural Features of the Glutamate Binding Site in Recombinant NR1/NR2A N-Methyl-d-aspartate Receptors Determined by Site-Directed Mutagenesis and Molecular Modeling. *Mol. Pharmacol.* 67:1470–1484

Chenard BL, Bordner J, Butler TW, Chambers LK, Collins MA, De Costa DL, Ducat MF, Dumont ML, Fox CB, Mena EE (1995) (1S,2S)-1-(4-hydroxyphenyl)-2-(4-hydroxy-4-phenylpiperidino)-1-propanol: a potent new neuroprotectant which blocks N-methyl-D-aspartate responses. *J. Med. Chem.* 38:3138–3145

Chenard BL, Menniti FS (1999) Antagonists selective for NMDA receptors containing the NR2B subunit. *Curr. Pharm. Des.* 5:381–404

Chetkovich DM, Sweatt JD (1993) NMDA receptor activation increases cyclic AMP in area CA1 of the hippocampus via calcium/calmodulin stimulation of adenylyl cyclase. *J. Neurochem.* 61:1933–1942

Chizh BA, Headley PM, Tzschentke TM (2001) NMDA receptor antagonists as analgesics: focus on the NR2B subtype. *Trends Pharmacol. Sci.* 22:636–642

Choi DW (1987) Ionic dependence of glutamate neurotoxicity. *J. Neurosci.* 7:369–379

Choi DW (1988) Glutamate neurotoxicity and diseases of the nervous system. *Neuron* 1:623–634

Choi DW, Maulucci-Gedde M, Kriegstein AR (1987) Glutamate neurotoxicity in cortical cell culture. *J. Neurosci.* 7:357–368

Choi UB, Kazi R, Stenzoski N, Wollmuth LP, Uversky VN, Bowen ME (2013) Modulating the intrinsic disorder in the cytoplasmic domain alters the biological activity of the N-methyl D-aspartate-sensitive glutamate receptor. *J. Biol. Chem.*

Choi UB, McCann JJ, Weninger KR, Bowen ME (2011) Beyond the random coil: stochastic conformational switching in intrinsically disordered proteins. *Struct. Lond. Engl. 1993* 19:566–576

Chowdhury D, Marco S, Brooks IM, Zandueta A, Rao Y, Haucke V, Wesseling JF, Tavalin SJ, Pérez-Otaño I (2013) Tyrosine Phosphorylation Regulates the Endocytosis and Surface Expression of GluN3A-Containing NMDA Receptors. *J. Neurosci.* 33:4151–4164

Christopoulos A (1998) Assessing the distribution of parameters in models of ligand–receptor interaction: to log or not to log. *Trends Pharmacol. Sci.* 19:351–357

Christopoulos A, Kenakin T (2002) G protein-coupled receptor allosterism and complexing. *Pharmacol. Rev.* 54:323–374

Chung HJ, Huang YH, Lau L-F, Huganir RL (2004) Regulation of the NMDA Receptor Complex and Trafficking by Activity-Dependent Phosphorylation of the NR2B Subunit PDZ Ligand. *J. Neurosci.* 24:10248–10259

Ciabarra AM, Sullivan JM, Gahn LG, Pecht G, Heinemann S, Sevarino KA (1995) Cloning and characterization of chi-1: a developmentally regulated member of a novel class of the ionotropic glutamate receptor family. *J. Neurosci.* 15:6498–6508

Clausen RP, Christensen C, Hansen KB, Greenwood JR, Lars Jørgensen, Micale N, Madsen JC, Nielsen B, Egebjerg J, Bräuner-Osborne H, Traynelis SF, Kristensen JL (2008) N-Hydroxypyrazolyl Glycine Derivatives as Selective N-Methyl-d-aspartic Acid Receptor Ligands. *J. Med. Chem.* 51:4179–4187

Clements JD, Westbrook GL (1991) Activation kinetics reveal the number of glutamate and glycine binding sites on the N-methyl-d-aspartate receptor. *Neuron* 7:605–613

Collingridge GL, Olsen RW, Peters J, Spedding M (2009) A nomenclature for ligand-gated ion channels. *Neuropharmacology* 56:2–5

Collins GGS (1990) Both agonists and antagonists of the strychnine-insensitive glycine site of N-methyl-D-aspartate receptors modulate polysynaptic excitations in slices of mouse olfactory cortex. *Naunyn. Schmiedebergs Arch. Pharmacol.* 342:677–682

Colquhoun D (1998) Binding, gating, affinity and efficacy: The interpretation of structure-activity relationships for agonists and of the effects of mutating receptors. *Br. J. Pharmacol.* 125:923–947

Colquhoun D, Hawkes AG (1977) Relaxation and Fluctuations of Membrane Currents that Flow through Drug-Operated Channels. *Proc. R. Soc. Lond. B Biol. Sci.* 199:231–262

Colquhoun D, Hawkes AG (1990) Stochastic Properties of Ion Channel Openings and Bursts in a Membrane Patch that Contains Two Channels: Evidence Concerning the Number of Channels Present when a Record Containing Only Single Openings is Observed. *Proc. R. Soc. Lond. B Biol. Sci.* 240:453–477

Colquhoun D, Hawkes AG (1995) A Q-Matrix Cookbook: How to Write Only One Program to Calculate the Single-Channel Macroscopic Predictions for Any Kinetic Mechanism In B. Sakmann & E. Neher, eds. Single-Channel Recording New York and London: Plenum Press, p. 483–587.

Colquhoun D, Sakmann B (1981) Fluctuations in the microsecond time range of the current through single acetylcholine receptor ion channels. *Nature* 294:464–466

Colquhoun D, Sakmann B (1985) Fast events in single-channel currents activated by acetylcholine and its analogues at the frog muscle end-plate. *J. Physiol.* 369:501–557

Colquhoun D, Sigworth FJ (1995) Fitting and Statistical Analysis of Single-Channel Records In B. Sakmann & E. Neher, eds. Single-Channel Recording New York and London: Plenum Press, p. 483–587.

Conn PJ, Pin J-P (1997) Pharmacology and Functions of Metabotropic Glutamate Receptors. *Annu. Rev. Pharmacol. Toxicol.* 37:205–237

Costa BM, Feng B, Tsintsadze TS, Morley RM, Irvine MW, Tsintsadze V, Lozovaya NA, Jane DE, Monaghan DT (2009) N-methyl-D-aspartate (NMDA) receptor NR2 subunit selectivity of a series of novel piperazine-2,3-dicarboxylate derivatives: preferential blockade of extrasynaptic NMDA receptors in the rat hippocampal CA3-CA1 synapse. *J. Pharmacol. Exp. Ther.* 331:618–626

Costa BM, Irvine MW, Fang G, Eaves RJ, Mayo-Martin MB, Skifter DA, Jane DE, Monaghan DT (2010) A Novel Family of Negative and Positive Allosteric Modulators of NMDA Receptors. *J. Pharmacol. Exp. Ther.* 335:614–621

Coyle JT (2012) NMDA Receptor and Schizophrenia: A Brief History. *Schizophr. Bull.* 38:920–926

Cryan JF, Sweeney FF (2011) The age of anxiety: role of animal models of anxiolytic action in drug discovery. *Br. J. Pharmacol.* 164:1129–1161

Cubelos B, Giménez C, Zafra F (2005) Localization of the GLYT1 Glycine Transporter at Glutamatergic Synapses in the Rat Brain. *Cereb. Cortex* 15:448–459

Cull-Candy SG, Leszkiewicz DN (2004) Role of Distinct NMDA Receptor Subtypes at Central Synapses. *Sci. Signal.* 2004:re16

Curtis DR, Phillis JW, Watkins JC (1959) Chemical Excitation of Spinal Neurones. *Nature* 183:611–612

Curtis DR, Watkins JC (1963) Acidic amino acids with strong excitatory actions on mammalian neurones. *J. Physiol.* 166:1–14

Dai J, Zhou H-X (2013) An NMDA Receptor Gating Mechanism Developed from MD Simulations Reveals Molecular Details Underlying Subunit-Specific Contributions. *Biophys. J.* 104:2170–2181

Danysz W, Parsons CG (2002) Neuroprotective potential of ionotropic glutamate receptor antagonists. *Neurotox. Res.* 4:119–126

Davies J, Evans RH, Herrling PL, Jones AW, Olverman HJ, Pook P, Watkins JC (1986) CPP, a new potent and selective NMDA antagonist. Depression of central neuron responses, affinity for [3H]D-AP5 binding sites on brain membranes and anticonvulsant activity. *Brain Res.* 382:169–173

Davies J, Watkins JC (1979) Selective antagonism of amino acid-induced and synaptic excitation in the cat spinal cord. *J. Physiol.* 297:621–635

Davies SN, Lodge D (1987) Evidence for involvement ofN-methylaspartate receptors in “wind-up” of class 2 neurones in the dorsal horn of the rat. *Brain Res.* 424:402–406

Dawson DA, Wadsworth G, Palmer AM (2001) A comparative assessment of the efficacy and side-effect liability of neuroprotective compounds in experimental stroke. *Brain Res.* 892:344–350

Delaney AJ, Sedlak PL, Autuori E, Power JM, Sah P (2012) Synaptic NMDA receptors in basolateral amygdala principal neurons are triheteromeric proteins: physiological role of GluN2B subunits. *J. Neurophysiol.*

Dickenson AH, Sullivan AF (1987) Evidence for a role of the NMDA receptor in the frequency dependent potentiation of deep rat dorsal horn nociceptive neurones following C fibre stimulation. *Neuropharmacology* 26:1235–1238

Dirnagl U, Iadecola C, Moskowitz MA (1999) Pathobiology of ischaemic stroke: an integrated view. *Trends Neurosci.* 22:391–397

Domino EF, Luby ED (2012) Phencyclidine/schizophrenia: one view toward the past, the other to the future. *Schizophr. Bull.* 38:914–919

Doyle DA, Cabral JM, Pfuetzner RA, Kuo A, Gulbis JM, Cohen SL, Chait BT, MacKinnon R (1998) The Structure of the Potassium Channel: Molecular Basis of K+ Conduction and Selectivity. *Science* 280:69–77

Dravid SM, Burger PB, Prakash A, Geballe MT, Yadav R, Le P, Vellano K, Snyder JP, Traynelis SF (2010) Structural Determinants of d-Cycloserine Efficacy at the NR1/NR2C NMDA Receptors. *J. Neurosci.* 30:2741 –2754

Dravid SM, Erreger K, Yuan H, Nicholson K, Le P, Lyuboslavsky P, Almonte A, Murray E, Mosley C, Barber J, French A, Balster R, Murray TF, Traynelis SF (2007) Subunit-specific mechanisms and proton sensitivity of NMDA receptor channel block. *J. Physiol.* 581:107–128

Dravid SM, Prakash A, Traynelis SF (2008) Activation of recombinant NR1/NR2C NMDA receptors. *J. Physiol.* 586:4425–4439

Dundas J, Ouyang Z, Tseng J, Binkowski A, Turpaz Y, Liang J (2006) CASTp: computed atlas of surface topography of proteins with structural and topographical mapping of functionally annotated residues. *Nucleic Acids Res.* 34:W116–W118

Durand GM, Bennett MV, Zukin RS (1993) Splice variants of the N-methyl-D-aspartate receptor NR1 identify domains involved in regulation by polyamines and protein kinase C. *Proc. Natl. Acad. Sci. U. S. A.* 90:6731 –6735

Durand GM, Gregor P, Zheng X, Bennett MV, Uhl GR, Zukin RS (1992) Cloning of an apparent splice variant of the rat N-methyl-D-aspartate receptor NMDAR1 with altered sensitivity to polyamines and activators of protein kinase C. *Proc. Natl. Acad. Sci.* 89:9359–9363

Eccles JC, Fatt P, Koketsu K (1954) Cholinergic and inhibitory synapses in a pathway from motor-axon collaterals to motoneurones. *J. Physiol.* 126:524–562

Ehlert FJ (1988) Estimation of the affinities of allosteric ligands using radioligand binding and pharmacological null methods. *Mol. Pharmacol.* 33:187–194

Endele S et al. (2010) Mutations in GRIN2A and GRIN2B encoding regulatory subunits of NMDA receptors cause variable neurodevelopmental phenotypes. *Nat. Genet.* 42:1021–1026

Epi4K Consortium et al. (2013) De novo mutations in epileptic encephalopathies. *Nature*

Erreger K, Dravid SM, Banke TG, Wyllie DJA, Traynelis SF (2005) Subunit-specific gating controls rat NR1/NR2A and NR1/NR2B NMDA channel kinetics and synaptic signalling profiles. *J. Physiol.* 563:345–358

Erreger K, Geballe MT, Kristensen A, Chen PE, Hansen KB, Lee CJ, Yuan H, Le P, Lyuboslavsky PN, Micale N, Jørgensen L, Clausen RP, Wyllie DJA, Snyder JP, Traynelis SF (2007) Subunit-Specific Agonist Activity at NR2A-, NR2B-, NR2C-, and NR2D-Containing N-Methyl-d-aspartate Glutamate Receptors. *Mol. Pharmacol.* 72:907–920

Erreger K, Traynelis SF (2005) Allosteric interaction between zinc and glutamate binding domains on NR2A causes desensitization of NMDA receptors. *J. Physiol.* 569:381–393

Erreger K, Traynelis SF (2008) Zinc inhibition of rat NR1/NR2A N-methyl-D-aspartate receptors. *J. Physiol.* 586:763–778

Evans RH, Francis AA, Hunt K, Oakes DJ, Watkins JC (1979) Antagonism of excitatory amino acid-induced responses and of synaptic excitation in the isolated spinal cord of the frog. *Br. J. Pharmacol.* 67:591–603

Evans RH, Francis AA, Jones AW, Smith DA, Watkins JC (1982) The effects of a series of omega-phosphonic alpha-carboxylic amino acids on electrically evoked and excitant

amino acid-induced responses in isolated spinal cord preparations. *Br. J. Pharmacol.* 75:65–75

Evans RH, Francis AA, Watkins JC (1977) Selective antagonism by Mg2+ of amino acid-induced depolarization of spinal neurones. *Experientia* 33:489–491

Evans RH, Francis AA, Watkins JC (1978)(a) Mg2+-like selective antagonism of excitatory amino acid-induced responses by α,ε-diaminopimelic acid, D-α-maminoadipate and HA-966 in isolated spinal cord of frog and immature rat. *Brain Res.* 148:536–542

Evans RH, Francis AA, Watkins JC (1978)(b) Mg2+-like selective antagonism of excitatory amino acid-induced responses by alpha, epsilon-diaminopimelic acid, D-alpha-aminoadipate and HA-966 in isolated spinal cord of frog and immature rat. *Brain Res.* 148:536–542

Faden AI, Demediuk P, Panter SS, Vink R (1989) The Role of Excitatory Amino Acids and NMDA Receptors in Traumatic Brain Injury. *Science* 244:798–800

Fage D, Voltz C, Scatton B, Carter C (1992) Selective release of spermine and spermidine from the rat striatum by N-methyl-D-aspartate receptor activation in vivo. *J. Neurochem.* 58:2170–2175

Falls WA, Miserendino MJ, Davis M (1992) Extinction of fear-potentiated startle: blockade by infusion of an NMDA antagonist into the amygdala. *J. Neurosci. Off. J. Soc. Neurosci.* 12:854–863

Farina AN, Blain KY, Maruo T, Kwiatkowski W, Choe S, Nakagawa T (2011) Separation of Domain Contacts Is Required for Heterotetrameric Assembly of Functional NMDA Receptors. *J. Neurosci.* 31:3565–3579

Feng B, Morley RM, Jane DE, Monaghan DT (2005) The effect of competitive antagonist chain length on NMDA receptor subunit selectivity. *Neuropharmacology* 48:354–359

Feng B, Tse HW, Skifter DA, Morley R, Jane DE, Monaghan DT (2004) Structure-activity analysis of a novel NR2C/NR2D-preferring NMDA receptor antagonist: 1-(phenanthrene-2-carbonyl) piperazine-2,3-dicarboxylic acid. *Br. J. Pharmacol.* 141:508–516

Ferraro TN, Hare TA (1985) Free and conjugated amino acids in human CSF: Influence of age and sex. *Brain Res.* 338:53–60

Fischer G, Mutel V, Trube G, Malherbe P, Kew JNC, Mohacsi E, Heitz MP, Kemp JA (1997) Ro 25–6981, a Highly Potent and Selective Blocker of N-Methyl-d-aspartate Receptors Containing the NR2B Subunit. Characterization in Vitro. *J. Pharmacol. Exp. Ther.* 283:1285–1292

Fletcher EJ, Lodge D (1988) Glycine reverses antagonism of N-methyl-D-aspartate (NMDA) by 1-hydroxy-3-aminopyrrolidone-2 (HA-966) but not by D-2-amino-5-phophonovalerate (D-AP5) on rat cortical slices. *Eur. J. Pharmacol.* 151:161–162

Forcina M, Ciabarra AM, Sevarino KA (1995) Cloning of chi-2: a putative member of the ionotropic glutamate receptor superfamily. *Soc. Neurosci. Abstr.* 21:438.433

Foster KA, McLaughlin N, Edbauer D, Phillips M, Bolton A, Constantine-Paton M, Sheng M (2010) Distinct Roles of NR2A and NR2B Cytoplasmic Tails in Long-Term Potentiation. *J. Neurosci.* 30:2676–2685

Frandsen A, Pickering DS, Vestergaard B, Kasper C, Nielsen BB, Greenwood JR, Campiani G, Fattorusso C, Gajhede M, Schousboe A, Kastrup JS (2005) Tyr702 is an important determinant of agonist binding and domain closure of the ligand-binding core of GluR2. *Mol. Pharmacol.* 67:703–713

Frizelle PA, Chen PE, Wyllie DJA (2006) Equilibrium Constants for (R)-[(S)-1-(4-Bromo-phenyl)-ethylamino]-(2,3-dioxo-1,2,3,4-tetrahydroquinoxalin-5-yl)-methyl]-phosphonic Acid (NVP-AAM077) Acting at Recombinant NR1/NR2A and NR1/NR2B N-Methyl-d-aspartate Receptors: Implications for Studies of Synaptic Transmission. *Mol. Pharmacol.* 70:1022–1032

Furukawa H, Gouaux E (2003) Mechanisms of activation, inhibition and specificity: crystal structures of the NMDA receptor NR1 ligand-binding core. *EMBO J.* 22:2873–2885

Furukawa H, Singh SK, Mancusso R, Gouaux E (2005) Subunit arrangement and function in NMDA receptors. *Nature* 438:185–192

Gaddum J (1945) Lognormal Distributions. *Nature* 156:463–466

Gardoni F, Sgobio C, Pendolino V, Calabresi P, Di Luca M, Picconi B (2012) Targeting NR2A-containing NMDA receptors reduces L-DOPA-induced dyskinesias. *Neurobiol. Aging* 33:2138–2144

Gielen M, Le Goff A, Stroebel D, Johnson JW, Neyton J, Paoletti P (2008) Structural Rearrangements of NR1/NR2A NMDA Receptors during Allosteric Inhibition. *Neuron* 57:80–93

Gielen M, Siegler Retchless B, Mony L, Johnson JW, Paoletti P (2009) Mechanism of differential control of NMDA receptor activity by NR2 subunits. *Nature* 459:703–707

Giese KP, Fedorov NB, Filipkowski RK, Silva AJ (1998) Autophosphorylation at Thr286 of the α Calcium-Calmodulin Kinase II in LTP and Learning. *Science* 279:870–873

Gladstone DJ, Black SE, Hakim AM (2002) Toward Wisdom From Failure Lessons From Neuroprotective Stroke Trials and New Therapeutic Directions. *Stroke* 33:2123–2136

Globus MY, Busto R, Dietrich WD, Martinez E, Valdes I, Ginsberg MD (1988) Intra-ischemic extracellular release of dopamine and glutamate is associated with striatal vulnerability to ischemia. *Neurosci. Lett.* 91:36–40

Graham BM, Langton JM, Richardson R (2011) Pharmacological enhancement of fear reduction: preclinical models. *Br. J. Pharmacol.* 164:1230–1247

Gray JA, Shi Y, Usui H, During MJ, Sakimura K, Nicoll RA (2011) Distinct Modes of AMPA Receptor Suppression at Developing Synapses by GluN2A and GluN2B: Single-Cell NMDA Receptor Subunit Deletion In Vivo. *Neuron* 71:1085–1101

Haack JA, Rivier J, Parks TN, Mena EE, Cruz LJ, Olivera BM (1990) Conantokin-T. A gamma-carboxyglutamate containing peptide with N-methyl-d-aspartate antagonist activity. *J. Biol. Chem.* 265:6025–6029

Habl G, Zink M, Petroianu G, Bauer M, Schneider-Axmann T, von Wilmsdorff M, Falkai P, Henn FA, Schmitt A (2009) Increased D-amino acid oxidase expression in the bilateral hippocampal CA4 of schizophrenic patients: a post-mortem study. *J. Neural Transm. Vienna Austria 1996* 116:1657–1665

Hald H, Ahring PK, Timmermann DB, Liljefors T, Gajhede M, Kastrup JS (2009) Distinct Structural Features of Cyclothiazide Are Responsible for Effects on Peak Current Amplitude and Desensitization Kinetics at iGluR2. *J. Mol. Biol.* 391:906–917

Hallett PJ, Dunah AW, Ravenscroft P, Zhou S, Bezard E, Crossman AR, Brotchie JM, Standaert DG (2005) Alterations of striatal NMDA receptor subunits associated with the development of dyskinesia in the MPTP-lesioned primate model of Parkinson's disease. *Neuropharmacology* 48:503–516

Hallett PJ, Standaert DG (2004) Rationale for and use of NMDA receptor antagonists in Parkinson's disease. *Pharmacol. Ther.* 102:155–174

Hamberger A, Runnerstam M, Nyström B, Starmark JE, von Essen C (1995) The neuronal environment after subarachnoid haemorrhage--correlation of amino acid and nucleoside levels with post-operative recovery. *Neurol. Res.* 17:97–105

Hansen K, Yuan H, Traynelis S (2007) Structural aspects of AMPA receptor activation, desensitization and deactivation. *Curr. Opin. Neurobiol.* 17:281–288

Hansen KB, Bräuner-Osborne H, Egebjerg J (2008) Pharmacological characterization of ligands at recombinant NMDA receptor subtypes by electrophysiological recordings and intracellular calcium measurements. *Comb. Chem. High Throughput Screen.* 11:304–315

Hansen KB, Clausen RP, Bjerrum EJ, Bechmann C, Greenwood JR, Christensen C, Kristensen JL, Egebjerg J, Bräuner-Osborne H (2005) Tweaking agonist efficacy at N-methyl-D-aspartate receptors by site-directed mutagenesis. *Mol. Pharmacol.* 68:1510–1523

Hansen KB, Furukawa H, Traynelis SF (2010) Control of Assembly and Function of Glutamate Receptors by the Amino-Terminal Domain. *Mol. Pharmacol.* 78:535 –549

Hansen KB, Naur P, Kurtkaya NL, Kristensen AS, Gajhede M, Kastrup JS, Traynelis SF (2009) Modulation of the Dimer Interface at Ionotropic Glutamate-Like Receptor δ2 by d-Serine and Extracellular Calcium. *J. Neurosci.* 29:907–917

Hansen KB, Ogden KK, Traynelis SF (2012) Subunit-Selective Allosteric Inhibition of Glycine Binding to NMDA Receptors. *J. Neurosci.* 32:6197–6208

Hansen KB, Tajima N, Risgaard R, Perszyk RE, Jorgensen L, Vance KM, Ogden KK, Clausen RP, Furukawa H, Traynelis SF (2013) Structural Determinants of Agonist Efficacy at the Glutamate Binding Site of NMDA Receptors. *Mol. Pharmacol.*

Hansen KB, Traynelis SF (2011) Structural and Mechanistic Determinants of a Novel Site for Noncompetitive Inhibition of GluN2D-Containing NMDA Receptors. *J. Neurosci.* 31:3650 –3661

Harsing Jr. LG, Matyus P (2013) Mechanisms of glycine release, which build up synaptic and extrasynaptic glycine levels: The role of synaptic and non-synaptic glycine transporters. *Brain Res. Bull.* 93:110–119

Hatton CJ, Paoletti P (2005) Modulation of Triheteromeric NMDA Receptors by N-Terminal Domain Ligands. *Neuron* 46:261–274

Hayashi T (1954) Effects of Sodium Glutamate on the Nervous System. *Keio J. Med.* 3:183–192

Hayashi T, Thomas GM, Huganir RL (2009) Dual Palmitoylation of NR2 Subunits Regulates NMDA Receptor Trafficking. *Neuron* 64:213–226

Hebb DO (1949) The Organization of Behavior. New York: Wiley & Sons.

Hedlund PB, Carson MJ, Sutcliffe JG, Thomas EA (1999) Allosteric regulation by oleamide of the binding properties of 5-hydroxytryptamine7 receptors. *Biochem. Pharmacol.* 58:1807–1813

Henson MA, Roberts AC, Pérez-Otaño I, Philpot BD (2010) Influence of the NR3A subunit on NMDA receptor functions. *Prog. Neurobiol.* 91:23–37

Herguedas B, Krieger J, Greger IH (2013) Chapter Thirteen - Receptor Heteromeric Assembly—How It Works and Why It Matters: The Case of Ionotropic Glutamate Receptors In Jesús Giraldo and Francisco Ciruela, ed. Progress in Molecular Biology and Translational Science Academic Press, p. 361–386.

Herron CE, Lester RA, Coan EJ, Collingridge GL (1985) Intracellular demonstration of an N-methyl-D-aspartate receptor mediated component of synaptic transmission in the rat hippocampus. *Neurosci. Lett.* 60:19–23

Hess SD, Daggett LP, Deal C, Lu CC, Johnson EC, Veliçelebi G (1998) Functional characterization of human N-methyl-D-aspartate subtype 1A/2D receptors. *J. Neurochem.* 70:1269–1279

Hestrin S, Nicoll RA, Perkel DJ, Sah P (1990) Analysis of excitatory synaptic action in pyramidal cells using whole-cell recording from rat hippocampal slices. *J. Physiol.* 422:203 –225

Hillered L, Hallström A, Segersvärd S, Persson L, Ungerstedt U (1989) Dynamics of extracellular metabolites in the striatum after middle cerebral artery occlusion in the rat monitored by intracerebral microdialysis. *J. Cereb. Blood Flow Metab. Off. J. Int. Soc. Cereb. Blood Flow Metab.* 9:607–616

Hillman BG, Gupta SC, Stairs DJ, Buonanno A, Dravid SM (2011) Behavioral analysis of NR2C knockout mouse reveals deficit in acquisition of conditioned fear and working memory. *Neurobiol. Learn. Mem.* 95:404–414

Hirai H, Kirsch J, Laube B, Betz H, Kuhse J (1996) The glycine binding site of the N-methyl-D-aspartate receptor subunit NR1: identification of novel determinants of co-agonist potentiation in the extracellular M3-M4 loop region. *Proc. Natl. Acad. Sci.* 93:6031–6036

Hogner A, Greenwood JR, Liljefors T, Lunn M-L, Egebjerg J, Larsen IK, Gouaux E, Kastrup JS (2003) Competitive Antagonism of AMPA Receptors by Ligands of Different Classes: Crystal Structure of ATPO Bound to the GluR2 Ligand-Binding Core, in Comparison with DNQX. *J. Med. Chem.* 46:214–221

Hollmann M (1999) Structure of Ionotropic Glutamate Receptors In P. D. P. Jonas & P. D. H. Monyer, eds. Ionotropic Glutamate Receptors in the CNS Handbook of Experimental Pharmacology. Springer Berlin Heidelberg, p. 3–98.

Hollmann M, Boulter J, Maron C, Beasley L, Sullivan J, Pecht G, Heinemann S (1993) Zinc potentiates agonist-lnduced currents at certain splice variants of the NMDA receptor. *Neuron* 10:943–954

Hollmann M, Heinemann S (1994) Cloned glutamate receptors. *Annu. Rev. Neurosci.* 17:31–108

Holm MM, Lunn M-L, Traynelis SF, Kastrup JS, Egebjerg J (2005) Structural determinants of agonist-specific kinetics at the ionotropic glutamate receptor 2. *Proc. Natl. Acad. Sci. U. S. A.* 102:12053–12058

Horak M, Vlcek K, Chodounska H, Vyklicky Jr L (2006) Subtype-dependence of N-methyl-d-aspartate receptor modulation by pregnenolone sulfate. *Neuroscience* 137:93–102

Horak M, Vlcek K, Petrovic M, Chodounska H, Vyklicky L (2004) Molecular Mechanism of Pregnenolone Sulfate Action at NR1/NR2B Receptors. *J. Neurosci.* 24:10318 –10325

Huang Y, Lu W, Ali DW, Pelkey KA, Pitcher GM, Lu YM, Aoto H, Roder JC, Sasaki T, Salter MW, MacDonald JF (2001) CAKbeta/Pyk2 kinase is a signaling link for induction of long-term potentiation in CA1 hippocampus. *Neuron* 29:485–496

Humphries C, Mortimer A, Hirsch S, de Belleroche J (1996) NMDA receptor mRNA correlation with antemortem cognitive impairment in schizophrenia. *Neuroreport* 7:2051–2055

Hunt DL, Castillo PE (2012) Synaptic plasticity of NMDA receptors: mechanisms and functional implications. *Curr. Opin. Neurobiol.* 22:496–508

Hunt DL, Puente N, Grandes P, Castillo PE (2013) Bidirectional NMDA receptor plasticity controls CA3 output and heterosynaptic metaplasticity. *Nat. Neurosci.* 16:1049–1059

Hvalby O, Hemmings HC, Paulsen O, Czernik AJ, Nairn AC, Godfraind JM, Jensen V, Raastad M, Storm JF, Andersen P (1994) Specificity of protein kinase inhibitor peptides and induction of long-term potentiation. *Proc. Natl. Acad. Sci.* 91:4761–4765

Igarashi K, Shirahata A, Pahk AJ, Kashiwagi K, Williams K (1997) Benzyl-polyamines: novel, potent N-methyl-D-aspartate receptor antagonists. *J. Pharmacol. Exp. Ther.* 283:533–540

Iino M, Ciani S, Tsuzuki K, Ozawa S, Kidokoro Y (1997) Permeation properties of Na+ and Ca2+ ions through the mouse epsilon2/zeta1 NMDA receptor channel expressed in Xenopus oocytes. *J. Membr. Biol.* 155:143–156

Ikeda K, Nagasawa M, Mori H, Araki K, Sakimura K, Watanabe M, Inoue Y, Mishina M (1992) Cloning and expression of the epsilon 4 subunit of the NMDA receptor channel. *FEBS Lett.* 313:34–38

Ikonomidou C, Turski L (2002) Why did NMDA receptor antagonists fail clinical trials for stroke and traumatic brain injury? *Lancet Neurol.* 1:383–386

Inanobe A, Furukawa H, Gouaux E (2005) Mechanism of Partial Agonist Action at the NR1 Subunit of NMDA Receptors. *Neuron* 47:71–84

Ishii T, Moriyoshi K, Sugihara H, Sakurada K, Kadotani H, Yokoi M, Akazawa C, Shigemoto R, Mizuno N, Masu M, Nakanishi S (1993) Molecular characterization of the family of the N-methyl-D-aspartate receptor subunits. *J. Biol. Chem.* 268:2836–2843

Jackson MB, Wong BS, Morris CE, Lecar H, Christian CN (1983) Successive openings of the same acetylcholine receptor channel are correlated in open time. *Biophys. J.* 42:109–114

Jahr CE, Stevens CF (1993) Calcium permeability of the N-methyl-D-aspartate receptor channel in hippocampal neurons in culture. *Proc. Natl. Acad. Sci.* 90:11573–11577

Jang M-K, Mierke DF, Russek SJ, Farb DH (2004) A steroid modulatory domain on NR2B controls N-methyl-d-aspartate receptor proton sensitivity. *Proc. Natl. Acad. Sci. U. S. A.* 101:8198–8203

Javitt DC (2007) Glutamate and schizophrenia: phencyclidine, N-methyl-D-aspartate receptors, and dopamine-glutamate interactions. *Int. Rev. Neurobiol.* 78:69–108

Javitt DC, Doneshka P, Zylberman I, Ritter W, Vaughan HG Jr (1993) Impairment of early cortical processing in schizophrenia: an event-related potential confirmation study. *Biol. Psychiatry* 33:513–519

Javitt DC, Steinschneider M, Schroeder CE, Arezzo JC (1996) Role of cortical N-methyl-D-aspartate receptors in auditory sensory memory and mismatch negativity generation: implications for schizophrenia. *Proc. Natl. Acad. Sci.* 93:11962–11967

Javitt DC, Zukin SR (1991) Recent advances in the phencyclidine model of schizophrenia. *Am. J. Psychiatry* 148:1301–1308

Jiang Y, Lee A, Chen J, Cadene M, Chait BT, MacKinnon R (2002)(a) The open pore conformation of potassium channels. *Nature* 417:523–526

Jiang Y, Lee A, Chen J, Cadene M, Chait BT, MacKinnon R (2002)(b) Crystal structure and mechanism of a calcium-gated potassium channel. *Nature* 417:515–522

Jiang Y, Lee A, Chen J, Ruta V, Cadene M, Chait BT, MacKinnon R (2003) X-ray structure of a voltage-dependent K+ channel. *Nature* 423:33–41

Jin R, Banke TG, Mayer ML, Traynelis SF, Gouaux E (2003) Structural basis for partial agonist action at ionotropic glutamate receptors. *Nat Neurosci* 6:803–810

Jin R, Clark S, Weeks AM, Dudman JT, Gouaux E, Partin KM (2005) Mechanism of Positive Allosteric Modulators Acting on AMPA Receptors. *J. Neurosci.* 25:9027–9036

Johansen JP, Cain CK, Ostroff LE, LeDoux JE (2011) Molecular mechanisms of fear learning and memory. *Cell* 147:509–524

Johnson JW, Ascher P (1987) Glycine potentiates the NMDA response in cultured mouse brain neurons. *Nature* 325:529–531

Johnston G a. R, Curtis DR, Davies J, Mcculloch RM (1974) Spinal interneurone excitation by conformationally restricted analogues of L-glutamic acid. *Nature* 248:804–805

Jones KS, VanDongen HMA, VanDongen AMJ (2002) The NMDA Receptor M3 Segment Is a Conserved Transduction Element Coupling Ligand Binding to Channel Opening. *J. Neurosci.* 22:2044–2053

Jones S, Gibb AJ (2005) Functional NR2B- and NR2D-containing NMDA receptor channels in rat substantia nigra dopaminergic neurones. *J. Physiol.* 569:209–221

Kalbaugh TL, Zhang J, Diamond JS (2009) Coagonist Release Modulates NMDA Receptor Subtype Contributions at Synaptic Inputs to Retinal Ganglion Cells. *J. Neurosci.* 29:1469–1479

Kalia LV, Kalia SK, Salter MW (2008) NMDA receptors in clinical neurology: excitatory times ahead. *Lancet Neurol.* 7:742–755

Kaniakova M, Lichnerova K, Vyklicky L, Horak M (2012) Single amino acid residue in the M4 domain of GluN1 subunit regulates the surface delivery of NMDA receptors. *J. Neurochem.*:n/a–n/a

Kanthan R, Shuaib A, Griebel R, Miyashita H (1995) Intracerebral Human Microdialysis In Vivo Study of an Acute Focal Ischemic Model of the Human Brain. *Stroke* 26:870–873

Karakas E, Simorowski N, Furukawa H (2009) Structure of the zinc-bound amino-terminal domain of the NMDA receptor NR2B subunit. *EMBO J.* 28:3910–3920

Karakas E, Simorowski N, Furukawa H (2011) Subunit arrangement and phenylethanolamine binding in GluN1/GluN2B NMDA receptors. *Nature* 475:249–253

Kashiwagi K, Masuko T, Nguyen CD, Kuno T, Tanaka I, Igarashi K, Williams K (2002) Channel blockers acting at N-methyl-D-aspartate receptors: differential effects of mutations in the vestibule and ion channel pore. *Mol. Pharmacol.* 61:533–545

Kasper C, Pickering DS, Mirza O, Olsen L, Kristensen AS, Greenwood JR, Liljefors T, Schousboe A, Wätjen F, Gajhede M, Sigurskjold BW, Kastrup JS (2006) The Structure of a Mixed GluR2 Ligand-binding Core Dimer in Complex with (S)-Glutamate and the Antagonist (S)-NS1209. *J. Mol. Biol.* 357:1184–1201

Kazi R, Gan Q, Talukder I, Markowitz M, Salussolia CL, Wollmuth LP (2013) Asynchronous Movements Prior to Pore Opening in NMDA Receptors. *J. Neurosci.* 33:12052–12066

Kemp JA, Foster AC, Leeson PD, Priestley T, Tridgett R, Iversen LL, Woodruff GN (1988) 7-Chlorokynurenic acid is a selective antagonist at the glycine modulatory site of the N-methyl-D-aspartate receptor complex. *Proc. Natl. Acad. Sci. U. S. A.* 85:6547–6550

Kenakin TP (2009) A Pharmacology Primer, Third Edition: Theory, Application and Methods 3rd ed. Academic Press.

Kew JN, Trube G, Kemp JA (1996) A novel mechanism of activity-dependent NMDA receptor antagonism describes the effect of ifenprodil in rat cultured cortical neurones. *J. Physiol.* 497 (Pt 3):761–772

Kew JNC, Trube G, Kemp JA (1998) State-dependent NMDA receptor antagonism by Ro 8-4304, a novel NR2B selective, non-competitive, voltage-independent antagonist. *Br. J. Pharmacol.* 123:463–472

Kim J-I et al. (2011) PI3Kγ is required for NMDA receptor-dependent long-term depression and behavioral flexibility. *Nat. Neurosci.* 14:1447–1454

Kinarsky L, Feng B, Skifter DA, Morley RM, Sherman S, Jane DE, Monaghan DT (2005) Identification of subunit- and antagonist-specific amino acid residues in the N-Methyl-D-aspartate receptor glutamate-binding pocket. *J. Pharmacol. Exp. Ther.* 313:1066–1074

Kinney GG, Sur C, Burno M, Mallorga PJ, Williams JB, Figueroa DJ, Wittmann M, Lemaire W, Conn PJ (2003) The Glycine Transporter Type 1 Inhibitor N-[3-(4′-Fluorophenyl)-3-(4′-Phenylphenoxy)Propyl]Sarcosine Potentiates NMDA Receptor-Mediated Responses In Vivo and Produces an Antipsychotic Profile in Rodent Behavior. *J. Neurosci.* 23:7586–7591

Kleckner NW, Dingledine R (1988) Requirement for Glycine in Activation of NMDA-Receptors Expressed in Xenopus Oocytes. *Science* 241:835–837

Kohda K, Wang Y, Yuzaki M (2000) Mutation of a glutamate receptor motif reveals its role in gating and δ2 receptor channel properties. *Nat. Neurosci.* 3:315–322

Köhr G, Seeburg PH (1996) Subtype-specific regulation of recombinant NMDA receptor-channels by protein tyrosine kinases of the src family. *J. Physiol.* 492:445–452

Kornau HC, Schenker LT, Kennedy MB, Seeburg PH (1995) Domain interaction between NMDA receptor subunits and the postsynaptic density protein PSD-95. *Science* 269:1737–1740

Korotkova T, Fuchs EC, Ponomarenko A, von Engelhardt J, Monyer H (2010) NMDA Receptor Ablation on Parvalbumin-Positive Interneurons Impairs Hippocampal Synchrony, Spatial Representations, and Working Memory. *Neuron* 68:557–569

Kotermanski SE, Johnson JW (2009) Mg2+ Imparts NMDA Receptor Subtype Selectivity to the Alzheimer's Drug Memantine. *J Neurosci* 29:2774–2779

Kristiansen LV, Huerta I, Beneyto M, Meador-Woodruff JH (2007) NMDA receptors and schizophrenia. *Curr. Opin. Pharmacol.* 7:48–55

Krogsgaard-Larsen P, Honoré T, Hansen JJ, Curtis DR, Lodge D (1980) New class of glutamate agonist structurally related to ibotenic acid. *Nature* 284:64–66

Krystal JH, Karper LP, Seibyl JP, Freeman GK, Delaney R, Bremner JD, Heninger GR, Bowers MB Jr, Charney DS (1994) Subanesthetic effects of the noncompetitive NMDA antagonist, ketamine, in humans. Psychotomimetic, perceptual, cognitive, and neuroendocrine responses. *Arch. Gen. Psychiatry* 51:199–214

Kumar J, Mayer ML (2013) Functional Insights from Glutamate Receptor Ion Channel Structures*. *Annu. Rev. Physiol.* 75:313–337

Kuner T, Seeburg PH, Robert Guy H (2003) A common architecture for K+ channels and ionotropic glutamate receptors? *Trends Neurosci.* 26:27–32

Kuner T, Wollmuth LP, Karlin A, Seeburg PH, Sakmann B (1996) Structure of the NMDA Receptor Channel M2 Segment Inferred from the Accessibility of Substituted Cysteines. *Neuron* 17:343–352

Kuryatov A, Laube B, Betz H, Kuhse J (1994) Mutational analysis of the glycine-binding site of the NMDA receptor: Structural similarity with bacterial amino acid-binding proteins. *Neuron* 12:1291–1300

Kussius CL, Popescu GK (2009) Kinetic basis of partial agonism at NMDA receptors. *Nat. Neurosci.* 12:1114–1120

Kussius CL, Popescu GK (2010) NMDA Receptors with Locked Glutamate-Binding Clefts Open with High Efficacy. *J. Neurosci.* 30:12474–12479

Kutsuwada T, Kashiwabuchi N, Mori H, Sakimura K, Kushiya E, Araki K, Meguro H, Masaki H, Kumanishi T, Arakawa M, Mishina M (1992) Molecular diversity of the NMDA receptor channel. *Nature* 358:36–41

Kuusinen A, Arvola M, Keinanen K (1995) Molecular dissection of the agonist binding site of an AMPA receptor. *EMBO J.* 14:6327–6332

Kwon H-B, Castillo PE (2008) Long-term potentiation selectively expressed by NMDA receptors at hippocampal mossy fiber synapses. *Neuron* 57:108–120

Labrie V, Fukumura R, Rastogi A, Fick LJ, Wang W, Boutros PC, Kennedy JL, Semeralul MO, Lee FH, Baker GB, Belsham DD, Barger SW, Gondo Y, Wong AHC, Roder JC (2009) Serine racemase is associated with schizophrenia susceptibility in humans and in a mouse model. *Hum. Mol. Genet.* 18:3227–3243

Labrie V, Roder JC (2010) The involvement of the NMDA receptor D-serine/glycine site in the pathophysiology and treatment of schizophrenia. *Neurosci. Biobehav. Rev.* 34:351–372

Lafon-Cazal M, Pietri S, Culcasi M, Bockaert J (1993) NMDA-dependent superoxide production and neurotoxicity. *Nature* 364:535–537

Laube B, Hirai H, Sturgess M, Betz H, Kuhse J (1997) Molecular Determinants of Agonist Discrimination by NMDA Receptor Subunits: Analysis of the Glutamate Binding Site on the NR2B Subunit. *Neuron* 18:493–503

Laube B, Kuhse J, Betz H (1998) Evidence for a Tetrameric Structure of Recombinant NMDA Receptors. *J. Neurosci.* 18:2954–2961

Laube B, Schemm R, Betz H (2004) Molecular determinants of ligand discrimination in the glutamate-binding pocket of the NMDA receptor. *Neuropharmacology* 47:994–1007

Lazareno S, Birdsall NJ (1995) Detection, quantitation, and verification of allosteric interactions of agents with labeled and unlabeled ligands at G protein-coupled receptors: interactions of strychnine and acetylcholine at muscarinic receptors. *Mol. Pharmacol.* 48:362–378

Lazo JS, Brady LS, Dingledine R (2007) Building a Pharmacological Lexicon: Small Molecule Discovery in Academia. *Mol. Pharmacol.* 72:1–7

Lee C-H, Gouaux E (2011) Amino Terminal Domains of the NMDA Receptor Are Organized as Local Heterodimers. *PLoS ONE* 6:e19180

Lee H, Kim JJ (1998) Amygdalar NMDA Receptors are Critical for New Fear Learning in Previously Fear-Conditioned Rats. *J. Neurosci.* 18:8444 –8454

Lehmann J, Hutchison AJ, McPherson SE, Mondadori C, Schmutz M, Sinton CM, Tsai C, Murphy DE, Steel DJ, Williams M (1988) CGS 19755, a selective and competitive N-methyl-D-aspartate-type excitatory amino acid receptor antagonist. *J. Pharmacol. Exp. Ther.* 246:65–75

Li Y, Krupa B, Kang J-S, Bolshakov VY, Liu G (2009) Glycine Site of NMDA Receptor Serves as a Spatiotemporal Detector of Synaptic Activity Patterns. *J. Neurophysiol.* 102:578–589

Li Y, Sacchi S, Pollegioni L, Basu AC, Coyle JT, Bolshakov VY (2013) Identity of endogenous NMDAR glycine site agonist in amygdala is determined by synaptic activity level. *Nat. Commun.* 4:1760

De Ligt J, Willemsen MH, van Bon BWM, Kleefstra T, Yntema HG, Kroes T, Vulto-van Silfhout AT, Koolen DA, de Vries P, Gilissen C, del Rosario M, Hoischen A, Scheffer H,

de Vries BBA, Brunner HG, Veltman JA, Vissers LELM (2012) Diagnostic Exome Sequencing in Persons with Severe Intellectual Disability. *N. Engl. J. Med.* 367:1921–1929

Liman ER, Tytgat J, Hess P (1992) Subunit stoichiometry of a mammalian K+ channel determined by construction of multimeric cDNAs. *Neuron* 9:861–871

Limpert E, Stahel WA, Abbt M (2001) Log-normal distributions across the sciences: keys and clues. *BioScience* 51:341–352

Lin C-H, Yeh S-H, Lu H-Y, Gean P-W (2003) The similarities and diversities of signal pathways leading to consolidation of conditioning and consolidation of extinction of fear memory. *J. Neurosci. Off. J. Soc. Neurosci.* 23:8310–8317

Lindahl JS, Keifer J (2004) Glutamate receptor subunits are altered in forebrain and cerebellum in rats chronically exposed to the NMDA receptor antagonist phencyclidine. *Neuropsychopharmacol. Off. Publ. Am. Coll. Neuropsychopharmacol.* 29:2065–2073

Lipton SA, Rosenberg PA (1994) Excitatory Amino Acids as a Final Common Pathway for Neurologic Disorders. *N. Engl. J. Med.* 330:613–622

Lisman J, Yasuda R, Raghavachari S (2012) Mechanisms of CaMKII action in long-term potentiation. *Nat. Rev. Neurosci.* 13:169–182

Liu L, Wong TP, Pozza MF, Lingenhoehl K, Wang Y, Sheng M, Auberson YP, Wang YT (2004) Role of NMDA Receptor Subtypes in Governing the Direction of Hippocampal Synaptic Plasticity. *Science* 304:1021 –1024

Liu XJ, Gingrich JR, Vargas-Caballero M, Dong YN, Sengar A, Beggs S, Wang S-H, Ding HK, Frankland PW, Salter MW (2008) Treatment of inflammatory and neuropathic pain by uncoupling Src from the NMDA receptor complex. *Nat. Med.* 14:1325–1332

Liu Y, Wong TP, Aarts M, Rooyakkers A, Liu L, Lai TW, Wu DC, Lu J, Tymianski M, Craig AM, Wang YT (2007) NMDA Receptor Subunits Have Differential Roles in Mediating Excitotoxic Neuronal Death Both In Vitro and In Vivo. *J. Neurosci.* 27:2846–2857

Lledo PM, Hjelmstad GO, Mukherji S, Soderling TR, Malenka RC, Nicoll RA (1995) Calcium/calmodulin-dependent kinase II and long-term potentiation enhance synaptic transmission by the same mechanism. *Proc. Natl. Acad. Sci.* 92:11175–11179

Lovinger DM, Wong KL, Murakami K, Routtenberg A (1987) Protein kinase C inhibitors eliminate hippocampal long-term potentiation. *Brain Res.* 436:177–183

Low C-M, Lyuboslavsky P, French A, Le P, Wyatte K, Thiel WH, Marchan EM, Igarashi K, Kashiwagi K, Gernert K, Williams K, Traynelis SF, Zheng F (2003) Molecular Determinants of Proton-Sensitive N-Methyl-d-aspartate Receptor Gating. *Mol. Pharmacol.* 63:1212–1222

Lu YM, Roder JC, Davidow J, Salter MW (1998) Src activation in the induction of long-term potentiation in CA1 hippocampal neurons. *Science* 279:1363–1367

Luby ED, Cohen BD, Rosenbaum G, Gottlieb JS, Kelley R (1959) Study of a new schizophrenomimetic drug; sernyl. *AMA Arch. Neurol. Psychiatry* 81:363–369

Lukasiewicz PD, Roeder RC (1995) Evidence for glycine modulation of excitatory synaptic inputs to retinal ganglion cells. *J. Neurosci.* 15:4592–4601

Lunn M-L, Hogner A, Stensbøl TB, Gouaux E, Egebjerg J, Kastrup JS (2003) Three-Dimensional Structure of the Ligand-Binding Core of GluR2 in Complex with the Agonist (S)-ATPA: Implications for Receptor Subunit Selectivity. *J. Med. Chem.* 46:872–875

Luo J, Wang Y, Yasuda RP, Dunah AW, Wolfe BB (1997) The Majority of N-Methyl-d-Aspartate Receptor Complexes in Adult Rat Cerebral Cortex Contain at Least Three Different Subunits (NR1/NR2A/NR2B). *Mol. Pharmacol.* 51:79–86

Luu P, Malenka RC (2008) Spike Timing-Dependent Long-Term Potentiation in Ventral Tegmental Area Dopamine Cells Requires PKC. *J. Neurophysiol.* 100:533–538

MacDermott AB, Mayer ML, Westbrook GL, Smith SJ, Barker JL (1986) NMDA-receptor activation increases cytoplasmic calcium concentration in cultured spinal cord neurones. *Nature* 321:519–522

Madry C, Betz H, Geiger JRP, Laube B (2010) Potentiation of glycine-gated NR1/NR3A NMDA receptors relieves Ca2+-dependent outward rectification. *Front. Mol. Neurosci.* 3:6

Madry C, Mesic I, Bartholomäus I, Nicke A, Betz H, Laube B (2007) Principal role of NR3 subunits in NR1/NR3 excitatory glycine receptor function. *Biochem. Biophys. Res. Commun.* 354:102–108

Magleby KL, Pallotta BS (1983) Burst kinetics of single calcium-activated potassium channels in cultured rat muscle. *J. Physiol.* 344:605–623

Makarova O, Kamberov E, Margolis B (2000) Generation of deletion and point mutations with one primer in a single cloning step. *BioTechniques* 29:970–972

Maki BA, Aman TK, Amico-Ruvio SA, Kussius CL, Popescu GK (2012) C-terminal Domains of N-Methyl-d-aspartic Acid Receptor Modulate Unitary Channel Conductance and Gating. *J. Biol. Chem.* 287:36071–36080

Makino C, Shibata H, Ninomiya H, Tashiro N, Fukumaki Y (2005) Identification of single-nucleotide polymorphisms in the human N-methyl-D-aspartate receptor subunit NR2D gene, GRIN2D, and association study with schizophrenia. *Psychiatr. Genet.* 15:215–221

Malayev A, Gibbs TT, Farb DH (2002) Inhibition of the NMDA response by pregnenolone sulphate reveals subtype selective modulation of NMDA receptors by sulphated steroids. *Br. J. Pharmacol.* 135:901–909

Malenka RC, Nicoll and RA (1999) Long-Term Potentiation--A Decade of Progress? *Science* 285:1870–1874

Malinow R, Schulman H, Tsien RW (1989) Inhibition of postsynaptic PKC or CaMKII blocks induction but not expression of LTP. *Science* 245:862–866

Mano I, Lamed Y, Teichberg VI (1996) A Venus Flytrap Mechanism for Activation and Desensitization of α-Amino-3-hydroxy-5-methyl-4-isoxazole Propionic Acid Receptors. *J. Biol. Chem.* 271:15299–15302

Martel M-A, Ryan TJ, Bell KFS, Fowler JH, McMahon A, Al-Mubarak B, Komiyama NH, Horsburgh K, Kind PC, Grant SGN, Wyllie DJA, Hardingham GE (2012) The Subtype of GluN2 C-terminal Domain Determines the Response to Excitotoxic Insults. *Neuron* 74:543–556

Martina M, B.-Turcotte M-E, Halman S, Tsai G, Tiberi M, Coyle JT, Bergeron R (2005) Reduced glycine transporter type 1 expression leads to major changes in glutamatergic neurotransmission of CA1 hippocampal neurones in mice. *J. Physiol.* 563:777–793

Martineau M, Baux G, Mothet J-P (2006) D-Serine signalling in the brain: friend and foe. *Trends Neurosci.* 29:481–491

Martucci L, Wong AHC, De Luca V, Likhodi O, Wong GWH, King N, Kennedy JL (2006) N-methyl-D-aspartate receptor NR2B subunit gene GRIN2B in schizophrenia and bipolar disorder: Polymorphisms and mRNA levels. *Schizophr. Res.* 84:214–221

Masuko T, Kuno T, Kashiwagi K, Kusama T, Williams K, Igarashi K (1999) Stimulatory and inhibitory properties of aminoglycoside antibiotics at N-methyl-D-aspartate receptors. *J. Pharmacol. Exp. Ther.* 290:1026–1033

Matsui T, Sekiguchi M, Hashimoto A, Tomita U, Nishikawa T, Wada K (1995) Functional Comparison of d-Serine and Glycine in Rodents: The Effect on Cloned NMDA Receptors and the Extracellular Concentration. *J. Neurochem.* 65:454–458

Matta JA, Ashby MC, Sanz-Clemente A, Roche KW, Isaac JTR (2011) mGluR5 and NMDA Receptors Drive the Experience- and Activity-Dependent NMDA Receptor NR2B to NR2A Subunit Switch. *Neuron* 70:339–351

Mattison HA, Hayashi T, Barria A (2012) Palmitoylation at Two Cysteine Clusters on the C-Terminus of GluN2A and GluN2B Differentially Control Synaptic Targeting of NMDA Receptors. *PLoS ONE* 7:e49089

Mattson MP (2003) Excitotoxic and excitoprotective mechanisms. *NeuroMolecular Med.* 3:65–94

Mayer ML (2006) Glutamate receptors at atomic resolution. *Nature* 440:456–462

Mayer ML (2011)(a) Emerging Models of Glutamate Receptor Ion Channel Structure and Function. *Structure* 19:1370–1380

Mayer ML (2011)(b) Structure and mechanism of glutamate receptor ion channel assembly, activation and modulation. *Curr. Opin. Neurobiol.* 21:283–290

Mayer ML, Westbrook GL (1987) Permeation and block of N-methyl-D-aspartic acid receptor channels by divalent cations in mouse cultured central neurones. *J. Physiol.* 394:501–527

Mayer ML, Westbrook GL, Guthrie PB (1984) Voltage-dependent block by Mg2+ of NMDA responses in spinal cord neurones. *Nature* 309:261–263

McGurk JF, Bennett MV, Zukin RS (1990) Polyamines potentiate responses of N-methyl-D-aspartate receptors expressed in xenopus oocytes. *Proc. Natl. Acad. Sci. U. S. A.* 87:9971–9974

Mcintosh TK, Vink R, Soares H, Hayes R, Simon R (1989) Effects of the N-methyl-D-aspartate receptor blocker MK-801 on neurologic function after experimental brain injury. *J. Neurotrauma* 6:247–259

McKay S, Griffiths N, Butters P, Thubron E, Hardingham G, Wyllie D (2012) Direct pharmacological monitoring of the developmental switch in NMDA receptor subunit composition using TCN 213, a GluN2A-selective, glycine-dependent antagonist. *Br. J. Pharmacol.* 166:924–937

McLennan H, Lodge D (1979) The antagonism of amino acid-induced excitation of spinal neurones in the cat. *Brain Res.* 169:83–90

Meddows E, Bourdellès BL, Grimwood S, Wafford K, Sandhu S, Whiting P, McIlhinney RAJ (2001) Identification of Molecular Determinants That Are Important in the Assembly of N-Methyl-d-aspartate Receptors. *J. Biol. Chem.* 276:18795–18803

Meguro H, Mori H, Araki K, Kushiya E, Kutsuwada T, Yamazaki M, Kumanishi T, Arakawa M, Sakimura K, Mishina M (1992) Functional characterization of a heteromeric NMDA receptor channel expressed from cloned cDNAs. *Nature* 357:70–74

Mena EE, Gullak MF, Pagnozzi MJ, Richter KE, Rivier J, Cruz LJ, Olivera BM (1990) Conantokin-G: a novel peptide antagonist to the N-methyl-D-aspartic acid (NMDA) receptor. *Neurosci. Lett.* 118:241–244

Miller B, Sarantis M, Traynelis SF, Attwell D (1992) Potentiation of NMDA receptor currents by arachidonic acid. *Nature* 355:722–725

Minematsu K, Fisher M, Li L, Davis MA, Knapp AG, Cotter RE, McBurney RN, Sotak CH (1993) Effects of a novel NMDA antagonist on experimental stroke rapidly and quantitatively assessed by diffusion-weighted MRI. *Neurology* 43:397–403

Miserendino MJ, Sananes CB, Melia KR, Davis M (1990) Blocking of acquisition but not expression of conditioned fear-potentiated startle by NMDA antagonists in the amygdala. *Nature* 345:716–718

Misra C, Brickley SG, Farrant M, Cull-Candy SG (2000) Identification of subunits contributing to synaptic and extrasynaptic NMDA receptors in Golgi cells of the rat cerebellum. *J. Physiol.* 524:147–162

Mody I, MacDonald JF (1995) NMDA receptor-dependent excitotoxicity: the role of intracellular Ca2+ release. *Trends Pharmacol. Sci.* 16:356–359

Moghaddam B, Javitt D (2012) From Revolution to Evolution: The Glutamate Hypothesis of Schizophrenia and its Implication for Treatment. *Neuropsychopharmacology* 37:4–15

Momiyama A, Feldmeyer D, Cull-Candy SG (1996) Identification of a native low-conductance NMDA channel with reduced sensitivity to Mg2+ in rat central neurones. *J. Physiol.* 494:479–492

Monaghan DT, Irvine MW, Costa BM, Fang G, Jane DE (2012) Pharmacological modulation of NMDA receptor activity and the advent of negative and positive allosteric modulators. *Neurochem. Int.* 61:581–592

Mony L, Kew JN, Gunthorpe MJ, Paoletti P (2009) Allosteric modulators of NR2B-containing NMDA receptors: molecular mechanisms and therapeutic potential. *Br. J. Pharmacol.* 157:1301–1317

Mony L, Zhu S, Carvalho S, Paoletti P (2011) Molecular basis of positive allosteric modulation of GluN2B NMDA receptors by polyamines. *EMBO J.* 30:3134–3146

Monyer H, Burnashev N, Laurie DJ, Sakmann B, Seeburg PH (1994) Developmental and regional expression in the rat brain and functional properties of four NMDA receptors. *Neuron* 12:529–540

Monyer H, Sprengel R, Schoepfer R, Herb A, Higuchi M, Lomeli H, Burnashev N, Sakmann B, Seeburg PH (1992) Heteromeric NMDA Receptors: Molecular and Functional Distinction of Subtypes. *Science* 256:1217–1221

Moriyoshi K, Masu M, Ishii T, Shigemoto R, Mizuno N, Nakanishi S (1991) Molecular cloning and characterization of the rat NMDA receptor. *Nature* 354:31–37

Morley RM, Tse H-W, Feng B, Miller JC, Monaghan DT, Jane DE (2005) Synthesis and Pharmacology of N1-Substituted Piperazine-2,3-dicarboxylic Acid Derivatives Acting as NMDA Receptor Antagonists. *J. Med. Chem.* 48:2627–2637

Morris GF, Bullock R, Marshall SB, Marmarou A, Maas A, Marshall LF (1999) Failure of the competitive N-methyl-D-aspartate antagonist Selfotel (CGS 19755) in the treatment of severe head injury: results of two phase III clinical trials. The Selfotel Investigators. *J. Neurosurg.* 91:737–743

Morris RGM, Anderson E, Lynch GS, Baudry M (1986) Selective impairment of learning and blockade of long-term potentiation by an N-methyl-D-aspartate receptor antagonist, AP5. *Nature* 319:774–776

Mosley CA, Acker TM, Hansen KB, Mullasseril P, Andersen KT, Le P, Vellano KM, Bräuner-Osborne H, Liotta DC, Traynelis SF (2010) Quinazolin-4-one Derivatives: A Novel Class of Noncompetitive NR2C/D Subunit-Selective N-Methyl-d-aspartate Receptor Antagonists. *J. Med. Chem.* 53:5476–5490

Mothet J-P, Parent AT, Wolosker H, Brady RO, Linden DJ, Ferris CD, Rogawski MA, Snyder SH (2000) d-Serine is an endogenous ligand for the glycine site of the N-methyl-d-aspartate receptor. *Proc. Natl. Acad. Sci.* 97:4926–4931

Mott DD, Doherty JJ, Zhang S, Washburn MS, Fendley MJ, Lyuboslavsky P, Traynelis SF, Dingledine R (1998) Phenylethanolamines inhibit NMDA receptors by enhancing proton inhibition. *Nat. Neurosci.* 1:659–667

Mott DD, Erreger K, Banke TG, Traynelis SF (2001) Open probability of homomeric murine 5-HT3A serotonin receptors depends on subunit occupancy. *J. Physiol.* 535:427–443

Muir KW (2006) Glutamate-based therapeutic approaches: clinical trials with NMDA antagonists. *Curr. Opin. Pharmacol.* 6:53–60

Mullasseril P, Hansen KB, Vance KM, Ogden KK, Yuan H, Kurtkaya NL, Santangelo R, Orr AG, Le P, Vellano KM, Liotta DC, Traynelis SF (2010) A subunit-selective potentiator of NR2C- and NR2D-containing NMDA receptors. *Nat. Commun.* 1:90

Müller T, Albrecht D, Gebhardt C (2009) Both NR2A and NR2B subunits of the NMDA receptor are critical for long-term potentiation and long-term depression in the lateral amygdala of horizontal slices of adult mice. *Learn. Mem.* 16:395–405

Näätänen R, Kähkönen S (2009) Central auditory dysfunction in schizophrenia as revealed by the mismatch negativity (MMN) and its magnetic equivalent MMNm: a review. *Int. J. Neuropsychopharmacol. Off. Sci. J. Coll. Int. Neuropsychopharmacol. CINP* 12:125–135

Nagy GG, Watanabe M, Fukaya M, Todd AJ (2004) Synaptic distribution of the NR1, NR2A and NR2B subunits of the N-methyl-d-aspartate receptor in the rat lumbar spinal cord revealed with an antigen-unmasking technique. *Eur. J. Neurosci.* 20:3301–3312

Naur P, Hansen KB, Kristensen AS, Dravid SM, Pickering DS, Olsen L, Vestergaard B, Egebjerg J, Gajhede M, Traynelis SF, Kastrup JS (2007) Ionotropic glutamate-like receptor δ2 binds d-serine and glycine. *Proc. Natl. Acad. Sci.* 104:14116–14121

Nayeem N, Zhang Y, Schweppe DK, Madden DR, Green T (2009) A nondesensitizing kainate receptor point mutant. *Mol. Pharmacol.* 76:534–542

Neyton J, Paoletti P (2006) Relating NMDA Receptor Function to Receptor Subunit Composition: Limitations of the Pharmacological Approach. *J. Neurosci.* 26:1331–1333

Nielsen BB, Pickering DS, Greenwood JR, Brehm L, Gajhede M, Schousboe A, Kastrup JS (2005) Exploring the GluR2 ligand-binding core in complex with the bicyclical AMPA analogue (S)-4-AHCP. *FEBS J.* 272:1639–1648

Niethammer M, Kim E, Sheng M (1996) Interaction between the C terminus of NMDA receptor subunits and multiple members of the PSD-95 family of membrane-associated guanylate kinases. *J. Neurosci.* 16:2157–2163

Nilsson P, Hillered L, Pontén U, Ungerstedt U (1990) Changes in cortical extracellular levels of energy-related metabolites and amino acids following concussive brain injury in rats. *J. Cereb. Blood Flow Metab. Off. J. Int. Soc. Cereb. Blood Flow Metab.* 10:631–637

Niswender CM, Conn PJ (2010) Metabotropic Glutamate Receptors: Physiology, Pharmacology, and Disease. *Annu. Rev. Pharmacol. Toxicol.* 50:295–322

Novelli A, Reilly JA, Lysko PG, Henneberry RC (1988) Glutamate becomes neurotoxic via the N-methyl-d-aspartate receptor when intracellular energy levels are reduced. *Brain Res.* 451:205–212

Nowak L, Bregestovski P, Ascher P, Herbet A, Prochiantz A (1984) Magnesium gates glutamate-activated channels in mouse central neurones. *Nature* 307:462–465

Nozaki C, Vergnano AM, Filliol D, Ouagazzal A-M, Le Goff A, Carvalho S, Reiss D, Gaveriaux-Ruff C, Neyton J, Paoletti P, Kieffer BL (2011) Zinc alleviates pain through high-affinity binding to the NMDA receptor NR2A subunit. *Nat. Neurosci.* 14:1017–1022

O'Roak BJ et al. (2012)(a) Sporadic autism exomes reveal a highly interconnected protein network of de novo mutations. *Nature* 485:246–250

O'Roak BJ et al. (2012)(b) Multiplex Targeted Sequencing Identifies Recurrently Mutated Genes in Autism Spectrum Disorders. *Science* 338:1619–1622

Ogden KK, Traynelis SF (2011) New advances in NMDA receptor pharmacology. *Trends Pharmacol. Sci.* 32:726–733

Ogden KK, Traynelis SF (2013) Contribution of the M1 transmembrane helix and pre-M1 region to positive allosteric modulation and gating of N-methyl-D-aspartate receptors. *Mol. Pharmacol.* 83:1045–1056

Olney JW (1969) Brain Lesions, Obesity, and Other Disturbances in Mice Treated with Monosodium Glutamate. *Science* 164:719–721

Omkumar RV, Kiely MJ, Rosenstein AJ, Min K-T, Kennedy MB (1996) Identification of a Phosphorylation Site for Calcium/Calmodulindependent Protein Kinase II in the NR2B Subunit of the N-Methyl-D-aspartate Receptor. *J. Biol. Chem.* 271:31670–31678

Ozyurt E, Graham DI, Woodruff GN, McCulloch J (1988) Protective effect of the glutamate antagonist, MK-801 in focal cerebral ischemia in the cat. *J. Cereb. Blood Flow Metab. Off. J. Int. Soc. Cereb. Blood Flow Metab.* 8:138–143

Panatier A, Theodosis DT, Mothet J-P, Touquet B, Pollegioni L, Poulain DA, Oliet SHR (2006) Glia-Derived d-Serine Controls NMDA Receptor Activity and Synaptic Memory. *Cell* 125:775–784

Paoletti P, Ascher P, Neyton J (1997) High-Affinity Zinc Inhibition of NMDA NR1–NR2A Receptors. *J. Neurosci.* 17:5711–5725

Paoletti P, Bellone C, Zhou Q (2013) NMDA receptor subunit diversity: impact on receptor properties, synaptic plasticity and disease. *Nat. Rev. Neurosci.* 14:383–400

Paoletti P, Neyton J, Ascher P (1995) Glycine-independent and subunit-specific potentiation of NMDA responses by extracellular Mg2+. *Neuron* 15:1109–1120

Papadakis M, Hawkins LM, Stephenson FA (2004) Appropriate NR1-NR1 Disulfide-linked Homodimer Formation Is Requisite for Efficient Expression of Functional, Cell Surface N-Methyl-D-aspartate NR1/NR2 Receptors. *J. Biol. Chem.* 279:14703–14712

Papouin T, Ladépêche L, Ruel J, Sacchi S, Labasque M, Hanini M, Groc L, Pollegioni L, Mothet J-P, Oliet SHR (2012) Synaptic and Extrasynaptic NMDA Receptors Are Gated by Different Endogenous Coagonists. *Cell* 150:633–646

Park-Chung M, Wu FS, Farb DH (1994) 3 alpha-Hydroxy-5 beta-pregnan-20-one sulfate: a negative modulator of the NMDA-induced current in cultured neurons. *Mol. Pharmacol.* 46:146 –150

Paul IA, Skolnick P (2003) Glutamate and Depression. *Ann. N. Y. Acad. Sci.* 1003:250–272

Perez-Otano I, Schulteis CT, Contractor A, Lipton SA, Trimmer JS, Sucher NJ, Heinemann SF (2001) Assembly with the NR1 Subunit Is Required for Surface Expression of NR3A-Containing NMDA Receptors. *J Neurosci* 21:1228–1237

Perin-Dureau F, Rachline J, Neyton J, Paoletti P (2002) Mapping the binding site of the neuroprotectant ifenprodil on NMDA receptors. *J. Neurosci. Off. J. Soc. Neurosci.* 22:5955–5965

Persson L, Hillered L (1992) Chemical monitoring of neurosurgical intensive care patients using intracerebral microdialysis. *J. Neurosurg.* 76:72–80

Persson L, Valtysson J, Enblad P, Warme PE, Cesarini K, Lewen A, Hillered L (1996) Neurochemical monitoring using intracerebral microdialysis in patients with subarachnoid hemorrhage. *J. Neurosurg.* 84:606–616

Petrenko AB, Yamakura T, Baba H, Shimoji K (2003) The Role of N-Methyl-d-Aspartate (NMDA) Receptors in Pain: A Review. *Anesth. Analg. Oct. 2003* 97:1108–1116

Petrovic M, Sedlacek M, Cais O, Horak M, Chodounska H, Vyklicky Jr L (2009) Pregnenolone sulfate modulation of N-methyl-d-aspartate receptors is phosphorylation dependent. *Neuroscience* 160:616–628

Petrovic M, Sedlacek M, Horak M, Chodounska H, Vyklický L Jr (2005) 20-oxo-5beta-pregnan-3alpha-yl sulfate is a use-dependent NMDA receptor inhibitor. *J. Neurosci. Off. J. Soc. Neurosci.* 25:8439–8450

Pettit DL, Perlman S, Malinow R (1994) Potentiated Transmission and Prevention of Further LTP by Increased CaMKII Activity in Postsynaptic Hippocampal Slice Neurons. *Science* 266:1881–1885

Philpot BD, Sekhar AK, Shouval HZ, Bear MF (2001) Visual experience and deprivation bidirectionally modify the composition and function of NMDA receptors in visual cortex. *Neuron* 29:157–169

Pin J-P, Duvoisin R (1995) The metabotropic glutamate receptors: Structure and functions. *Neuropharmacology* 34:1–26

Plested AJR, Mayer ML (2007) Structure and Mechanism of Kainate Receptor Modulation by Anions. *Neuron* 53:829–841

Plested AJR, Vijayan R, Biggin PC, Mayer ML (2008) Molecular Basis of Kainate Receptor Modulation by Sodium. *Neuron* 58:720–735

Popescu G, Auerbach A (2003) Modal gating of NMDA receptors and the shape of their synaptic response. *Nat. Neurosci.* 6:476–483

Popescu G, Robert A, Howe JR, Auerbach A (2004) Reaction mechanism determines NMDA receptor response to repetitive stimulation. *Nature* 430:790–793

Premkumar L, Auerbach A (1996) Identification of a High Affinity Divalent Cation Binding Site near the Entrance of the NMDA Receptor Channel. *Neuron* 16:869–880

Preskorn SH, Baker B, Kolluri S, Menniti FS, Krams M, Landen JW (2008) An Innovative Design to Establish Proof of Concept of the Antidepressant Effects of the NR2B Subunit Selective N-Methyl-D-Aspartate Antagonist, CP-101,606, in Patients With Treatment-Refractory Major Depressive Disorder. *J. Clin. Psychopharmacol.* 28:631–637

Priestley T, Laughton P, Myers J, Le Bourdellés B, Kerby J, Whiting PJ (1995) Pharmacological properties of recombinant human N-methyl-D-aspartate receptors comprising NR1a/NR2A and NR1a/NR2B subunit assemblies expressed in permanently transfected mouse fibroblast cells. *Mol. Pharmacol.* 48:841–848

Ptak CP, Ahmed AH, Oswald RE (2009) Probing the Allosteric Modulator Binding Site of GluR2 with Thiazide Derivatives. *Biochemistry (Mosc.)* 48:8594–8602

Puddifoot C, Chen P, Schoepfer R, Wyllie D (2009) Pharmacological characterization of recombinant NR1/NR2A NMDA receptors with truncated and deleted carboxy termini expressed in Xenopus laevis oocytes. *Br. J. Pharmacol.* 156:509–518

Punnakkal P, Jendritza P, Köhr G (2012) Influence of the intracellular GluN2 C-terminal domain on NMDA receptor function. *Neuropharmacology* 62:1985–1992

Qin F (2004) Restoration of Single-Channel Currents Using the Segmental k-Means Method Based on Hidden Markov Modeling. *Biophys. J.* 86:1488–1501

Qin F, Auerbach A, Sachs F (1996) Estimating single-channel kinetic parameters from idealized patch-clamp data containing missed events. *Biophys. J.* 70:264–280

Qin F, Auerbach A, Sachs F (1997) Maximum likelihood estimation of aggregated Markov processes. *Proc. R. Soc. B Biol. Sci.* 264:375–383

Qin S, Zhao X, Pan Y, Liu J, Feng G, Fu J, Bao J, Zhang Z, He L (2005) An association study of the N-methyl-D-aspartate receptor NR1 subunit gene (GRIN1) and NR2B subunit gene (GRIN2B) in schizophrenia with universal DNA microarray. *Eur. J. Hum. Genet. EJHG* 13:807–814

Qiu S, Hua Y, Yang F, Chen Y, Luo J (2005) Subunit Assembly of N-Methyl-d-aspartate Receptors Analyzed by Fluorescence Resonance Energy Transfer. *J. Biol. Chem.* 280:24923–24930

Qureshi AI, Ali Z, Suri MFK, Shuaib A, Baker G, Todd K, Guterman LR, Hopkins LN (2003) Extracellular glutamate and other amino acids in experimental intracerebral hemorrhage: an in vivo microdialysis study. *Crit. Care Med.* 31:1482–1489

Raditsch M, Ruppersberg JP, Kuner T, Günther W, Schoepfer R, Seeburg PH, Jahn W, Witzemann V (1993) Subunit-specific block of cloned NMDA receptors by argiotoxin636. *FEBS Lett.* 324:63–66

Rambhadran A, Gonzalez J, Jayaraman V (2010) Subunit Arrangement in N-Methyl-d-aspartate (NMDA) Receptors. *J. Biol. Chem.* 285:15296–15301

Rambhadran A, Gonzalez J, Jayaraman V (2011) Conformational Changes at the Agonist Binding Domain of the N-Methyl-d-Aspartic Acid Receptor. *J. Biol. Chem.* 286:16953–16957

Ransom RW, Stec NL (1988) Cooperative modulation of [3H]MK-801 binding to the N-methyl-D-aspartate receptor-ion channel complex by L-glutamate, glycine, and polyamines. *J. Neurochem.* 51:830–836

Rauner C, Köhr G (2011) Triheteromeric NR1/NR2A/NR2B Receptors Constitute the Major N-Methyl-d-aspartate Receptor Population in Adult Hippocampal Synapses. *J. Biol. Chem.* 286:7558–7566

Rebola N, Carta M, Lanore F, Blanchet C, Mulle C (2011) NMDA receptor-dependent metaplasticity at hippocampal mossy fiber synapses. *Nat. Neurosci.* 14:691–693

Rebola N, Lujan R, Cunha RA, Mulle C (2008) Adenosine A2A receptors are essential for long-term potentiation of NMDA-EPSCs at hippocampal mossy fiber synapses. *Neuron* 57:121–134

Reed BT, Sullivan SJ, Tsai G, Coyle JT, Esguerra M, Miller RF (2009) The glycine transporter GlyT1 controls N-methyl-D-aspartic acid receptor coagonist occupancy in the mouse retina. *Eur. J. Neurosci.* 30:2308–2317

Reynolds IJ (1990) Arcaine uncovers dual interactions of polyamines with the N-methyl-D-aspartate receptor. *J. Pharmacol. Exp. Ther.* 255:1001–1007

Reynolds IJ, Miller RJ (1989) Ifenprodil is a novel type of N-methyl-D-aspartate receptor antagonist: interaction with polyamines. *Mol. Pharmacol.* 36:758–765

Riaza Bermudo-Soriano C, Perez-Rodriguez MM, Vaquero-Lorenzo C, Baca-Garcia E (2012) New perspectives in glutamate and anxiety. *Pharmacol. Biochem. Behav.* 100:752–774

Riou M, Stroebel D, Edwardson JM, Paoletti P (2012) An Alternating GluN1-2-1-2 Subunit Arrangement in Mature NMDA Receptors. *PLoS ONE* 7:e35134

Risgaard R, Hansen KB, Clausen RP (2010) Partial Agonists and Subunit Selectivity at NMDA Receptors. *Chem. - Eur. J.* 16:13910–13918

Roberson ED, Sweatt JD (1996) Transient Activation of Cyclic AMP-dependent Protein Kinase during Hippocampal Long-term Potentiation. *J. Biol. Chem.* 271:30436–30441

Robertson CS, Clifton GL, Grossman RG, Ou CN, Goodman JC, Borum P, Bejot S, Barrodale P (1988) Alterations in cerebral availability of metabolic substrates after severe head injury. *J. Trauma* 28:1523–1532

Rock DM, Macdonald RL (1992) The polyamine spermine has multiple actions on N-methyl-D-aspartate receptor single-channel currents in cultured cortical neurons. *Mol. Pharmacol.* 41:83–88

Rodrigues SM, Schafe GE, LeDoux JE (2001) Intra-amygdala blockade of the NR2B subunit of the NMDA receptor disrupts the acquisition but not the expression of fear conditioning. *J. Neurosci. Off. J. Soc. Neurosci.* 21:6889–6896

Rosenberg D, Artoul S, Segal AC, Kolodney G, Radzishevsky I, Dikopoltsev E, Foltyn VN, Inoue R, Mori H, Billard J-M, Wolosker H (2013) Neuronal d-Serine and Glycine Release Via the Asc-1 Transporter Regulates NMDA Receptor-Dependent Synaptic Activity. *J. Neurosci.* 33:3533–3544

Rosenmund C, Stern-Bach Y, Stevens CF (1998) The Tetrameric Structure of a Glutamate Receptor Channel. *Science* 280:1596–1599

Rossi P, Sola E, Taglietti V, Borchardt T, Steigerwald F, Utvik JK, Ottersen OP, Köhr G, D'Angelo E (2002) NMDA Receptor 2 (NR2) C-Terminal Control of NR Open Probability Regulates Synaptic Transmission and Plasticity at a Cerebellar Synapse. *J. Neurosci.* 22:9687–9697

Rothman SM, Olney JW (1987) Excitotoxity and the NMDA receptor. *Trends Neurosci.* 10:299–302

Salussolia CL, Corrales A, Talukder I, Kazi R, Akgul G, Bowen M, Wollmuth LP (2011)(a) Interaction of the M4 Segment with Other Transmembrane Segments Is Required for Surface Expression of Mammalian α-Amino-3-hydroxy-5-methyl-4-isoxazolepropionic Acid (AMPA) Receptors. *J. Biol. Chem.* 286:40205–40218

Salussolia CL, Prodromou ML, Borker P, Wollmuth LP (2011)(b) Arrangement of Subunits in Functional NMDA Receptors. *J. Neurosci.* 31:11295–11304

Sanacora G, Treccani G, Popoli M (2012) Towards a glutamate hypothesis of depression: An emerging frontier of neuropsychopharmacology for mood disorders. *Neuropharmacology* 62:63–77

Sanes JR, Lichtman JW (1999) Can molecules explain long-term potentiation? *Nat. Neurosci.* 2:597–604

Santangelo Freel RM, Ogden KK, Strong KL, Khatri A, Chepiga KM, Jensen HS, Traynelis SF, Liotta DC (2013) Synthesis and Structure Activity Relationship of

Tetrahydroisoquinoline-based Potentiators of GluN2C and GluN2D Containing N-Methyl-D-Aspartate Receptors. *J. Med. Chem.*

Santini E, Muller RU, Quirk GJ (2001) Consolidation of extinction learning involves transfer from NMDA-independent to NMDA-dependent memory. *J. Neurosci. Off. J. Soc. Neurosci.* 21:9009–9017

Sanz-Clemente A, Gray JA, Ogilvie KA, Nicoll RA, Roche KW (2013) Activated CaMKII Couples GluN2B and Casein Kinase 2 to Control Synaptic NMDA Receptors. *Cell Reports* 3:607–614

Sattler R, Xiong Z, Lu W-Y, Hafner M, MacDonald JF, Tymianski M (1999) Specific Coupling of NMDA Receptor Activation to Nitric Oxide Neurotoxicity by PSD-95 Protein. *Science* 284:1845–1848

Säveland H, Nilsson OG, Boris-Möller F, Wieloch T, Brandt L (1996) Intracerebral microdialysis of glutamate and aspartate in two vascular territories after aneurysmal subarachnoid hemorrhage. *Neurosurgery* 38:12–19; discussion 19–20

Saver JL (2013) The 2012 Feinberg Lecture Treatment Swift and Treatment Sure. *Stroke* 44:270–277

Savtchenko LP, Rusakov DA (2007) The optimal height of the synaptic cleft. *Proc. Natl. Acad. Sci. U. S. A.* 104:1823–1828

Schetz JA, Sibley DR (1997) Zinc Allosterically Modulates Antagonist Binding to Cloned D1 and D2 Dopamine Receptors. *J. Neurochem.* 68:1990–1997

Schneggenburger R (1996) Simultaneous measurement of Ca2+ influx and reversal potentials in recombinant N-methyl-D-aspartate receptor channels. *Biophys. J.* 70:2165–2174

Schneggenburger R (1998) Altered voltage dependence of fractional Ca2+ current in N-methyl-D-aspartate channel pore mutants with a decreased Ca2+ permeability. *Biophys. J.* 74:1790–1794

Schorge S, Colquhoun D (2003) Studies of NMDA Receptor Function and Stoichiometry with Truncated and Tandem Subunits. *J. Neurosci.* 23:1151–1158

Schorge S, Elenes S, Colquhoun D (2005) Maximum likelihood fitting of single channel NMDA activity with a mechanism composed of independent dimers of subunits. *J. Physiol.* 569:395–418

Scott DB, Blanpied TA, Swanson GT, Zhang C, Ehlers MD (2001) An NMDA Receptor ER Retention Signal Regulated by Phosphorylation and Alternative Splicing. *J. Neurosci.* 21:3063–3072

Sgambato-Faure V, Cenci MA (2012) Glutamatergic mechanisms in the dyskinesias induced by pharmacological dopamine replacement and deep brain stimulation for the treatment of Parkinson's disease. *Prog. Neurobiol.* 96:69–86

Sharma G, Stevens CF (1996) Interactions between two divalent ion binding sites in N-methyl-d-aspartate receptor channels. *Proc. Natl. Acad. Sci.* 93:14170–14175

Sheinin A, Shavit S, Benveniste M (2001) Subunit specificity and mechanism of action of NMDA partial agonist D-cycloserine. *Neuropharmacology* 41:151–158

Shen K, Meyer T (1999) Dynamic Control of CaMKII Translocation and Localization in Hippocampal Neurons by NMDA Receptor Stimulation. *Science* 284:162–167

Sheng M, Cummings J, Roldan LA, Jan YN, Jan LY (1994) Changing subunit composition of heteromeric NMDA receptors during development of rat cortex. *Nature* 368:144–147

Shinozaki H, Konishi S (1970) Actions of several anthelmintics and insecticides on rat cortical neurones. *Brain Res.* 24:368–371

Siegler Retchless B, Gao W, Johnson JW (2012) A single GluN2 subunit residue controls NMDA receptor channel properties via intersubunit interaction. *Nat. Neurosci.* 15:406–413

Simon RP, Swan JH, Griffiths T, Meldrum BS (1984) Blockade of N-methyl-D-aspartate Receptors May Protect against Ischemic Damage in the Brain. *Science* 226:850–852

Smothers CT, Woodward JJ (2007) Pharmacological Characterization of Glycine-Activated Currents in HEK 293 Cells Expressing N-Methyl-D-aspartate NR1 and NR3 Subunits. *J. Pharmacol. Exp. Ther.* 322:739–748

Smothers CT, Woodward JJ (2009) Expression of Glycine-Activated Diheteromeric NR1/NR3 Receptors in Human Embryonic Kidney 293 Cells Is NR1 Splice Variant-Dependent. *J. Pharmacol. Exp. Ther.* 331:975–984

Sobolevsky AI, Beck C, Wollmuth LP (2002) Molecular Rearrangements of the Extracellular Vestibule in NMDAR Channels during Gating. *Neuron* 33:75–85

Sobolevsky AI, Prodromou ML, Yelshansky MV, Wollmuth LP (2007) Subunit-specific contribution of pore-forming domains to NMDA receptor channel structure and gating. *J. Gen. Physiol.* 129:509–525

Sobolevsky AI, Rosconi MP, Gouaux E (2009) X-ray structure, symmetry and mechanism of an AMPA-subtype glutamate receptor. *Nature* 462:745–756

Sobolevsky AI, Yelshansky MV, Wollmuth LP (2003) Different Gating Mechanisms in Glutamate Receptor and K+ Channels. *J. Neurosci.* 23:7559–7568

South SM, Kohno T, Kaspar BK, Hegarty D, Vissel B, Drake CT, Ohata M, Jenab S, Sailer AW, Malkmus S, Masuyama T, Horner P, Bogulavsky J, Gage FH, Yaksh TL, Woolf CJ, Heinemann SF, Inturrisi CE (2003) A Conditional Deletion of the NR1 Subunit of the NMDA Receptor in Adult Spinal Cord Dorsal Horn Reduces NMDA Currents and Injury-Induced Pain. *J. Neurosci.* 23:5031–5040

Srinivasan R, Sailasuta N, Hurd R, Nelson S, Pelletier D (2005) Evidence of elevated glutamate in multiple sclerosis using magnetic resonance spectroscopy at 3 T. *Brain J. Neurol.* 128:1016–1025

Standaert DG, Testa CM, Young AB, Penney JB Jr (1994) Organization of N-methyl-D-aspartate glutamate receptor gene expression in the basal ganglia of the rat. *J. Comp. Neurol.* 343:1–16

Standley S, Roche KW, McCallum J, Sans N, Wenthold RJ (2000) PDZ domain suppression of an ER retention signal in NMDA receptor NR1 splice variants. *Neuron* 28:887–898

Stern-Bach Y, Bettler B, Hartley M, Sheppard PO, O'Hara PJ, Heinemann SF (1994) Agonist selectivity of glutamate receptors is specified by two domains structurally related to bacterial amino acid-binding proteins. *Neuron* 13:1345–1357

Sucher NJ, Akbarian S, Chi CL, Leclerc CL, Awobuluyi M, Deitcher DL, Wu MK, Yuan JP, Jones EG, Lipton SA (1995) Developmental and regional expression pattern of a novel NMDA receptor- like subunit (NMDAR-L) in the rodent brain. *J. Neurosci.* 15:6509–6520

Sugihara H, Moriyoshi K, Ishii T, Masu M, Nakanishi S (1992) Structures and properties of seven isoforms of the NMDA receptor generated by alternative splicing. *Biochem. Biophys. Res. Commun.* 185:826–832

Sun L, Liu SJ (2007) Activation of extrasynaptic NMDA receptors induces a PKC-dependent switch in AMPA receptor subtypes in mouse cerebellar stellate cells. *J. Physiol.* 583:537–553

Sun Y, Olson R, Horning M, Armstrong N, Mayer M, Gouaux E (2002) Mechanism of glutamate receptor desensitization. *Nature* 417:245–253

Suzuki A, Josselyn SA, Frankland PW, Masushige S, Silva AJ, Kida S (2004) Memory reconsolidation and extinction have distinct temporal and biochemical signatures. *J. Neurosci. Off. J. Soc. Neurosci.* 24:4787–4795

Swan JH, Meldrum BS (1990) Protection by NMDA Antagonists Against Selective Cell Loss Following Transient Ischaemia. *J. Cereb. Blood Flow Metab.* 10:343–351

Talukder I, Borker P, Wollmuth LP (2010) Specific sites within the ligand-binding domain and ion channel linkers modulate NMDA receptor gating. *J. Neurosci. Off. J. Soc. Neurosci.* 30:11792–11804

Talukder I, Wollmuth LP (2011) Local constraints in either the GluN1 or GluN2 subunit equally impair NMDA receptor pore opening. *J. Gen. Physiol.* 138:179–194

Tao Y-X, Rumbaugh G, Wang G-D, Petralia RS, Zhao C, Kauer FW, Tao F, Zhuo M, Wenthold RJ, Raja SN, Huganir RL, Bredt DS, Johns RA (2003) Impaired NMDA Receptor-Mediated Postsynaptic Function and Blunted NMDA Receptor-Dependent Persistent Pain in Mice Lacking Postsynaptic Density-93 Protein. *J. Neurosci.* 23:6703–6712

Teichert RW, Jimenez EC, Twede V, Watkins M, Hollmann M, Bulaj G, Olivera BM (2007) Novel Conantokins from Conus parius Venom Are Specific Antagonists of N-Methyl-D-aspartate Receptors. *J. Biol. Chem.* 282:36905–36913

Thiels E, Weisz DJ, Berger TW (1992) In vivo modulation ofN-methyl-d- aspartate receptor-dependent long-term potentiation by the glycine modulatory site. *Neuroscience* 46:501–509

Thomas CG, Krupp JJ, Bagley EE, Bauzon R, Heinemann SF, Vissel B, Westbrook GL (2006) Probing N-Methyl-d-aspartate Receptor Desensitization with the Substituted-Cysteine Accessibility Method. *Mol. Pharmacol.* 69:1296–1303

Thomson AM, Walker VE, Flynn DM (1989) Glycine enhances NMDA-receptor mediated synaptic potentials in neocortical slices. *Nature* 338:422–424

Tingley WG, Roche KW, Thompson AK, Huganir RL (1993) Regulation of NMDA receptor phosphorylation by alternative splicing of the C-terminal domain. *Nature* 364:70–73

Tovar KR, McGinley MJ, Westbrook GL (2013) Triheteromeric NMDA Receptors at Hippocampal Synapses. *J. Neurosci.* 33:9150–9160

Traynelis SF, Hartley M, Heinemann SF (1995) Control of Proton Sensitivity of the NMDA Receptor by RNA Splicing and Polyamines. *Science* 268:873–876

Traynelis SF, Wollmuth LP, McBain CJ, Menniti FS, Vance KM, Ogden KK, Hansen KB, Yuan H, Myers SJ, Dingledine R (2010) Glutamate Receptor Ion Channels: Structure, Regulation, and Function. *Pharmacol. Rev.* 62:405 –496

Tsai G, Ralph-Williams RJ, Martina M, Bergeron R, Berger-Sweeney J, Dunham KS, Jiang Z, Caine SB, Coyle JT (2004) Gene knockout of glycine transporter 1: Characterization of the behavioral phenotype. *Proc. Natl. Acad. Sci. U. S. A.* 101:8485–8490

Tsien JZ, Chen DF, Gerber D, Tom C, Mercer EH, Anderson DJ, Mayford M, Kandel ER, Tonegawa S (1996)(a) Subregion- and Cell Type–Restricted Gene Knockout in Mouse Brain. *Cell* 87:1317–1326

Tsien JZ, Huerta PT, Tonegawa S (1996)(b) The Essential Role of Hippocampal CA1 NMDA Receptor–Dependent Synaptic Plasticity in Spatial Memory. *Cell* 87:1327–1338

Ulbrich MH, Isacoff EY (2007) Subunit counting in membrane-bound proteins. *Nat. Methods* 4:319–321

Ulbrich MH, Isacoff EY (2008) Rules of engagement for NMDA receptor subunits. *Proc. Natl. Acad. Sci.* 105:14163–14168

Vance KM, Hansen KB, Traynelis SF (2012) GluN1 splice variant control of GluN1/GluN2D NMDA receptors. *J. Physiol.* 590:3857–3875

Vance KM, Simorowski N, Traynelis SF, Furukawa H (2011) Ligand-specific deactivation time course of GluN1/GluN2D NMDA receptors. *Nat. Commun.* 2:294

Vicini S, Wang JF, Li JH, Zhu WJ, Wang YH, Luo JH, Wolfe BB, Grayson DR (1998) Functional and Pharmacological Differences Between RecombinantN-Methyl-D-Aspartate Receptors. *J. Neurophysiol.* 79:555 –566

Villarroel A, Burnashev N, Sakmann B (1995) Dimensions of the narrow portion of a recombinant NMDA receptor channel. *Biophys. J.* 68:866–875

Volianskis A, Bannister N, Collett VJ, Irvine MW, Monaghan DT, Fitzjohn S, Jensen MS, Jane DE, Collingridge GL (2012) Different NMDAR subtypes mediate induction of LTP and two forms of STP at CA1 synapses in the rat hippocampus in vitro. *J. Physiol.*

Vyklický L, Benveniste M, Mayer ML (1990) Modulation of N-methyl-D-aspartic acid receptor desensitization by glycine in mouse cultured hippocampal neurones. *J. Physiol.* 428:313–331

Wagner AK, Fabio A, Puccio AM, Hirschberg R, Li W, Zafonte RD, Marion DW (2005) Gender associations with cerebrospinal fluid glutamate and lactate/pyruvate levels after severe traumatic brain injury. *Crit. Care Med.* 33:407–413

Walker DL, Davis M (2008) Amygdala infusions of an NR2B-selective or an NR2A-preferring NMDA receptor antagonist differentially influence fear conditioning and expression in the fear-potentiated startle test. *Learn. Mem. Cold Spring Harb. N* 15:67–74

Walker DL, Ressler KJ, Lu K-T, Davis M (2002) Facilitation of conditioned fear extinction by systemic administration or intra-amygdala infusions of D-cycloserine as assessed with fear-potentiated startle in rats. *J. Neurosci. Off. J. Soc. Neurosci.* 22:2343–2351

Wang JH, Feng DP (1992) Postsynaptic protein kinase C essential to induction and maintenance of long-term potentiation in the hippocampal CA1 region. *Proc. Natl. Acad. Sci. U. S. A.* 89:2576–2580

Ward SE, Bax BD, Harries M (2010) Challenges for and current status of research into positive modulators of AMPA receptors. *Br. J. Pharmacol.* 160:181–190

Watanabe J, Beck C, Kuner T, Premkumar LS, Wollmuth LP (2002) DRPEER: A Motif in the Extracellular Vestibule Conferring High Ca2+ Flux Rates in NMDA Receptor Channels. *J. Neurosci.* 22:10209–10216

Watanabe M, Inoue Y, Sakimura K, Mishina M (1992) Developmental changes in distribution of NMDA receptor channel subunit mRNAs. *Neuroreport* 3:1138–1140

Watkins JC (1962) The Synthesis of Some Acidic Amino Acids Possessing Neuropharmacological Activity. *J. Med. Pharm. Chem.* 5:1187–1199

Watkins JC (2000) L-Glutamate as a Central Neurotransmitter: Looking Back. *Biochem. Soc. Trans.* 28:297–309

Waxman EA, Lynch DR (2005) N-Methyl-D-aspartate Receptor Subtype Mediated Bidirectional Control of p38 Mitogen-activated Protein Kinase. *J. Biol. Chem.* 280:29322–29333

Weitlauf C, Honse Y, Auberson YP, Mishina M, Lovinger DM, Winder DG (2005) Activation of NR2A-containing NMDA receptors is not obligatory for NMDA receptor-dependent long-term potentiation. *J. Neurosci. Off. J. Soc. Neurosci.* 25:8386–8390

Weston MC, Schuck P, Ghosal A, Rosenmund C, Mayer ML (2006) Conformational restriction blocks glutamate receptor desensitization. *Nat. Struct. Mol. Biol.* 13:1120–1127

White HS, McCabe RT, Armstrong H, Donevan SD, Cruz LJ, Abogadie FC, Torres J, Rivier JE, Paarmann I, Hollmann M, Olivera BM (2000) In vitro and in vivo characterization of conantokin-R, a selective NMDA receptor antagonist isolated from the venom of the fish-hunting snail Conus radiatus. *J. Pharmacol. Exp. Ther.* 292:425–432

Wilcox KS, Fitzsimonds RM, Johnson B, Dichter MA (1996) Glycine regulation of synaptic NMDA receptors in hippocampal neurons. *J. Neurophysiol.* 76:3415–3424

Williams K (1993) Ifenprodil discriminates subtypes of the N-methyl-D-aspartate receptor: selectivity and mechanisms at recombinant heteromeric receptors. *Mol. Pharmacol.* 44:851 –859

Williams K (1994) Subunit-specific potentiation of recombinant N-methyl-D-aspartate receptors by histamine. *Mol. Pharmacol.* 46:531–541

Williams K (1995) Pharmacological properties of recombinant N-methyl-D-aspartate (NMDA) receptors containing the epsilon 4 (NR2D) subunit. *Neurosci. Lett.* 184:181–184

Williams K, Dawson VL, Romano C, Dichter MA, Molinoff PB (1990) Characterization of polyamines having agonist, antagonist, and inverse agonist effects at the polyamine recognition site of the NMDA receptor. *Neuron* 5:199–208

Williams K, Romano C, Molinoff PB (1989) Effects of polyamines on the binding of [3H]MK-801 to the N-methyl-D-aspartate receptor: pharmacological evidence for the existence of a polyamine recognition site. *Mol. Pharmacol.* 36:575–581

Williams K, Zappia AM, Pritchett DB, Shen YM, Molinoff PB (1994) Sensitivity of the N-methyl-D-aspartate receptor to polyamines is controlled by NR2 subunits. *Mol. Pharmacol.* 45:803–809

Wo GZ, Oswald RE (1995) Unraveling the modular design of glutamate-gated ion channels. *Trends Neurosci.* 18:161–168

Wollmuth LP, Kuner T, Sakmann B (1998) Adjacent asparagines in the NR2-subunit of the NMDA receptor channel control the voltage-dependent block by extracellular Mg2+. *J. Physiol.* 506:13–32

Wollmuth LP, Kuner T, Seeburg PH, Sakmann B (1996) Differential contribution of the NR1- and NR2A-subunits to the selectivity filter of recombinant NMDA receptor channels. *J. Physiol.* 491:779–797

Wolosker H (2006) D-Serine Regulation of NMDA Receptor Activity. *Sci. Signal.* 2006:pe41

Wong AYC, Fay A-ML, Bowie D (2006) External Ions Are Coactivators of Kainate Receptors. *J. Neurosci.* 26:5750–5755

Wong AYC, MacLean DM, Bowie D (2007) Na+/Cl− Dipole Couples Agonist Binding to Kainate Receptor Activation. *J. Neurosci.* 27:6800–6809

Wong EH, Kemp JA, Priestley T, Knight AR, Woodruff GN, Iversen LL (1986) The anticonvulsant MK-801 is a potent N-methyl-D-aspartate antagonist. *Proc. Natl. Acad. Sci. U. S. A.* 83:7104–7108

Woo T-UW, Walsh JP, Benes FM (2004) Density of glutamic acid decarboxylase 67 messenger RNA-containing neurons that express the N-methyl-D-aspartate receptor subunit NR2A in the anterior cingulate cortex in schizophrenia and bipolar disorder. *Arch. Gen. Psychiatry* 61:649–657

Wood MW, VanDongen HM, VanDongen AM (1995) Structural conservation of ion conduction pathways in K channels and glutamate receptors. *Proc. Natl. Acad. Sci.* 92:4882–4886

Woolf CJ, Salter MW (2000) Neuronal Plasticity: Increasing the Gain in Pain. *Science* 288:1765–1768

Wu FS, Gibbs TT, Farb DH (1991) Pregnenolone sulfate: a positive allosteric modulator at the N-methyl-D-aspartate receptor. *Mol. Pharmacol.* 40:333 –336

Wu L-J, Zhuo M (2009) Targeting the NMDA receptor subunit NR2B for the treatment of neuropathic pain. *Neurotherapeutics* 6:693–702

Wyllie DJA, Béhé P, Colquhoun D (1998) Single-channel activations and concentration jumps: comparison of recombinant NR1a/NR2A and NR1a/NR2D NMDA receptors. *J. Physiol.* 510:1–18

Wyllie DJA, Chen PE (2007) Taking The Time To Study Competitive Antagonism. *Br. J. Pharmacol.* 150:541–551

Wyllie DJA, Livesey MR, Hardingham GE (2013) Influence of GluN2 subunit identity on NMDA receptor function. *Neuropharmacology*

Xia H, Hornby Z., Malenka R. (2001) An ER retention signal explains differences in surface expression of NMDA and AMPA receptor subunits. *Neuropharmacology* 41:714–723

Yamamoto T, Rossi S, Stiefel M, Doppenberg E, Zauner A, Bullock R, Marmarou A (1999) CSF and ECF glutamate concentrations in head injured patients. *Acta Neurochir. Suppl.* 75:17–19

Yao Y, Harrison CB, Freddolino PL, Schulten K, Mayer ML (2008) Molecular mechanism of ligand recognition by NR3 subtype glutamate receptors. *EMBO J.* 27:2158

Ylilauri M, Pentikäinen OT (2012) Structural Mechanism of N-Methyl-D-Aspartate Receptor Type 1 Partial Agonism. *PLoS ONE* 7:e47604

Yuan H, Erreger K, Dravid SM, Traynelis SF (2005) Conserved Structural and Functional Control of N-Methyl-d-aspartate Receptor Gating by Transmembrane Domain M3. *J. Biol. Chem.* 280:29708–29716

Yuan H, Hansen KB, Vance KM, Ogden KK, Traynelis SF (2009) Control of NMDA Receptor Function by the NR2 Subunit Amino-Terminal Domain. *J. Neurosci.* 29:12045–12058

Zafra F, Aragon C, Olivares L, Danbolt NC, Gimenez C, Storm-Mathisen J (1995)(a) Glycine transporters are differentially expressed among CNS cells. *J. Neurosci.* 15:3952–3969

Zafra F, Gomeza J, Olivares L, Aragón C, Giménez C (1995)(b) Regional Distribution and Developmental Variation of the Glycine Transporters GLYT1 and GLYT2 in the Rat CNS. *Eur. J. Neurosci.* 7:1342–1352

Zarei MM, Dani JA (1995) Structural basis for explaining open-channel blockade of the NMDA receptor. *J. Neurosci.* 15:1446–1454

Zhang L, Peoples RW, Oz M, Harvey-White J, Weight FF, Brauneis U (1997) Potentiation of NMDA receptor-mediated responses by dynorphin at low extracellular glycine concentrations. *J. Neurophysiol.* 78:582–590

Zhang W, Howe JR, Popescu GK (2008) Distinct gating modes determine the biphasic relaxation of NMDA receptor currents. *Nat. Neurosci.* 11:1373–1375

Zhang X-X, Bunney BS, Shi W-X (2000) Enhancement of NMDA-induced current by the putative NR2B selective antagonist ifenprodil. *Synapse* 37:56–63

Zheng F, Erreger K, Low CM, Banke T, Lee CJ, Conn PJ, Traynelis SF (2001) Allosteric interaction between the amino terminal domain and the ligand binding domain of NR2A. *Nat. Neurosci.* 4:894–901

Zhorov BS, Tikhonov DB (2004) Potassium, sodium, calcium and glutamate-gated channels: pore architecture and ligand action. *J. Neurochem.* 88:782–799

Zhu S, Stroebel D, Yao CA, Taly A, Paoletti P (2013) Allosteric signaling and dynamics of the clamshell-like NMDA receptor GluN1 N-terminal domain. *Nat. Struct. Mol. Biol.* 20:477–485